Ford Aerospace
955115 - Final
Vol. 2 (Appendix A-D)

(NASA-CR-162370) PHASE 1 OF THE FIRST SOLAR SMALL POWER SYSTEM EXPERIMENT (EXPERIMENTAL SYSTEM NO. 1). VOLUME 2: APPENDIX A - D Final Report (Ford Aerospace and Communications) 279 p HC A13/MF A01 N79-33574

Unclas G3/44 38928



274

## FOREWORD

This final report documents the technical studies conducted by Ford Aerospace & Communications Corporation, Aeronutronic Division under Contract 955115 to the California Institute of Technology Jet Propulsion Laboratory (JPL) in Pasadena, California. The JPL Technical Manager was Mr. J. R. Womack.

This is a three volume report prepared by the Aeronutornic Division. Subcontractors were the WDL Division of Ford Aerospace & Communications Corporation, Palo Alto, California; United Stirling of Sweden (USS), Malmö, Sweden; Sundstrand Energy Systems, Rockford, Illinois.

The WDL Division was responsible for the concentrator and electrical subsystems. USS provided information on Stirling engines, and Sundstrand supplied information on organic Rankine-Cycle Engines. Additional supporting information was provided by Garrett AiResearch Manufacturing Company, Phoenix, Arizona (closed-cycle Brayton engines); Solar Turbines International, San Diego, California (open-cycle Brayton engines); and Williams Research, Walled Lake, Michigan (open-cycle Brayton engines). Also, the following divisions of the Ford Motor Company provided expertise: Glass Division, Scientific Research Laboratory, and the Manufacturing Planning Group.

The key personnel for the studies documented in this final report are listed below:

- Aeronutronic Division, Ford Aerospace & Communications Corporation

  N. L. Cowden - Program Manager

  R. L. Pons - Technical Manager and Systems Analysis

  T. B. Clark - Optics and Assistant Technical Manager

  D. B. Osborn - Thermodynamics

  E. D. Avetta - Design

  D. C. Jackson - Structures

- WDL Division, Ford Aerospace & Communications Corporation

  H. J. Sund - Subcontract Manager

  I. E. Lewis - Concentrator Subsystem

  J. L. Knorpp - Electrical Subsystem

- United Stirling (USS)

  W. Percival - Consultant to Aeronutronic and Marketing Representative of USS

  Y. Håland - Program Manager for Solar/Stirling Applications

- Sundstrand

  M. Santucci - Principal Investigator, Organic Rankine Engine

- Garrett

  L. Six - Principal Investigator, Closed-Cycle Brayton Engine

- Solar Turbines International

  M. Gramlich

- Williams Research

  R. Mandel

- Ford Motor Company Manufacturing Planning Group

  W. Nagle

T. B. Clark was the editor of these reports.

APPENDIX A

CONCENTRATOR SUBSYSTEM SELECTION AND DEFINITION

CONTENTS FOR APPENDIX A

CONTENTS FOR APPENDIX A (Continued)

CONTENTS FOR APPENDIX A (Continued)

# SECTION 1

# INTRODUCTION

This Appendix summarizes the results of the effort to define the recommended conceptual design of the solar concentrator subsystem. The concentrator subsystem is defined as the combination of: (1) the structural/mechanical framework which supports the receiver/heat engine/generator assembly, (2) the point focusing collector/reflector, (3) the pedestal supporting the reflector, (4) the electrical drive and tracking subsystem, and (5) the foundation footings.

The baseline concentrator represents a combination of the utilization of proven, reliable components and technology but with the addition of innovative and advanced fabrication techniques to reduce costs. In-depth trade studies and analyses stating the reasons and providing justification for selection of the baseline concentrator are explained in this Appendix. In addition, critical parametric concentrator data affecting overall system configuration selection have been identified.

## 1.1 OBJECTIVES

The basic objective of the concentrator selection task was to investigate all viable concepts; to study various concentrator configurations which would fulfill the requirements of this program; and to recommend the baseline concept from a reliability, performance and cost point of view. Selection of the proposed concept was based on the optimum use of near term technologies which could result in operable hardware within the 3½, 4½, and 6½ year startup times, but yet show potential for commercial success in the late 1980's.

The primary criteria used are listed below, in descending order of importance.

(1) High operational reliability

(2) Minimum risk of program schedule failure

(3) High potential for commercialization

(4) Low Phase II and III program costs.

Other parameters which were considered as potential risks to the overall program objectives were:

- Performance
- Efficiency
- Production costs

- Operational costs
- Unscheduled maintenance
- Human safety
- Community acceptance.

## 1.2 STUDY APPROACH

The requirements of the program stress near term reliability and performance, but with the objective of future commercialization. Therefore, the approach was to extend familiar microwave technology to solar applications. This would provide a base of proven hardware and performance with minimal risk which can be modified for solar applications in a cost effective manner. The concentrator subsystem performance requirements are actually less stringent than those normally imposed by microwave communications systems. The critical differences which affect cost, performance, and reliability have been identified. The major consideration for overall concept and individual components was low cost of basic materials in a form adapted to high quantity fabrication and installation.

The extensive experience and expertise of the Ford Motor Company Glass Division, Scientific Research Laboratories, and Manufacturing Planning groups have been used to provide assistance and guidance in the development, design, manufacturing feasibility and estimated costs of the various concentrator components. This support was particularly aimed at future large scale production, i.e., 1990 technology and production rates of 100 to 5000 stations of 1 MWe generating capacity per year.

# SECTION 2

## CONCENTRATOR CONCEPT EVALUATION AND TRADE STUDIES

Table 1 breaks down the concentrator subsystem into major components and identifies particular configurations which exhibited potential for further investigation and study. A preliminary evaluation and screening of each candidate was made based on qualitative cost, performance, and reliability information. In-depth trade studies were then performed on the qualifying candidates and a particular concept was selected, consistent with the overall system concept.

## 2.1 CONCENTRATOR PERFORMANCE REQUIREMENTS, INTERFACES AND SPECIFICATIONS

### 2.1.1 PERFORMANCE PARAMETERS

Performance requirements for the concentrator subsystem have been divided into two types - defined and derived. The defined system requirements are quite broad and impose minimal restrictions on the concentrator configuration design. The derived requirements represent values obtained from system trade studies for the baseline configuration, which were updated during the study.

The defined system requirements for the SPSE program have been established by JPL and are summarized in Table 2. Table 3 lists the major derived parameters and how they were obtained.

### 2.1.2 INTERFACE CRITERIA

The primary interface is with the receiver/engine/generator* package. Table 4 lists the major areas to which this package has an impact on the concentrator design.

The other significant interface is with the site preparation work. Installation and checkout requires that the site be cleared and accessible, that subsurface soil conditions be known, that utility interfaces are available, that security is maintained, etc.

*Commonly referred to as the power module.

TABLE 1. CONCENTRATOR COMPONENTS MATRIX

| RECEIVER/POWER CONVERSION UNIT LOCATION | RECEIVER SUPPORT | REFLECTIVE SURFACE MATERIAL | REFLECTOR STRUCTURE | REFLECTOR ARRANGEMENT | OPTICAL GEOMETRY |
|---|---|---|---|---|---|
| • Prime Focus<br>• Reflector<br>• Pedestal<br>• Ground | • Quadripod<br>• Tripod<br>• Bipod<br>• Multi-pod<br>• Separate Structure | • Metallized Plastic Film<br>• Polished Metal<br>• 2nd Surface Draw-Fusion Glass<br>• 2nd Surface Float Glass | • Conventional Back Structure<br>• Front Bracing (Proprietary) | • Continuous Surface<br>• Individual Facets<br>• Fresnel<br>• Modified Fresnel or Truncated | • Conventional Newtonian<br>• Cassegrainian & Multiple Bounce<br>• Offset & Full Parabola<br>• Fresnel Configurations<br>• Circular & Non-Circular |

| AXES ORIENTATION | LOWER AXIS BEARING | UPPER AXIS DRIVE | LOWER AXIS DRIVE | AXIS DRIVE POWER | TRACKING CONTROL |
|---|---|---|---|---|---|
| • Elevation Over Azimuth<br>• Equatorial Mount<br>• X-Y Mount | • Wheel & Track<br>• Inverted Track<br>• Turn Table<br>• Shaft-Mounted Bearing Pairs<br>• Kingpost | • Linear Actuator<br>• Gears<br>• Traction<br>• Roller Chain<br>• Wire Rope<br>• Rack & Pinion | • Linear Actuator<br>• Gears<br>• Traction<br>• Roller Chain<br>• Wire Rope<br>• Rack & Pinion | • AC Electric<br>• DC Electric<br>• Pneumatic<br>• Hydraulic | • Closed-loop Auto-track with Optical Sun Sensor<br>• Open-loop Program Track Ephemeris Data<br>• Closed-loop Auto-track with Thermal Sensor<br>• Combinations |

TABLE 2. DEFINED PERFORMANCE PARAMETERS

| ITEM NO. | CONCENTRATOR PARAMETER DESCRIPTION | DEFINED SYSTEM REQUIREMENTS |
|---|---|---|
| 01 | Concentrator Configuration | Point-Focusing Distributed Collector, Energy Conversion at the Collector |
| 02 | Concentrator Size | Sufficient Size and Quantity to Maintain 1 MWe of Rated Power to the Utility Grid (Sensitivity Analysis to be Conducted for 0.5 MWe to 10.0 MWe Range) |
| 03 | Concentrator Schedule | Operate 1 MWe System Within 4-1/2 Year Start-up Time (3-1/2 & 6-1/2 Year Start up Times to also be addressed) |
| 04 | Concentrator Life | 30 Years |
| 05 | System Annual Capacity Factor | Concentrator System to be Compatible with an Annual Capacity Factor of 0.4 (no storage, 0.7 C.F. and Stand-alone Systems to also be addressed) |

2.1.3 ENVIRONMENTAL SPECIFICATIONS

The concentrator (and other subsystems comprising the plant) must be capable of operating in and surviving the appropriate environments summarized in Table 5. Overall system performance calculations were made using the 1967 Barstow Insolation and Weather data.

2.2 BASIC CONCENTRATOR CONCEPTS

A point focusing concentrator consists of three fundamental elements:

- An Optical System - the mirror(s) which focus the incoming insolation into the receiver aperture.
- A Pedestal System - a two-axis mechanism drive which points the optical system at the sun.
- A Solar Tracking System - instrumentation and logic to furnish the position of the sun and control the pedestal axis drives.

TABLE 3. DERIVED PERFORMANCE PARAMETERS

| ITEM NO. | CONCENTRATOR PARAMETER DESCRIPTION | DERIVED CONCENTRATOR REQUIREMENTS | BASIS OF SELECTION |
|---|---|---|---|
| 1 | Collector Diameter | 8m to 26m | Diameter range sufficient to accommodate possible engine options. Value for specific engine set by systems analysis. (Section 3.1.1.3 of report) |
| 2 | Elevation Travel Range (Horizon 0° Reference) | ∿+10° to +90° | Minimum angle of ∿+10° set by time sufficient solar energy available for operation, including warm-up. (Non-operating travel of ∿0° desirable for maintenance.) Limit of +90° required for Southern regions of the U.S. |
| 3 | Azimuth Travel Range (South 0° Reference) | ±114° | Value based on operation anywhere within Continental U.S. |
| 4 | Rim Angle | 65° | System trade studies (Section 3.1.1.1 of report) |
| 5 | Emergency Defocus Rate | ∿5°/Min. | Required to move the concentrated beam across the receiver lip rapidly enough to prevent excessive heating. Used only in a malfunction. |
| 6 | Average Panel Reflectivity | Maximum Possible | System trade studies (Section 3.1.1.1 of report) show optimum value is the maximum possible, i.e., glass |
| 7 | Surface Slope Error | ∿0.15° (2.6 mr) | System trade studies (Section 3.1.1.1 of report) |
| 8 | Pointing Error | ∿0.10° (1.7 mr) | System trade studies (Section 3.1.1.1 of report) |

TABLE 4. CONCENTRATOR INTERFACE WITH RECEIVER/ENGINE/ALTERNATOR

| ITEM | RECEIVER/ENGINE/GENERATOR (POWER MODULE) DESIGN CHARACTERISTICS | EFFECT ON CONCENTRATOR |
|---|---|---|
| 1 | Physical Size | • Configuration of Support System<br>• Amount of Shadowing and Blockage |
| 2 | Weight and Center of Gravity | • Sizing of Mechanical Drive Components<br>• Foundation Requirements<br>• Pedestal Member Sizing<br>• Support Structure Configuration and Sizing |
| 3 | Vibration | • Support Structure Rigidity<br>• Reflector Structure Stiffness |
| 4 | Cooling and Electrical Line Requirements (Including Instrumentation) | • Provisions for Mounting Fan/Radiator for Engine Cooling (Stirling Engine)<br>• Provisions for Routing and Supporting Cooling and Electrical Lines |
| 5 | Control (Starting, Synchronizing, shut-down, etc.) | • Provisions for Control Cables |
| 6 | Access/Maintenance Requirements | • No Access Platforms or Stairs Planned. External Lift Servicing Only.<br>• Power Module Removal/Replacement<br>• Power Module Servicing Requirements |
| 7 | Tilting/Tipping Restraints | • Type of Axis Configuration Which Can be Utilized |
| 8 | Closure Requirements for Receiver Door | • Insolation Level Detector and Logic Command |
| 9 | Emergency Defocusing Requirements | • Servo Capability and Logic to Move the Concentrator in the Event of an Emergency (Overheat, Loss of Load, etc.) |
| 10 | Installation Requirements | • Lifting Equipment Required<br>• East of Mounting, Including Minimum Elevation Angle<br>• Alignments Required |
| 11 | Safety Hazards | • Leakage of Sodium Can Cause Corrosion of Concentrator Components |

TABLE 5. ENVIRONMENTAL SPECIFICATIONS

| ITEM NO. | ENVIRONMENTAL PARAMETER | ENVIRONMENTAL SPECIFICATION |
|---|---|---|
| 01 | Wind Speed (M/S) at Reference Height of 10m (30 ft) * | Frequency (%) |
| | 0-2 | 29 |
| | 2-4 | 21 |
| | 4-6 | 19 |
| | 6-8 | 14 |
| | 8-10 | 8 |
| | 10-12 | 5 |
| | 12-14 | 3 |
| | 14- | Less than 1 |
| | * Wind velocity profile varies exponentially with height to 0.15 power from this reference | |
| 02 | Wind Rise Rate | Max. 0.01 $m/s^2$ (1.3 mph/min During Stow |
| 03 | Stowage Initiation | To be selected based on loss of direct beam insolation vs plant cost. |
| 04 | Max survival wind speed (any position)* | 25 M/S (50 mph) |
| 05 | Max survival wind speed (stow) | 40 M/S (90 mph) |
| 06 | Dust (No damage) | Dust devils with wind speeds to 17 M/S |
| 07 | Temperature | $-30^oC$ to $+50^oC$ ($-20^oF$ to $+120^oF$) |
| 08 | Earthquake (No damage) | Seismic Zone 3 |
| 09 | Snow (Survival) | 5 $lb/ft^2$ @ Rate of 1 ft/24 hrs |
| 10 | Average Annual/Rain | 750 mm (30 in) |
| 11 | Maximum 24 hour rain | 75 mm (3 in) |
| 12 | Ice (No damage) | 50 mm (2 in) thick layers |
| 13 | Hail (Any Orientation) | |
| | - Diameter | 20 mm (3/4 in) |
| | - Specific Gravity | 0.9 |
| | - Terminal Velocity | 20 M/S (65 fps) |
| 14 | Hail (Survival) | |
| | - Diameter | 25 mm (1 in) |
| | - Specific Gravity | 0.9 |
| | - Terminal Velocity | 23 M/S (75 fps) |
| 15 | Sandstorm (No damage) | MIL-STD-810B, Method 510 |
| 16 | Lightning (Direct Hit) | Single Collector & Controller Destruction |
| 17 | Lightning (Adjacent Hit) | Minimal Collector & Controller Damage |

*Max operating wind speed = 13 m/s (29 mph)

Each of these elements is discussed in the following paragraphs.

## 2.2.1 OPTICAL SYSTEMS

The optical system geometric arrangements which have been considered are:

- Symmetric Newtonian
- Symmetric Cassegrainian
- Segmented Fresnel
- Offset Newtonian with circular or noncircular aperture

The basic configurations of these candidates are described below.

2.2.1.1 Symmetrical Newtonian (Prime Focus). The most straight-forward point focusing optical system is a symmetrical paraboloidal mirror with a receiver mounted at the focus as shown in Figure 1. The receiver aperture (opening) is located at the mirror focal plane. The only significant parameter for a Newtonian system is the rim angle ($\theta_R$) which is directly related to the focal length/diameter ratio (F/D).

2.2.1.2 Cassegrainian and Multiple Bounce. One disadvantage of simple prime focus systems is that the relatively heavy power module must be structurally supported behind the focal plane. This problem can be reduced with Cassegrain optics, which uses a hyperbolic secondary reflector to refocus the image to an arbitrary point on the optical axis, as shown in Figure 2. A convenient structural location for the receiver is near the vertex of the reflector. However, the advantage of repositioning the power module is greatly outweighed by: (1) the greatly increased reflectance losses, (2) the requirement to actively cool the secondary mirror to prevent overheating, and (3) a redesign of the sodium reflux boiler to add heat pipes or pumps since the fluid must be returned against gravity. It is possible in theory to add a third or fourth mirror so as to position the receiver off the centerline but this only compounds the problems of losses and cooling the optics, and was not considered further.

2.2.1.3 Fresnel System. A Fresnel reflecting system is made up of a number of annular mirrors with a common focal point (Figure 3). This configuration has basically the same optical characteristics as a conventional Newtonian system but the depth of the reflector structure is less. In order to prevent blockage from one mirror ring to the next, gaps are provided between the reflecting annuli. This results in increased structural diameter of about 20 percent for a typical rim angle of 60°, based on the limiting case of a large number of rings.

Another alternative is Fresnel refracting optics (Fresnel lens). Serious problems include the losses in the lens, two surfaces to maintain, and the unfavorable position of the receiver. Further development is required to determine the applicability of refracting Fresnel systems. Due to these problems, this concept was not considered further.

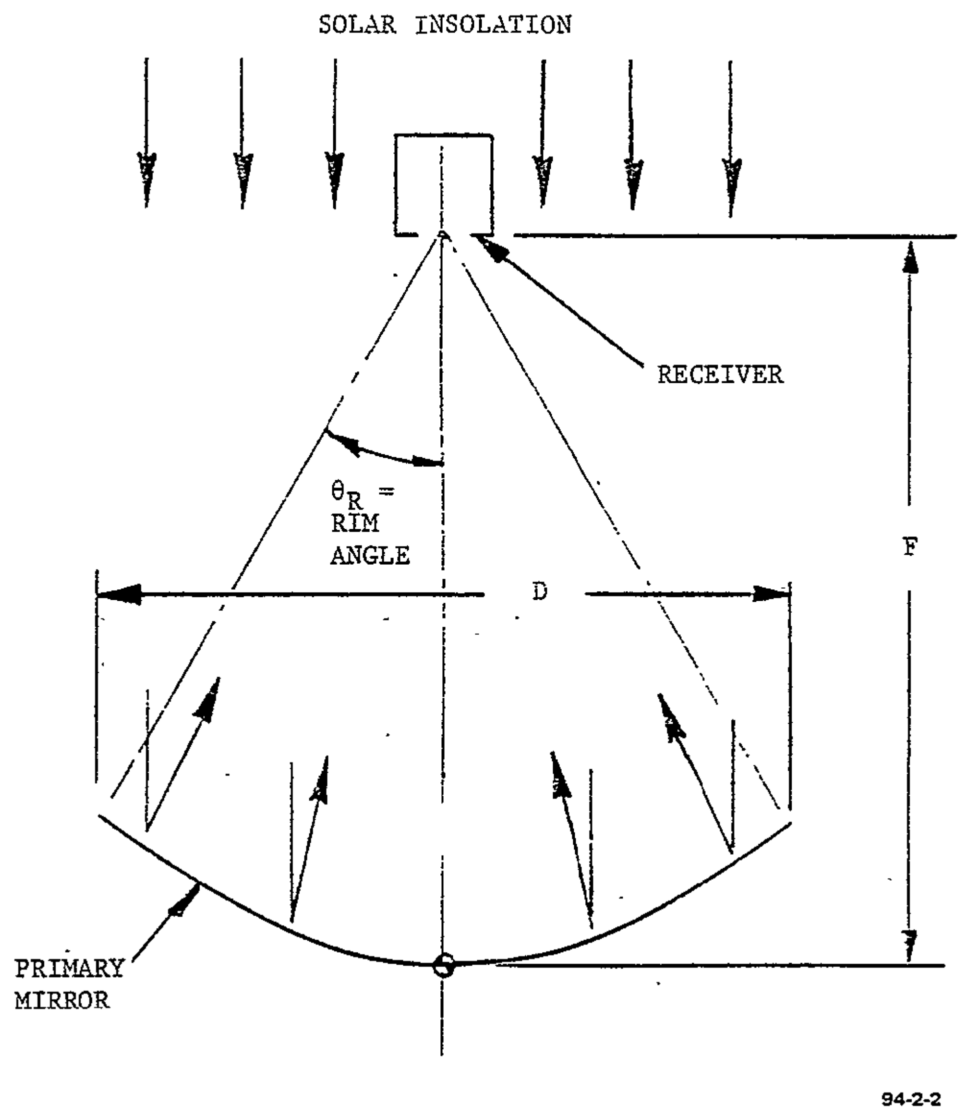


FIGURE 1. NEWTONIAN (PRIME FOCUS) OPTICAL SYSTEM

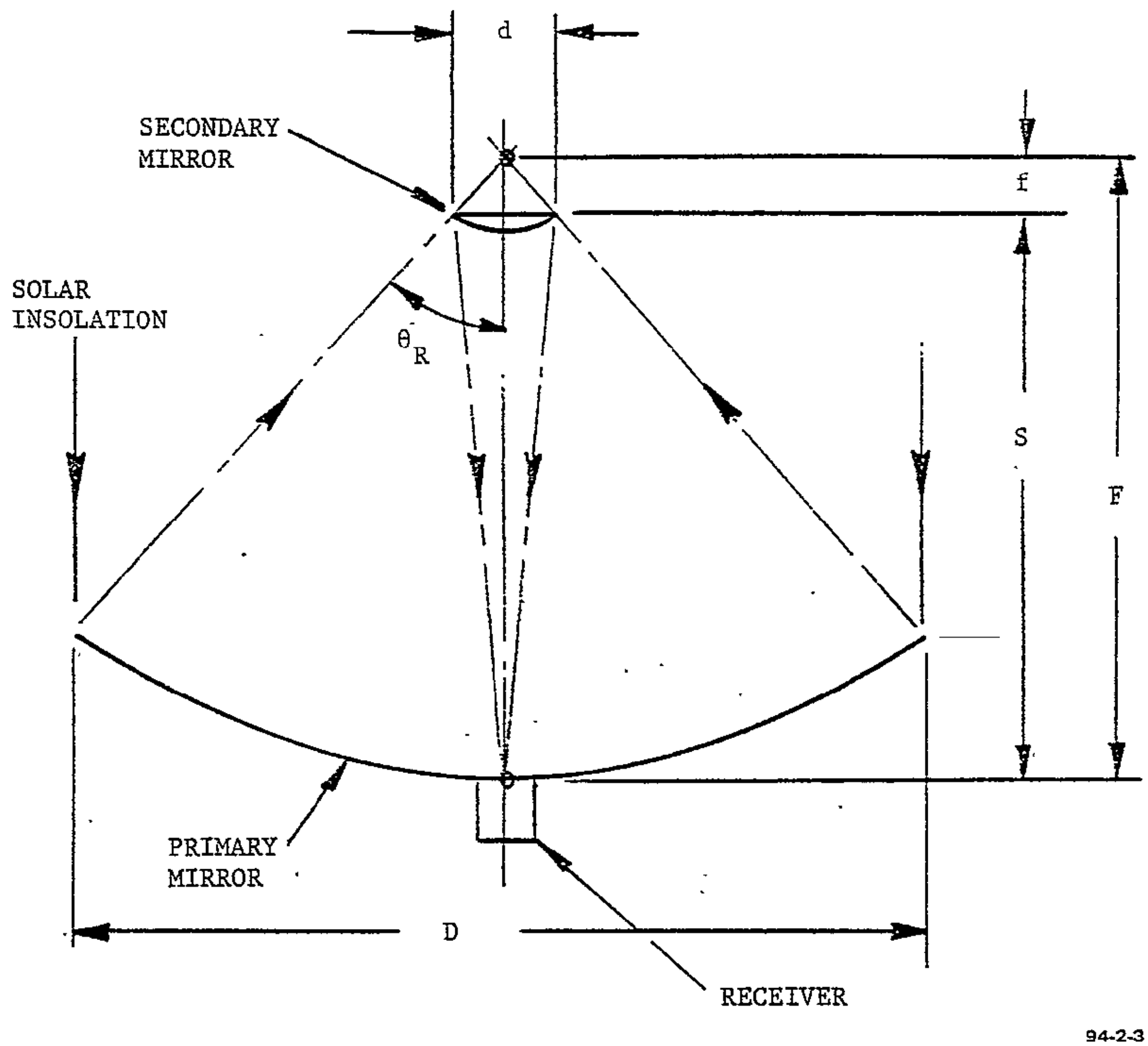


FIGURE 2. SYMMETRICAL CASSEGRAIN OPTICAL SYSTEM

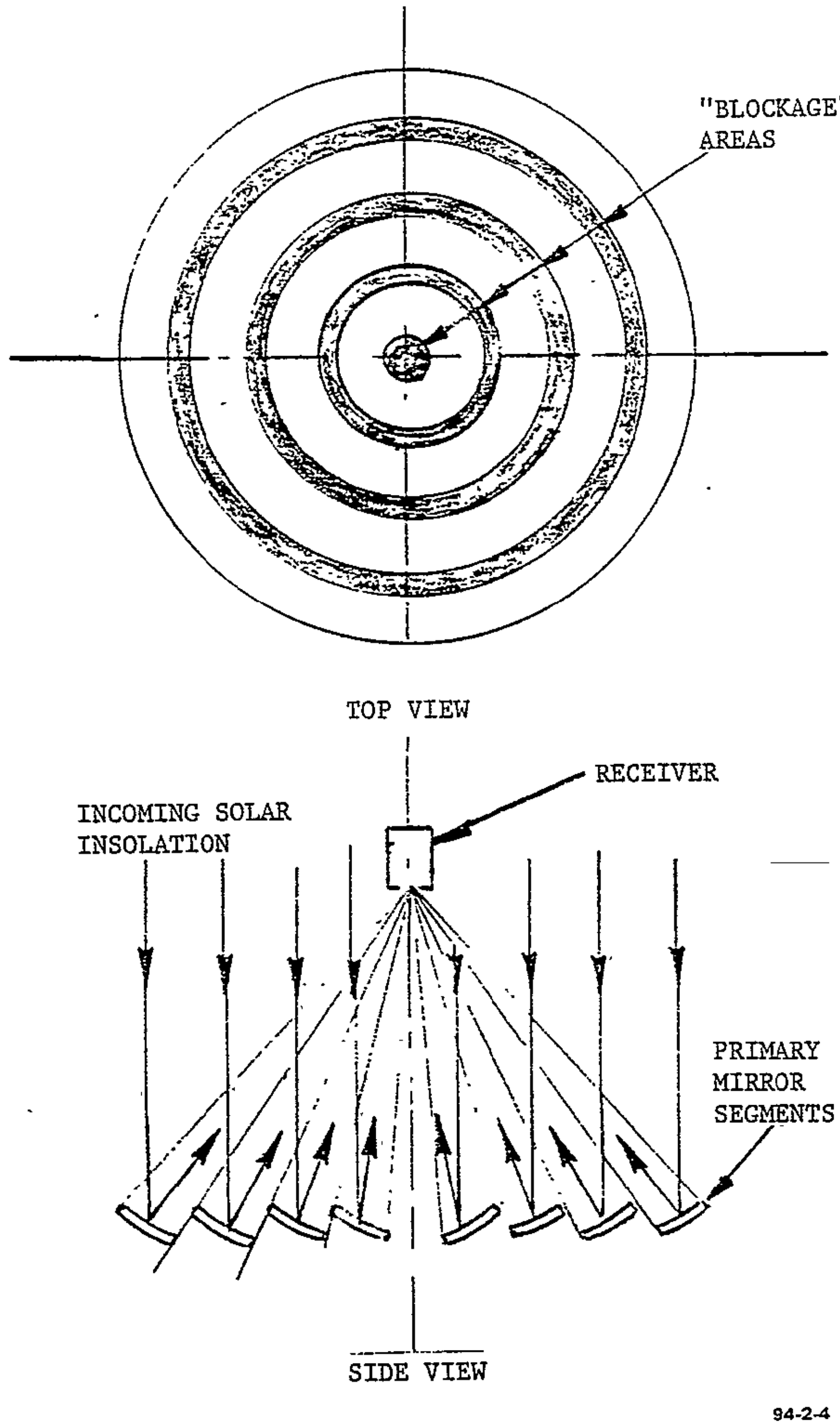


FIGURE 3. FRESNEL REFLECTOR

2.2.1.4 Nonsymmetric Newtonian Systems. Two nonsymmetric systems were investigated since they are low profile configurations. The first uses an off-axis segment of a paraboloid with the receiver located at the focal point and canted with respect to the paraboloid axis. This system in conjunction with a particular Az/El mount arrangement makes it possible to have no solar blockage and to position a power module which is nonrotating with respect to gravity.

The second offset configuration that was considered is essentially a half-symmetric paraboloid. This is potentially attractive because the reflector height is 0.707 of that for an equal area symmetric system. This results in significant reduction in elevation wind moments and counterbalancing problems.

2.2.2 PEDESTAL SYSTEMS

A two-axis pedestal system is required for continuously tracking the sun. In general, the two axes of rotation can be identified as primary (fixed to the ground) and secondary (usually orthogonal to the primary axis to give maximum spatial coverage with minimum axis travel). Common pedestal systems include polar or equatorial mounts (HA/DEC), elevation over azimuth (Az/El), and X/Y (first axis parallel to the ground). These arrangements are shown in Figure 4.

The primary geometric and kinematic factors that were considered in selecting a pedestal geometry are:

- The total angular travel required in each axis.
- The angular rates required in each axis for suntracking.
- The attitude variations of the power module for Newtonian or Cassegrain Systems.

Other factors which are similar for all the configurations are the wind stowing rates and the emergency defocus rate. The latter requires a movement of approximately $5^{\circ}$ per minute in at least one axis. Worst case stowing rate is slightly less than $5^{\circ}$/min.

2.2.2.1 Polar (HA/DEC) Mount (Primary axis elevation equal to site latitude). Polar or HA/DEC geometry is attractive for tracking celestial targets such as the sun, because the secondary axis travel is minimal and the primary axis tracking rates are low; namely $\pm 23.5^{\circ}$ motion in DEC and $0.25^{\circ}$/minute HA velocity. The total required hour-angle travel depends on the site latitude and the minimum elevation selected for solar collection, as plotted in Figure 5. The attitude motions can be described by the elevation angle of the receiver axis and a roll angle about its axis, relative to a vertical plane. These are plotted in Figure 6, showing that the receiver must be operable over a considerable two-dimensional attitude range.

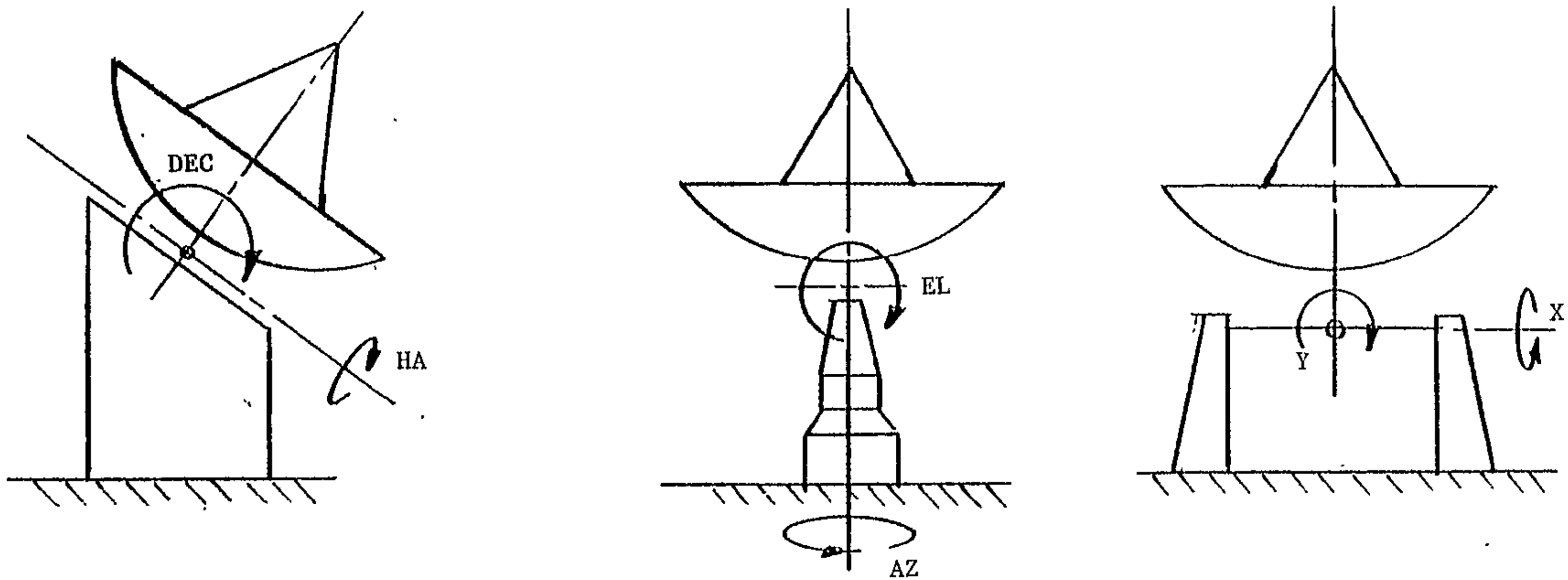


HA/DEC AZ-EL X-Y

94-2-5

FIGURE 4. AXIS GEOMETRIC ARRANGEMENTS

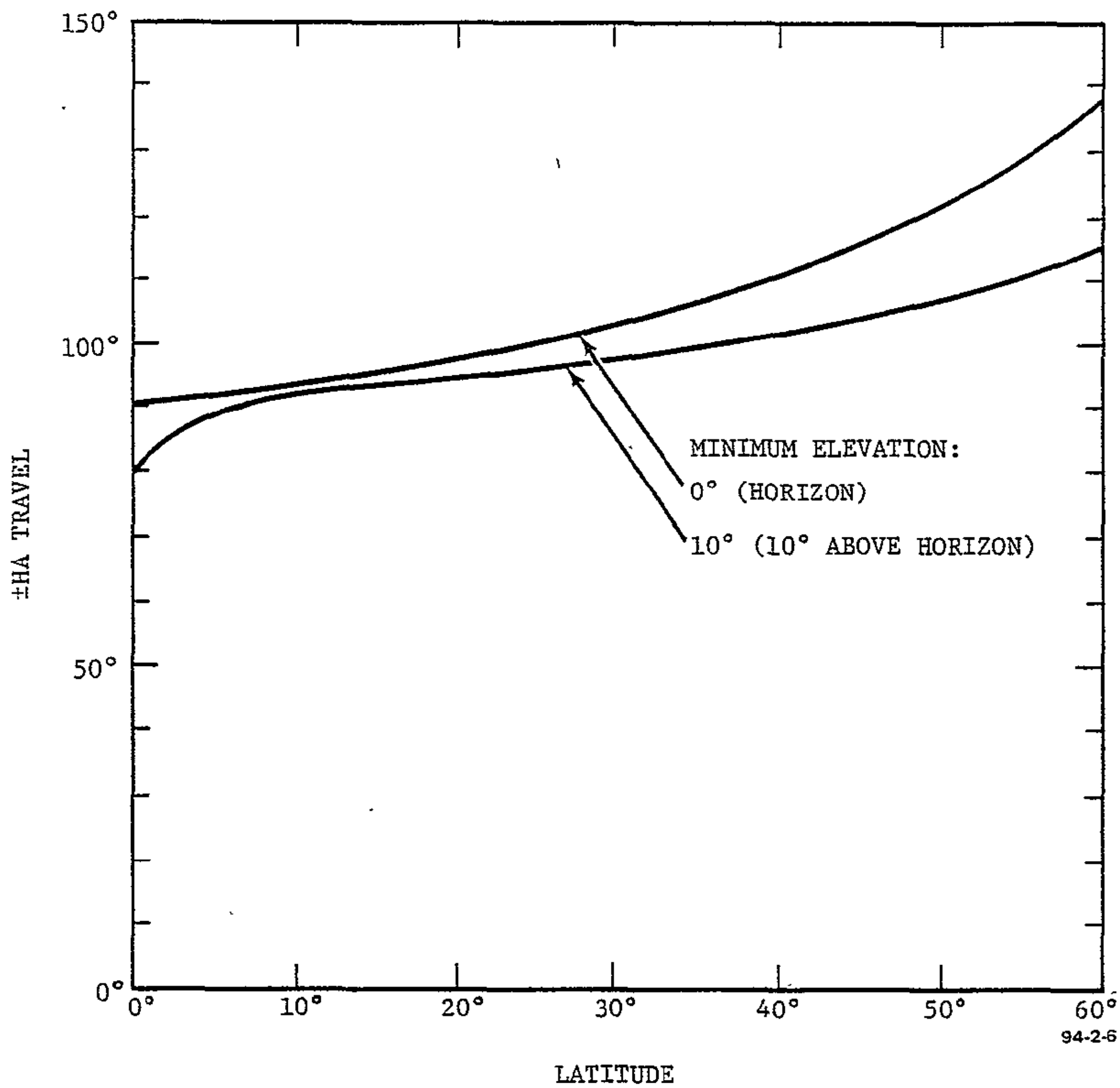


FIGURE 5. MAXIMUM HOUR ANGLE COVERAGE

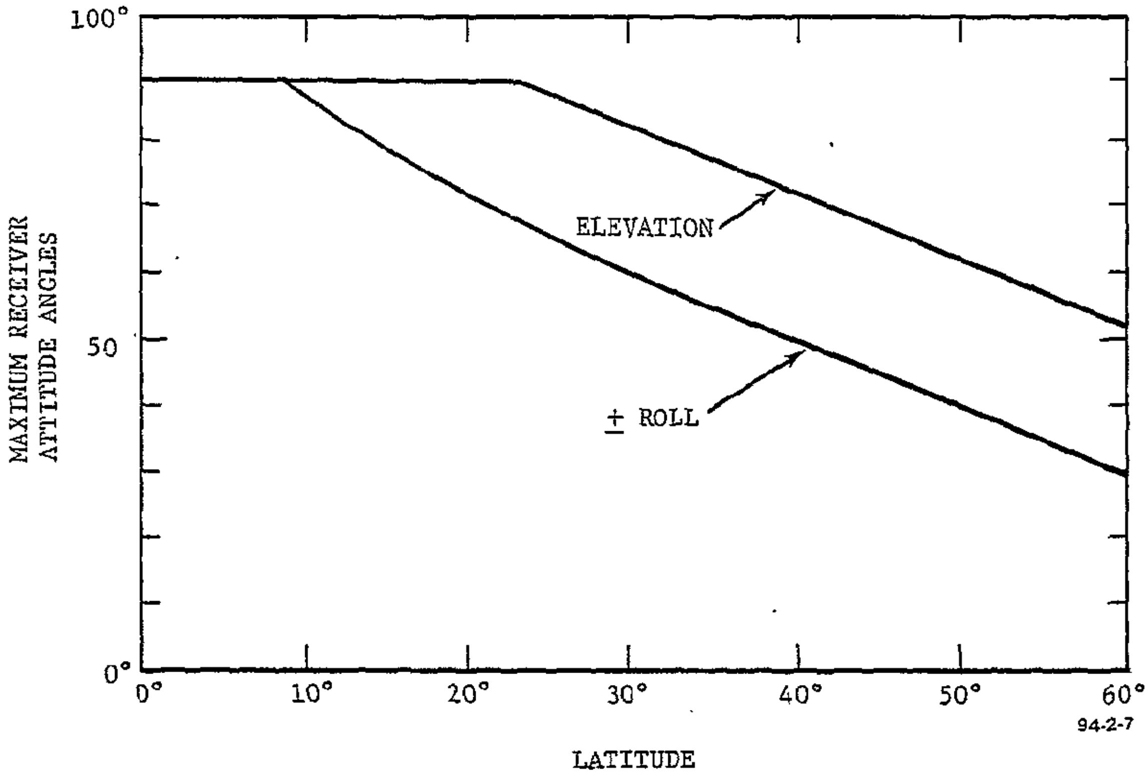


FIGURE 6. RECEIVER ATTITUDE VARIATIONS FOR HA/DEC PEDESTAL

2.2.2.2 Az/El Mount (Primary Axis Vertical). The generally desirable characteristic of Az/El mounts is their near symmetry with respect to vertical (gravity). The required elevation travel is from operational horizon to maximum elevation (Figure 6). The required azimuth travel again depends on latitude and operational horizon, and is plotted in Figure 7.

The maximum elevation tracking rate is approximately earth rate times the cosine of latitude, i.e., always less than 0.25°/min. The maximum azimuth rate, on the other hand, is proportional to the secant of maximum elevation times cos(23.5°), and becomes quite large in the summer for southern latitudes near the tropics. This so-called "keyhole" rate is plotted in Figure 8. The required azimuth rate for southern U.S. sites such as Miami, FL. or Brownsville, TX. is comparable to the emergency defocus rate of 5°/min.

The receiver attitude variations for an Az/El configuration encompass the entire operational elevation range, but there is no roll - the angular motion of the receiver is one-dimensional.

2.2.2.3 X-Y Mount (Primary "X" Axis Horizontal). This axis arrangement has been used for microwave antennas to avoid the zenith keyhole problem. The X-Y geometry, of course, has a rate keyhole near its primary axis, but for solar tracking applications where the primary axis is oriented north-south, the closest the sun can ever come to the primary axis is the same as the operational horizon elevation. For a 10° horizon, the maximum earth rate magnification is about six for the X axis (∿1.5°/min. maximum rate).

The required X axis travel range is approximately ±90° minus the horizon elevation. Y axis travel requires a value of (latitude + 23.5°) in the southern direction (winter noon) and half-azimuth swing minus 90° in the northern direction (summer horizon). Since most X-Y mount configurations are inherently symmetric about both X and Y, this implies that full above-horizon coverage is required. The receiver maximum roll angle is about ±90° because at sunrise and sunset the reflector is laid over on its side.

2.2.3 SOLAR TRACKING SYSTEMS

Tracking involves positioning the concentrator to focus the solar image on the receiver aperture. In addition to the prime tracking function, there are several other functional requirements:

- Automatic repositioning to sunrise orientation after nightfall.
- Manual operation at each concentrator for maintenance and testing.
- Defocusing of the receiver for emergency conditions (e.g., receiver or engine overheating).
- Stowing at zenith position for high wind conditions.

The latter two functions are executed from external logic inputs.

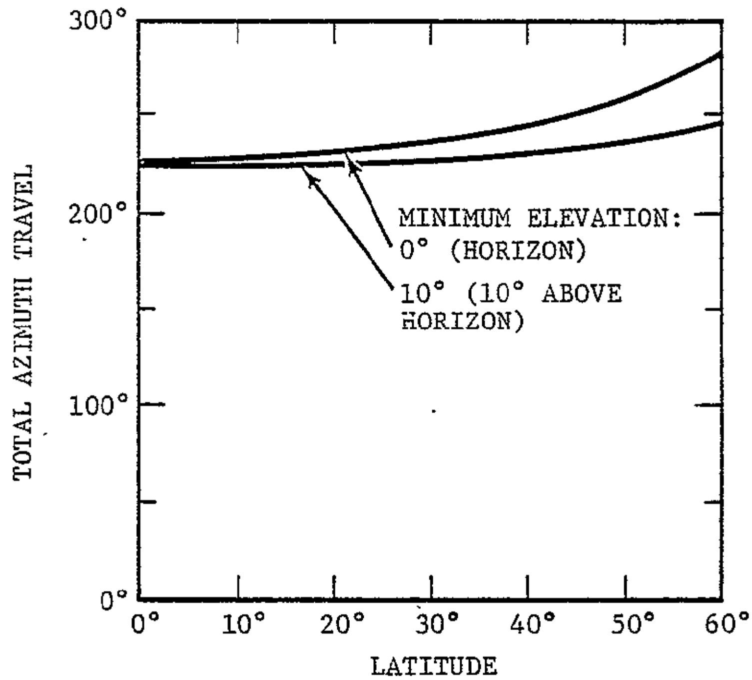


FIGURE 7. AZIMUTH COVERAGE

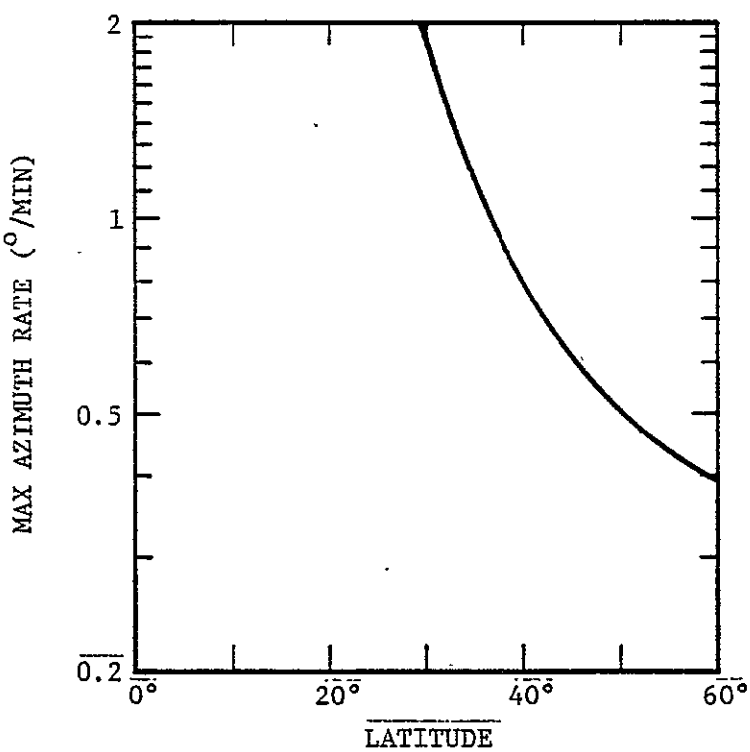


FIGURE 8. AZIMUTH TRACKING RATES

Ways of implementing the normal daytime solar tracking function are briefly described below. All of these tracking systems are adaptable to any two-axis pedestal configuration.

2.2.3.1 Ephemeris Program Tracking. Solar ephemeris data is computed at appropriate time intervals to provide adequate solar pointing resolution and converted to mount axis angle coordinates. The computation can be performed either onboard each concentrator or by a central field computer. The concentrator axis angles are then updated by repositioning until the measured axis angles correspond with the updated ephemeris angles.

The antenna axis angles can be measured in various ways including:

- On-axis digital encoders
- Synchro or resolver to digital conversion
- High speed shaft revolution counters with a "zero reference marker"

It is usually necessary for periodic measured-angle calibrations to be made in order to account for such effects as gravity sag, pedestal misalignments, and angle measuring system nonlinearity and offset. Variation between units will likely require calibration checks to be performed on each individual concentrator.

2.2.3.2 Thermal Autotracking. The ideal suntracking system is one that uses actual measurements of the image at the receiver to generate error signals from which the pedestal axis angles can be corrected to center the image. One concept would be to locate four wide-angle flux sensors in a symmetric array around the outside of the receiver aperture. When the image is not centered, the readings of two opposite sensors will be unequal. The difference in readings are normalized to the average incoming flux to generate true angular error signals that are independent to the flux level. This normalization procedure (automatic gain control) is the conventional method of generating tracking error signals in microwave antenna autotracking systems. These 2-dimensional error signals are then transmitted to the position control/servo system for processing to control the movement of the pedestal tracking axes. The control logic for this type of autotracking system is, in principle, the same as for program tracking. Namely, axis positions are updated whenever the error reaches some specified tolerance level. The fundamental problem is to obtain a sensor which can withstand the concentrated flux (10,000 suns, maximum) without burning up.

2.2.3.3 Optical Autotracking. Optical autotracking is accomplished using a device which measures the sun's direction in two angular coordinates relative to the instrument axis. This sensor is mounted on the concentrator structure so that the image is centered on the receiver aperture when the output angles are zero. The outputs of the sensor can then be regarded as tracking error signals for the two pedestal axes. Axis positions are updated when the error reaches a predetermined level. This scheme minimizes mechanical tracking errors, with the exception of gravity sag. The angular deflections of the mounting point of the error sensor will not, in general, be the same as is required to collimate the image, but by careful selection of the mounting point the errors can be reduced to an acceptable value.

Optical autotracking requires the sensor have a relatively narrow field of view to prevent tracking problems on cloudy or diffuse days. This implies the need for an additional coarse optical error sensing device with wide field of view, and tracker to determine whether the direct insolation level is adequate for power collection. There must also be some coarse program to permit nighttime movement to the next day's sunrise position, and to keep the sun within the coarse sensor field of view during extended cloudy periods.

2.2.3.4 Hybrid Tracking Systems. Another option is to use a fine auto-tracking system in conjunction with a coarse program track system. In this scheme the program track accuracy need only be adequate to position the concentrator within the field of view of the fine tracking sensor, which alleviates the more stringent requirements for pointing angle measurement (axis encoding) and calibration accuracy that are necessary for pure program tracking.

A feature of hybrid systems is that they provide a ready means for self-calibration of the axis angle encoding systems. This is done by making periodic (say hourly) comparisons of the measured axis angles versus the true sun ephemeris to generate a two-axis calibration table, which can subsequently be used for refining the program track operation on cloudy days. This self-calibration can be done either onboard each concentrator or centrally.

## 2.3 CONFIGURATION VERSUS PERFORMANCE/COST MATRICES

The inherent advantages and disadvantages were evaluated for all the previously identified concentrator concepts in each of the following categories:

- External versus enclosed concentrators
- Pedestal/optical systems
- Tracking control systems.

The pedestal and optical systems were combined because of their close dependence.

The initial screening was conducted based on preliminary analyses of performance, cost, and reliability. The goal was to be able to identify those concepts which did not merit further consideration when judged against the others.

### 2.3.1 EXTERNAL VERSUS ENCLOSED CONCENTRATIONS

2.3.1.1 Enclosed Concentrators. The concentrator can be enclosed within a protective transparent cover. This concept was not selected for the following reasons:

(1) Weight of Power Module. An advantage of an enclosure is that the concentrator could be lighter weight (and less costly) since it is not subjected to wind loads. However, when the power module is mounted at the focal point the support for this rotating weight cannot be a lightweight concentrator structure. The gravity moment loads resulting from the power module are a major contributor to the design of the structural and mechanical components of the concentrator.

(2) High Life Cycle Costs. The age deterioration of the exposed plastic enclosure and its replacement costs required during the design life are prohibitive*. Data on the mechanical and optical properties of the enclosure is very limited. Useful life of the plastics cannot be predicted accurately at this time. Considerable process development is needed which might improve the enclosure material, but this will not be available within the time frame required.

(3) High Maintenance/Cleaning Costs. The surface of the enclosure that requires cleaning is over three times greater than the surface of the unenclosed concentrator, even if only the sun path area is cleaned. The surface to be cleaned is higher, more difficult to reach, and requires more expensive maintenance equipment. The enclosure also requires maintenance of its pressurization equipment.

(4) Possible Size Limitation. Concentrators ranging up to 26 meters in diameter were considered, which are larger than the enclosures under development.

(5) Environmental Impact. The large enclosures have a greater impact on the aesthetics than unenclosed structures because of larger ground area which is covered and/or shadowed and the greater height. Also larger amounts of cleaning solutions and water are required for maintenance.

*Sandia Laboratories Report SAND78-8265, October 1978, "Prototype/Second Generation Heliostat Evaluation and Recommendations"

2.3.1.2 External Concentrator. The standard external concentrator is existing technology and requires no heavy development. This concept will exhibit high operational reliability based on proven equipment, offers no risk of schedule failure as all concepts and components are fully developed, and will achieve lower life cycle cost for commercial success.

2.3.2 PEDESTAL/OPTICAL SYSTEMS

2.3.2.1 Elevation Over Azimuth Configurations. Advantages of the Az-El types are easy alignment, minimum gravity moments, the least swept volume, the lowest primary axis torques, the use of a single primary axis bearing, and the simplest (and least costly) structural load path from the primary bearing to the ground. The only general disadvantage is the azimuth velocity keyhole problem at sites near or below the tropics (Paragraph 2.2.2.2).

2.3.2.2 Hour Angle/Declination Axis Configuration (Polar Mount). The advantages are the elimination of the velocity keyhole problem, and the least amount of secondary axis travel. HA/DEC disadvantages are that they require site-peculiar structural designs between the ground and the primary axis, require more complicated gimbal structures, have more swept volume, and are subjected to higher axis torques and bending moments.

2.3.2.3 XY Configurations. The only advantage of the XY concept in solar tracking is the elimination of the velocity keyhole problem. (This virtue is also shared by the HA/DEC types except the declination travel required is much less than that of the Y travel of an XY mount.) The big disadvantage in XY is the ungainly structure required to provide approximately $180^{\circ}$ of X travel and $90^{\circ}$ of Y travel. For these reasons the XY concept (and all concepts having primary axis tilts, other than vertical or polar) were dropped from further consideration.

2.3.2.4 Receiver Axis Orientation. In most of the concepts the receiver aperture axis of symmetry is colinear with the theoretical paraboloid axis and orthogonal to the secondary axis, which is "normal". Deviations from that symmetrical configuration were considered as they show the potential for minimizing or eliminating the rotation of the gravity vector with respect to the receiver and/or improving accessibility to the power module.

2.3.2.5 Number of Reflections. The single bounce is obviously superior in performance than any of the multiple bounce configurations. However, the two-bounce concept was briefly considered in an attempt to determine if there were any significant advantages.

2.3.2.6 Reflector Aperture Symmetry. Nonsymmetrical reflectors generally require the reflector panel area to exceed the solar aperture area by 30 to 50 percent, thus greatly increasing panel and structure costs.

2.3.2.7 Pedestal/Optical Concept Screening. The 12 concepts summarized in Figures 9 through 20 were selected as candidate pedestal/optical configurations for the program. The evaluation rationale is shown on each figure, and a summary tabulated in Table 6. Four concepts were retained for an in-depth investigation summarized in Paragraph 2.4:

Concept 2 - Inverted Track Az/El

Concept 3 - Yoke Az/El

Concept 4 - Turret Az/El

Concept 11 - Conventional Ha/Dec

It was further concluded that conventional single surface paraboloid optics is the most cost effective for the present requirements.

2.3.3 TRACKING CONTROL SYSTEMS

Preliminary comparisons of the various conceptual solar tracking and servo drive systems were made to determine which should be retained for further analysis. The critical components and driving cost factors of each concept have been identified. Technology development and risk are also considered.

2.3.3.1 Program Tracking. The critical elements of a program tracking system are:

- Ephemeris Data Generation: Can be done with disc storage or computed in real time. Only one computation is needed for the entire field.

- Data Transmission to Concentrators: Because of very low rates, data can be serially transmitted on a single line, multiplexed with other collector control functions.

- Axis Angle Encoding System: A number of well developed systems are available. Selection requires a trade of cost versus accuracy.

- Data Processing and Control Logic Electronics: Inexpensive implementation with standard IC's and/or microprocessors.

- Concentrator Structure: Contributes to tracking error because of deflections between encoding transducers and concentrator optical axis.

Program tracking implementation is straightforward with standard components and technology. The advantage of this technique is that it does not require any optical sensors. The potential disadvantages are that attaining desired accuracies may require expensive angle encoding and/or structural stiffening, and the calibration of systematic errors requires time-consuming field measurements on each concentrator.

## CONCEPT EVALUATION

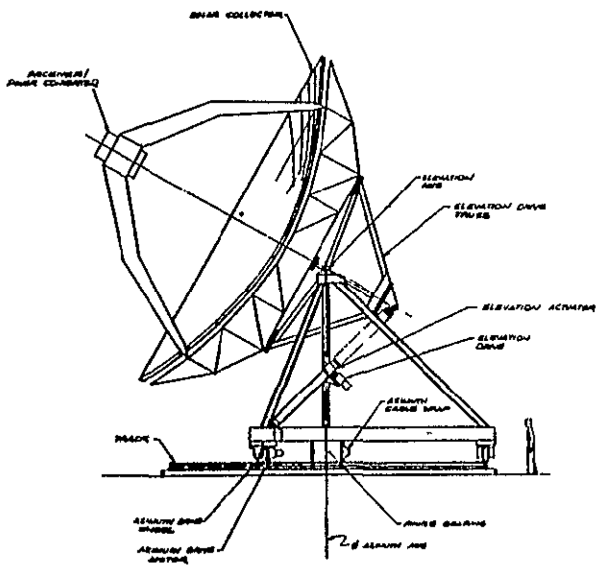

This concentrator configuration was suggested during the SPSE proposal stage. It is basically a "lightweight" version of the conventional microwave wheel and track antennas. This concept has exhibited proven performance during the past few decades and is extremely reliable. However, the large reduction in weight allowed in the transformation from microwave to solar technology (due mainly to relaxed pointing error requirements and lower survival wind conditions) created an overturning problem with the solar concentrator during operational wind conditions (~ 30 mph). Several potential remedies were investigated, i.e. adding back more structural weight, adding counterweight, adding wheel/rail holddown mechanisms and/or adding thrust capability with a pintle bearing. All of these fixes were found to be costly, and if implemented, would drive the overall concept cost above other comparable configurations under consideration. Even though the open, widespread space frame configuration provides advantages in terms of azimuth gear ratio efficiencies, it also requires a large, and consequently, costly, foundation. Therefore, the major virtues that made this configuration attractive for microwave use do not necessarily appear to be directly applicable to solar.

94-2-32

FIGURE 9. CONCEPT 1 - CONVENTIONAL WHEEL AND TRACK, AZ-EL, ONE BOUNCE

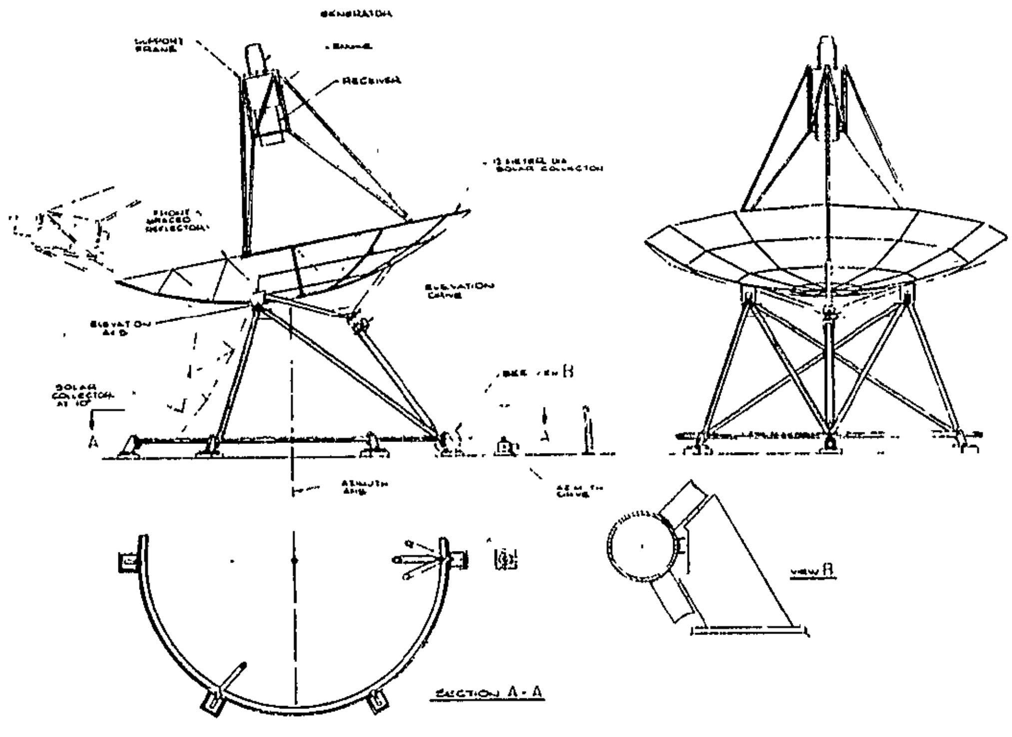


## CONCEPT EVALUATION

This concept represents a solution to the overturning problem cited with Concept #1. The rotating tubular track is captured between six pairs of wheels mounted on piers anchored to the ground. This design must consider the bending and torsional stresses and deflections developed in this track. Loads from the reflector are transmitted down the alidade structure to three "hard points" on the track which do not always fall directly over three of the six wheel pairs. Another problem is that the radial compliance of the track would allow it to go out-of-round, approaching a six-lobed cam, and thus destroying the necessary good contact between the track and the canted wheels. Nevertheless it was judged that a tubular track with adequate cross sectional area could be economically provided. This configuration has the advantages of allowing for the elimination of the central pintle bearing along with a much simpler (are consequently lower cost) track foundation. In addition, it still maintains the gear ratio advantage and lightweight structure identified in Concept #1.

94-2-33

FIGURE 10. CONCEPT 2 - INVERTED WHEEL AND TRACK, AZ-EL, ONE BOUNCE

## CONCEPT EVALUATION

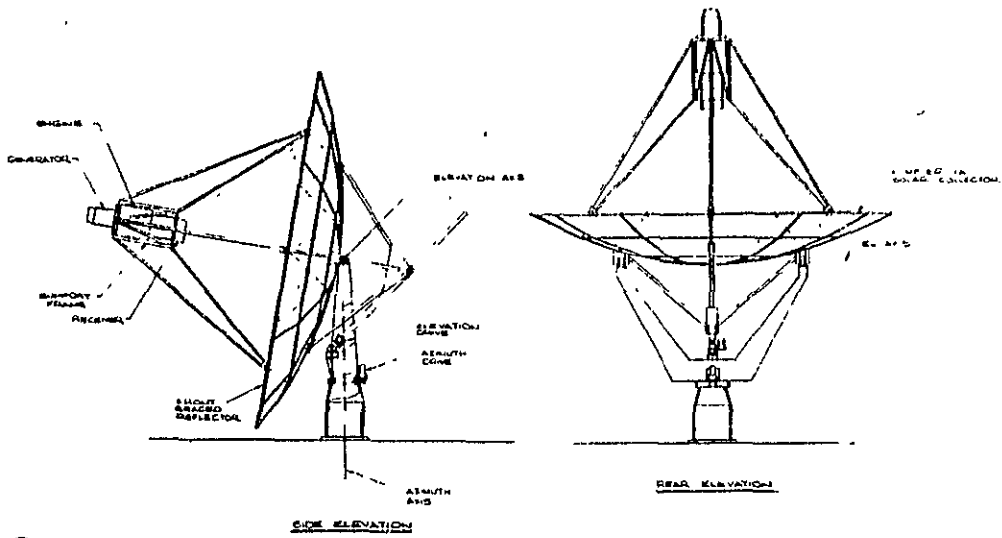


This configuration is another converted cousin of a microwave antenna, having an azimuth turntable bearing supporting a box beam yoke, and being driven in elevation by a center-mounted machine screw actuator. The main disadvantage with this concept is that the elevation bearing loads are carried down the yoke arms a relatively long distance to the small turntable bearing. As a result of the low mounting location of the azimuth bearing, high moment loads have to be reacted through the bearing, thus requiring high bearing performance and consequential high cost. Fabrication of the large yoke weldment may also prove costly. The azimuth gear ratio advantage identified in Concept #1 and #2 cannot be provided by this configuration. It does, however, have the advantages of proven performance and known reliability based on past microwave experience. The basic design is quite compact and consists of very few member components when compared to the open, space frame type configurations. This allows for simplicity and ease of shop assembly and field installation (resulting in lower costs). The foundation offers no real advantage or disadvantage when compared with the other concepts.

94-2-34

FIGURE 11. CONCEPT 3 - YOKE, TURNTABLE BEARING, AZ-EL, ONE BOUNCE

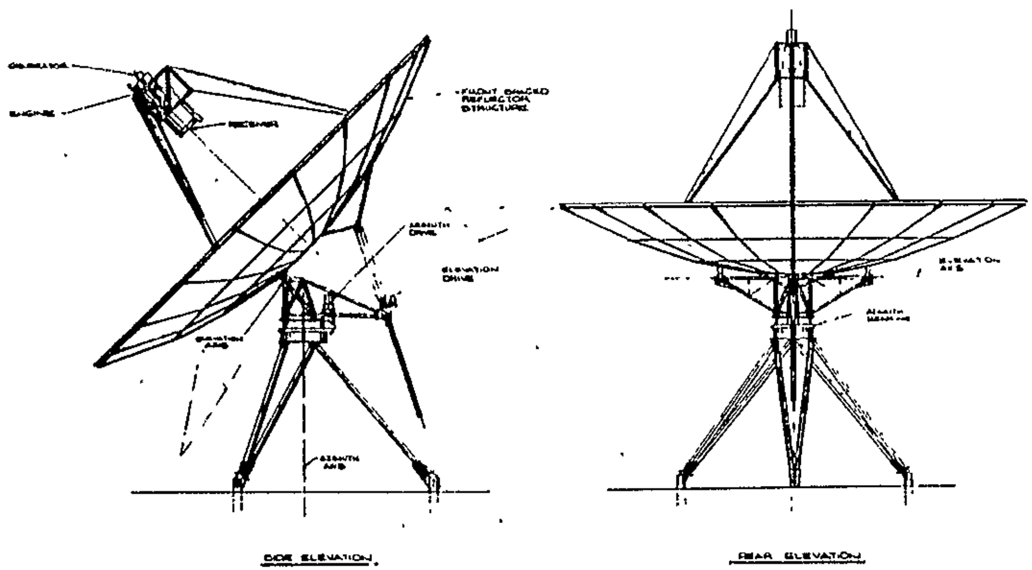

## CONCEPT EVALUATION

This concept is another Az-El turntable concept which has improved stiffness over the yoke configuration shown in Concept #3. The azimuth bearing is higher and closer to the wind and gravity centers. The elevation actuator has been shifted to a more effective position. The structure between the azimuth bearing, the elevation bearings, and the actuator drive support point is a rigid trussed structure which efficiently transmits loads axially without imposing major flexural loads, a necessary feature in transferring loads with the least structural steel weight. The foundation is spread out and can be constructed relatively inexpensively. The azimuth drive system is compact and allows for convenient shop assembly and alignment. The only disadvantage of this configuration is the low azimuth gear ratio created by the relatively small azimuth bearing. This overall concept appears to be quite efficient in load transfer, relatively stiff and potentially low in cost.

94-2-35

FIGURE 12. CONCEPT 4 - TURRET, TURNTABLE BEARING, AZ-EL, ONE BOUNCE

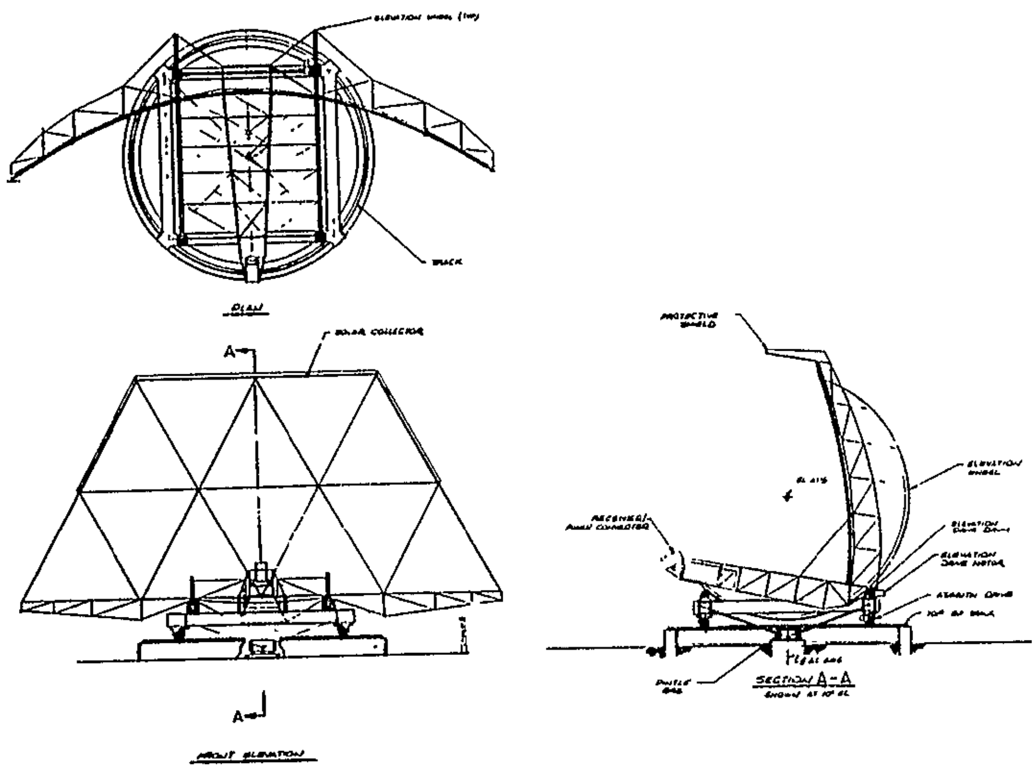


## CONCEPT EVALUATION

This concept was developed to provide a low profile, low torque concentrator having the azimuth and elevation axes intersecting at or near the wind and gravity centers. The receiver is offset from the reflector aperture which eliminates blockage loss and allows orienting the power conversion equipment without regard to minimum package envelope/blockage. It has the additional virtue that the receiver/power package can be positioned close to the ground for maintenance. There are major disadvantages, however. The solar energy is approaching the receiver from a semi-circle and thus the receiver acceptance angle is twice as wide as it is tall, creating receiver solar flux design problems. While the structure may be aesthetically pleasing, it is, in fact, structurally complicated and high in cost when compared with some of the other concepts. Again, the wheel and track foundation and pintle bearing requirement introduce additional cost into this concept. The advantages appear to be more than overshadowed by the design and cost problems associated with this configuration.

94-2-36

FIGURE 13. CONCEPT 5 - WHEEL AND TRACK, OFFSET, LOW PROFILE, AZ-EL, ONE BOUNCE

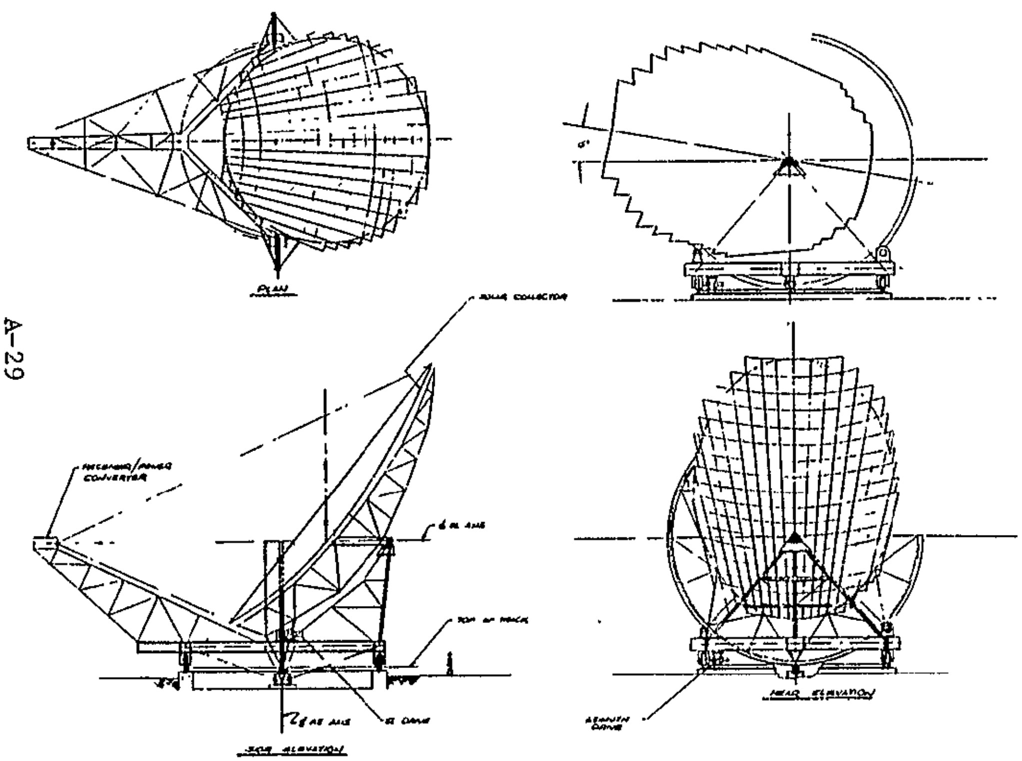

## CONCEPT EVALUATION

This concept is a prime focused offset paraboloid with the receiver axis, the elevation axis, and the paraboloid axis sharing the same line. The arrangement provides a free (invisible) solar rotary joint, allowing the receiver to be mounted external of the secondary axis so that it sees no change in gravity vector, simplifying the receiver design, making the power conversion package more accessible and allowing for a thermal storage system to be included.

This was an attempt to combine the features of an Az-El type mount with single axis receiver rotation while maintaining the one bounce optical advantage. However, its offset reflector increases the focal length and requires approximately 50% more panel and panel support structure area than the usable solar aperture area, and thus is very expensive. It is also quite apparent that the receiver support structure is more extensive than conventional tripod or quadripod supports. The elevation bearing and drive system is complicated and complex, requiring many structural members. The foundation and pintle post design add even greater cost to this already expensive concept. The cost penalty incurred for not having to tilt the receiver far outweigh any advantages associated with this concept. It could only be justified if a stationary power conversion package or massive thermal storage was required.

94-2-37

FIGURE 14. CONCEPT 6 - HOGG HORN, WHEEL AND TRACK, OFFSET, AZ-EL, ONE BOUNCE

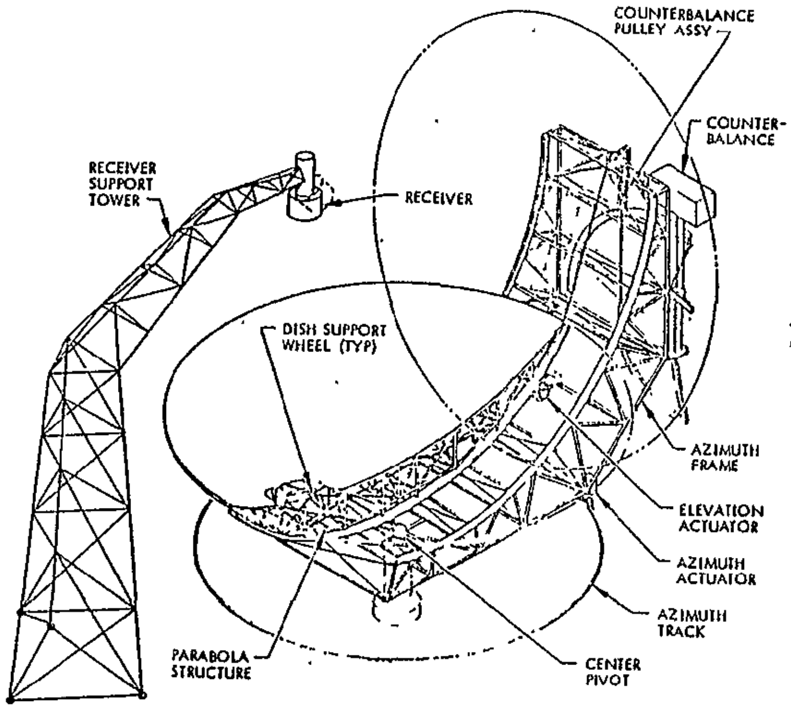


## CONCEPT EVALUATION

This concept, proposed by G.S. Perkins of JPL, has azimuth, elevation and paraboloid axes which intersect at a point contained by the receiver aperture. With the receiver on a ground mounted tower, the attachment must provide an Az/El gimbal which moves in correspondence with Az/El reflector motions. This gimbal action could be driven either by structure and cables extending from the reflector or by separately slaved small gimbal mounted motors and gear trains. For the FACC SPSC concept, however, the receiver cannot be separately rotated from the engine/generator assembly due to the rigid heat transport lines. Also the non-rigid connection between the receiver and primary reflector would introduce alignment errors between the two. A unique advantage of this scheme is that the stow position is at the lowest possible profile. This concept, however, suffers from many of the same problems that were identified with some of the earlier discussed concepts, i.e. large receiver support structure, high foundation costs of azimuth track, pintle and tower, complex elevation drive mechanism and multi-membered structural framework support. Many desirable features proposed by G.S. Perkins for the sun tracking collector will be incorporated into the selected FACC concept, notably the tracker control concept of position control trimmed by sun sensor, tracking error of 0.1° countering construction costs, optimal restraint points for paraboloid radial trusses, and conventional materials.

94-2-38

FIGURE 15. CONCEPT 7 - PERKINS, UNCOUPLED RECEIVER, WHEEL AND TRACK, AZ-EL, ONE BOUNCE

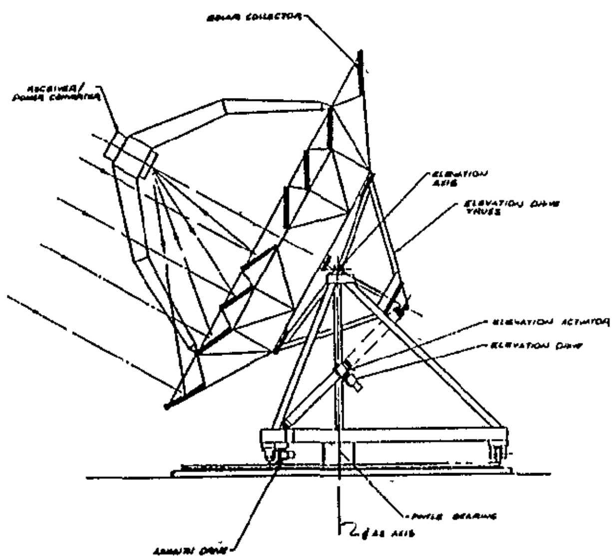


## CONCEPT EVALUATION

Since this reflector can be put on virtually any of the mounts under consideration, only the pros and cons of the Fresnel reflector itself were investigated. The symmetrical Fresnel reflector was considered because it has potential advantages in that the reflector support could approach a flat circular structure as opposed to the conventional deep paraboloid. However, since each panel must have a clear path to the receiver, edges of adjacent panels must be separated in the radial direction, causing the reflector structure area to increase by about 20% for a $60^{\circ}$ rim angle. As stated in JPL Advanced Technology Development Progress Report, June '78, #5102-67; "In order for the Fresnel reflector to be viable, the benefits from the structures and materials must outweight the loss in performance for the selected F/D" The FACC study determined no structural or material benefits. A reported advantage of the Fresnel concept is that the reflector structure is shallow compared to a single surface paraboloid resulting in potentially reduced unbalance moments and wind drag in the zenith stow position. On the other hand, the major operating wind loads, primarily drag and axis torques, can be expected to be no less than for an equivalent single surface paraboloid, based on wind tunnel test data by JPL and others. Namely, peak drag and moments on analogous porous reflectors are generally proportional to the total useful reflector area. Distributing equal loads over a broader span requires more structural material, for equivalent structural strength and stiffness. Finally, the inherent shallowness of the optical system is not really a structural advantage, since depth near the structural center is always required to efficently support wind and gravity loads. On the above grounds and structural complexity considerations, this concept is clearly more expensive than a conventional single surface paraboloid.

94-2-39

FIGURE 16. CONCEPT 8 - REFLECTING FRESNEL, WHEEL AND TRACK, AZ-EL, ONE BOUNCE

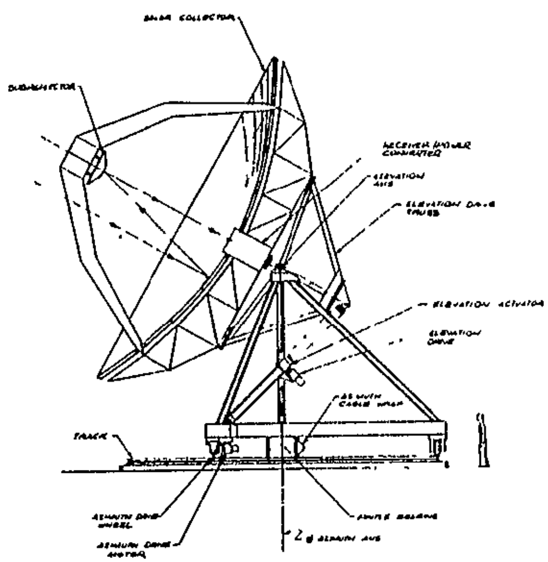

## CONCEPT EVALUATION

This is a Cassegrainian reflector system which could be mounted on any pedestal axis arrangement. It comprises a two-mirror system with the paraboloidal mirror for a primary reflector and a confocal hyperboloidal mirror as a secondary reflector to converge solar rays back to the vertex of the paraboloid. Its major advantage is that the power conversion package, including the receiver, can be mounted near the reflector vertex and thus remove heavy components from the relatively thin, minimum shadow, tripod structure. However, the cost of providing a stronger tripod structure is much lower than the cost of increasing the reflector size to compensate for secondary reflector losses (~ 10%) due to the additional surface absorption of energy and specular reflectance. This configuration would only become attractive over the conventional one-bounce systems if the receiver/engine/generator assembly weight or size was unusually high, or that thermal storage became a requirement.

94-2-40

FIGURE 17. CONCEPT 9 - CONVENTIONAL CASSEGRAIN, WHEEL AND TRACK, AZ-EL, TWO BOUNCE

## CONCEPT EVALUATION

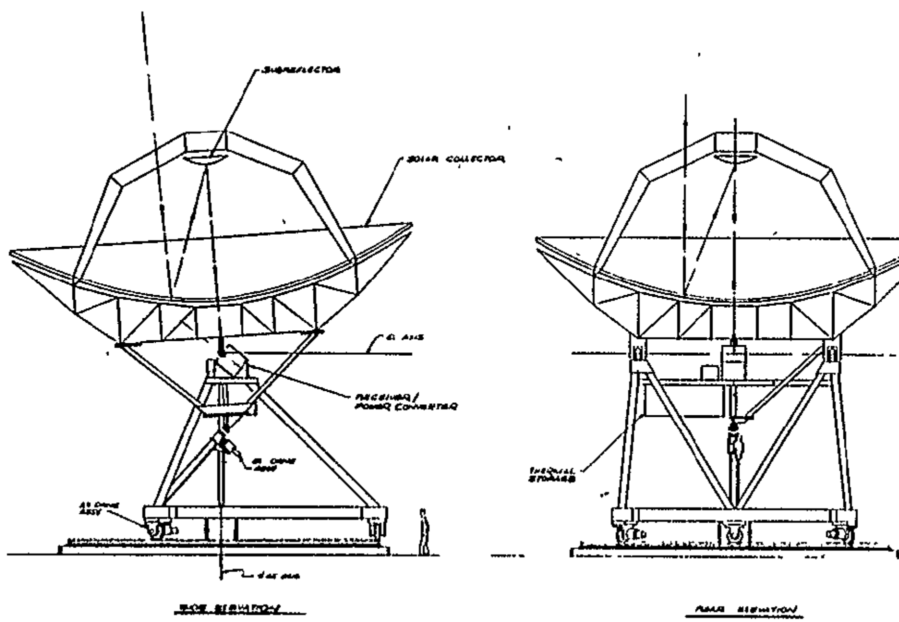

This scheme was to study the situation wherein the receiver would not be required to tilt in elevation. It is a Cassegrainian, two bounce system, suffering the additional secondary reflector losses. The larger problem, however, is that the receiver must accept energy from the sub-reflector which is moving $\pm$ 40$^{o}$ about the receiver axis, the result being that the flux distribution is varying throughout the day within the receiver. This was considered to be a more severe condition than changing the gravity vector on the prime focus receiver. This concept would be further considered only if receiver/engine/generator assembly weight or size became unmanagable, if the requirement for a non-tilt receiver was mandated or if thermal storage was desired.

94-2-41

FIGURE 18. CONCEPT 10 - CASSEGRAIN, NONTILT RECEIVER, WHEEL AND TRACK, AZ-EL, TWO BOUNCE

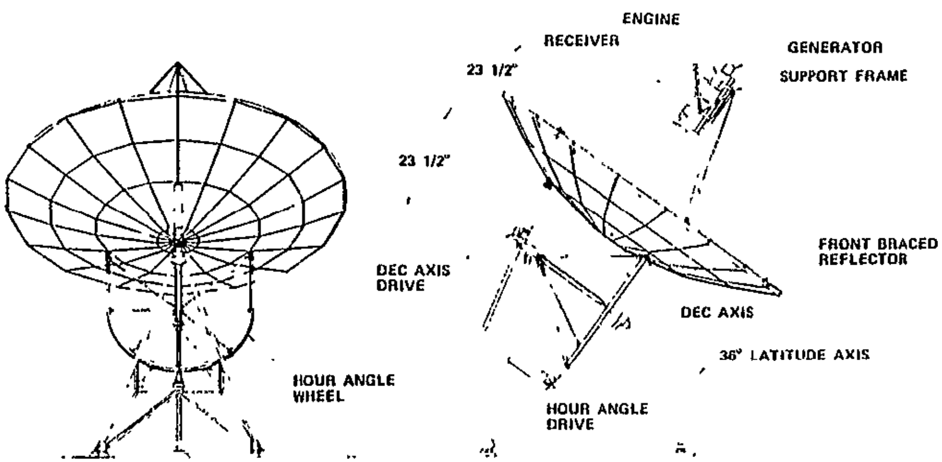


## CONCEPT EVALUATION

This concept is a conventional prime focus hour-angle/declination (Ha/Dec) concentrator assembly, and is being used extensively in microwave communication and radio telescope activities. It is one of the lightest weight structures considered on the SPSL program. Some of the other major advantages of this concept is that it has no azimuth "keyhole" problems as do the Az-El mounts; it has limited daily and annual secondary axis travel (max. ± 23½°/year) which lends itself to an inexpensive actuator drive mechanism; the tracking system can be simple due to the coincidence of the hour angle axis with the earth's polar axis; and the open space frame structure allows for low cost foundation footings. Reflector slope errors due to gravity and wind are much more severe for a Ha/Dec configuration than an Az/El, however the FACC front-braced reflector concept minimizes this effect. Similiarly the front bracing reduces the large moment about the hour-angle axis which is normally a Ha/Dec disadvantage. One disadvantage is that the tilt of the primary axis depends upon the site latitude which varies the pedestal configuration. Another potential problem is that the receiver/engine/generator package must be capable of rolling side to side as well as tilting in elevation. The site-peculiar design problem can be economically solved, and if the power conversion package roll can be accounted for economically in the receiver design, this concept represents a very lightweight, stiff, cost-effective design.

94-2-42

FIGURE 19. CONCEPT 11 - NEWTONIAN PRIME FOCUS, CONVENTIONAL HA/DEC, ONE BOUNCE

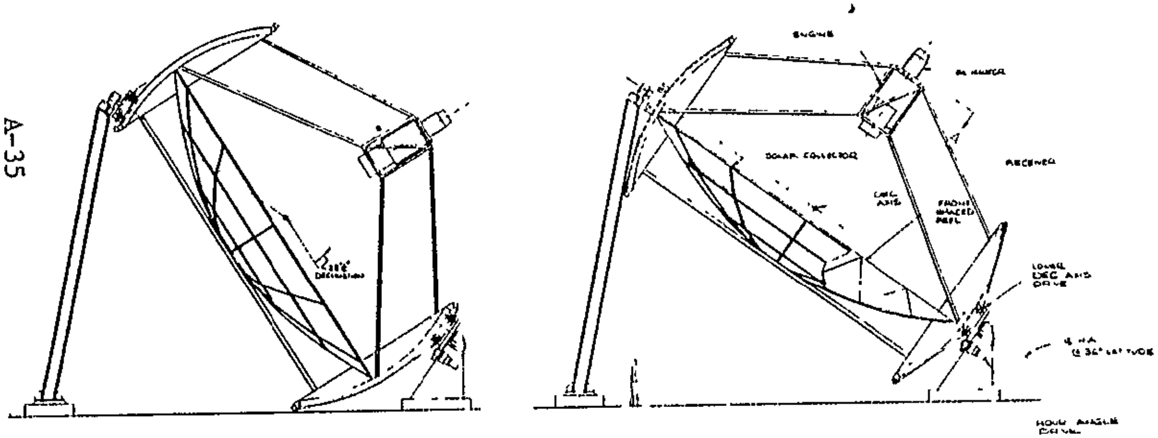

## CONCEPT EVALUATION

This is a Ha/Dec design invented and constructed in 1901 by Mr. Eneas. It has been designed such that the structure center of gravity lies on the primary axis and therefore has minimum hour-angle drive torque requirements. Another unique feature is that since it can rotate 360 degrees about the hour angle, the receiver/engine/generator package can be positioned such that it is within a few feet of the ground for accessibility and/or maintenance. The stow wind position can be at a reduced height. It also displays a novel declination rocker bearing. The declination axis drive mechanism is complex, however the travel of $\pm 23\frac{1}{2}^{\circ}$ is required only once per year. The two disadvantages of the Ha/Dec mount identified in Concept #13 are still inherent in this design. Due to development of the declination axis drive mechanism, this concept does not warrant further investigation unless the 6½ year time period was selected.

94-2-43

FIGURE 20. CONCEPT 12 - ENEAS, ROCKER BEARING, HA/DEC, ONE BOUNCE

TABLE 6. PEDESTAL/OPTICAL CONCEPT EVALUATION SUMMARY

| CONCEPT NO. | CONFIGURATION | STEERABLE AXIS ARRANGEMENT | RECEIVER AXIS ORIENTATION | REFLECTOR APERTURE TYPE | NO. OF REFL. | DISTINGUISHING FEATURES | RETAIN OR REJECT DECISION |
|---|---|---|---|---|---|---|---|
| [illegible] | Conventional Wheel & Track | Az-El | Orthogonal to Secondary | On-Axis Symmetrical | One | • Utilizes Proven Microwave Antenna Technology<br>• Lightweight Open Space Frame Structure<br>• Overturning Problem and High Cost Foundation | Reject |
| [illegible] | Inverted Wheel & Track | Az-El | Orthogonal to Secondary | On-Axis Symmetrical | One | • Eliminates Pintle Bearing and Has Low Cost Foundation<br>• Lightweight, Non-Overturning Open Structure<br>• Cost and Stress Problem with Azimuth Track | Retain |
| [illegible] | Yoke & Turntable Bearing | Az-El | Orthogonal to Secondary | On-Axis Symmetrical | One | • Uses Conventional Microwave Technology<br>• Compact Design, Easily Assembled and Installed<br>• High Bearing Loads, Expensive & Compliant Yoke | Retain |
| [illegible] | Turret & Turntable Bearing | Az-El | Orthogonal to Secondary | On-Axis Symmetrical | One | • High Azimuth Bearing & Efficient Load Transfer<br>• Low Cost Structure & Foundation, Easy Assembly<br>• Complicated Azimuth Gear Reduction Due to Small Bearing | Retain |
| 5 | Low Profile Wheel & Track | Az-El | Canted 30° to Paraboloid Axis | Offset Half Reflector | One | • Low Profile, Low Torque Concentrator<br>• Low Blockage and Convenient Power Conversion Package<br>• Receiver Flux Problem and Complex Structure | Reject |
| 6 | Hogg Horn Wheel & Track | Az-El | Co-Linear with Secondary Axis | Offset Circular | One | • Non-Tilt and Convenient Power Conversion Package<br>• Larger Amount of Collector Area Required<br>• Complicated and Complex Elevation Bearing & Drive System | Reject |
| 7 | Perkins Wheel & Track | Az-El | Gimballed and Uncoupled | On-Axis or Off-Axis | One | • Low Stow Profile & Separate Power Conversion Package<br>• High Foundation Costs of Track, Pintle and Tower<br>• Complex Elevation Drive Mechanism & High Cost Structure | Reject |
| 8 | Fresnel Reflector | Az-El | Orthogonal to Secondary | Symmetrical Fresnel | One | • Requires Larger Reflector Panel Support Structure<br>• Provides No Inherent Advantages Over Parabolic Structures<br>• Complex Panel Support Structure Required | Reject |
| [illegible] | Conventional Cassegrain | Az-El | Orthogonal to Secondary | On-Axis Symmetrical | Two | • Rigid and Convenient Mounting for Power Conversion Pack<br>• Suffers from Energy Losses due to Double Bounce Required<br>• Utilizes Proven Microwave Technology | Reject |
| 10 | Cassegrain Non-Tilt Receiver | Az-El | Canted ±40° to Paraboloid Axis | On-Axis Symmetrical | Two | • Non-Tilt, Convenient Power Conversion Package<br>• Suffers from Excessive Energy Losses Due to Double Bounce<br>• Flux Distribution Problem on Receiver a Problem | Reject |
| 11 | Conventional Ha/Dec | Ha/Dec | Orthogonal to Secondary | On-Axis Symmetrical | One | • Utilizes Proven Microwave Technology<br>• Eliminates "Keyhole", Lightweight and Stiff<br>• Requires Two Axis Receiver Roll & Primary Axis Variation | Retain |
| 12 | Enaa Ha/Dec | Ha/Dec | Orthogonal to Secondary | On-Axis Symmetrical | One | • Low Stow Profile & Convenient Access to Power Package<br>• Complicated Elevation Drive Mechanism<br>• Requires Two Axis Receiver Roll & Primary Axis Variation | Reject |

2.3.3.2 Optical Autotracking. The critical elements of the optical autotracking system are:

- Optical Error Sensor: Hardware developed and used by FACC and others using differentially shadowed photocells; only requires detailed design for low production cost and high reliability.

- Data Transmission: No angle data is required for pure autotracking.

- Angle Encoding: Not required except for several coarse accuracy limit switches and positioning logic.

- Control Logic Electronics: Requires more analog and less digital than program track; straightforward and inexpensive.

- Concentrator Structure: The deflection between the sensor and optical axes can be significantly reduced by selecting a sensor whose mounting point deflections accurately track the optical deflections.

The advantage of this system is that ephemeris generation and angle encoding are not required. The potential disadvantages are that more frequent cleaning, inspection, and alignment may be required due to physical degradation of the tracking sensor response caused by aging, dust, etc. In addition, there may be some long-term differential degradation of the individual photosensitive elements of the tracking sensor. Optical tracking sensors have also had a history of erratic behavior during periods of partial cloud coverage.

2.3.3.3 Hybrid-Program/Optical Autotrack. The critical elements of a hybrid tracking system basically include all elements required for both pure program or pure autotrack. The potential advantages of a hybrid system are:

- The required program track accuracy is relatively coarse; i.e., only good enough to get into the field of view of the fine optical sensor (about 1 to 2 mrad). This reduces costs of angle encoding and structural stiffness.

- Because of self-calibration capability, field alignment requirements are minimal.

- Because a single element tracking sensor can be used in conjunction with a single peaking algorithm, sensor degradation and electronics drift have no effect on tracking accuracy.

2.3.3.4 Thermal Autotracking. The critical elements of a thermal autotracking system are the same as for optical autotracking, with the exception of the error sensing elements. These are optical flux sensors which are arranged around the periphery of the receiver to sense image offsets by comparison of the "halo" fluxes on two opposite sides of the aperture. The major problem is to find a sensor which can withstand the peak flux of approximately

10,000 suns during emergency defocus conditions. A survey of available components indicate that no such devices are currently available. For this reason thermal autotracking was not considered further.

2.3.3.5 Axis Drive and Servo Configuration. All tracking systems generate axis position error signals, which must be used to control the axis drives. The two basic methods of closing the loop around these error signals are:

(1) Continuous control where the drive rates are modulated as some function of the error signals, e.g., proportional or proportional plus integral control.

(2) Discontinuous (bang-bang) control, where the axis positions are updated in discrete increments at discrete times.

Discontinuous control systems require a maximum tracking error of about $0.1^o$ rms. This permits step increments of up to $0.2^o$, which are executed less than twice a minute. These steps can be performed in a quasi open-loop manner; i.e., turn on a motor until it has traveled to where it should be and then turn it off. This requires only simple switching controls and possibly dynamic braking.

Continuous proportional-type controllers require continuous modulation of some drive parameter (usually motor speed). This, in turn, requires a power amplifier with controllable output which is more expensive than switching controls. Another disadvantage of continuous control is that it is always working, i.e., some torque is always being applied. The long term rms torque level can be expected to be about half the running torque due to friction and/or imbalance. Discontinuous systems will have less than a 5% duty cycle and therefore consume much less daily energy.

2.3.3.6 Summary of Tracking and Drive System Screening. It is concluded that the three conventional tracking control schemes; i.e., program track, optical autotrack, and hybrid all have potential for low cost and minimal risk, but require more detailed analysis to determine the optimum configuration (see Paragraph 2.4.4.2). Discontinuous control is clearly more cost effective and reliable than continuous control. The actual hardware configuration; i.e., type of motors and switching components requires further definition and study (see Paragraph 2.4.4.1).

## 2.4 CONCEPT SUBSYSTEM TRADE STUDIES

The major components of the concentrator are evaluated in detail in the following paragraphs. These elements are:

- Reflector Surface Panels
- Reflector Structure and Receiver Support System
- Pedestal Systems
- Tracking Control Systems
- Foundation Concepts
- Site Implementation.

### 2.4.1 REFLECTOR SURFACE PANELS

The proper design of the reflector surface panels is the key to an effective solar concentrator. Fabrication of acceptable double curvature panels must be achieveable within the time frame of the program; therefore, it was necessary to take a realistic look at present technology. Design concepts were selected based on the progress and test data to date.

2.4.1.1 Criteria for Design of Reflector Panels. The reflector panels must be accurate, have the capability of being aligned, and have a high specular reflectivity. Reflectivity must be preserved under conditions of adverse environment, such as hail, sand abrasion, thermal cycling, and accumulation of dirt. The accuracy of the reflective surface (slope error) must be maintained under thermal stress or gravity sag. Also the panels should be cost effective in terms of useful life versus acquisition cost and be economical to maintain. Finally, the materials used in the construction of the panels must be compatible with the collector concept, i.e., lend itself to a double curvature panel construction.

Panel selection encompassed four areas: (1) reflective materials and optical surfaces, (2) reflective surface degradation characteristics, (3) glass forming techniques, and (4) reflector panel construction.

2.4.1.2 Reflective Materials and Optical Surfaces. Reflective materials which have been considered fall into one of three categories; (1) metallized glass, (2) metallized plastic film, and (3) polished metal.

a. Metallized Glass. High reflectivity glass surfaces are made by depositing silver or aluminum on either the first (front) or second (back) surfaces. Investigation of existing first surface reflectors has led to the conclusion that none has demonstrated that it can withstand the applicable environmental conditions and retain an acceptable level of reflectivity for a sufficient lifetime to be cost effective. Attempts to protect the exposed reflective surface from oxidation with a transparent material have resulted in diminished specular reflectance when the protective material becomes scratched. The only material found to be partially resistant to abrasion of sand and dirt is glass. The conclusion was that first surface reflectors are not developed sufficiently for use on this program.

Flat glass made by both float and draw fusion processes exhibit excellent optical properties. Silvered flat samples of both products have been tested for specular beam spreading (Reference 1), and the one sigma beam widths were below 0.5 milliradian. This smoothness is the result of the surface being formed without contact with solid surfaces. One surface of float glass is formed on a liquid tin surface, the other in contact with the atmosphere. Draw fusion glass surfaces are both atmospheric formed, i.e., two separately drawn sheets are fused together in the atmosphere.

The reflectivity of glass is primarily determined by its thickness, the iron oxide content, the oxidation state of the iron, the reflective metal and the method of metal deposition. Figure 21 (from Reference 2 and supplemented by FACC), illustrates these variations. Data points for float glass lie on nearly straight lines, one for each iron content, which converge at 94 to 95 percent reflectivity and zero thickness. Good correlation for float glass is obtained between the observed reflectivity and predictions based on Surowiec's work (Figures 22 and 23), but correlation is poor for glass made by other processes, notably ASG Lustra Sheet. The accepted explanation of this anomaly is that the oxidation state distribution of ferrous (FeO) and ferric oxide ($Fe_2O_3$) for float glass is consistent at 25 percent and 75 percent, respectively, due to the nonoxidizing atmosphere required by the molten tin. However, glass formed in an oxidizing atmosphere will have a lower unreduced (ferrous) oxide content. Ferrous oxide (FeO) strongly absorbs light in the 1.0 μm solar region (see Figure 24), but the reduced (ferric) oxide absorbs predominantly in the 0.34 μm region (where much less of the solar spectrum is absorbed). Therefore, substantial improvement in transmittance and reflectance can be achieved by forming glass in an oxidizing atmosphere. The ASG Lustra Sheet and Corning 0317 glasses are examples of this improved reflectance performance and do not follow Surowiec's formulation predictions based on float glass iron oxide distribution. Obviously, it is desirable to make solar mirror glass in an oxidizing atmosphere to achieve the benefits of low ferrous oxide content and therefore maximum specular reflectivity.

Figure 25 illustrates the specular characteristics of the candidate materials. Also shown on this figure is the reflectance in terms of the standard solar profile (Reference 3).

Table 7 compiles the properties of mirrors made of glass, plastic film and polished metal. The reflectance factors identified in the table are those developed by Pettit (Reference 1) to define the reflectance distribution function ρ (Δθ) in the following format:

$$\rho(\Delta\theta) = \frac{\rho_s}{R_1 + R_2}\left(\frac{R_1}{2\pi\sigma_1^2} e^{\frac{-\Delta\theta^2}{2\sigma_1^2}} + \frac{R_2}{2\pi\sigma_2^2} e^{\frac{-\Delta\theta^2}{2\sigma_2^2}}\right)$$

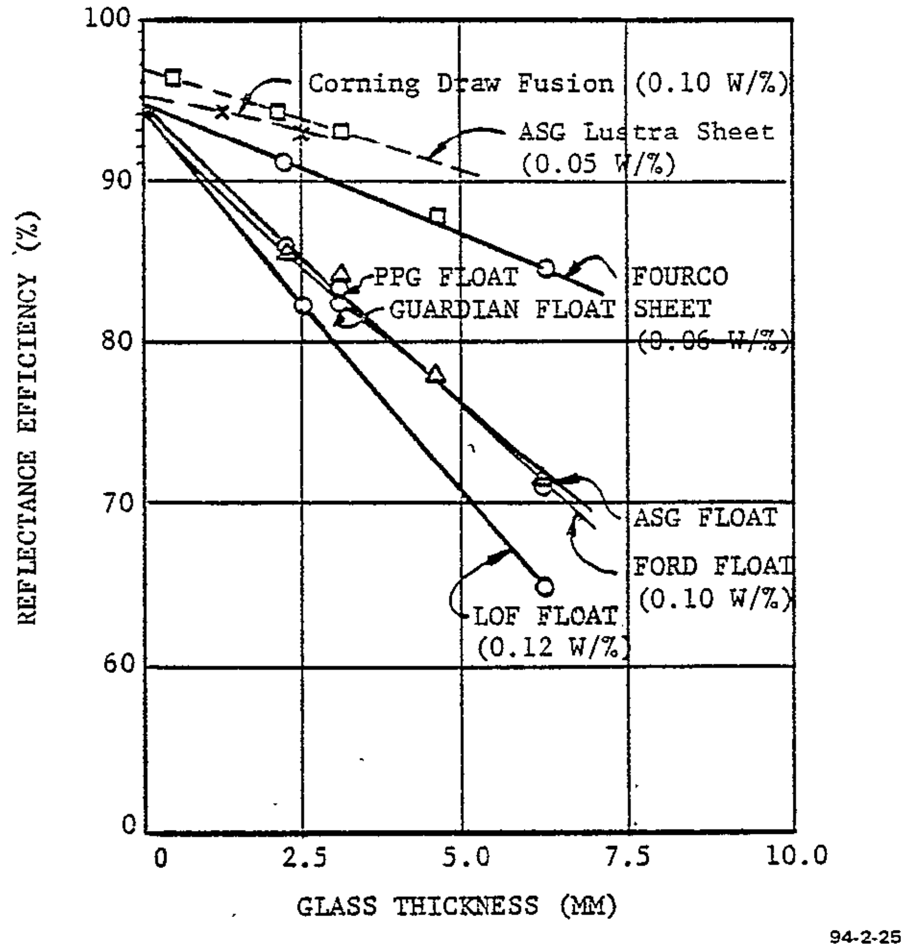


FIGURE 21. TOTAL REFLECTANCE EFFICIENCY (REFLECTIVITY) FOR MIRRORS USING VARIOUS GLASSES

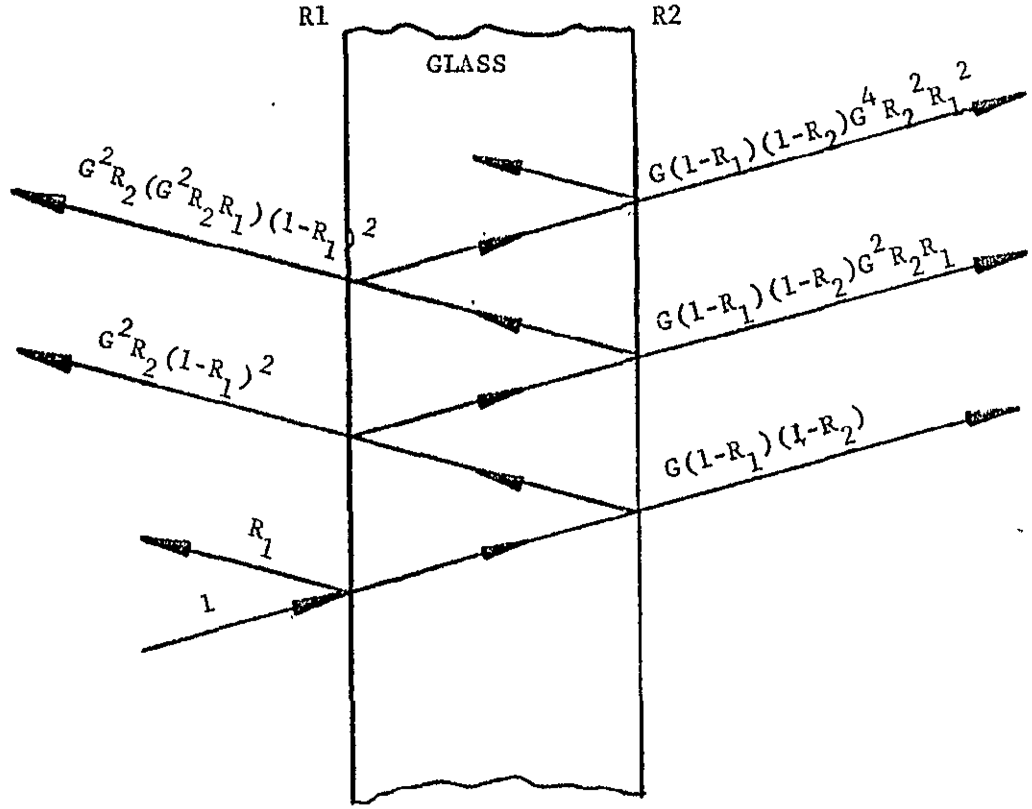


$$\%T = G(1-R_1)(1-R_2)\left[1 + G^2R_2R_1 + G^4R_2^{\,2}R_1^{\,2} + \bullet \bullet \bullet\right]$$

$$= \frac{G(1-R_1)(1-R_2)}{1-G^2R_1R_2}$$

$$\%R = R_1 + GR_2^{\,2}(1-R_1)^2\left[1 + G^2R_2R_1 + G^4R_2^{\,2}R_1^{\,2} + \bullet \bullet \bullet\right]$$

$$= R_1 + \frac{G^2R_2(1-R_1)^2}{1-G^2R_1R_2}$$

WHERE $R_1$ = REFLECTANCE FROM PART SURFACE OR 0.04 FROM $R = \left(\frac{N-1}{N-2}\right)^2$

$R_2$ = REFLECTANCE FROM BACK SURFACE OR 0.04 FOR TRANSMISSION MEASUREMENTS AND 0.95 FOR REFLECTANCE MEASUREMENTS, AND

G = TRANSMISSION EFFICIENCY IN THE GLASS

94-2-26

FIGURE 22. TRANSMISSION AND REFLECTANCE EQUATIONS DEVELOPED BY R. SUROWIEC

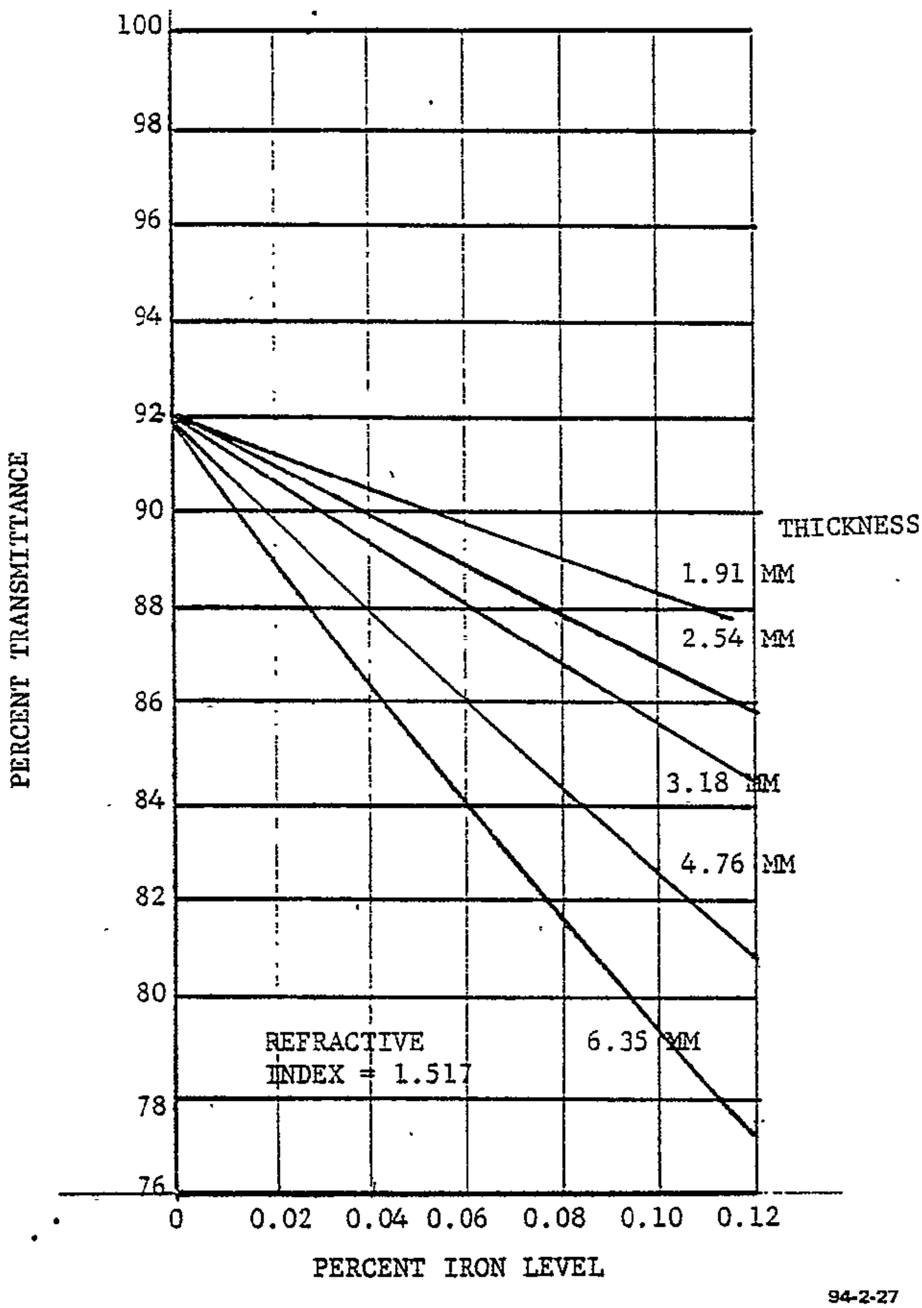


FIGURE 23. SOLAR TRANSMITTANCE AS A FUNCTION OF IRON LEVEL FROM R. SUROWIEC'S DATA

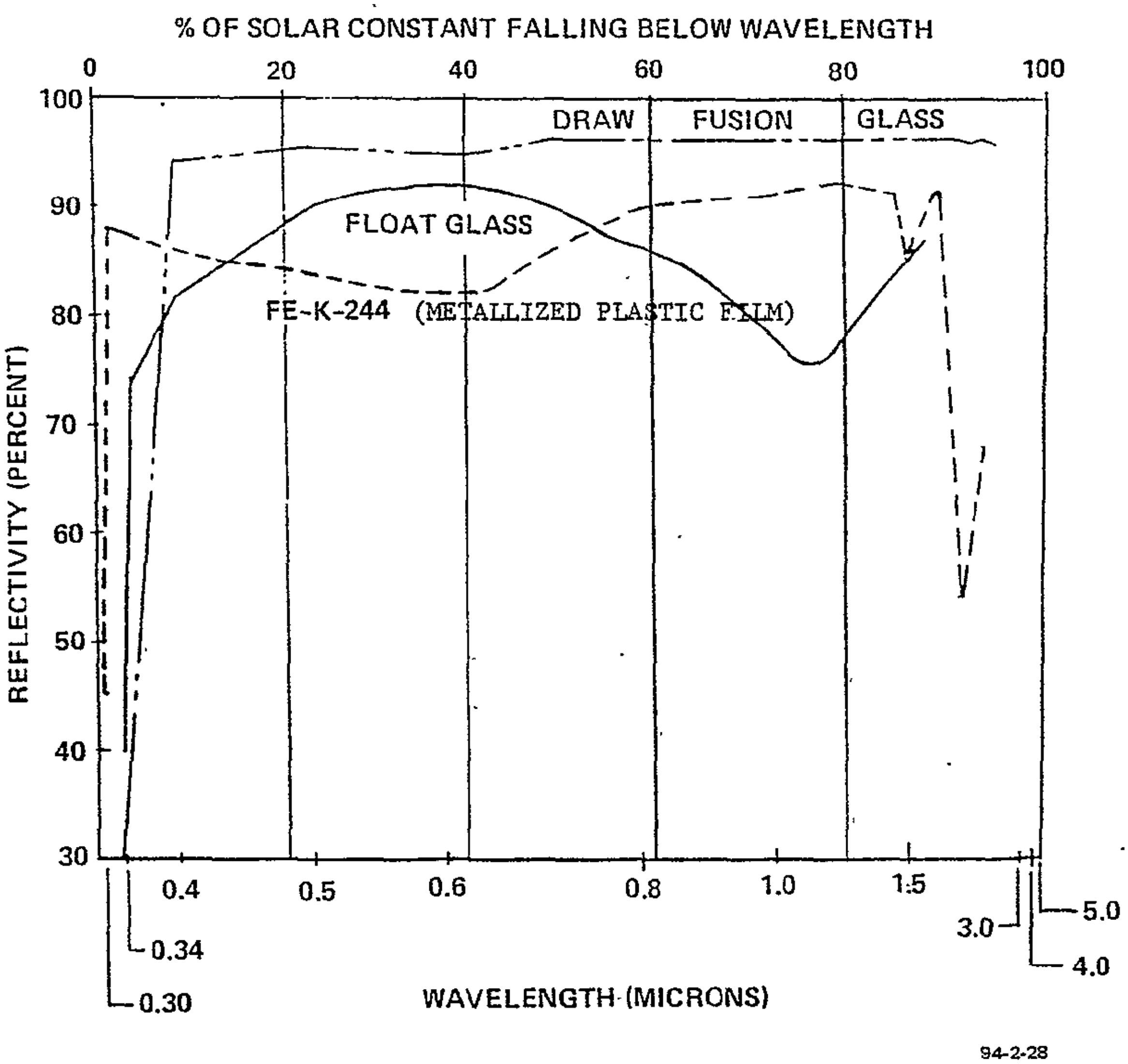


FIGURE 24. REFLECTIVITY OF CANDIDATE MATERIALS VERSUS SOLAR WAVELENGTH

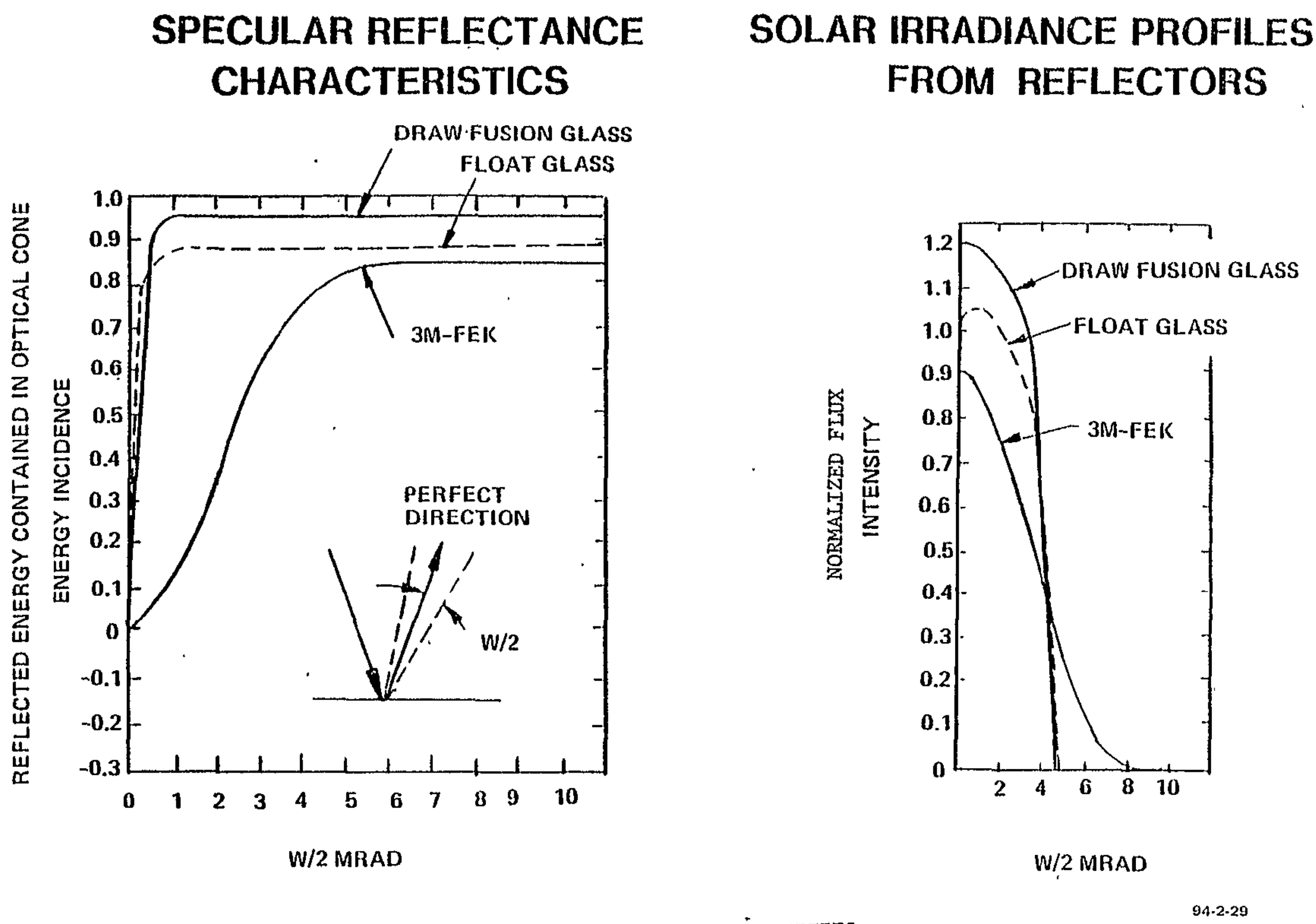


FIGURE 25. SPECULARITY PROPERTIES

TABLE 7. MIRROR MATERIAL PROPERTIES

| REFLECTIVE MATERIALS | PETTIT REFLECTANCE [illegible]ORS (NEW/UNWEATHERED MATERIAL) | | | | HEMISPHERICAL REFLECTIVITY | WEIGHT | THERMA[illegible]PANSION COEFFICIENT |
|---|---|---|---|---|---|---|---|
| | $R_1$ | σ 1 (mrad) | $R_2$ | σ 2 (mrad) | $\rho_s$ | $(kg/m^2)$ | $(IN/IN/^{o}F \times 10^{-6})$ |
| **METALLIZED GLASS** | | | | | | | |
| 0.090" Float/Silver 0.05 % Iron Oxide | .87 | ½ | - | - | .88 $^{+1}_{-5}$ | 6.5 | 4.7 - 5.2 |
| 0.08 Iron Oxide | .86 | ½ | - | - | .86 $^{+1}_{-5}$ | 6.5 | " " |
| Microsheet/0.0045" Silvered | .78 | 1.1 | .18 | 6.2 | .95 $^{+1}_{-5}$ | 0.32 | - |
| Draw Fusion/2nd Surf. Silvered - Corning #0317 0.058" tk | .95 | 0.25 | - | - | .96 | 4.2 | 4.8 |
| Draw Fusion/Silvered Corning #7806/0.050" tk | .95 | 0.25 | - | - | .95 $^{+1}_{-1}$ | - | - |
| Draw Fusion Corning #7806 Mod 0.090" | .94 | 0.25 | - | - | .94 | - | 3.6 |
| 1st Surf. Silver with Silicatious Coating over 0.090 tk Glass | .97 | ½ | - | - | .97 | 6.2 | 4.7 - 5.2 |
| **METALLIZED PLASTIC FILM** | | | | | | | |
| 3M-FEK244 | .85 | .9 | - | - | .85 $^{+1}_{-4}$ | 0.17 | 0.2 |
| 3M Scotchcal 5400 | .85 | 1.9 | - | - | .85 $^{+1}_{-4}$ | 0.17 | 0.2 |
| Sheldahl G405600 | .80 | 1.3 | 0.7 | 30.9 | .87 $^{+1}_{-4}$ | 0.16 | - |
| **POLISHED METAL** | | | | | | | |
| Alzac - ⊥ to Roll Marks | 0.54 | .42 | .31 | 10.1 | .85 $^{+1}_{-3}$ | Variable | 13.3 |
| - ‖ to Roll Marks | 0.60 | .29 | .25 | 7.1 | .85 | - | - |
| Coilzak (0.025) | 0.55 | .3 | .32 | 8.0 | .85 $^{+1}_{-3}$ | 2.0 | 13.3 |

Where $\rho_s$ is the hemispherical solar reflectivity and $\rho$ is the reflectivity within $\Delta\theta$, the angular deviation of the reflected beam.

In summary, the attributes of second-surface metallized glass mirrors are:

- Optical smoothness (high specularity)
- High reflectivity
- Abrasion resistance (long life)
- Low cost raw materials
- Well developed glass technology
  - Uniformity in production quantities
  - Thickness accuracy
- Structural stability
- Low thermal expansion

Its disadvantages are:

- Iron oxide absorption producting a decrease in reflectivity
- Problems with developing a cost-effective double curvature process
- Low tensile strength (brittle material)

b. Metallized Plastic Film. The metallized plastic film reflective materials identified in Table 7 were thoroughly investigated. The attractive aspects of metallized plastic films are its availability, relatively low cost and demonstrated ability to conform to doubly contoured surfaces. The greatest single disadvantage is the uncertain (apparently short) useful life of plastic film subjected to the outdoor environments of sun, sand, dirt abrasion, dirt film, and cleaning processes (Reference 4). Of further concern is the fact that the thermal expansion coefficient of the metallized plastic film is nearly an order of magnitude larger than any candidate substrate material. The resulting differential expansion will place large shear strain on the adhesive bonding. This combined with the diaphragm stress normally present in doubly contoured panels will have the tendency to make the film peel loose from the edges of the panel.

c. Polished Metal. Polished and surface-treated sheetmetal have the basic problem of retaining specularity and reflectivity under the adverse environmental conditions normally experienced by solar concentrators. Evaluation of products such as Alcoa's Coilzac in the EMMA and EMMAQUA desert tests revealed substantial reflective losses (Reference 4).

2.4.1.3 Reflective Surface Degradation. The exposed surface of a glass mirror is much harder and therefore more abrasion resistant than all the other candidate solar reflector materials. The relative abrasion rates of primarily glass and acrylic plastic, were demonstrated by blowing silica flour onto glass and acrylic plastic surfaces (Reference 4). Plain acrylic transmissivity loss was almost an order of magnitude larger than for glass for equal abrasion. Swedlow proprietary coated acrylic had about double the transmittance loss of glass.

Reflectivity measurements conducted after accelerated and real time exposure at the Desert Sunshine Exposure Tests facility further demonstrate the vulnerability of acrylic and Teflon reflector candidates. After 129 weeks of EMMAQUA testing (8 suns intensity and surface cooled with water spray) and cleaning, the least-cost reflector film (Scotchcal) had lost 19 percent total reflectivity, and anodized aluminum had lost 10 percent. The same tests performed on glass samples showed a 3 percent nonrecoverable decrease in reflectivity. A milky appearance of the glass samples was observed following the test which was attributed to alkali leeching taking place with the glass. Glass manufacturers believe this leeching effect can be controlled by proper adjustments of the manufacturing processes and materials.

Dust storms and other weather conditions play the major role in determining properties of a mirror under outdoor exposure (Reference 5). The present system concept minimizes reflectivity and dust losses by a preventive maintenance and cleaning plan. With proper maintenance, the baseline borosilicate glass mirrors should last many years, with minimal loss of optical performance.

2.4.1.4 Glass Forming Techniques. Two basic processes to form glass for solar reflector applications are being developed: (1) the elastic (cold) forming technique, which bonds a deflected flat sheet to a preformed substrate; and (2) the plastic (hot) forming technique which utilizes the plastic and thermal setting characteristics of glass to effect the desired configuration. Each of these processes has been investigated to determine which should yield the best end result when applied to a double curvature glass sheet.

a. Elastic (Cold) Forming. Elastic forming is accomplished by deflecting flat sheet glass onto a contoured male mold or onto a shaped substrate such as machined cellular glass. Deflection with a distributed force (e.g., vacuum bags) is required to prevent glass breakage. When elastically curved glass is bonded to a proper substrate, the combined structure has much greater structural rigidity than the glass alone, and maintains the glass sheet at the proper curvature. The range of stresses calculated for a typical doubly curved glass strip is shown in Figure 26. These results are based on the bending component and diaphragm stresses corresponding to a cylindrical strip (curvature in long direction) being pulled down to a sphere of radius equal to the average curvature of each panel. A key item is to have a bond which will keep the glass "glued" to the substrate for a 30 year life.

Glass is a brittle-fracture material which fails in tension starting from microscopic surface cracks. These cracks are present in all glass surfaces

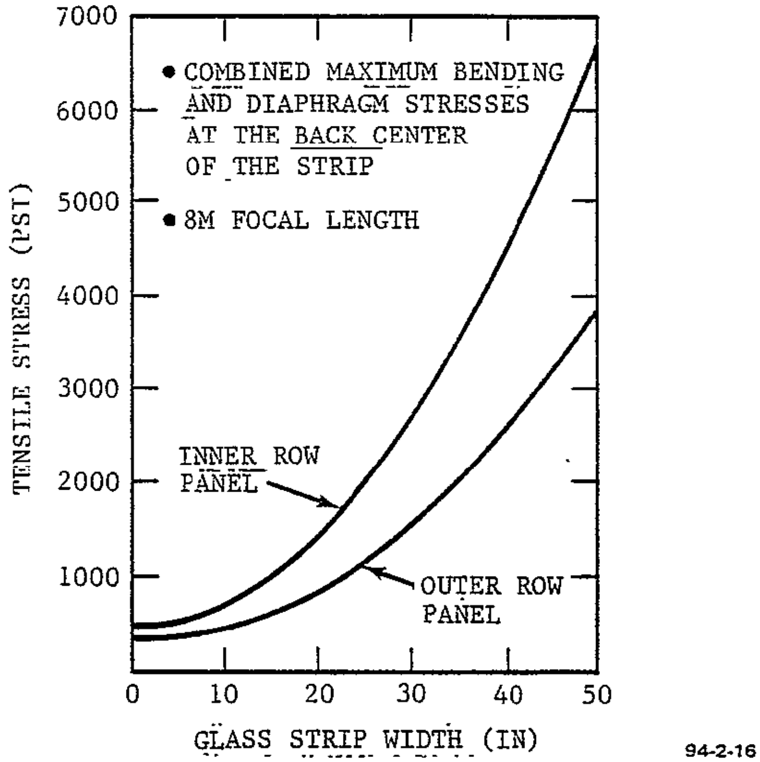


FIGURE 26. MAX TENSILE STRESS DUE TO ELASTIC CURVING

and grow at rates dependent on tensile stress levels and moisture. Glass is also subject to static fatigue, a phenomena that relates breaking stress inversely with the duration of stress (Reference 6). The statistical nature of the observed strength properties of glass is summarized in Reference 7 as, "The standard deviation observed in strength data from replicate samples is between 10 and 25% (or higher) of the mean . . . . This variation in the strength of glass, coupled with static fatigue, leads to long-term practical tensile strengths for glass as low as 2000 psi. Using a safety factor of two, the usual design strength of glass is about 1000 psi. But careful consideration of problems and design can raise this limit to 3000 psi for an annealed product and 20,000 psi for a tempered product". The allowable design stresses for the back surface of a typical panel for this application will be between 1500 and 2500 psi for normal operation and 2500 and 3500 psi for survival in high winds. Two favorable conditions will permit the use of the high end of the stress range recommended in Reference 7. These are:

(1) The peak tensile stress is only at the center of the facet, but the 1000 psi limit was imposed to prevent edge flaws from propagating to total fracture.

(2) The most highly stressed surface is covered with silver and copper or aluminum and paint and thus protected from abrasion and moisture.

Argoud (Reference 8) built nine elastically curved spherical mirrors which were mounted in a test collector. The peak tensile stress at the center on the silver side was 2300 psi indicating an allowable design stress above 2000 psi. However, more testing is required to evaluate the static fatigue of such a configuration using samples constructed of the proposed materials. This testing should consist of loading complete sandwich structures; i.e., glass, core, and backskin of various spherical radii to fast fracture failure in order to determine long term fracture stress levels on a statistical basis. From these data, allowable design stress criteria for a cost-optimized breakage rate could be established and strip widths for reflector panels could be optimized.

b. Plastic (Hot) Curving. Two methods have been developed for hot forming glass to double curvatures: Sagging, where heat softened glass is shaped by gravity onto a mold, and Pressing, where heat-softened glass is formed between two molds.

Much development work has been devoted to the sagging of low cost automotive window glass. Windshield laminates are sagged on special frames which support only the edges of the glass. The smoothness of the glass is preserved since it is contacted only by the atmosphere. Note, however, that automotive glass has almost no curvature in one direction (nearly conical sections) and the shapes have very little diaphragm displacement.

To produce the accurate double curvature required for solar applications, the glass must be sagged into an open or solid mold of the correct contour. It will require experimental work to be able to soften the glass just enough to form the curve without significantly degrading the micro-smoothness (markoff). Glass formed by the hot mold sagging technique at Corning is expected to improve in quality. The Ford Glass Division, under a contract with Sandia, is also evaluating the accuracies that can be economically achieved by hot sagging of single and double sheets (specimen plus forming backup) into both open and solid molds, as well as developing temperature and time controls, radiation baffles, and fixture frames. They will also investigate gas hearth sagging techniques and a combination method of curving without a mold to an approximate shape, and achieving the exact curve by elastic (cold) forming.

The other method of hot glass curving is press forming. Sheets of glass are cut to shape and heated above the softening point in a furnace. The proper shape is obtained by pressing between matched molds whose surfaces are designed to preserve the micro-surface finish of the softened glass. Donnelly Mirrors, Inc. has developed a proprietary method for pressing curved glass. They believe that slope errors can be held within 1 mrad, but the value of the micro-surface finish is unclear since there is no accepted test method for measuring specularity of doubly curved surfaces. The press they are building could make pieces as large as 30" x 30".

In conclusion, hot pressed glass will be available within the required time frame. Gravity sagging development is proceeding and may be available soon.

2.4.1.5 Panel Design. As previously concluded, second-surface silvered, low (unreduced) iron content glass holds the greatest promise for high reflectivity, optically smooth and durable reflector surfaces. The task remains to develop the means of contouring the glass accurately to achieve the double curvature required by the parabolic reflector and to provide adequate support to permit the glass to withstand the rigors of the environment. A tabulation of various means of achieving this objective is contained in Table 8. Each concept has been carried forward to a design configuration and predicted performance. The selection was narrowed to the three concepts described in the following paragraphs, two of which are considered viable and a third which has several advantages but has been discarded for reasons discussed below.

a. Multiple Facet and Frame Concept. This concept has glass sections (facets) bonded to raised pads of a lightweight foam-filled stamped steel structure as shown in Figure 27. The glass facets are pie-shaped pieces of single strength draw fusion glass which have been heat softened and pressed to the desired curvatures. Piece sizes are about 30 x 30 inches. The facets are silvered in the curved condition and copper or aluminum cladding is then layered over the silver followed by conventional mirror back paint to form a stand alone silver protection. These facets are supported by a stamped steel structure which holds the facets in correct optical relationship to each other and which transfers wind and gravity loads of the individual facets to the structural hard points of the reflector truss structure. The panel structure consists of two sheets of 28 Ga. (0.015 inch) steel, stamped to shape, including glass facet mounting pads on the front sheet. The steel sandwich is corrosion protected with zinc plating after fabrication. The two sheets are edge welded together to form a 2 inch deep core cavity which is filled with structural foam, establishing a stable dimensional spacing between the thin sheets of steel such that they form a strong and rigid sandwich structure.

Five to eight glass facets are attached to the raised pads stamped in the sheet metal by a bond of silicone rubber. By proper proportioning of area to thickness, this rubber bond will allow the glass shell to expand almost independently of the steel sandwich, thereby virtually eliminating thermal stress caused by differential expansion of unlike materials. Support pads are on 8 to 10 inch centers such that the heat strengthened, 0.090 inch thick glass can support survival wind loads, and resist hail impact. Since the steel sandwich structure shields the glass facets from wind, only the hail impact is considered the controlling design consideration. Annealed glass, 0.125 inch thick, supported similarly, survived hail impact in tests except at edges and corners (Reference 9). Edge preparation and heat strengthening of pressed glass facets is expected to survive 25mm (1 inch) hail at 23m/sec (75 fps). However, testing will be required to demonstrate this performance.

Steel sandwich bending stresses were calculated utilizing standard equations for a rectangular plate singly supported at 4 corners. The results, contained in Table 9, indicate stress levels that are easily within allowable limits for common carbon steels.

TABLE 8. CONCEPT MATRIX FOR DOUBLE CURVATURE SOLAR CONCENTRATOR PANELS

| OPTICAL SURFACE STRUCTURAL CONCEPT | METALIZED 2ND SURFACE GLASS | METALIZED 1ST SURFACE GLASS | METALIZED PLASTIC THIN SHEET | METALIZED PLASTIC THICK SHEET | ELECTROPLATED SURFACE | POLISHED METAL SURFACE |
|---|---|---|---|---|---|---|
| **SANDWICHES:** | | | | | | |
| 1. Fabricated sandwich | • Thick curved 2nd surf. glass, back skin and core, adhesive ass'y. on fixture. | • Thick curved 1st surf. glass, back skin and core, adhesive ass'y. on fixture | • Two curved structural sheets, core material adhesively bonded with metalized plastic film bonded on fixture. | • Metalized thick plastic sheet, core material, back skin adhesively bonded on fixture. | • Metal plated curved sheet front, core, sheet back adhesively bonded on fixture. | • Mechanically polished sheet, curved, core, sheet back adhesively bonded on fixture. |
| 2. Molded sandwich | • Molded structural foam sandwich with 2nd surf. glass microsheet. | • Molded structural foam sandwich with 1st surf. glass microsheet. | • Molded structural foam sandwich with metalized plastic film adhesively bonded on. | | • Molded structural foam sandwich with electroplated foil adhesively bonded on. | • Molded structural foam sandwich with mechanically polished foil adhesively bonded on. |
| **FRAME STRUCTURES:** | | | | | | |
| 1. Sheet and fabricated frame (antenna panel). | • Mosaic of flat 2nd surf. facets on antenna panel.<br>• Mosaic of spherical 2nd surf. facets on antenna panel. | • 1st surface metal on glass microsheet bonded on antenna panel.<br>• Mosaic of 1st surf. facets on antenna panel. | • Metalized plastic film with adhesive back on antenna panel. | • Metalized thick plastic sheet bonded to extruded fabricated plastic frame on fixture. | • Metal electroplated sheetmetal as front surface of antenna panel. | • Mechanically polished sheetmetal (Stainless Steel) as front surface of antenna panel. |
| 2. Molded ribbed frame. | • Molded fiberglass ribbed structure with 2nd surf. glass microsheet. | • Molded plastic ribbed structure with 1st surf. glass microsheet. | • Molded Fiberglass ribbed structure with metalized plastic film adhesively bonded on. | • Metalized thick plastic sheet bonded to molded plastic ribbed frame. | • Molded fiberglass ribbed structure with electroplated foil adhesively bonded on. | • Molded fiberglass ribbed structure with mechanically polished foil adhesively bonded on. |
| 3. Stamped metal frame (ex. auto hood construction) | • Mosaic of flat 2nd surf. glass facets bonded on stamped metal panel.<br>• 2nd surf. microsheet bonded on stamped metal panel.<br>• Mosaic of 2nd surf. facets bonded onto stamped metal. | • Mosaic of flat 1st surf. glass facets bonded on stamped metal panel.<br>• 1st surf. microsheet bonded on stamped metal panel.<br>• Mosaic of 1st surf. glass facets bonded onto stamped metal panel. | • Metalized plastic film adhesively bonded on stamped metal frame. | | • Stamped metal panel, metal plated. | • Stamped metal panel, mechanically polished. |
| **SHELLS:** | | | | | | |
| 1. Self supporting sheet. | • Two sheets of curved glass, 2nd surf. metalized, vinyl in between (auto wind screen) | • Two sheets of curved glass, 1st surf. metalized, vinyl in between (auto wind screen) | • Single curved sheet with metalized plastic film adhesively bonded on. | • Metalized single curved thick plastic sheet. | • Single curved sheetmetal plated. | • Single curved sheetmetal with polished surface. |

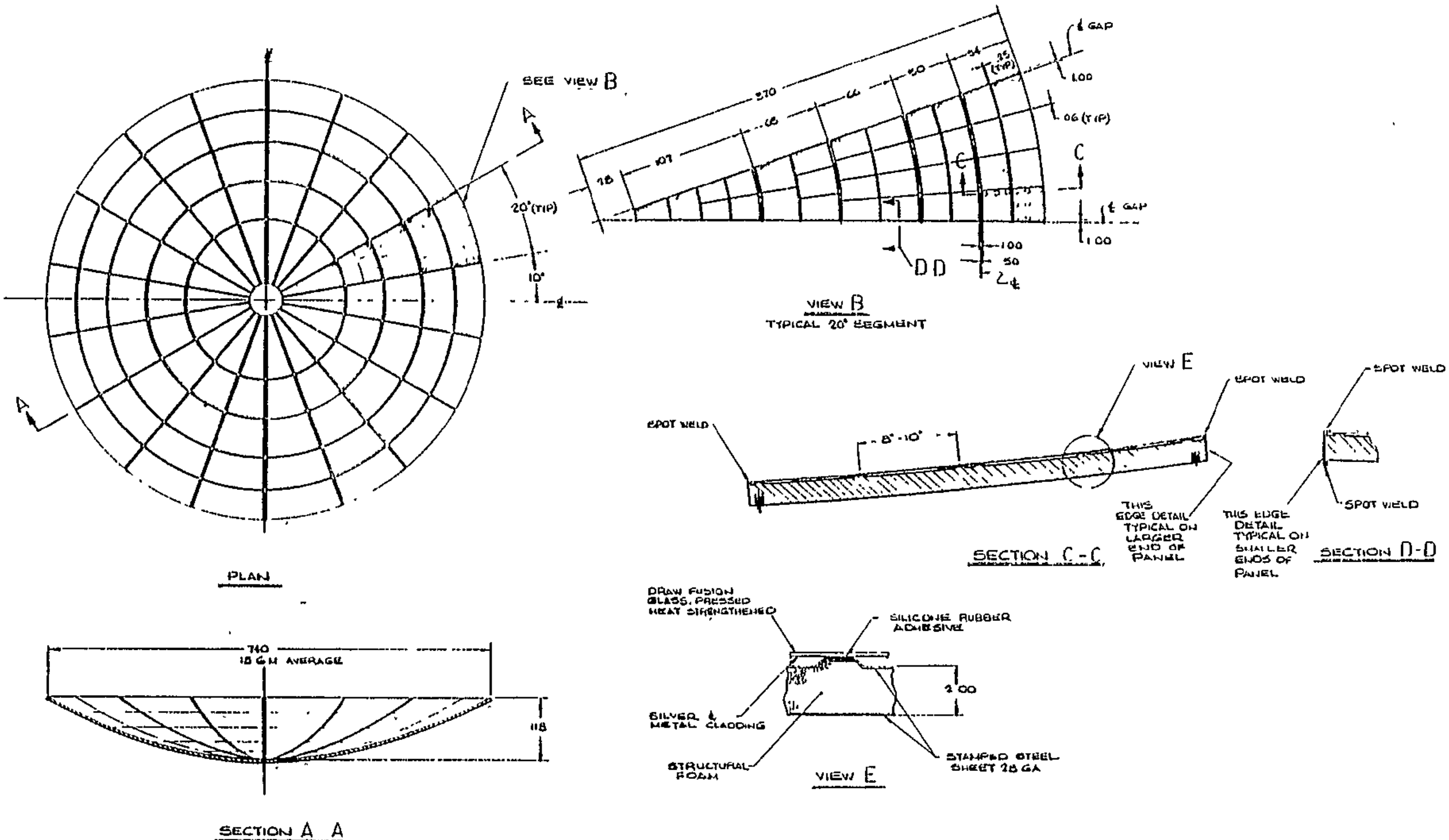


94-2-30

FIGURE 27. MULTIPLE FACET REFLECTOR PANEL DESIGN

TABLE 9. STEEL SANDWICH BENDING STRESS

| Panel Row | Stress (psi) | |
|---|---|---|
| | Inner | Outer |
| Gravity loading | 1,010 | 1,440 |
| 30 mph wind: loading on back | 2,270 | 2,860 |
| 90 mph wind: loading stowed | 5,130 | 13,240 |

b. Cellular Glass Sandwich Concept. The second viable concept that was developed is a sandwich structure where the glass is the front structural member in addition to providing the reflective surface (Figure 28). The back sandwich skin is steel and the core is cellular glass. Since the glass (0.05 inch thickness) is part of the structure, it must extend continuously across the length of the panel to carry the skin tensile load. Glass piece lengths in the order of 120 inches will be available as flat glass but not as doubly curved within the required time span, therefore strips 120 inches long and tapered up to 12 to 16 inches wide will be elastically deformed to the required curvatures.

Table 10 shows overall glass stress prediction for elastic forming as a function of thermal, wind, and gravity loading. Stresses fall within the expected design allowables.

Optical performance of the elastically curved silvered fusion glass will be as high as for the flat glass. Slope errors for Argoud's first test panels were about 0.6 mrad (Reference 8), so it should be possible to hold production panels to 0.5 mrad rms. Life of the cellular glass currently appears to be a serious question, which must be resolved before a final decision is made for its use.

c. Self Supporting Shell Concept. The third concept considered consists of two identical pieces of 0.090 inch glass, hot formed to the desired contour, and bonded together to act as one piece, 0.180 thick. The second surface of the front laminate is silvered. The two pieces would be sagged together with the back piece contacting the mold. The rear glass provides an excellent water vapor barrier to protect the silver if an adequate edge seal is provided.

A disadvantage of this concept is that the unsupported length of glass panel must be limited to 60 inches maximum to maintain the allowable stress level at 30,000 psi (survival wind), a level which is already optimistic for present state-of-the-art glass tempering. The baseline reflector panel configuration requires glass panels of 120 inches in length, so the thickness of the laminate would have to be increased to 0.380 inch in order to keep the stress to an acceptable level. This effect results in increased cost, weight, and solar absorption considerably beyond the other two previously described concepts. Therefore, this concept has not been considered further.

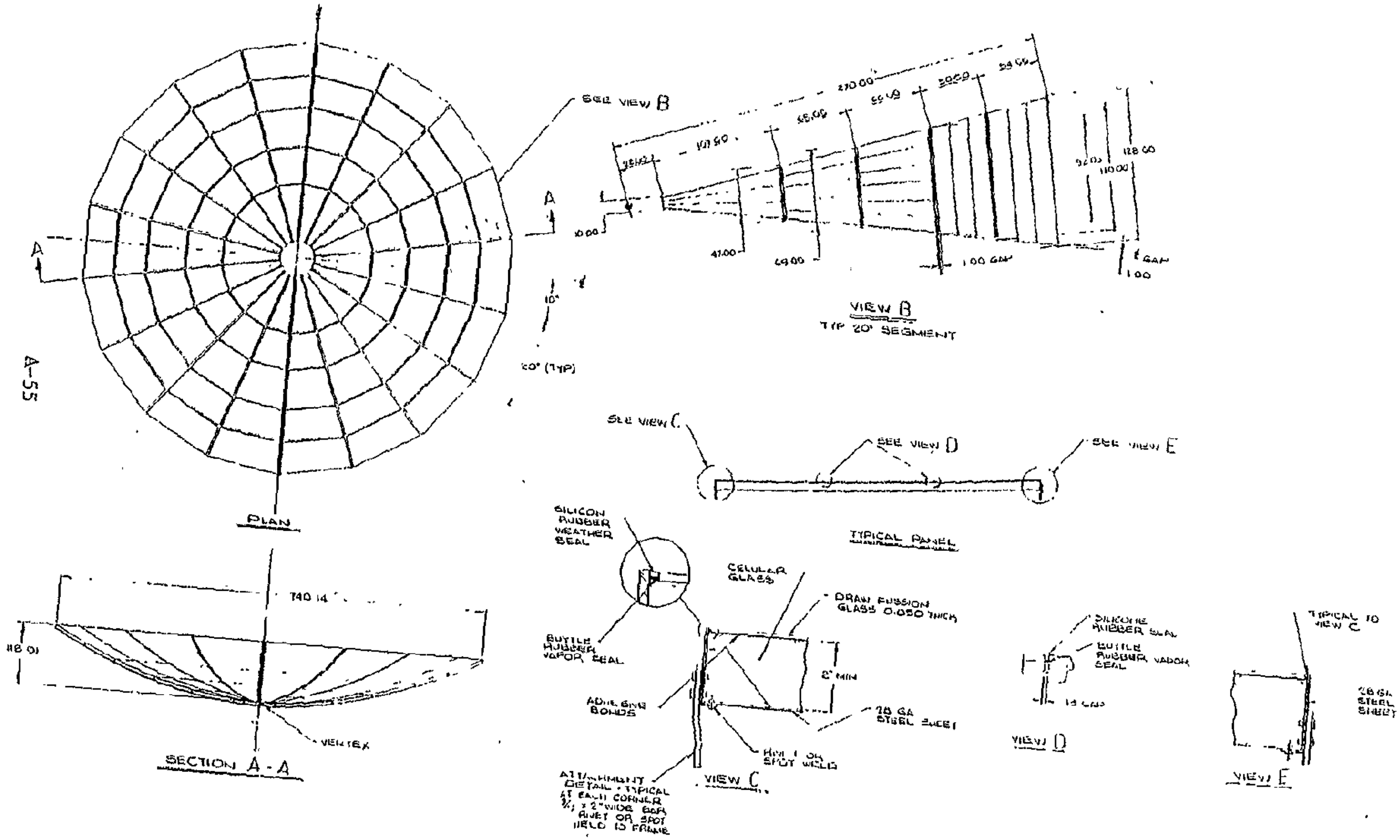


FIGURE 28. CELLULAR GLASS SANDWICH REFLECTOR PANEL DESIGN

94-2-31

TABLE 10. ELASTICALLY CURVED GLASS PANEL STRESSES

| LOADING CONDITIONS | STRESS CONTRIBUTION (PSI) | TOTAL GLASS STRESS (PSI) | | |
|---|---|---|---|---|
| | | AT CENTER | | AT EDGE |
| | | AT FRONT OF GLASS (CONCAVE) | AT BACK OF GLASS (CONVEX) | FRONT & BACK |
| <u>Innermost Row of Panels</u> | | | | |
| Gravity (Zenith) | -265 | -169 | +763 | -546 |
| 30 MPH Wind (Horizon) | | | | |
| (a) Back, $C_p$ = 1.4 | +585 | +681 | +1613 | +304 |
| (b) Front, $C_p$ = 1.65 | -643 | -547 | +1671 | -924 |
| Gravity + 90 MPH Wind (Zenith) | +1237 | +1333 | +2265 | +956 |
| <u>Outermost Row of Panels</u> | | | | |
| Gravity (Zenith) | -235 | -189 | +623 | -461 |
| 30 MPH Wind (Horizon) | | | | |
| (a) Back, $C_p$ = .45 | +362 | +408 | +1220 | +136 |
| (b) Front, $C_p$=1.3 | -603 | -557 | +255 | -829 |
| Gravity + 90 MPH Wind (Zenith) | +3059 | +3105 | +3917 | +2833 |

LEGEND: + = Tension Stress
- = Compression Stress

Highlights of the three panel designs which were considered are summarized below:

- Multiple facet and frame concept

  Advantages:

  1. Light-weight
  2. Easily produced
  3. Low cost (See Table 11)
  4. Thermally stable
  5. Good optical performance (See Table 12)

  Disadvantages:

  1. "Markoff" may be large (i.e., poor micro-smoothness resulting in a less specular surface)

- Cellular glass sandwich concept

  Advantages:

  1. Cellular glass contour can be easily and accurately formed.
  2. Markoff should be small
  3. Light-weight construction
  4. Low cost (See Table 11)
  5. Good optical performance (See Table 12)

  Disadvantages:

  1. Glass curvature at edges contribute indeterminant slope error
  2. Compound stresses developed in doubly bent glass. Test data needed to evaluate the levels

TABLE 11. FAR TERM PANEL CONSTRUCTION COST ESTIMATE

(Cost $/Ft$^2$)

| Panel Component Breakdown | Multiple Facet/Frame | | Cellular Glass Sandwich | |
|---|---|---|---|---|
| | 6 MSF* | 300 MSF* | 6 MSF* | 300 MSF* |
| Glass | 0.84 | 0.50 | 0.78 | 0.50 |
| Silver/Copper/Paint | 0.07 | 0.04 | 0.06 | 0.04 |
| Mirroring Labor | 0.50 | 0.20 | 0.20 | 0.10 |
| Adhesives | 0.07 | 0.05 | 0.30 | 0.25 |
| Hot Pressing | 0.68 | 0.45 | - - | - - |
| Steel Frame | 0.43 | 0.31 | - - | - - |
| Steel Sheet | - - | - - | 0.50 | 0.40 |
| Foam | 0.40 | 0.31 | - - | - - |
| Cellular Glass | - - | - - | 0.75 | 0.65 |
| Attachment Hardware | 0.06 | 0.05 | 0.06 | 0.05 |
| Manufacturing | 0.38 | 0.25 | 0.72 | 0.48 |
| Total Cost | \$3.43/Ft$^2$ | \$2.16/Ft$^2$ | \$3.37/Ft$^2$ | \$2.47/Ft$^2$ |

* Production Rates of: 6 MSF (Million Sq Ft/Year) = 100 Sites
300 MSF (Million Sq Ft/Year) = 5000 Sites

TABLE 12. PANEL OPTICAL PERFORMANCE (ESTIMATED)

| Performance Parameter | Multiple Facet & Frame Concept | Cellular Glass Sandwich Concept |
|---|---|---|
| Slope Error (Source): | | |
| • Manufacturing | 1.2 mrad rms | 1.0 mrad rms |
| • Assembly | 0.2 mrad rms | N/A |
| • Thermal Distortion* | Negligible | See Note |
| • Gravity Distortion | 0.5 mrad rms | 0.5 mrad rms |
| • Wind Distortion (6M/S) | 0.2 mrad rms | 0.2 mrad rms |
| Reflectivity - New | 0.94 | 0.95 |
| Specular Beam Width | TBD (>0.5 mrad rms) | ≤ 0.5 mrad rms |

*Determination of thermal distortion for the cellular glass sandwich concept will require further analysis. Thermal distortion can be controlled by manufacturing panels with materials having compensating thermal expansion properties. Studies are needed to determine if this is a cost-effective approach.

- Self-supporting shell concept

  Advantages:

  1. Silvered surface protected by second piece of glass
  2. Mark-off is potentially low.

  Disadvantages:

  1. Must be very thick (approximately 0.38 inch) to withstand required loading when made in 120-inch sheets. This increases cost, weight, and solar absorption.

2.4.1.6 Reflector Panel Summary. It is concluded that:

- Second surface silvered glass offers the best long term reflective surface.
- Draw fusion glass has better reflectivity than float glass.
- Metallized plastic film and polished metal have been eliminated because the (already poor) optical properties cannot be maintained for an economical lifetime.
- Measurement technique is needed to verify the specularity and reflectivity of doubly curved surfaces.

It was decided to use draw fusion, second surface silvered glass and carry forward panel designs of both the multiple facet/frame and the cellular glass sandwich concepts, but eliminate the self-supporting shell concept.

## 2.4.2 REFLECTOR STRUCTURE AND RECEIVER SUPPORT SYSTEM

Two basic concepts were investigated in the evaluation of cost-effective approaches for the reflector structure and receiver support. These were the rear and front brace configurations. The front-braced concept is unique for solar applications in that the reflector structure is in front of the mirrors. (This is not a viable design for microwave use because of several technical reasons.) The investigation included detailed structural analyses for operational and survival conditions. Also various configurations of the power module (receiver/engine/generator) support structure were evaluated. Variables such as materials, finishes, fabrication and assembly techniques, and alignment schemes were considered. The criteria for selection of the most cost-effective structural concept was a comparison of the costs of the basic structure (other variables are approximately the same for both concepts). The major parameter which affects the cost of the reflector structure is its weight, therefore weight was used as the primary index of cost. Both concepts were rated on equal structural survival capability and equal solar energy collection.

2.4.2.1 Analysis Methods. The basic analysis tools which were used in the investigation of the reflector structure concepts were the Large Frame, Forsum, and RMS Slope Error computer programs. The first two codes are standard programs used for the detailed structural analysis of large parabolic dishes and were originally developed for microwave antennas. The RMS Slope Error code uses the structural deformation data from the other programs to compute the rms slope errors for the reflecting panel supports. The contribution of the structural deformation to the pointing error is included in the calculations.

2.4.2.2 Power Module Support Structure Selection. The power module support concept is applicable to either front or rear braced configurations. The two factors of importance are the number of legs used and the point at which the structure is attached to the reflector structure.

a. Number of Legs. Preliminary studies quickly narrowed the choice to either a tripod or a quadripod support structure. A tripod is preferred because it is simpler, has less solar blockage/shadowing and is less costly. It is structurally more efficient to have the receiver support legs terminate adjacent to the support points of the reflector structure (i.e. simplified load paths). Since there are three support points between the reflector assembly and the pedestal (the two upper axis bearings and the actuator), this is another advantage of using a tripod. Therefore, a tripod power module support structure was selected.

b. Reflector Attachment Location. The radial point at which the tripod support structure is attached to the reflector structure has an effect on blockage (i.e. blockage of the reflected rays from reaching the receiver). Minimum blockage (zero) is achieved by locating the attachments at the rim of the concentrator, but this is undesirable from a structural standpoint. Preliminary studies indicate the optimum point is about three quarters of the distance from the center to the rim, subject to detailed analysis.

2.4.2.3 Reflector Structural Analysis Studies. The loads acting on the structure are induced by gravity, wind, and thermal effects. The wind loads were derived from pressure distribution data obtained from wind tunnel tests conducted and reported by JPL. External gravity loads (from panels and the power module), thermal loads, and the structure gravity loads were computed for several limiting cases.

The analysis of the reflector and power module support structures was accomplished by the use of the Large Frame computer program. One half of the structure was modeled and analyzed as a pin-jointed, three-dimensional truss. The model for the stress and deflection analysis utilized an arbitrary loading system having, in general, no axis of symmetry.

a. Rear Braced Structure. The design of the rear braced concept was based on reflector structures for microwave antennas. The structure for both this design and the front braced concept was designed to survive (in the stowed position) 40 m/s winds with a minimum factor safety against material yielding of 1.1. The initial analysis was performed for a typical 12-meter diameter reflector.

b. Front Braced Structure. The front braced structure is an innovative derivative of the conventional rear braced reflector structures currently used on many microwave antennas. An artists' conception of a typical structural layout for a ~12 m diameter is shown in Figure 29. Note that the design consists of a series of radial and circumferential structural members. A 12 meter diameter was analyzed for the same conditions used for the rear braced concept. Results were also obtained for larger concentrators.

c. Comparison of Structural Analyses. A fair comparison between the rear and front braced reflector structures requires that each have the same solar energy collecting capability, i.e., equivalent apertures. The front braced concept obviously has more shadowing/blockage, therefore the size of the concentrator must be increased to compensate for this effect. A first order analysis of the shadowing/blocking (summarized below) indicates that the front braced structure must have a diameter of 12.25 meters to have an aperture equivalent to that of a 12-meter rear braced structure. Thus, the weight, RMS slope errors, and pointing errors calculated for the front braced structure must be scaled to account for the change in diameter. Scaling laws were derived for each of these parameters and the results analyzed.

Table 13 presents the comparison of the various parameters for the 12-meter diameter rear braced structure and the scaled-up (12.25 meter) front braced structure. These data indicate that the front braced structure is still approximately 12 percent lighter in weight (and hence less expensive) and has better performance in terms of RMS slope error and pointing error than the rear braced structure. For this reason, the front braced reflector panel support configuration was selected as being the most cost-effective concept.

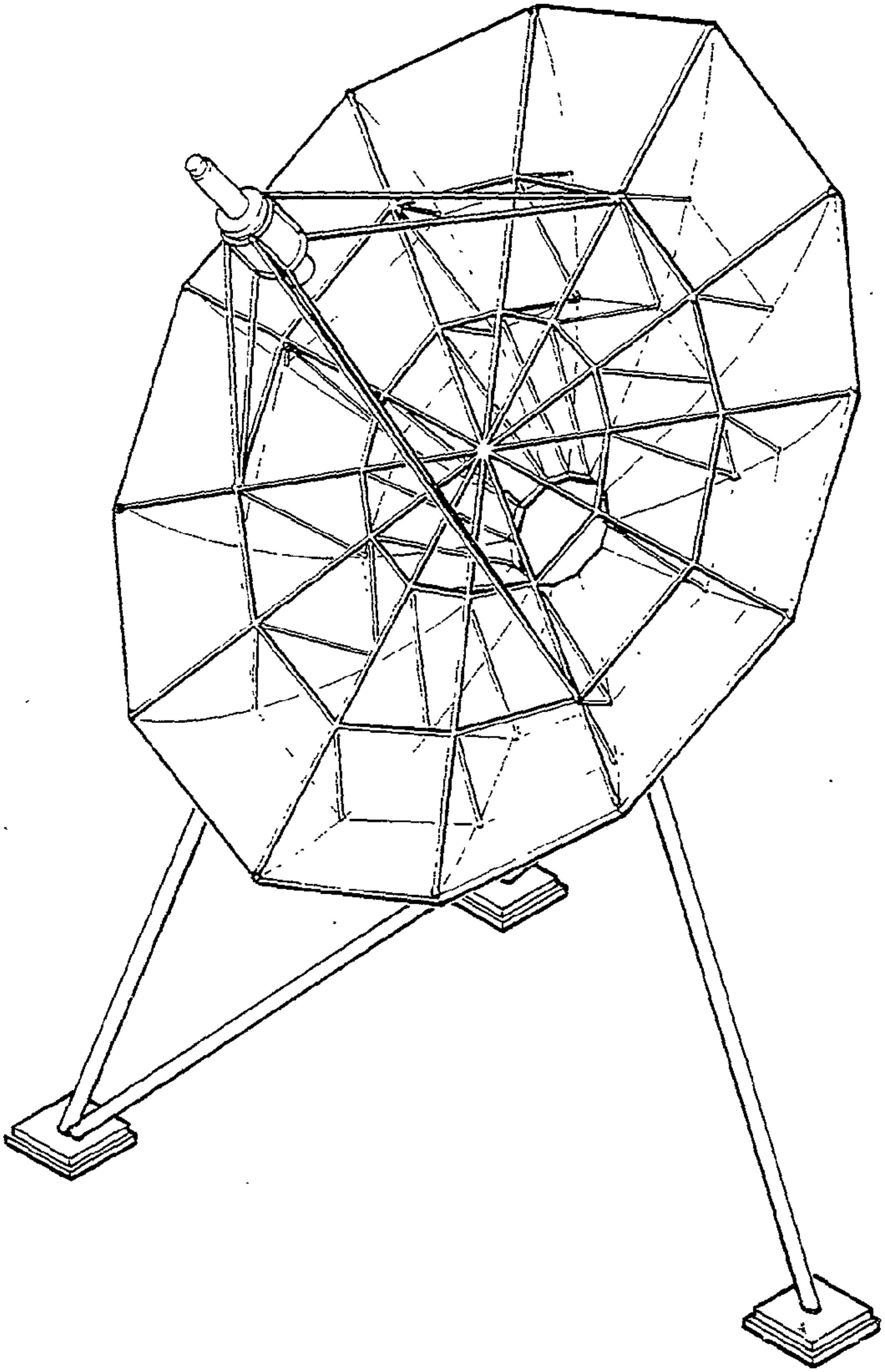


FIGURE 29. ARTIST'S CONCEPTION OF FRONT BRACED SOLAR CONCENTRATOR

2.4.2.4 Solar Shadowing/Blockage. Shadowing and blocking due to the tripod structure and due to the front structure (for the front structure concept) was analyzed for the two concepts. The determination of shadowing is straightforward; however, the detailed analysis of blocking is more complicated and only an approximate analysis was made for this study. This analysis was based on simple geometric relations based on the ~0.5 degree solar disc diameter and perfect reflecting surfaces.

The combined shadowing/blocking pattern for the 12-meter front structure dish used for the analysis is shown in Figure 30. The areas considered are the central power module (defined as the receiver and apex support in the figure), the radial trusses (9), hoops (12), and the tripod (3). The terms "primary blockage" and "secondary blockage" refer to shadowing and blocking, respectively.

TABLE 13. STRUCTURAL COMPARISON OF REAR AND FRONT BRACED STRUCTURE

| Parameter | Rear Braced Structure (12m) | | Front Braced Structure (12.25m) | |
|---|---|---|---|---|
| | Outboard Supports* | Inboard Supports* | Outboard Supports* | Inboard Supports* |
| Weight (lb.) | 4200 | 4500 | 3600 | 3700 |
| Worse Case Slope Error (mrad) | | | | |
| • Radial | 0.2 | 0.3 | 0.2 | 0.3 |
| • Tangential | 0.4 | 0.7 | 0.3 | 0.4 |
| Worse Case Absolute Pointing Error (mrad) | | | | |
| • Gravity | 1.2 | 1.8 | 0.8 | 0.8 |
| • Wind | 0.3 | 0.5 | 0.2 | 0.2 |
| Worse Case Relative Pointing Error (mrad) | | | | |
| • Gravity | 0.3 | 0.4 | 0.2 | 0.2 |
| • Wind | 0.05 | 0.1 | 0.05 | 0.05 |

*Outboard and inboard supports represent two different positions for attaching the three support points to the two bearings and the actuator. The outboard support was about 55 percent of the distance between the center and the edge, the inboard about 25 percent.

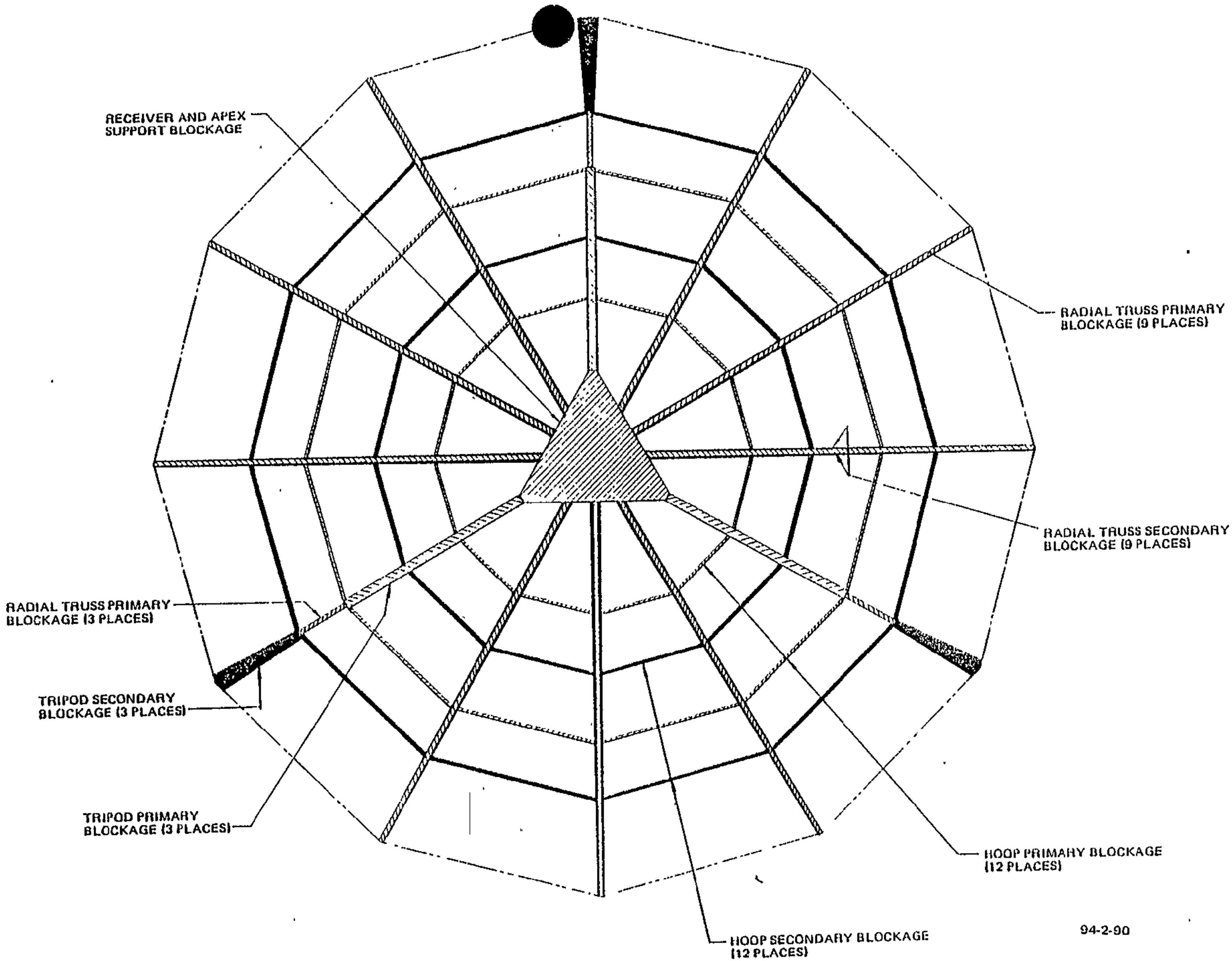


FIGURE 30. SHADOWING/BLOCKAGE AREAS FOR THE FRONT STRUCTURE CONCEPT (12M DIAMETER)

The shadowing/blockage for the 12-meter diameter concepts are summarized in Table 14. The front braced configuration has a loss of about 9 percent due to shadowing/blockage compared to 4.4 percent for a conventional structure. Additional calculations were performed for an 18.6 meter front structure concentrator which was optimized by carefully selecting truss height and hoop member positions in relationship to the surface panel sizes. The total solar loss for the larger dish was 7.6 percent compared to a conventional structure solar loss of 3.4 percent.

Another feature of the front-braced concept is the use of gaps between surface panels. The panels are oriented such that gaps fall into the blockage areas, which saves actual mirror material, reduces tolerances, and provides a reduction in wind force.

TABLE 14. SHADOWING/BLOCKAGE SUMMARY

(12 Meter Diameter - 113 Meter$^2$ Aperture Area)

| Reflector Support Concept | Area, $m^2$ | | | Percent of Aperture |
|---|---|---|---|---|
| | Shadowing | Blockage | Total | |
| Front-Braced* | | | | |
| Power Module | 2.03 | --- | 2.03 | 1.80 |
| Tripod Legs | 1.06 | 0.79 | 1.85 | 1.64 |
| Radial Trusses | 2.67 | 0.75 | 3.42 | 3.02 |
| Hoop Members | 1.11 | 1.71 | 2.82 | 2.50 |
| | 6.87 | 3.25 | 10.12 | 9.0% |
| Conventional Back-Braced** | | | | |
| Power Module | 2.04 | --- | 2.04 | 1.81 |
| Tripod Legs | 1.89 | 1.03 | 2.92 | 2.58 |
| | 3.93 | 1.03 | 4.96 | 4.4% |

* (Net Aperture Area = 102.9$m^2$)
** (Net Aperture Area = 108.2$m^2$)

2.4.2.5 Wind Loads. The front braced concept eliminates the conventional exposed rear structural members, which greatly reduces the critical wind forces on all components of the concentrator. This was demonstrated in the wind tunnel tests conducted by the Jet Propulsion Laboratory (Reference 10). The tests showed a significant effect for side winds; the no-back-structure reflector had 40 percent less force than a "structure with minimum counter-weight". This reduction is particularly important to the critical survival condition in the stowed zenith position, although detailed calculations will require aerodynamic data for specific designs.

The use of gaps between the reflector panels also reduces the wind loads by a small amount for certain wind directions. Reference 11 presents detailed surface pressure distribution data for solid and porous reflectors. Additional data is presented in Reference 12.

2.4.2.6 Pedestal Loads. The front braced concept reduces the loads that are transmitted to the pedestal. This is due to a lighter weight reflector and tripod, but even more important is that the reflector surface moves closer to the axes of rotation. Thus, gravity moments are reduced; calculations show the unbalance gravity moment for the front braced concept is 25 percent less than the moment for a conventional rear braced structure. Finally, the closer location also reduces operating and survival wind moments for a combined reduction in forces on structural and mechanical components of the pedestal and foundation.

2.4.3 PEDESTAL SYSTEMS

The pedestal to be used has important cost and performance implications on the selection of the baseline concentrator configuration. The choice was narrowed down to four candidates in paragraph 2.3.2.2: (1) Az-El Inverted Track, (2) Az-El Low Turntable (Yoke), (3) Az-El High Turntable (Turret), and (4) Conventional HA/DEC. Table 15 summarizes the features of each concept.

Two components are common to all four candidates namely, secondary axis bearings and secondary axis drives. Trade studies were conducted to determine the best hardware for the SPS application in terms of performance, cost, and risk. It was determined that the bearings should be spherical roller-bearing type, and the secondary drive should be a machine screw actuator.

2.4.3.1 Comparisons of Pedestal Systems. A simplified diagram and summary of the features of each candidate is presented in Figure 31.

a. Az-El Inverted Track (concept No. 2). The linear actuator is a 10 ton machine screw device with a stroke of 13 feet and is driven by a worm and wheel gear coupled to a single stage speed reducer and motor. The top of the actuator connects to a truss on the reflector structure and the bottom of the actuator is pinned to a point on the rotating azimuth torus ring. There is a six-member tubular space frame connecting the two elevation bearings to three structural base work points, one of which is shared by the elevation actuator base on the azimuth torus ring. This alidade is a rigid wide base structure comprised of efficient, low-cost steel members. The azimuth torus ring

TABLE 15. SUMMARY OF CANDIDATE PEDESTAL CONCEPTS

| Description | Concept #2 | Concept #3 | Concept #4 | Concept # 11 |
|---|---|---|---|---|
| Axis Arrangement | AZ-EL | | | HA/DEC |
| Secondary Axis Bearing | SELF-ALIGNING, PAIR OF PILLOW BLOCK BEARINGS | | | |
| Secondary Structure (Rotating) | Large Space-Frame Alidade. Axially Loaded Members. | Yoke Weldment. Flexurally Loaded Members | Small space Frame. Axially Loaded Members. | |
| Secondary Axis Drive | Linear Actuator | | | |
| Primary Axis Bearing | Wheel & Inverted Track | Turntable Rolling Element | | Self-aligning Pair of Pillow Block Bearings |
| Primary Axis Drive | Roller Chain On AZ Track | Bull Gear Integral With Bearing | | Roller Chain On HA Wheel |
| Primary Structure (Non-rotating) | Six Small Weldments (Wide Base) | Steel Cone On Concrete Cylinder (Narrow Base) | Six Legged Space Frame (Wide Base) | 5 Legged Space Frame (Site Peculiar and Wide Base) |
| Foundation (Reference Only) | Six Piers | Large Circular Or "X" Pad | Three Piers | |

CONCEPT NO. 2

AZ-EL INVERTED TRACK

CONCEPT NO. 3

AZ-EL LOW TURNTABLE (YOKE)

CONCEPT NO. 4

AZ-EL HIGH TURNTABLE (TURRET)

CONCEPT NO. 11

CONVENTIONAL HA/DEC

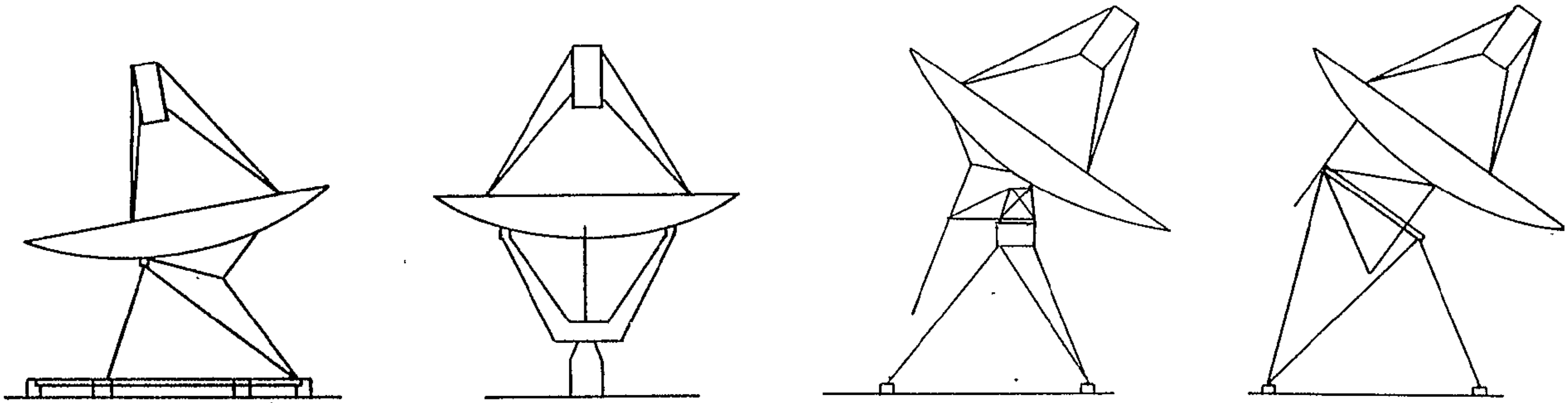

**Concept No. 2**

- Az-El axis arrangement
- Secondary axis pillow-block bearings
- Large axially loaded space-frame alidade structure
- Linear actuator secondary drive
- Inverted wheel and track primary axis bearing
- Roller chain primary axis drive
- Six small weldments for base structure

**Concept No. 3**

- Az-El axis arrangement
- Secondary axis pillow-block bearings
- Flexually loaded yoke weldment structure
- Linear actuator secondary drive
- Turntable rolling element primary axis bearing
- Bull gear and pinion primary axis drive
- Steel cone and concrete cylinder for base structure

**Concept No. 4**

- Az-El axis arrangement
- Secondary axis pillow-block bearings
- Small axially loaded space-frame alidade structure
- Linear actuator secondary drive
- Turntable rolling element primary axis bearing
- Bull gear and pinion primary axis drive
- Six legged space frame for base structure

**Concept No. 11**

- Ha/Dec axis arrangement
- Secondary axis pillow-block bearings
- Small axially loaded space-frame alidade structure
- Linear actuator secondary drive
- Primary axis pillow-block bearings
- Roller chain primary axis drive
- Five legged space frame for base structure

94-2-200

Figure 31. CANDIDATE PEDESTAL SYSTEMS

rotates, and is captured by six pairs of canted wheels. The torus has a ring diameter of 25 feet and a section outer diameter of 9 inches with a 0.50 inch wall. The canted wheels are nominally 6 inch diamter, mounted on bearings and have circular contact faces to conform to the torus. Thus the azimuth system provides freedom to rotate in azimuth and restrain radial, axial, and moment loads in the same way a conventional rolling element turntable bearing does.

The concentrator is driven in azimuth by means of a roller chain. There is one drive sprocket and two idler sprockets which hold the chain into 180 degrees of contact with the drive sprocket. The drive sprocket is driven by a gear reducer and motor.

The inverted track bearing is an integral part of this concept and other alternatives such as turntable bearing types or conventional wheel and track types do not apply. The inverted track provides a natural wheel structure on which can be placed either a segmented bull gear (segmented because the diameter is too large for any known gear cutting machine) or a channel section which guides a roller chain. The available drive types do not include single linear actuators because the stroke is more than 180 degrees and it is impossible to achieve this with a linear actuator without resorting to complicated and compliant scissors links. The only feasible concepts considered were either a bull gear and pinion final drive or a roller chain and sprocket. The roller chain was selected based on cost. The tolerances of a roller chain drive would be eliminated by use of corrective autotracking.

Several problems exist with the Az-El inverted track concept which have a direct impact on its use for this program:

(1) Torsional and bending stresses in the track. Since the hard points on the torus are usually not directly over the wheels, the load is taken to the wheels in bending and torsion of the track. Because the wheels occur at 60 degree intervals and the hard points occur at 120 degree intervals, the three track deflections are equal and no pointing error results. Nevertheless, the bending and torsional loads result in a heavy and expensive track. Solution of this problem requires a cost-element trade study of ring diameter, track section diameter, thickness and number of wheel pairs.

(2) Wheel/track contact stresses. The ideal case has perfect conformity of the wheel and track, (line contact) which results in an acceptable contact stress of 98,000 psi (survival). In reality, the wheel contact radius must be larger than the torus section radius in order to avoid point loading and destructive stresses caused by wheel and track misalignments and deflections. The major deflection problem will be caused by the horizontal component of the gravity load taken by the wheels which will deflect the track in the ring direction, reducing the effective ring diameter. The reduction in track diameter will cause the tubular section to move down a line parallel to the lower wheel axis which would cause point contact on a fully conforming wheel. Therefore the wheel contact radius must be increased. Solutions to this problem require further design studies to

investigate the cant angle of the wheels, number of wheels, wheel diameter and width, rectangular track sections, self-aligning wheels, and tire material.

(3) Fabrication, Shipping and Field Assembly of the Torus Track. The third problem with this concept is in designing joints in the torus track which will permit shipping and economical field assembly. The joints must transmit the torsional and bending moments and yet not interfere with the rolling contact surfaces.

These problems require further study and this concept is classified as a high risk.

b. Az-El Yoke (Concept No. 3). This concept requires either a single turntable bearing, or a pair of bearings supported by a short king post such that the upper bearing will accommodate radial and thrust loads and the lower bearing take the radial loads. Several bearing designs were considered including a cross roller bearing, a king post two-bearing system, and a reinforced teflon turntable bearing. A single four-point contact ball bearing was selected as the best design.

Azimuth drive candidates evaluated in terms of cost, performance, and risk were: (1) external bull gear/single pinion, (2) internal bull gear/single pinion, (3) internal bull gear/3 idler, center pinion, (4) planetary-differential type, and (5) planetary-conventional type. The external bull gear with single pinion was selected.

The major problems identified with this concept are:

(1) The azimuth bearing is far below the elevation bearings, thus the moment on the turntable bearing due to survival wind is high, driving up the cost of the bearing.

(2) The yoke is a large and expensive slender structure which transfers loads by means of bending stresses, which is inefficient from a weight and cost standpoint.

(3) Moment loads are transferred from the collector to the ground via a relatively small diameter cylindrical structure, so the foundation will will be more expensive than it would if the loads were passed to the ground through points that are spread apart.

These problems are less severe than for Concept No. 2, and the design risk is classified as low.

c. Az-El Turret (Concept No. 4). The mechanical components of this configuration are nearly identical to those of Concept No. 3. The major differences are in the structural design. The secondary structure yoke is replaced by the open space frame turret with a transition to the large cylindrical azimuth bearing housing assembly. The elevation actuator passes completely behind the turret, eliminating the requirement for a yoke. This permits raising the azimuth bearing to a point nearer the center of wind and gravity load application, reducing its loads and moments.

The primary structure (between the ground and the azimuth bearing) is higher than on Concept No. 3, and therefore lends itself to a tripod space-frame design rather than the cylindrical pier design. The tripod transmits loads in an efficient axial manner, providing a lighter weight structure. Also the tripod base structure requires a lower cost foundation (three simple piers) than does the cylindrical tower (large concrete pad to resist overturning).

This concept is a leading candidate because of well-proven, virtually no-risk mechanical subsystems; and because of minimum structural requirements (i.e. an efficient, low-cost structure).

d. Conventional HA/DEC (Concept No. 11). This concept has linear actuator deceleration drive with a 25 ton machine screw providing ± 23.5 degrees of DEC stroke. The hour angle bearings consist of a pair of self-aligning pillow block bearings, which form the least expensive primary axis bearing system of all four concepts. The hour angle bearings are shop mounted to the simple tube shaft, to which structural members are field bolted to form the hour-angle wheel. The hour angle drive system is composed of a roller chain attached to the ends of the hour angle drive wheel, and guided by a channel section on the wheel periphery. There is an idler sprocket on either side of the drive sprocket, providing 180 degrees contact with the drive sprocket, similar to the aximuth drive arrangement on Concept No. 2. The rigid space frame carrying the HA bearing and drive loads to the ground is a five-legged truss mounted to three piers. This is the lightest weight concept of the four under consideration.

The requirements and loads for the declination drive are similar to those for the elevation drives, and the selected drive is again the machine screw actuator. The stroke is only 47 degrees, rather than the 80 degrees required for Az-El.

The hour angle drive has a requirement for a travel of 195 degrees which is outside the range of linear actuators. The choices considered were pinion and gear versus sprocket and roller chain; roller chains were selected for the reasons outlined in Concept No. 2.

HA/DEC has some peculiar disadvantages which need careful consideration. These are:

(1) The reflector is subjected to much larger gravity load variations than an Az-El concept. Also the gravity slope errors cannot be compensated by initial alignment since rotation is ± 90 degrees about the hour-angle axis. Usually these distortions prohibit considering a HA-DEC concept, however, the front-braced structure minimizes them.

(2) The primary structure requires a modification for each latitude (i.e. site dependent).

(3) The reflector is higher off the ground in the noon position than an Az-El concentrator. However, the front-braced reflector concept minimizes the height.

(4) The power module is subjected to a daily roll component (in addition to tilt) which presents a problem for receivers or engines which are not capable of operating on their side. A sodium reflux boiler is an example because the liquid in the receiver cannot be allowed to flow into the vapor pipe and restrict the vapor flow. This problem can be solved by designing a counter-rotating frame or cage for the power module, but at added expense, complexity, and risk.

2.4.3.2 Selection of Pedestal Systems. The selection of the baseline system was based on an evaluation of performance, cost, risk, and compatibility with the power module (receiver/engine/generator). Preliminary designs of all concepts have been based on the same requirements for survival, and tracking (stiffness).

a. Performance. The risk of the concepts not meeting performance goals are evaluated as follows:

(1) Concept No. 2 presently has the risk that the inverted track can not be designed to provide a cost-effective 30 year wheel/track contact life. Detail design, analysis and (probable) testing would be required to demonstrate this capability.

(2) Concept No. 3 has virtually no performance risk, having been designed and built in numerous versions as microwave antennas by FACC and others.

(3) Concept No. 4 has little performance risk because the detailed design studies carried out during the Phase I effort, and the similarity with existing hardware.

(4) Concept No. 11 has some performance risk even though it is a simple structure. The problem lies in the present uncertainty about the roller chain safety, life and maintenance costs. The safety issue (gravity unbalance load on the chain) would be resolved during a detail design. The life and maintenance cost require a determination of the frequency of chain cleaning, lubrication and retensioning.

b. Costs. Structural steel subassembly costs were estimated based on information supplied by the Ford Manufacturing Feasibility Department. Mechanical component costs were estimated based on quotes from qualified vendors. In all cases, costs were based on production quantities of 100 to 5000 1 MWe sites annually in ∿ 1990 (1978 base dollars).

TABLE 16. CANDIDATE PEDESTAL COST COMPARISONS FOR TYPICAL 12 METER DIAMETER; QUANTITY: 100 SITES ANNUALLY IN 1990 (1978 $)

| Element | AZ-EL Inverted Track Concept No. 2 | AZ-EL Yoke Concept No. 3 | AZ-EL Turret Concept No. 4 | HA/DEC Concept No. 11 |
|---|---|---|---|---|
| Secondary Axis Bearings | $0.2 K | $0.2 K | $0.2 K | $0.2 K |
| Secondary Axis Drives | 0.8 | 0.8 | 0.8 | 0.7 |
| Secondary Structure | 3.5 | 2.5 | 1.3 | 1.3 |
| Primary Axis Bearing | 0.6 | 1.2 | 1.0 | 0.3 |
| Primary Axis Drives | 0.9 | 1.6 | 1.7 | 1.5 |
| Primary Structure | 0.3 | 0.6 | 1.4 | 1.6 |
| Drive Motors/ Controllers | 0.3 | 0.3 | 0.3 | 0.3 |
| Tracking Control System | 0.6 | 0.6 | 0.6 | 0.6 |
| Foundation* | 0.8 | 1.0 | --- | --- |
| Erection* | 0.4 | 0.2 | --- | 0.4 |
| Reflector* | 0.1 | 0.2 | --- | --- |
| TOTAL | $8.5 K | $9.2 K | $7.3 K | $6.9 K |

*Represents Additional Cost Only Relative To Concept No. 4.

The pedestal system has the most variable cost, and for comparative costing purposes each concentrator pedestal assembly was divided into the common structural elements. Table 16 summarizes the estimated costs of the individual elements for each of the four concepts based on a typical concentrator of 12 meter diameter.

c. Cost Risk. The cost risks associated with each concept are:

(1) Concept No. 2 rates "high" due to design risks associated with the inverted track and wheel design.

(2) Concept No. 3 rates "low" risk. A small design risk is associated with the yoke plate weldment compliance, buckling, and weight vs cost.

(3) Concept No. 4 rates "low" risk. Current development work has not uncovered any risk areas for this concept.

(4) Concept No. 11 rates "medium" due to design risk associated with the hour angle drive.

d. Interface Compatibility. A problem exists with the HA/DEC daily roll of the sodium receiver. No solution currently exists except to design a complex and costly "cage" which counteracts the roll and allows the receiver to operate properly.

e. Selection Summary. The results of the pedestal concept evaluation is summarized in Table 17. It is apparent that Concept No. 4, the Az-El turret design, shows consistently better overall performance and cost potential than the other three. Therefore, this concept was selected as the baseline pedestal design.

TABLE 17. PEDESTAL CONCEPT SELECTION CRITERIA SUMMARY

| Selection Criteria | Concept No. 2 AZ-EL Inverted Track | Concept No. 3 AZ-EL Yoke | Concept No. 4 AZ-EL Turret | Concept No. 11 HA/DEC |
|---|---|---|---|---|
| Anticipated Performance | Same | Same | Same | Same |
| Performance Risk* | High | Low | Low | Medium |
| Anticipated Cost | Medium | High | Low | Low |
| Cost Risk (Meet Estimated Goals) | High | Low | Low | Medium |
| Interface with Power Module (Receiver) | No Impact | No Impact | No Impact | A Problem |

*30 year life

## 2.4.4 TRACKING CONTROL SYSTEM

Tracking control is composed of the drive control system and the tracking system.

2.4.4.1 Drive Control System. The drive control system consists of a drive motor for each axis and the electronics required to control each motor. Figure 32 shows the relationship between AC and DC control systems as a function of cost and horsepower. It is apparent why an AC motor and control system is recommended. Another advantage is that AC motors have no brushes to replace, thus minimizing the maintenance.

Since the tracking accuracies for SPS do not require continuous sun tracking, a bang-bang stepping type drive system is the obvious choice. This is because of simplicity, relatively low cost, and long life. Figure 33 depicts the general arrangement of this typical motor control arrangement. Cost, reliability and maintenance dictates the following parameters:

- Motor: 230 or 480 V AC 3 phase (compatible with power system)
- Controls: Solid state switches (zero crossing actuation)
- Prime Power: 230 or 240 V AC, 3 phase, delta.

2.4.4.2 Tracking System. The three tracking systems qualifying for further consideration (paragraph 2.3.3) were: (1) Program Track, (2) Optical Track, and (3) Hybrid Track.

a. Program Track. Program track consists of a station control computer connected to each concentrator with a bit serial current loop communication link. The computer:

- Generates ephemeris data for concentrator position including timing, elevation sag correction, and angle to actuator position conversion.
- Transmits absolute position commands to each concentrator.
- Issues special commands to individual concentrators, such as stow, defocus, close or open receiver door, etc.
- Monitors status of each concentrator.

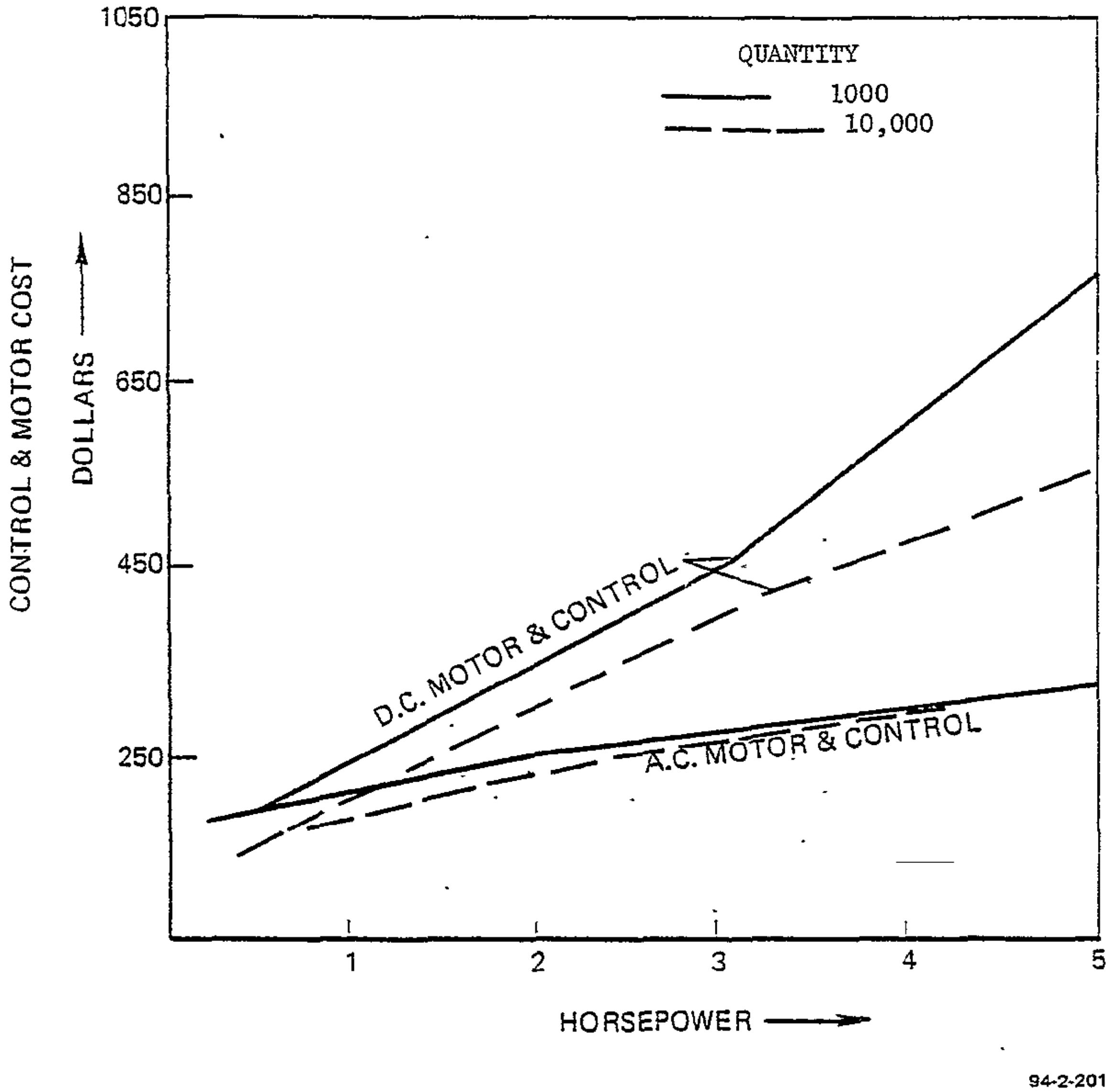


FIGURE 32. CONTROL & MOTOR COST VS HORSEPOWER

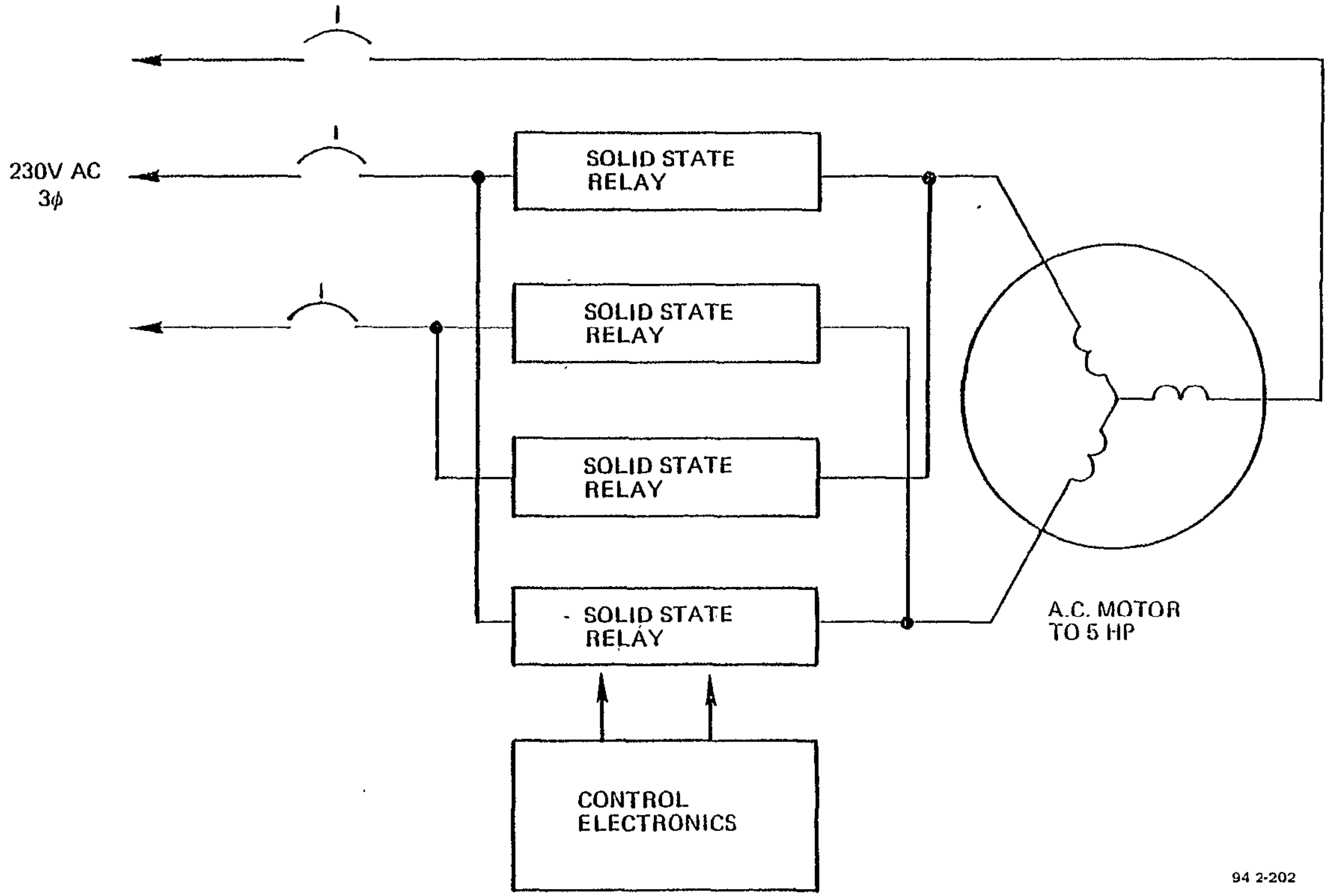


FIGURE 33. TYPICAL 3$\phi$ A.C. CONTROL SCHEMATIC

Each concentrator performs the following functions:

- Receives and decodes absolute position commands and other control functions.
- Generates encoded axis position data from position transducers.
- Accepts status inputs from concentrator transducers and reports to station control.
- Switches AC solid state relays for each axis to cause axis to move to commanded position.

Figure 34 is a block diagram description of the program track system.

The position transducers are expensive items. The choices are absolute encoders, synchros/potentiometers, or incremental encoders. Absolute encoders are too expensive. Synchros (resolvers) require analog to digital conversion and are relatively complex and expensive. Potentiometers are also relatively expensive, considering the required accuracy and resolution of about 0.01° needed to meet an overall tracking accuracy of 0.1° (1.7 mrad). Also an analog to digital conversion is required.

An incremental encoding scheme is the most attractive for this application. The most economical and reliable method for detecting axis position is the use of electromagnetic proximity switches to count motor shaft revolutions. Resolution of 0.01° is no problem, considering motor shaft rotation is in excess of 100,000 times axis rotation.

b. Optical Autotracking. Optical tracking consists of coarse and fine tracking sun sensors. The coarse sensors provide initial acquisition. Each axis is positioned independently to within the field of view of the fine tracking sensors. Hysteresis tracking would be employed to maintain fine pointing within the required accuracies, and the coarse tracking sensors would be inhibited. A computer-driven reference sensor would also be pointed at the sun to obtain direct insolation data. A decision to terminate optical tracking would be made when the direct insolation drops below a predetermined level. A reacquisition provision would be included in the optical tracking logic. This technique is illustrated in Figure 35.

Under ideal conditions this approach works fine. However, for cloud layers, scattered clouds, etc., refinements to the tracking mode logic are required.

c. Hybrid Tracking. A hybrid system consists of a coarse program track in conjunction with a fine optical tracking system. The program track function is the same as described in paragraph b. except that the accuracy requirement is reduced to about $\pm 0.4°$ (7 mrad) which is adequate to keep the sun in the field of view of the fine "steptrack" optical system. The key feature is the ability to optically track the sun with a limited angular field of view. This allows the feature of self-calibration to be added, i.e., corrections can be applied to the ephemeris inputs and stored in the microprocessor. The

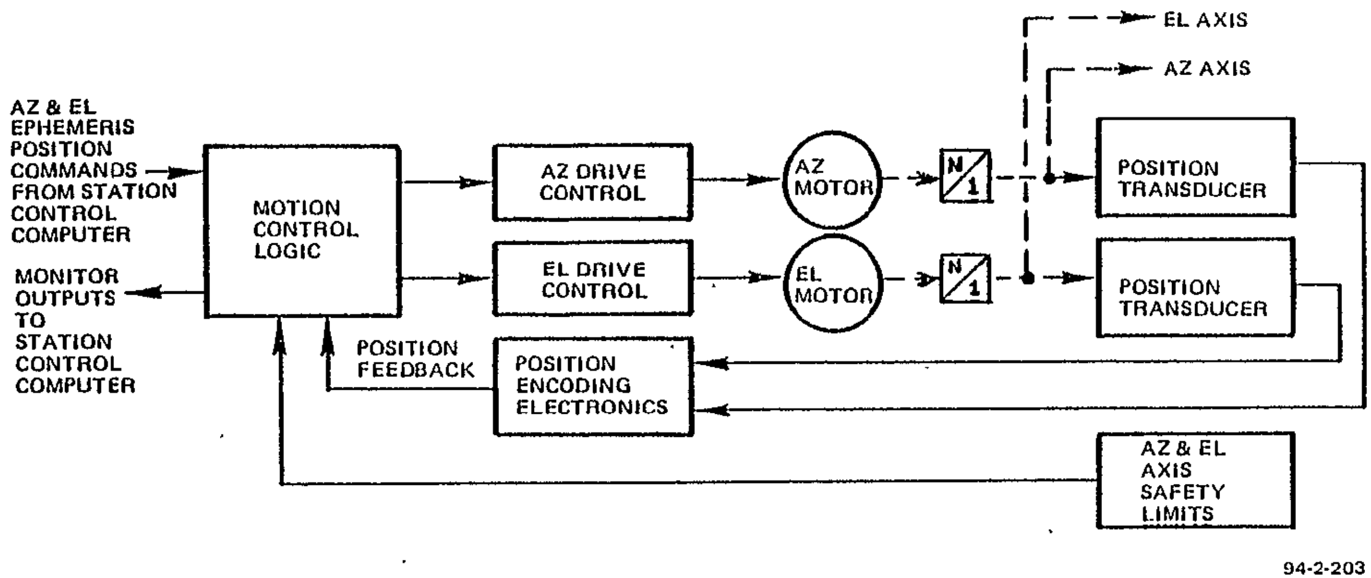


FIGURE 34. BLOCK DIAGRAM OF PROGRAM TRACK

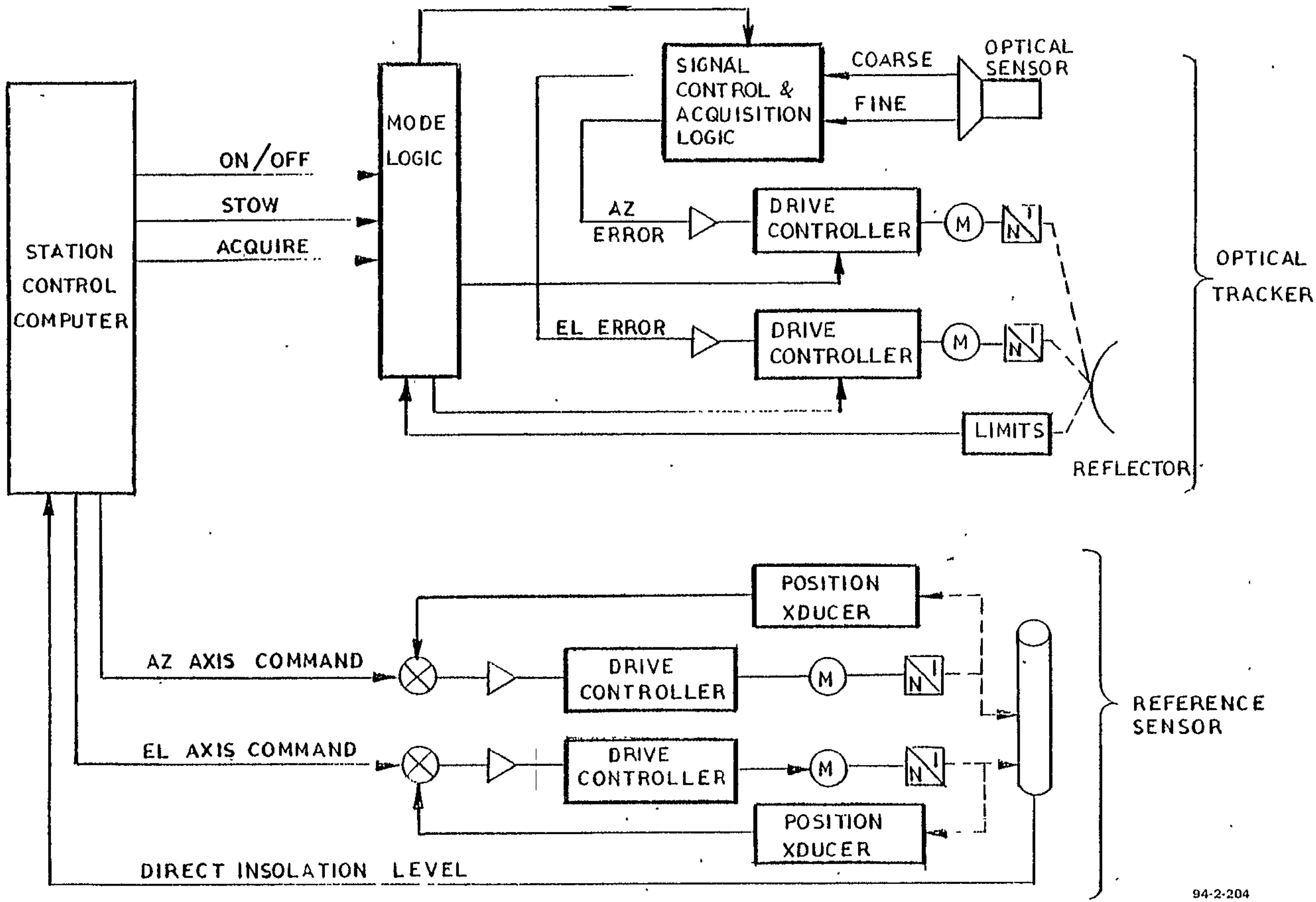


FIGURE 35. OPTICAL TRACKING TECHNIQUE

steptrack feature is accomplished by two step sizes, one slightly larger than the sun's movement, and the other slightly smaller. By this method, the collector will either catch up with the sun or let the sun catch up. A block diagram of this scheme is shown on Figure 36.

d. Conclusions and Selections. Table 18 is an estimate of the various costs for the three tracking systems. Program track has been subdivided into two versions; one with no changes in the structure (from optical or hybrid tracking); and the other with a stiffened, more accurate structure plus an extensive alignment process.

Program tracking with an improved structure was ruled out as too costly. Program tracking with an unchanged structure appears to be cost competetive, however, the tracking error is excessive. Optical tracking is slightly more expensive, but because of acquisition problems this system was eliminated. Therefore, the selection is the Hybrid Tracking System. The advantages of hybrid tracking are:

(1) Deflections of the structure due to wind, gravity or other semi-static effects are automatically accounted for.

(2) The optical sensor is immune to drift and offset effects and provides a simple, reliable means of optically boresighting the collector and removing errors due to the gear train which affect the encoded axis position.

(3) Zero reference position for each axis is not critical since errors are self-calibrated and stored.

(4) A table of average corrections can be generated and stored to be used from day to day, and will provide improved pointing even in the event of optical sensor failure.

(5) The condition of the drive and encoding system can be evaluated by daily transmission of the average correction effects to the station computer. This is used to define maintenance actions.

(6) Installation and alignment is minimal because of the self-calibration feature.

## 2.4.5 FOUNDATION CONCEPTS

The construction cost of the foundation to support the concentrator is a major cost factor and a trade study was made to determine the most economical foundation design.

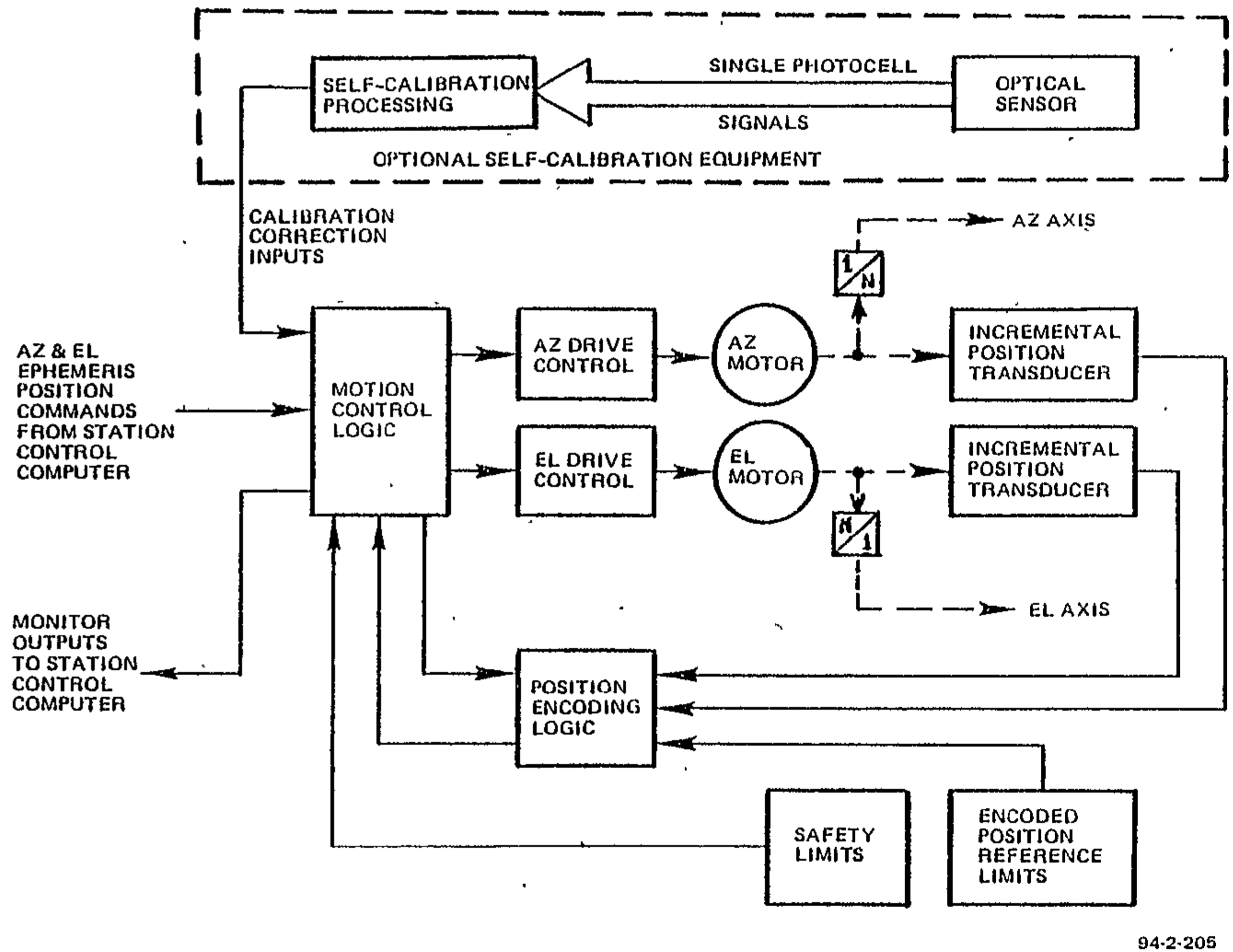


FIGURE 36. HYBRID TRACKING SYSTEM: PROGRAM CONTROL WITH INCREMENTAL POSITION FEEDBACK.

TABLE 18. RELATIVE COSTS OF TRACKING SYSTEMS PER CONCENTRATOR

| | Program Track | | Optical Track | Hybrid Track |
|---|---|---|---|---|
| | Unchanged Structure | Improved Structure | | |
| Position Transducers | $150 | $250 | $ 50 | $150 |
| Electronics | 300 | 300 | 300 | 350 |
| Optical Sensor and Cables | 0 | 0 | 100 | 60 |
| Structure | 0 | 1200 | 0 | 0 |
| Installation and Alignment | 150 | 800 | 0 | 0 |
| Site Insolation Sensor Pedestal | 0 | 0 | 230 | 0 |
| Total | $600 | $2250 | $680 | $560 |
| RMS Tracking Error (mrad) | 7 | 2 | 2 | 2 |

NOTE: Ephemeris commands are obtained from Station Control Computer at negligible cost.

The many factors which influence the cost of the foundation are listed below.

(1) Soil conditions at the site:

- Soil layers and types
- Shear modulus and secant modulus
- Bearing capacity
- Penetration data
- Presence of a water layer

(2) Concentrator size and type of base (a relationship between the foundation loading and concentrator diameter was derived. Also considered was the way the structure distributes the forces and the overturning moment to the foundation).

(3) Design wind loads.

(4) Allowable operational and ultimate structural deflections.

(5) Factor of safety for overturning,

(6) Type of foundation designed,

(7) Total number of foundations at each site (possible use of specialized equipment for high volume foundations), and

(8) Type of construction methods.

A study of foundation costs was made for soil conditions typical of the Southwestern United States. Concentrator diameters of 8, 12, 18 and 26 meters were used with a ring girder foundation (Figure 37); a spread footing with concrete pedestal (Figure 38); and piles (Figure 39). Table 19 summarizes the foundation costs for quantities of 100 sites annually.

The results in Table 19 show a pile foundation is obviously the most economical. A pile made of timber was the type selected. It has a minimum 30-year life span and provides the best friction at the lowest cost. One timber friction-pile is used under each concentrator leg.

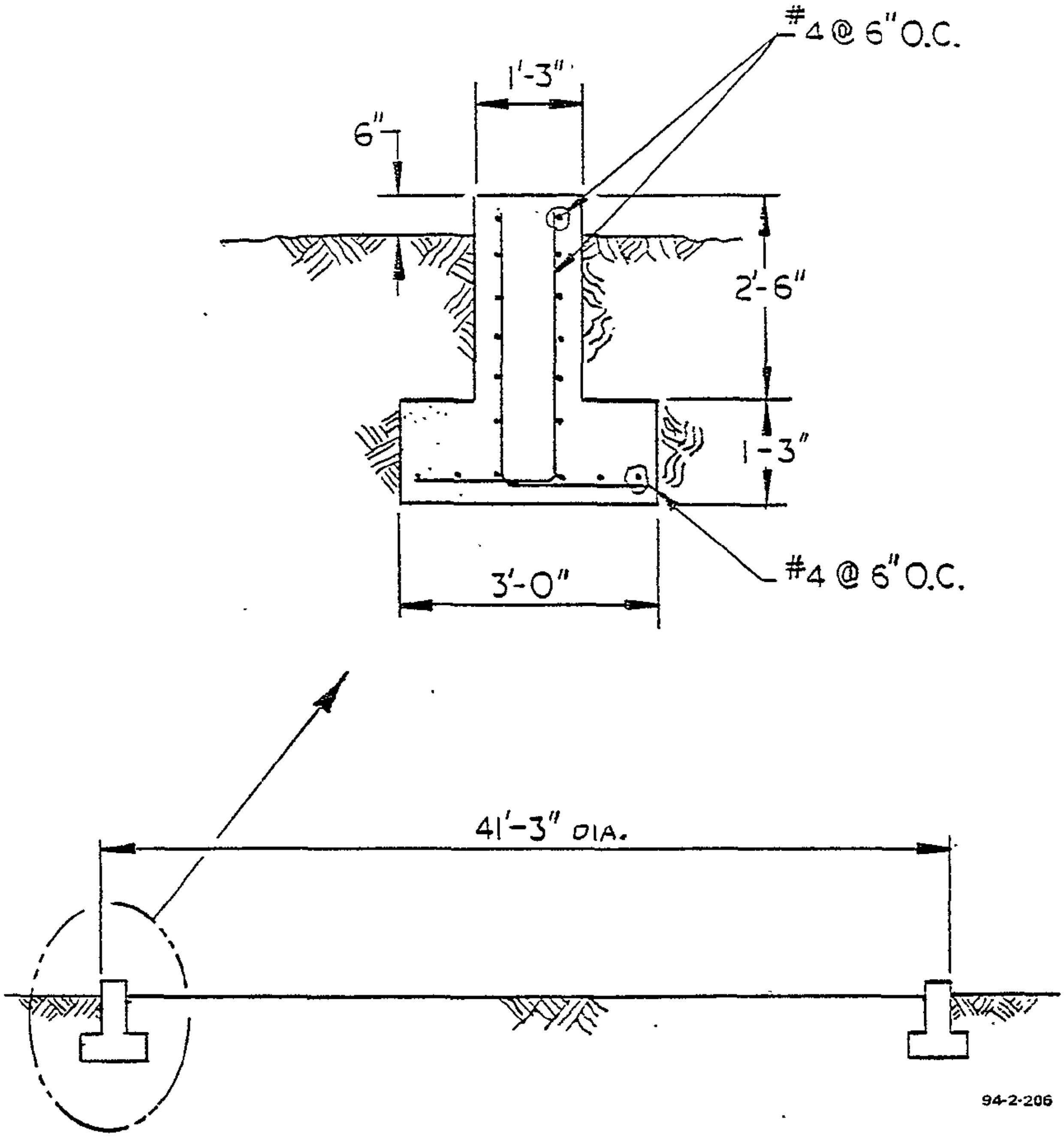


FIGURE 37. TYPICAL RING GIRDER FOUNDATION CONFIGURATION

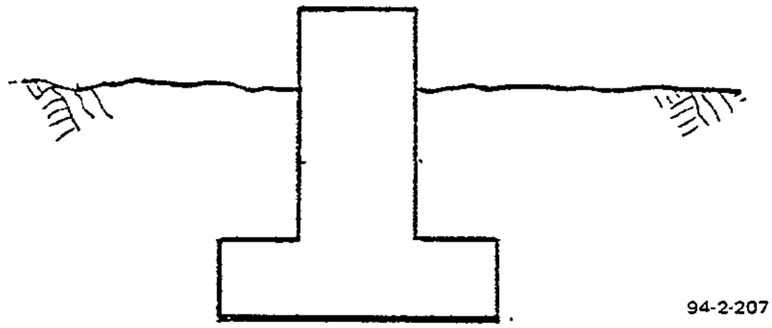


FIGURE 38. SKETCH OF SPREAD FOOTING

TABLE 19. SUMMARY OF FOUNDATION COSTS (100 SITES ANNUALLY)

| Type of Foundation | Size of Concentrator (m) | Foundation Cost Per $m^2$ of Concentrator Aperture |
|---|---|---|
| Ring Girder* | 16 | $60/m$^2$ |
| Pedestal* | 8<br>12<br>18<br>26 | 49<br>48<br>32<br>25 |
| Pile With Pile Cap | 12 | 23 |
| Pile With Grade Beam | 12<br>18 | 18<br>17 |
| Pile With Beam Steel | 12<br>18 | 10<br>11 |

*High cost due to excavation and concrete form work.

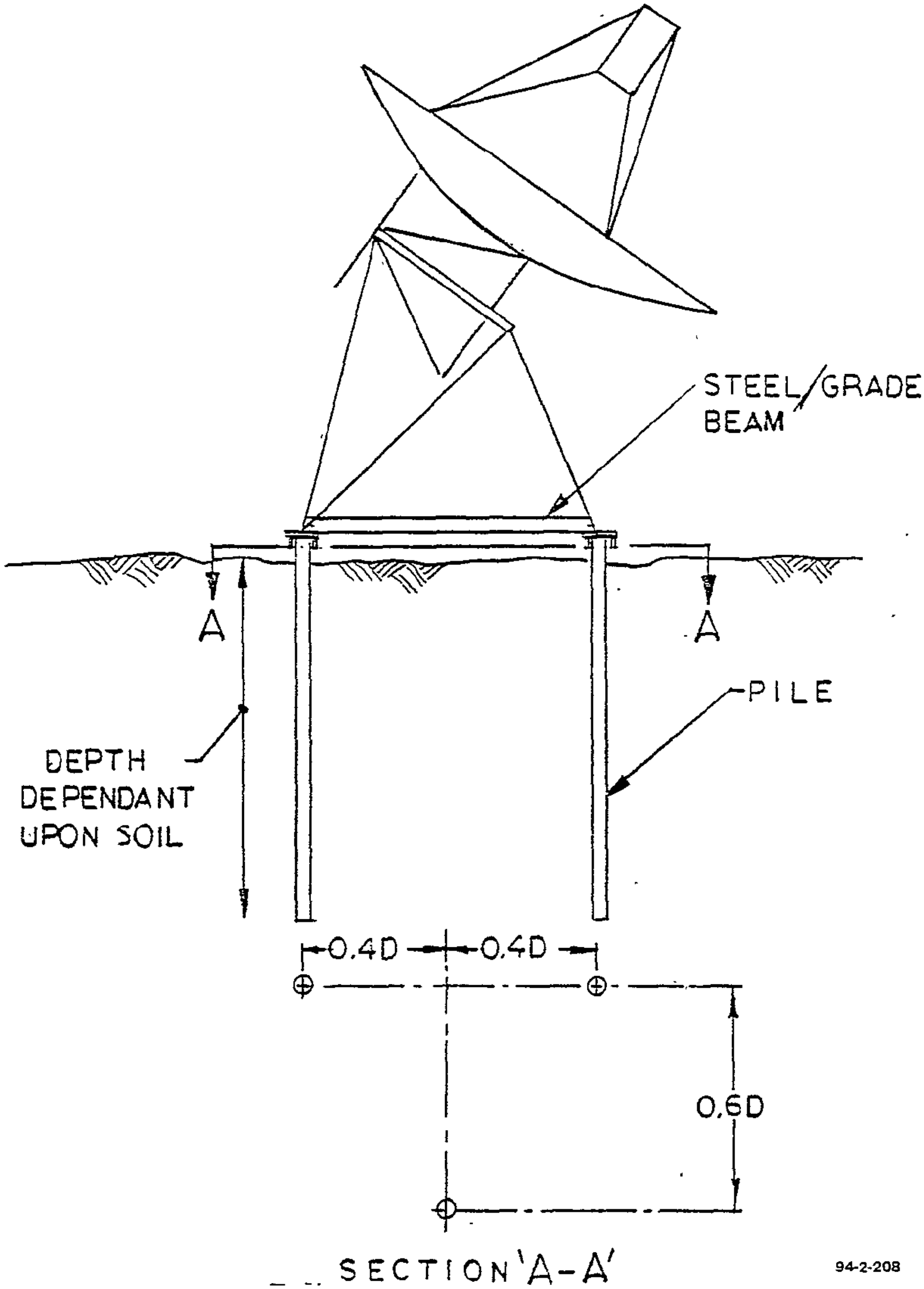


FIGURE 39. TYPICAL PILE FOUNDATION CONFIGURATION

## 2.5 PARAMETRIC COST STUDIES

The concentrator cost (fabricated and installed) is a key parameter in determining the plant energy cost ($\overline{BBEC}$), and the cost/square meter of aperture is an important input in selecting an optimum size. Also investigated was the cost effect as the quantity of small power systems varied from 100 to 5000 sites annually. Other cost analyses that were performed for surface reflectivity, slope error, rim angle, and the equipment weight at the focal point.

### 2.5.1 COST VS DIAMETER AND PRODUCTION RATE

The cost of the concentrator has been determined for aperture diameters ranging from 8 meters to 26 meters, and for various production rates of 1.0 MWe plants. The results are expressed in $\$/m^2$ of aperture area and plotted in Figure 40. A further breakdown of costs for the far term, 5000 sites/yr case is shown on Figure 41. The itemized lists of component and activity costs are tabulated for 100, 500, 1000, and 5000 sites and for diameter variations on Tables 20 through 23.

### 2.5.2 REFLECTIVITY COST ANALYSIS

Systems studies demonstrated that the reflectivity of the concentrator should be as high as possible - commensurate, of course, with the type of material used for the reflective surface. Two materials were chosen for investigation: a metallized plastic film (3M aluminized KE-K-244), and a second-surface draw fusion glass. The reflectivities are 0.86 and 0.95, respectively.

The cost comparison between the two materials was made on the basis of equal reflected energy, that is, the aperture area of a concentrator using tape was increased by 0.95/0.86 or 10.5 percent to provide an equivalent comparison with glass. However, this size increase must also be included in the rest of the concentrator (structure, etc.), which typically costs 5 to 6 times more per unit area than for reflective panels. When all these costs are accounted for the initial capital costs of tape is actually 0.5 to 5.5 percent more expensive than glass, depending on quantity. (This despite the fact the tape panels cost only about 60 percent those for glass on a \$/unit-aperture-area basis.) The real disadvantage, however, is the fact that the tape will have to be replaced several times during the 30-year life, which is an expensive process. Glass is currently predicted to last the entire period (subject to verification tests), plus has the advantage of much better specularity and aging characteristics. These reasons resulted in the decision to recommend draw fusion glass for the baseline concentrator.

### 2.5.3 SURFACE SLOPE ERROR COST ANALYSIS

The cost implications of slope errors 50 percent higher and 50 percent lower than the baseline value of 2.6 milliradians (0.15 degree) were investigated. The contributors to the slope error are: (1) panel manufacturing tolerance, (2) panel gravity and thermal distortion, (3) reflector structure/panel

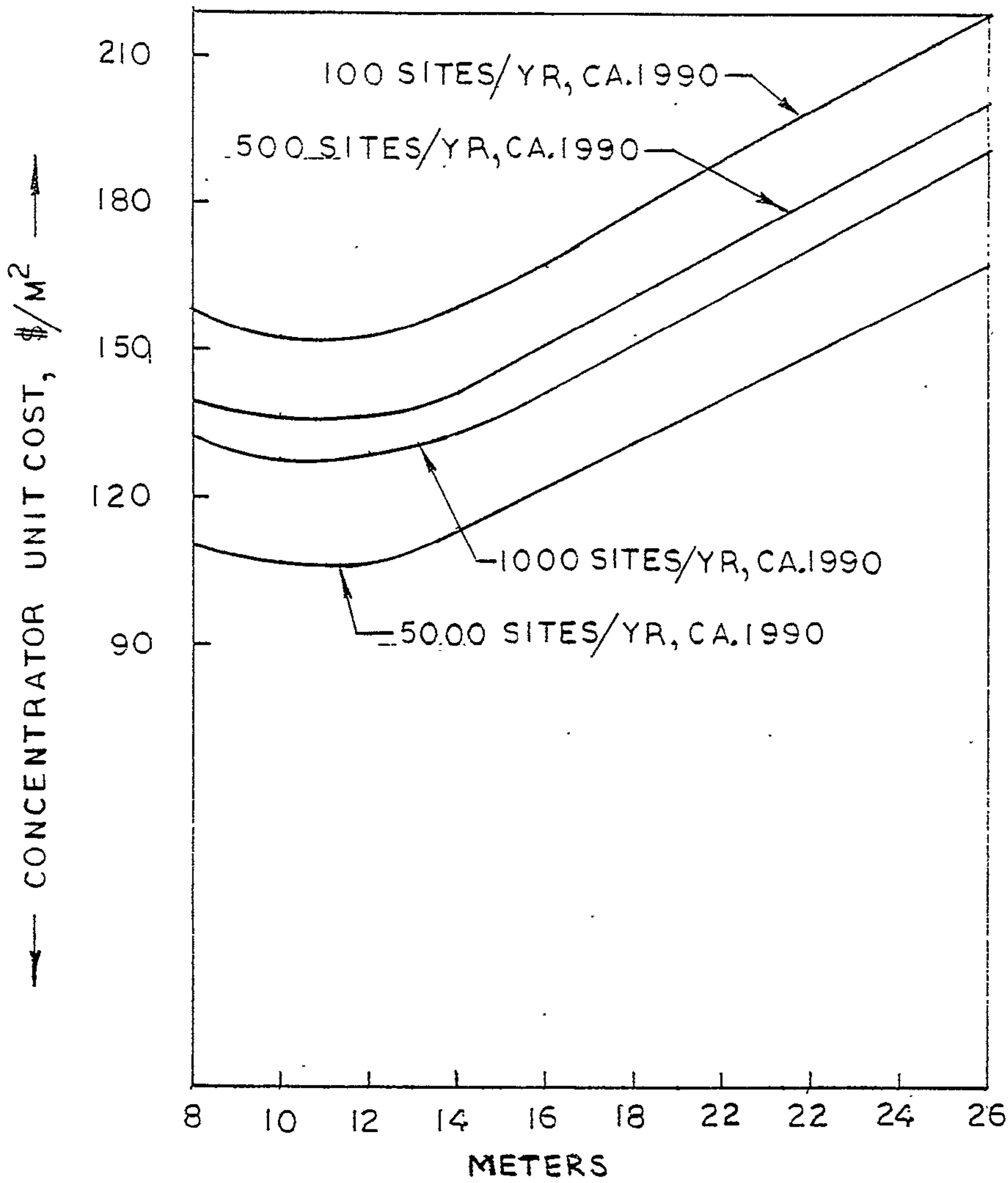


FIGURE 40. INSTALLED CONCENTRATOR COST

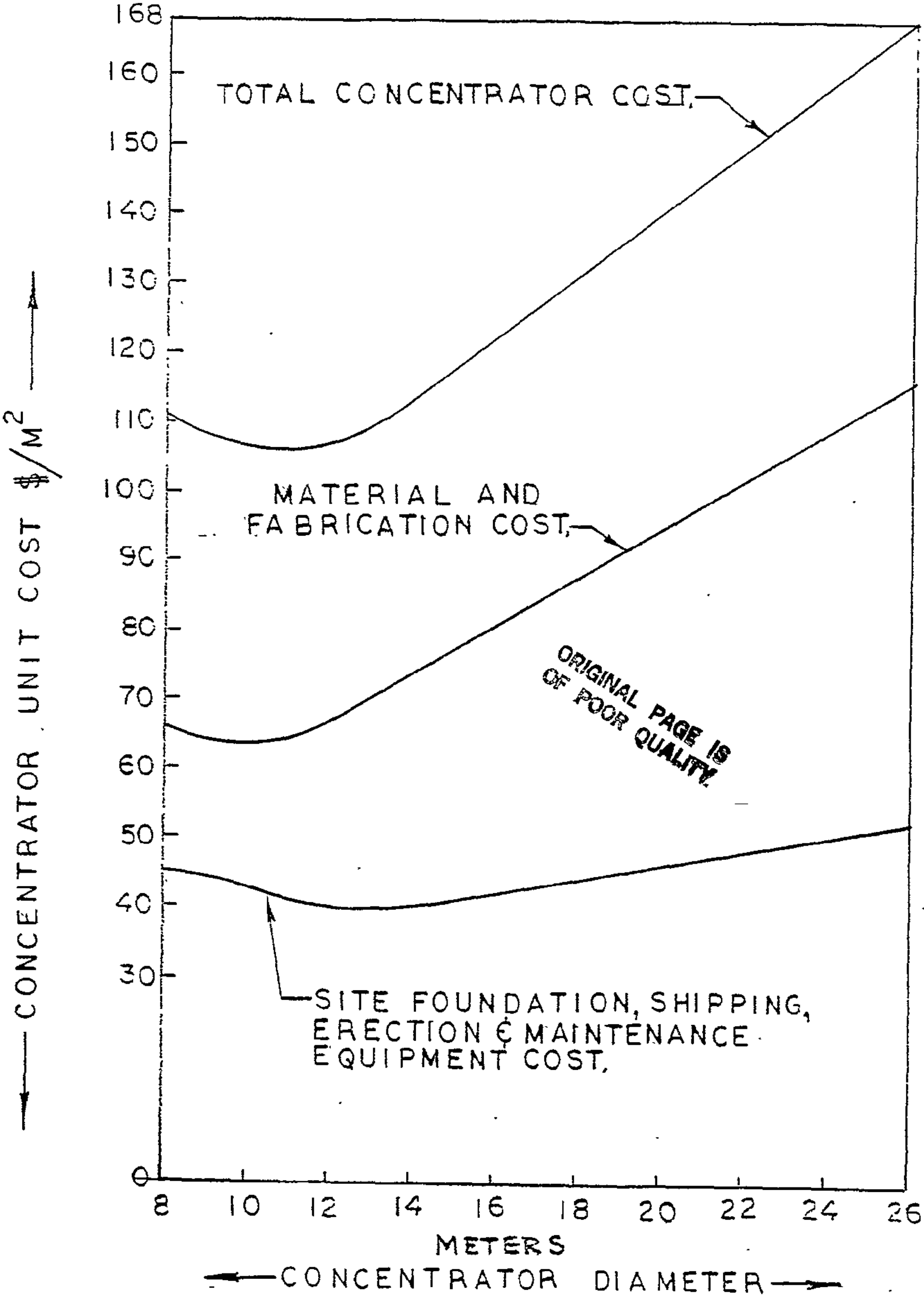


FIGURE 41. COST BREAKDOWN FOR 5000 SITES PER YEAR IN 1990



C-2

TABLE 20. CONCENTRATOR COSTS VS DIAMETER (100 SITES, CA 1990)

| Concentrator Component | Nominal Diameter/Cost ($/M$^2$) | | | | | | |
|---|---|---|---|---|---|---|---|
| | 8M | 10M | 12M | 14M | 16M | 18M | 26M |
| Reflective panels | | | | | | | |
| • Material | $ 20/M$^2$ | $ 20/M$^2$ | $ 20/M$^2$ | $ 20/M$^2$ | $ 20/M$^2$ | $ 21/M$^2$ | $ 22/M$^2$ |
| • Labor | 17 | 16 | 16 | 17 | 17 | 17 | 17 |
| Structure | | | | | | | |
| • Material | 26 | 27 | 31 | 37 | 43 | 49 | 75 |
| • Labor | 9 | 9 | 9 | 9 | 9 | 9 | 9 |
| Mechanical | 23 | 22 | 22 | 22 | 23 | 24 | 30 |
| Tracking Control | 7 | 5 | 4 | 3 | 2 | 2 | 1 |
| Foundation | 11 | 10 | 9 | 9 | 10 | 11 | 11 |
| Erection | 32 | 29 | 27 | 25 | 26 | 27 | 27 |
| Shipping | 4 | 5 | 5 | 6 | 6 | 6 | 8 |
| Project Operation | 3 | 3 | 3 | 3 | 3 | 3 | 3 |
| Maintenance Equip. | 7 | 7 | 7 | 8 | 8 | 9 | 16 |
| Total | $159/M$^2$ | $153/M$^2$ | $153/M$^2$ | $159/M$^2$ | $167/M$^2$ | $178/M$^2$ | $219/M$^2$ |

NOTE: 1978 Base Year Dollars

TABLE 21. CONCENTRATOR COSTS VS DIAMETER (500 SITES, CA 1990)

| Concentrator Component | Nominal Diameter/Cost ($/M$^2$) | | | | | | |
|---|---|---|---|---|---|---|---|
| | 8M | 10M | 12M | 14M | 16M | 18M | 26M |
| Reflective Panels | | | | | | | |
| • Material | $ 18/M$^2$ | $ 18/M$^2$ | $ 18/M$^2$ | $ 18/M$^2$ | $ 18/M$^2$ | $ 19/M$^2$ | $ 20/M$^2$ |
| • Labor | 15 | 14 | 14 | 15 | 15 | 15 | 15 |
| Structure | | | | | | | |
| • Material | 24 | 25 | 29 | 35 | 41 | 47 | 72 |
| • Labor | 8 | 8 | 8 | 8 | 8 | 8 | 8 |
| Mechanical | 20 | 19 | 19 | 19 | 20 | 20 | 25 |
| Tracking Control | 5 | 4 | 3 | 2 | 2 | 2 | 1 |
| Foundation | 10 | 9 | 8 | 8 | 9 | 10 | 10 |
| Erection | 29 | 27 | 25 | 23 | 24 | 25 | 25 |
| Shipping | 4 | 5 | 5 | 6 | 6 | 6 | 8 |
| Project Operation | 2 | 2 | 2 | 2 | 2 | 2 | 2 |
| Maintenance Equip. | 6 | 6 | 6 | 6 | 7 | 8 | 15 |
| Total | $141/M$^2$ | $137/M$^2$ | $137/M$^2$ | $142/M$^2$ | $152/M$^2$ | $162/M$^2$ | $201/M$^2$ |

NOTE: 1978 Base Year Dollars

TABLE 22. CONCENTRATOR COSTS VS DIAMETER (1000 SITES, CA 1990)

| Concentrator Component | Nominal Diameter/Cost ($/M²) | | | | | | |
|---|---|---|---|---|---|---|---|
| | 8M | 10M | 12M | 14M | 16M | 18M | 26M |
| Reflective Panels | | | | | | | |
| • Material | 17 | 17 | 17 | 17 | 17 | 18 | 19 |
| • Labor | 14 | 13 | 13 | 14 | 14 | 14 | 14 |
| Structure | | | | | | | |
| • Material | 23 | 24 | 28 | 33 | 39 | 45 | 70 |
| • Labor | 7 | 7 | 7 | 7 | 7 | 7 | 7 |
| Mechanical | 18 | 17 | 17 | 17 | 18 | 19 | 23 |
| Tracking Control | 5 | 3 | 3 | 2 | 1 | 1 | 1 |
| Foundation | 10 | 9 | 8 | 8 | 9 | 10 | 10 |
| Erection | 27 | 25 | 23 | 21 | 22 | 23 | 23 |
| Shipping | 4 | 5 | 5 | 6 | 6 | 6 | 8 |
| Project Operation | 2 | 2 | 2 | 2 | 2 | 2 | 2 |
| Maintenance Equip. | 6 | 6 | 6 | 6 | 7 | 8 | 14 |
| Total | $133/M² | $128/M² | $129/M² | $133/M² | $142/M² | $153/M² | $191/M² |

NOTE: 1978 Base Year Dollars

TABLE 23. CONCENTRATOR COSTS VS DIAMETER (5000 SITES, CA 1990)

| Concentrator Component | Nominal Diameter/Cost ($/M²) | | | | | | |
|---|---|---|---|---|---|---|---|
| | 8M | 10M | 12M | 14M | 16M | 18M | 26M |
| Reflective Panels | | | | | | | |
| • Material | $ 13/M² | $ 13/M² | $ 13/M² | $ 13/M² | $ 13/M² | $ 14/M² | $ 15/M² |
| • Labor | 10 | 9 | 9 | 10 | 10 | 10 | 10 |
| Structure | | | | | | | |
| • Material | 19 | 20 | 23 | 29 | 35 | 40 | 64 |
| • Labor | 6 | 6 | 6 | 6 | 6 | 6 | 6 |
| Mechanical | 15 | 14 | 14 | 14 | 15 | 16 | 20 |
| Tracking Control | 3 | 2 | 2 | 2 | 1 | 1 | 1 |
| Foundation | 9 | 8 | 7 | 7 | 8 | 9 | 9 |
| Erection | 25 | 23 | 21 | 20 | 21 | 21 | 21 |
| Shipping | 4 | 5 | 5 | 6 | 6 | 6 | 8 |
| Project Operation | 1 | 1 | 1 | 1 | 1 | 1 | 1 |
| Maintenance Equip. | 6 | 6 | 6 | 6 | 6 | 7 | 13 |
| Total | $111/M² | $107/M² | $107/M² | $114/M² | $122/M² | $131/M² | $168/M² |

NOTE: 1978 Base Year Dollars

alignment tolerance, (4) gravity and thermal distortion of the reflector structure and (5) wind distortion of the reflector structure and panels. Average wind forces are small for 98 percent of the annual operating time at the Barstow, Ca. site. However, the larger wind forces for the remaining 2 percent of operation have important implications for the design and have been included.

The baseline design surface slope errors (2.6 milliradians; 0.15 degrees) are allocated for the five different concentrator diameters in Table 24. The cost associated with each component affected by the surface slope error change was determined relative to the baseline concept. The total concentrator costs for the three values of slope error are plotted on Figure 42. These results are based on 5000 sites annually, circa 1990.

Relaxing the 2.6 milliradian surface slope error by 50 percent decreases total concentrator costs by 8 percent, whereas increasing it by the same amount increases costs by an average 20 percent. These results were included in the systems cost analysis to determine which configuration has the lowest energy costs (BBEC).

2.5.4 CONCENTRATOR RIM ANGLE COST ANALYSIS

Evaluation of rim angle involves trade-offs among such parameters as structural weight and stiffness, size of components for the Az-El drive subsystem, radius of curvature of the concentrator surface, and the required size of the concentrator supports. A large rim angle (for a given concentrator diameter) leads to short tripod legs, relatively smaller bending moments, and less blockage; a smaller angle leads to a flatter, easier-to-fabricate paraboloidal surface, but the radial truss diagonal members may be heavier.

This investigation considered rim angles in the range of 50 degrees to 70 degrees for the front-braced concept. The factors summarized above were evaluated in terms of cost versus rim angle; the results are shown in Figure 43. Note that the minimum lies in the vicinity of a 65 degree rim angle.

2.5.5 POWER MODULE WEIGHT/COST ANALYSIS

Power module (receiver/engine/generator) weight primarily affects the tripod support structure, the reflector structure, and the pedestal. A structural analysis resulted in the following general rules:

(1) Each 500 lb weight increment (227 kg) at the apex increases the the tripod leg maximum forces and weight by 5 percent. This in turn increases total solar blockage/shadowing by ∿ 0.1 percent.

(2) Each 500 lb weight increment at the tripod apex increases the maximum force in key structural elements such that the total reflector weight increases 1.1 percent.

TABLE 24. SURFACE SLOPE ERROR BUDGET FOR BASELINE CONDITION (2.6 MILLIRADIANS)

| | | Nominal Diameter | | | | |
|---|---|---|---|---|---|---|
| | | 8M | 12M | 18M | 18.6M | 26M |
| A. | Panel Manufacturing | 1.5 | 1.5 | 1.5 | 1.5 | 1.4 |
| | Panel Gravity & Thermal | 1.25 | 1.25 | 1.25 | 1.25 | 1.25 |
| | Structure/Panel Alignment | 1.69 | 1.67 | 1.59 | 1.55 | 1.3 |
| | Structure Gravity & Thermal | 0.2 | 0.3 | 0.6 | 0.7 | 1.2 |
| | RSS Subtotal | 2.59 | 2.59 | 2.59 | 2.59 | 2.58 |
| | Wind; 98% Operating Time Structure & Panels | 0.2 | 0.2 | 0.2 | 0.2 | 0.3 |
| | RSS Total (98%) | 2.6 | 2.6 | 2.6 | 2.6 | 2.6 |
| B. | Above Subtotal | 2.59 | 2.59 | 2.59 | 2.59 | 2.58 |
| | Wind; 1.8% Operating Time Structure & Panels | 1.0 | 1.0 | 1.1 | 1.1 | 1.3 |
| | RSS Total (1.8%) | 2.8 | 2.8 | 2.8 | 2.8 | 2.9 |
| C. | Above Subtotal | 2.59 | 2.59 | 2.59 | 2.59 | 2.58 |
| | Wind; 0.2% Operating Time Structure & Panels | 1.8 | 1.9 | 2.0 | 2.1 | 2.5 |
| | RSS Total (0.2%) | 3.2 | 3.2 | 3.3 | 3.3 | 3.6 |

- All Values in mrad
- Radial and Tangential Slope Errors are Combined
- All Values are 1$\sigma$

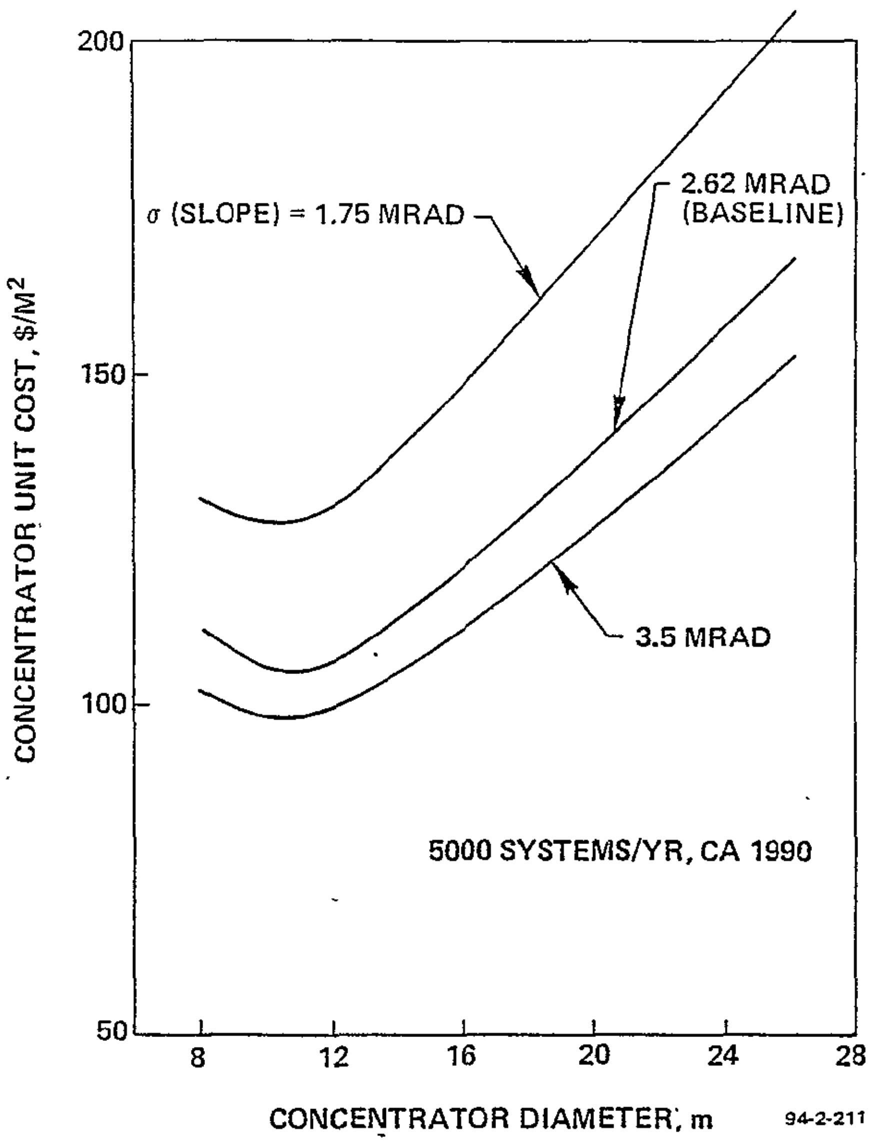


FIGURE 42. THE EFFECT OF SLOPE ERROR ON CONCENTRATOR COST

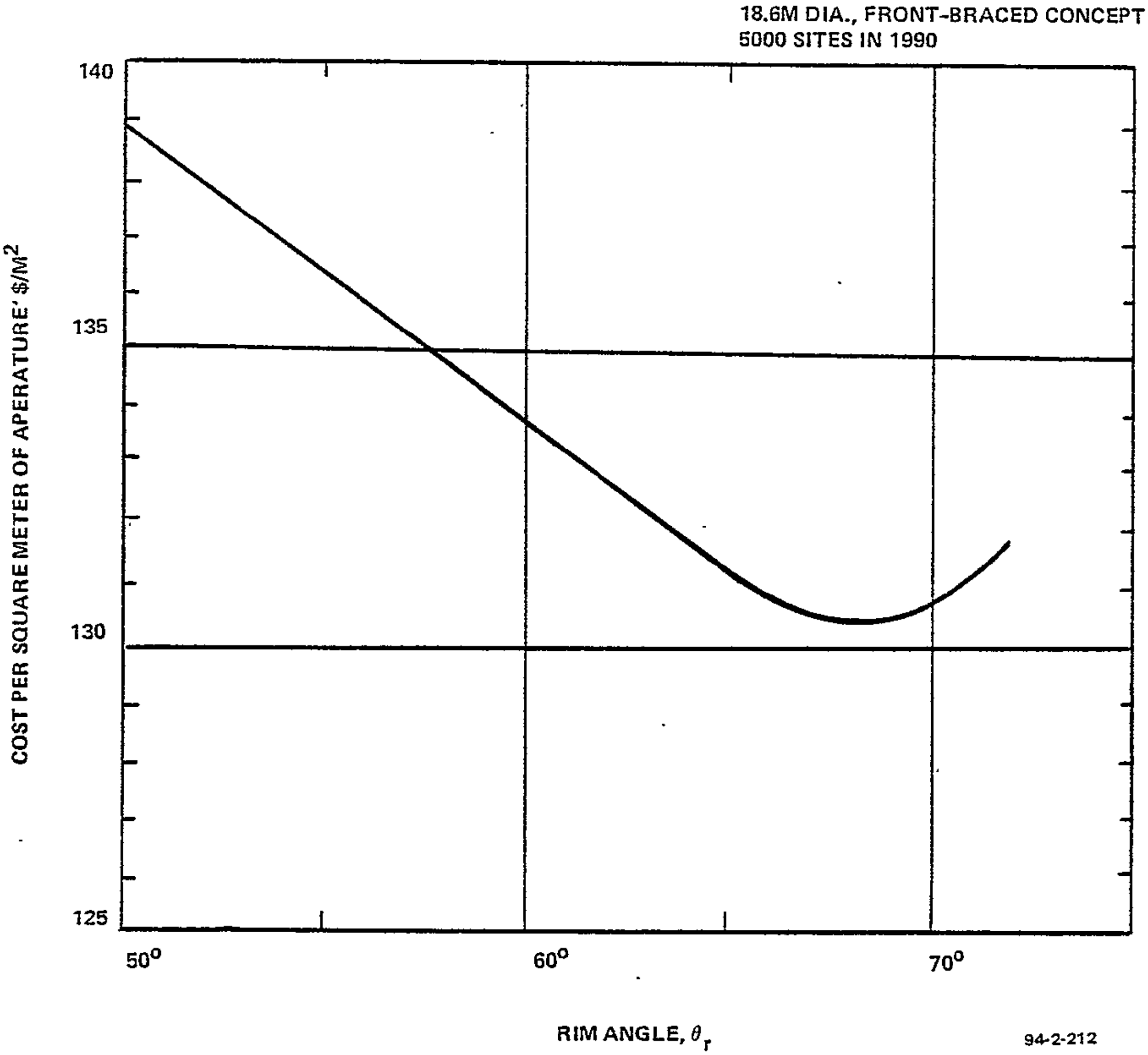


FIGURE 43. EFFECT OF RIM ANGLE ON CONCENTRATOR COST

(3) Each additional 500 lb weight increment at the tripod apex increases the weight at the top of the pedestal by 5 percent, and increases the gravity unbalance moment at the elevation axis by 12 percent. This results in half of the pedestal structural components increasing in weight by 6 percent, half of the mechanical components and drive motors increasing in weight or power by 4 percent, and the foundation cost is increased 1 percent.

(4) Combining these factors results in a concentrator cost increase of 1.1 percent for each 500 lb (227 kilogram) increment in the power module weight. The breakdown for the various components are shown in Table 25. In addition the total solar blockage/shadowing is increased approximately 0.1 percent, due to the larger tripod legs.

TABLE 25. COST EFFECT OF WEIGHT INCREASE AT TRIPOD APEX (PER 500 POUNDS)

| Component/Task | Baseline Cost | Cost Increase |
|---|---|---|
| Panels | 15.9% | |
| Tripod-Material | 3.4 x .05 = | 0.17% |
| Labor | 1.1 | |
| Reflector-Material | 7.9 x .011 = | 0.09 |
| Labor | 2.3 | |
| Pedestal-Material | 14.0 x .06/2 = | 0.42 |
| Labor | 5.5 | |
| Supports for Equipment | 0.8 | |
| Mechanical Components | 13.9 x .04/2 = | 0.28 |
| Drive Motors | 1.0 x .04/2 = | 0.02 |
| Tracking Control | 0.8 | |
| Foundation | 6.0 x .01 = | 0.06 |
| Erection & Cranes | 16.3 | |
| Shipping-Panels | 1.5 | |
| Balance | 2.1 x .02 = | 0.04 |
| Project Operation | 2.0 | |
| Maintenance Equipment | 5.5 | |
| | 100.0% | 1.1% |

NOTE: Baseline is the nominal 18m diameter concentrator, far term, 100-1 MWe sites.

## SECTION 3

## SELECTED CONCEPT COMPONENT DEFINITION

The previous sections have presented analyses used in the selection of concentrator concept components. This section: (1) describes the baseline concentrator hardware in more detail, (2) provides calculated performance data, (3) discusses various fabrication and/or procurement techniques, (4) reviews operation and maintenance requirements, and (5) provides an analysis of predicted subsystem reliability. Life Cycle cost estimates and sensitivity analyses are presented in Sections 4 and 5, respectively.

The information presented in this section is based on the 4-1/2 or 6-1/2 year program, however, the system is basically the same for the 3-1/2 year case.

### 3.1 CONCENTRATOR COMPONENT DESCRIPTION

#### 3.1.1 REFLECTOR PARAMETERS

The concentrator reflector that was selected by the system level analysis for the 4-1/2 and 6-1/2 year program has an aperture area of 272 square meters with an average diameter of 18.6 meters and a rim-angle of 65 degrees. The performance parameters associated with this selection are a reflectivity of 95%, an average dust/dirt degradation factor of 95 percent, a solar blockage shadowing factor of 92 percent, a rms surface slope error of 2.6 milliradians and rms tracking accuracy of 1.7 milliradians. Each 1 MWe site contains 19 azimuth-elevation type concentrators (18 plus 1 for storage requirements).

#### 3.1.2 REFLECTOR SURFACE PANELS

Two reflector panel constructional concepts were chosen for further development and testing, as described in Paragraph 2.4.1. Both concepts are pie-shaped gores. There are five rows in the radial direction, and 18 panels in each row. The average panel length is 2.3 meters (7.7 feet); the average panel width is 1.3 meter (4.4 ft).

Figure 44 depicts the manufacturing steps used for one concept. It is a sandwich formed by the reflective glass, cellular glass and sheet steel. The glass sheet chosen for production is Corning draw fusion process, Code 7806 modified glass. Prototypes made in Phase II would be of Code 0317 since 7806 will not be available until production quantities are required. Chemical silvering will be applied to the glass in the flat condition by a conventional process line. The metal cladding, probably copper, would be applied on the same line.

The cellular glass material selected for Phase III panels is Foamsil made by Pittsburgh-Corning Corporation. It is a cellular borosilicate glass made without $H_2S$ gasses in the porosity and has virtually the same cost as soda lime glass. The advantage over soda lime glass is that borosilicate offers more resistance to stress rate corrosion, and therefore has more design margin. Also the potential for $H_2S$ attack on the silver is eliminated. The current

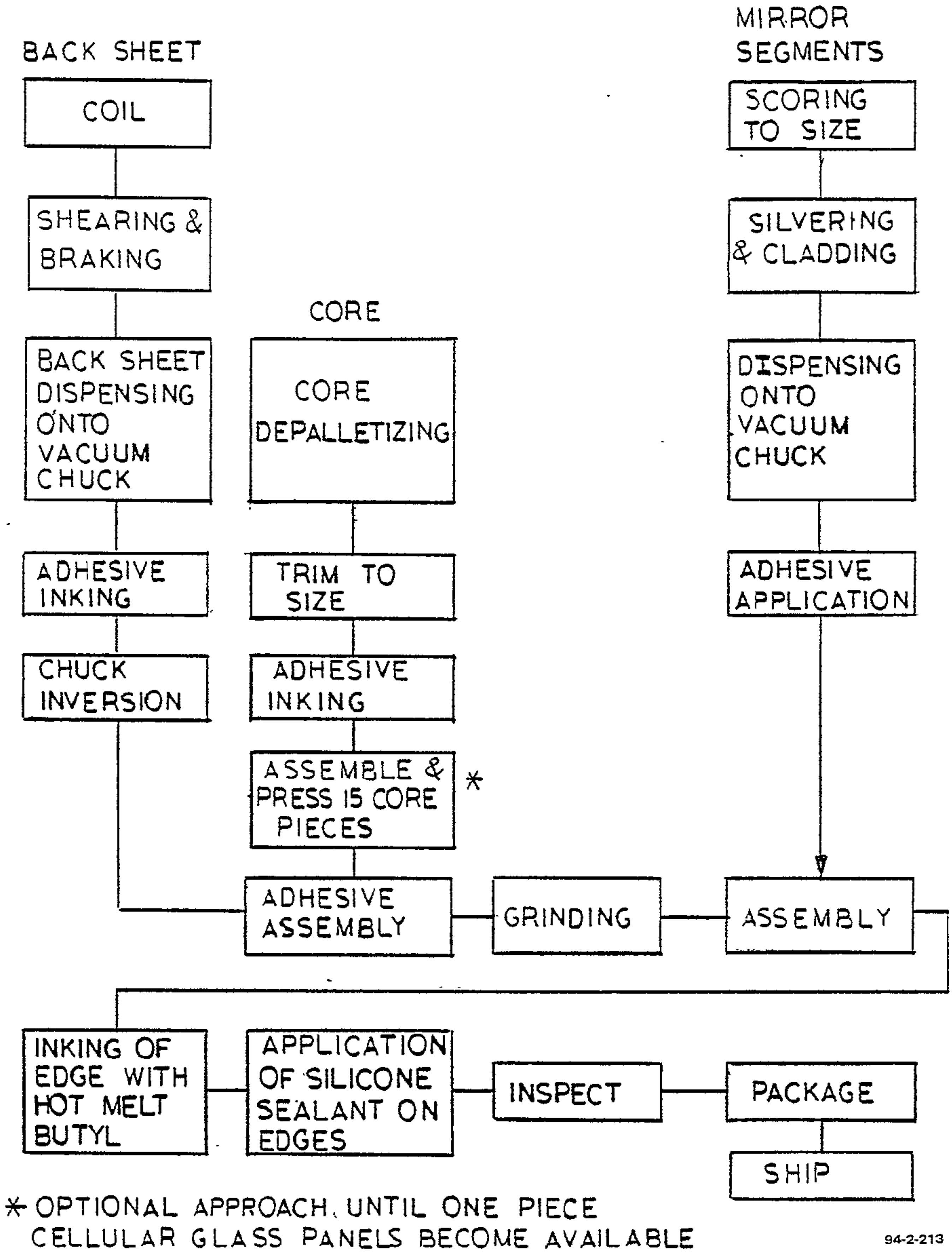


FIGURE 44. FLOW CHART OF MIRROR PANEL MANUFACTURING – GLASS SANDWICH DESIGN

expectation is that no cellular glass production facility will be able to produce blocks large enough for monolithic core members required for SPS within the time period needed. Therefore, adhering one block to another to form a core blank will be required. Various adhesive techniques would be tested to determine the best approach.

Manufacturing tasks for the baseline panel configuration are outlined on Figure 45. Six to eight pie-shaped facets are made of low unreduced iron draw-fusion glass. As with the previous concept, glass would initially be Code 0317 Corning, replaced by Code 7806 as available. The glass is scored to size and heat softened. It is press formed and cooled rapidly enough to impart additional strength.

The convex side of the pressed glass is chemically silvered and clad with a protective metal such as copper. Conventional "paint" used for architectural mirrors is layered over the cladding, the type used will be based on deterioration studies now in progress by Sandia Laboratories. The curved mirror facets are supported by a stamped 28 gauge galvanized carbon sheet steel sandwich structure separated by 2 inches of organic structural foam. The attachment of the mirror facets to the steel/foam sandwich is by means of a layer of silicone rubber adhesive which allows the glass to expand independently of the steel sandwich. Final glass thickness (0.050" to 0.093") and substrate attachment (with or without pads) will be developed later. Attachment of the panels to the concentrator is by means of stamped steel clips which are mounted to the sandwich and bolted to the truss reflector structure.

### 3.1.3 REFLECTOR STRUCTURE AND RECEIVER SUPPORT SYSTEM

The concept selected for the reflector structure and receiver support system is a unique derivative of the reflector backup structure currently used throughout the industry for communications antennas. This concept (proprietary) has the principal support structure for the panels located in front of the reflecting surface, which significantly enhances the inherent stiffness of the trussed structure. The truss depth can be made larger without any impact on the distance of its centroid from the elevation axis (thus without any increase in gravity and wind overturning movements) which improves the distribution of loads within the structure by providing direct rim-to-rim connection. Figures 46 and 47 depict the structure in front of and behind the reflective surface, respectively.

The reflector structure is a space truss composed of trusses radiating from the center (Figure 48). Torsional bracing is provided in the planes of the bottom chords for additional stiffness and stability. The joints of the top and bottom chords of the radial trusses are connected in the circumferential direction by hoop members. A typical joint is shown in Figure 49. As noted in the figure, the structure is made of square tubing approximately 2-inches in cross section. The tubing is mashed to form the cost-effective joints.

### 3.1.4 PEDESTAL SUPPORT STRUCTURE

The selected azimuth-elevation concentrator is shown in Figure 50. A major advantage of this concept is the ability to position the central azimuth

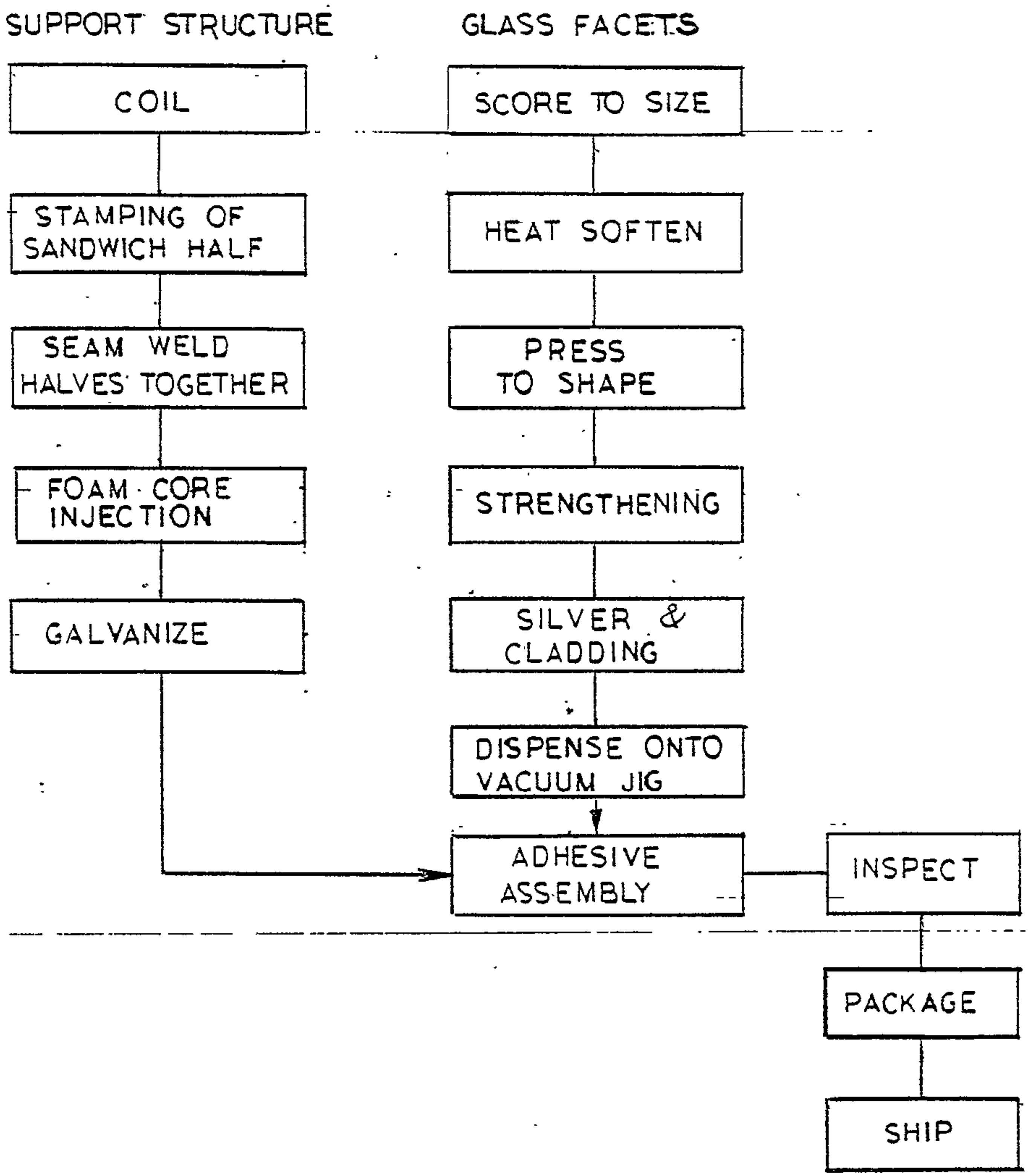


FIGURE 45. FLOW CHART OF MIRROR PANEL MANUFACTURING
PRESSED GLASS FACET DESIGN (BASELINE)

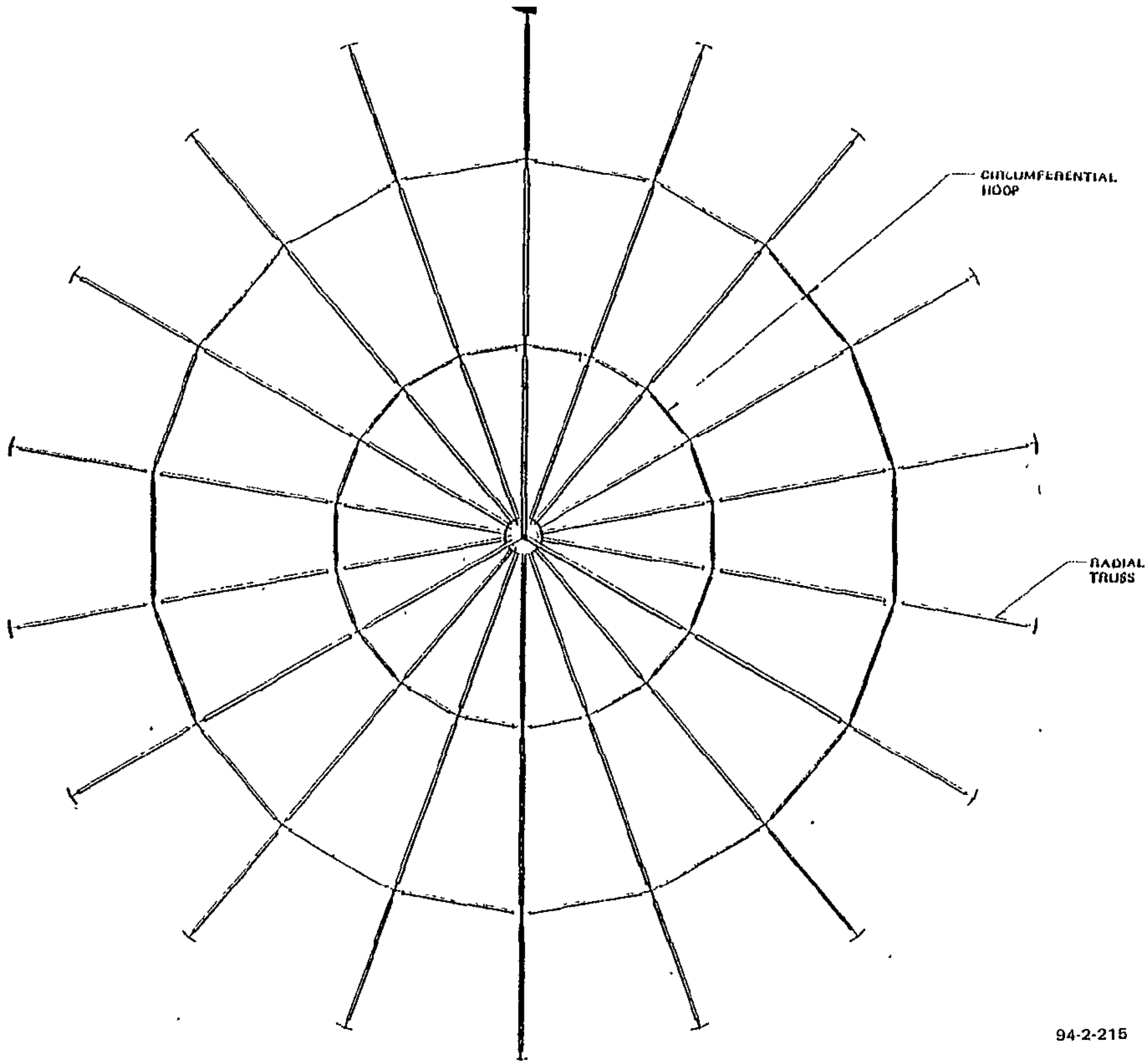


FIGURE 46. FRONT VIEW OF STRUCTURE FOR 18.6 METER DIAMETER CONCENTRATOR

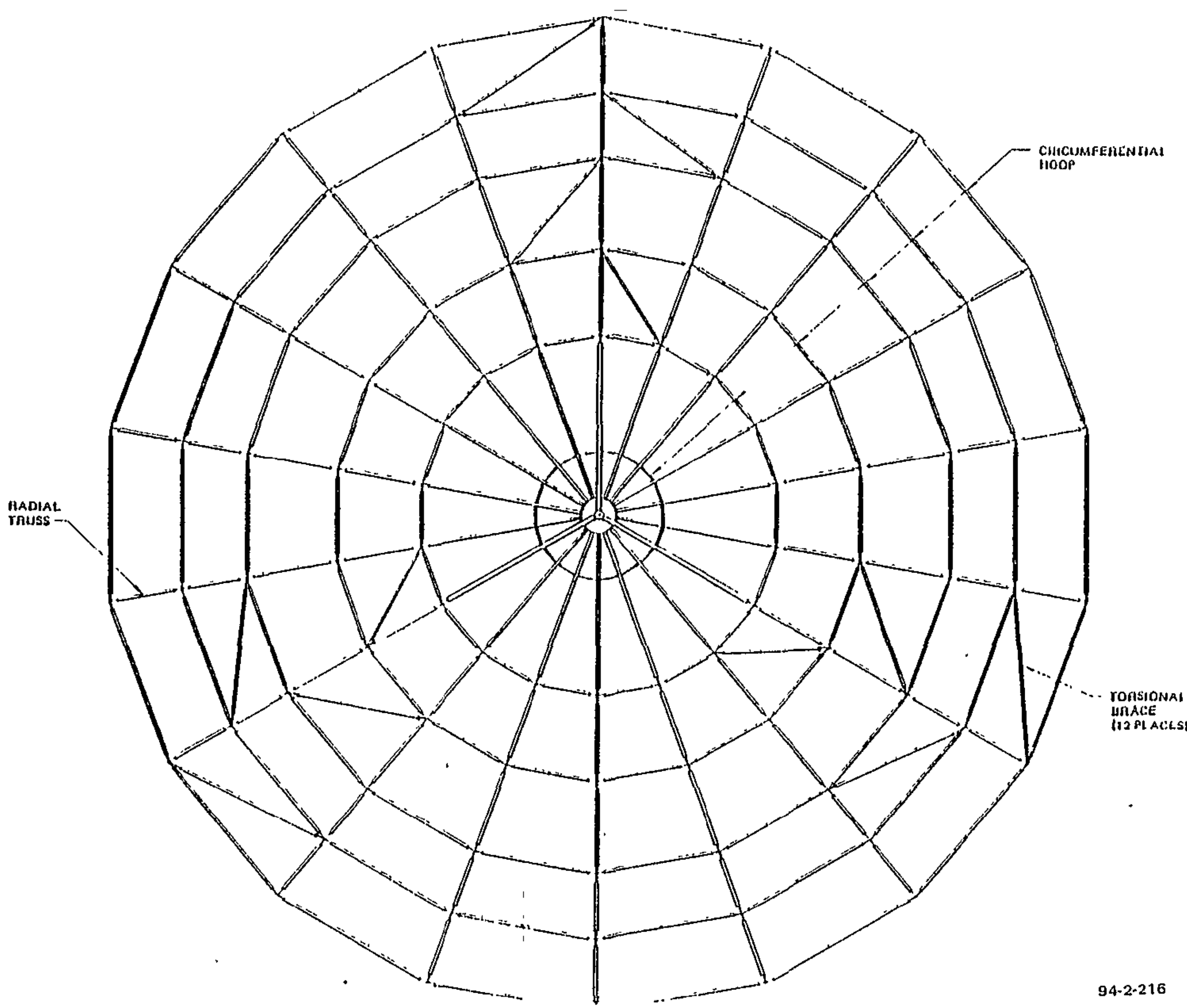


FIGURE 47. REAR VIEW OF STRUCTURE FOR 18.6 METER DIAMETER CONCENTRATOR

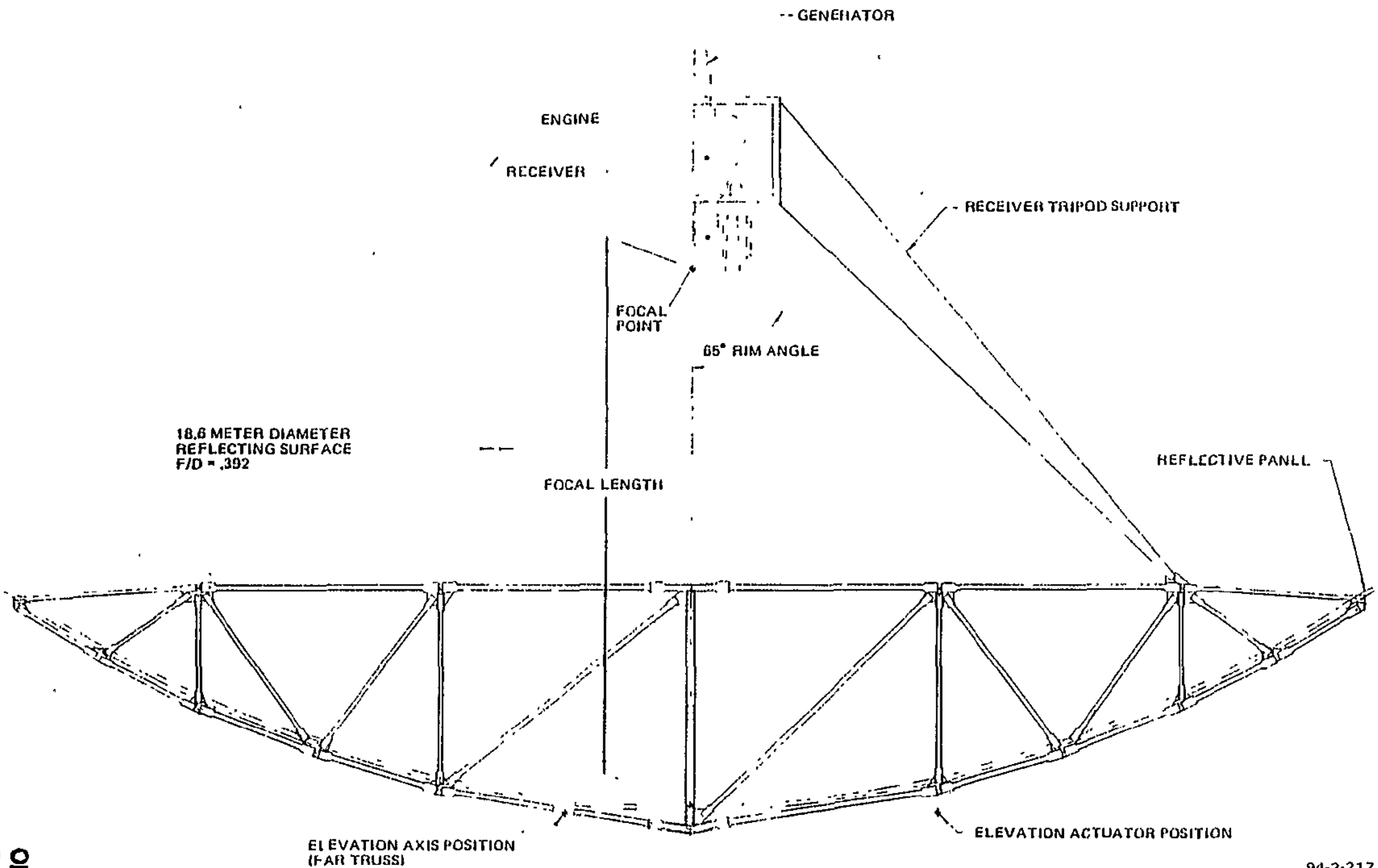


FIGURE 48. RADIAL TRUSS FOR FRONT BRACED 18.6 METER CONCENTRATOR

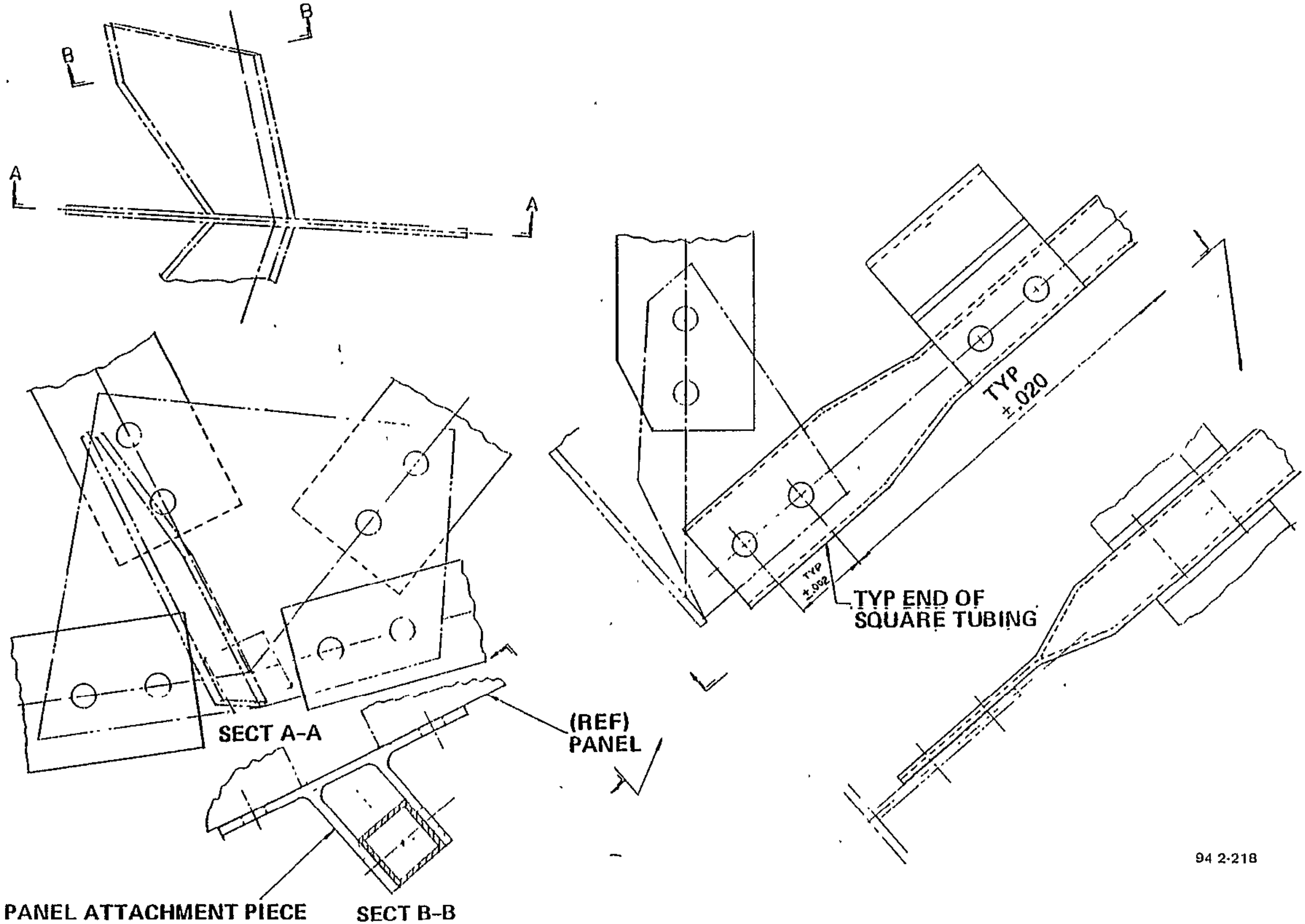


FIGURE 49. TYPICAL REFLECTOR TRUSS JOINT

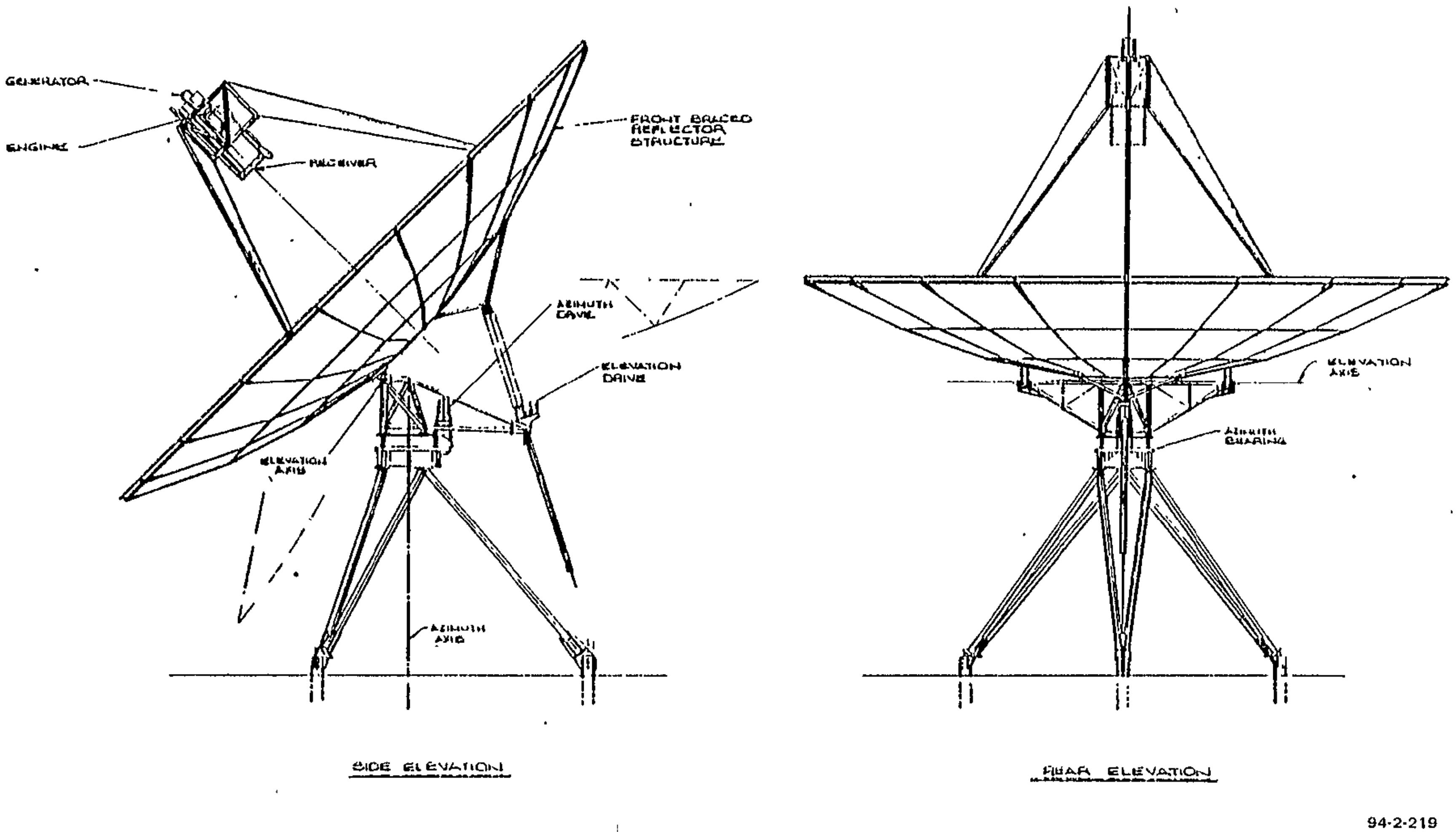


FIGURE 50. BASELINE FRONT-BRACED 18.6 METER SOLAR CONCENTRATOR/POWER MODULE CONCEPT

bearing at an optimum height whereby minimizing the overall cost. The following features are an important part of this concept and are discussed in detail.

- Tall fixed pedestal which spreads loads to the three foundation piles.
- Short azimuth-rotating turret structure which collects loads from the three reflector support points and transfers them to the azimuth bearing.
- Azimuth bearing and drive.

3.1.4.1 Fixed Pedestal. The pedestal consists of three dual structural members (six total) transferring loads from three points on the underside of the azimuth bearing housing to the three foundation piles. All construction is steel and it is anticipated that square tubing will prove to be the most economical for volume fabrication. Weathering steel (such as Cor-Ten) will be used to provide 30-year life with no maintenance or corrosion problems. Access provisions are not required as part of each concentrator since the special maintenance/cleaning vehicle (described in Section 3.5) will provide easy access to any point on the concentrator.

3.1.4.2 Turret Structure. The turret structure shown in Figure 51 is the uppermost portion of the pedestal. It rotates above the azimuth bearing housing and supports the two elevation bearings and the elevation actuator. The turret structure is a space-frame consisting of four connected tetrahedrons fabricated of square steel tubing and bolted to the top flange of the upper azimuth bearing housing. The design will utilize simple shop assembly techniques and bolted field erection. Tubing members are sized to support maximum design loads plus safety factor and no secondary or redundant bracing is required.

### 3.1.5 AZIMUTH BEARING AND HOUSING

The azimuth bearing shown in Figure 51 consists of a 4-point contact ball bearing having a ball pitch diameter of 54 inches, a bore of 48 inches and an outside diameter of 61.8 inches. This configuration, in which the balls contact the races at angles of 45° with respect to the axis of rotation, provides a turntable-type of bearing. This bearing is capable of simultaneously supporting axial loads (vertical in this case) radial (horizontal) loads and moment loads about any diametrical axis. Neoprene lip oil seals are provided to seal in lubricant and exclude moisture and dirt. Grease fittings are installed in the bore of the inner race so that grease can be introduced directly into the ball path through drilled passages. The outer race of the bearing, which is the stationary member, is mounted on the flange of the lower bearing housing by bolts passing through the bearing race. An accurately machined pilot shoulder is provided on the bearing outer race which fits closely with a corresponding pilot on the lower bearing housing. This ensures that the roundness is maintained when the bearing is installed. The inner race of the bearing is similarly mounted on the upper bearing housing. The bearing housings, both upper and lower, are cylinders with the same diameter as the ball races, and have wide top and bottom flanges. The deep section provides stiffness for

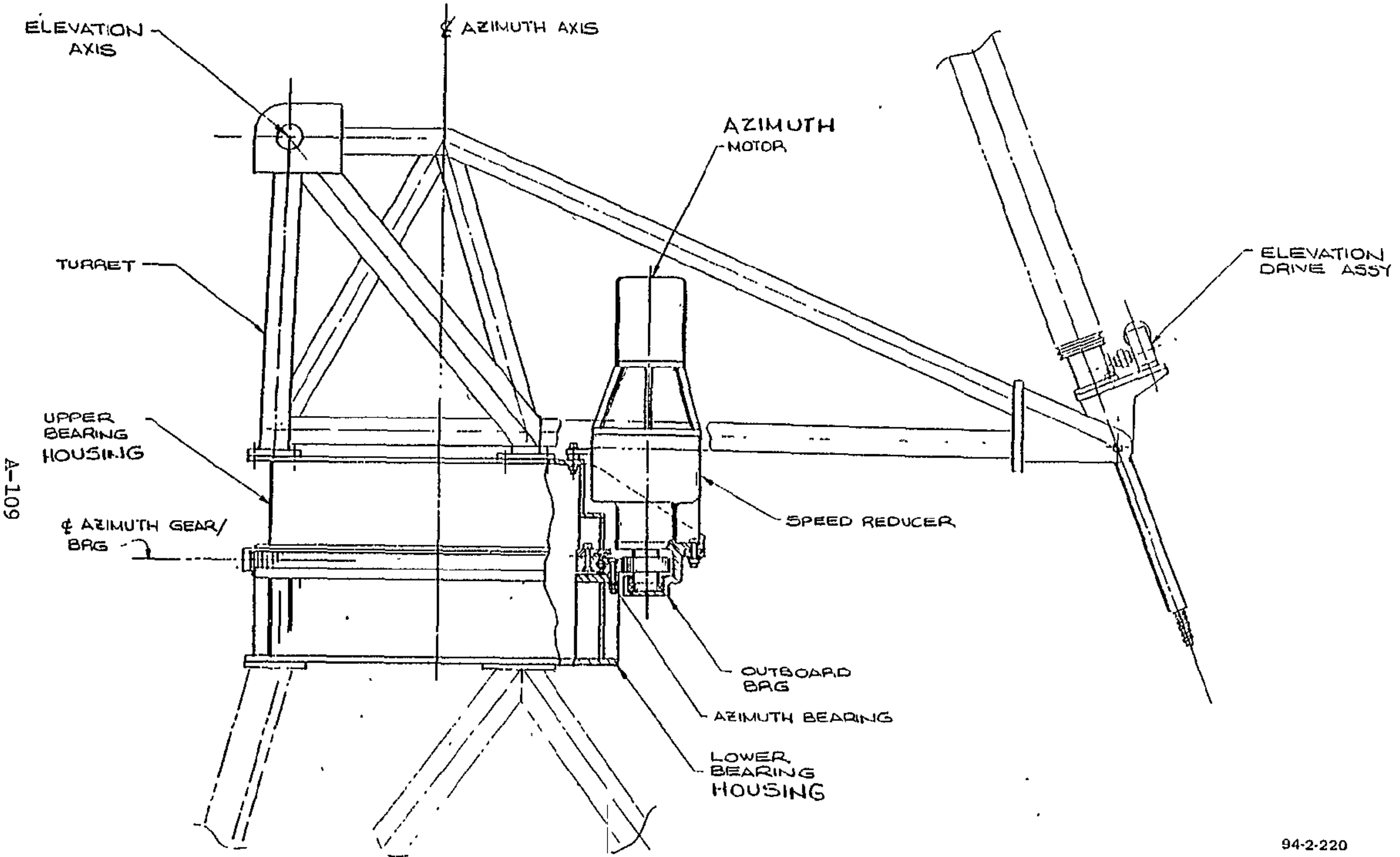


FIGURE 51. TURRET AND ASSOCIATED HARDWARE FOR BASELINE CONCENTRATOR

supporting the bearing, and it effectively resists vertical bending loads. The wide flanges provide stiffness to resist radial loads and maintain roundness. The teeth are cut on the outer periphery of the bearing which forms the bull gear for the azimuth drive. The bearing races are made from forgings of a hardened alloy steel. The ball paths of the raceways are case hardened to ensure that all stresses are well below allowable limits for strength and durability. The ball paths are hardened to a minimum of Rockwell 'C' 30, which provides both core hardness adequate for bending strength of the integral gear teeth and surface hardness for durability.

### 3.1.6 ELEVATION AXIS BEARINGS

The elevation axis is supported by two identical, self aligning, spherical roller bearings housed in cast steel pillow blocks. The bearings are preloaded during factory assembly to remove internal clearance to increase stiffness. Each pillow block is bolted to the pedestal structure with high-strength bolts. The self-aligning feature minimizes the load on the bearings due to any misalignment and also alleviates the need for accurate alignment of bearings on site. The bearings are lubricated with special grease used for high contact pressure conditions.

The bearing size was selected so the dynamic load rating is in excess of the operational loads imposed by gravity and operational winds. This insures bearing life in excess of the 30 year life of the concentrator. The static load rating of the selected bearing is in excess of the survival loads imposed by gravity and survival wind with the concentrator in its stow position. Survival and operational load analysis was performed in accordance with AFBMA (Anti-Friction Bearing Manufacturers' Association) standards.

### 3.1.7 AZIMUTH DRIVE SYSTEM

The azimuth drive system consists of a stationary bull gear (integral with the azimuth bearing outer race), a pinion and an electric motor-driven speed reducer which is mounted on the upper or moving bearing housing. Figure 52 is a photograph of an azimuth drive on a 36 foot antenna of the same type proposed for SPS.

The drive gear set consists of a bull gear with 122 teeth and a pinion with 14 teeth. Gear teeth are 2 diametral pitch, 25 degree contact angle. The bull gear has 4 inch face width and the pinion 4.5 inch. Hardness of the bull gear is approximately 30 Rockwell "C" and the pinion Rockwell 'C' 35. The overall ratio required for the drive system is 126,000:1. This provides 5 degree per minute maximum velocity with a 1750 rpm motor. Final drive ratio is 8.7:1 and the speed reducer ration is 14,500:1. The speed reducer selected is an off-the-shelf Winsmith Model 61 differential planetary with a special mounting flange.

### 3.1.8 ELEVATION DRIVE SYSTEM

The elevation drive system is composed of a machine screw actuator and a speed reducer. The base of the actuator is attached to a trunnion bracket which

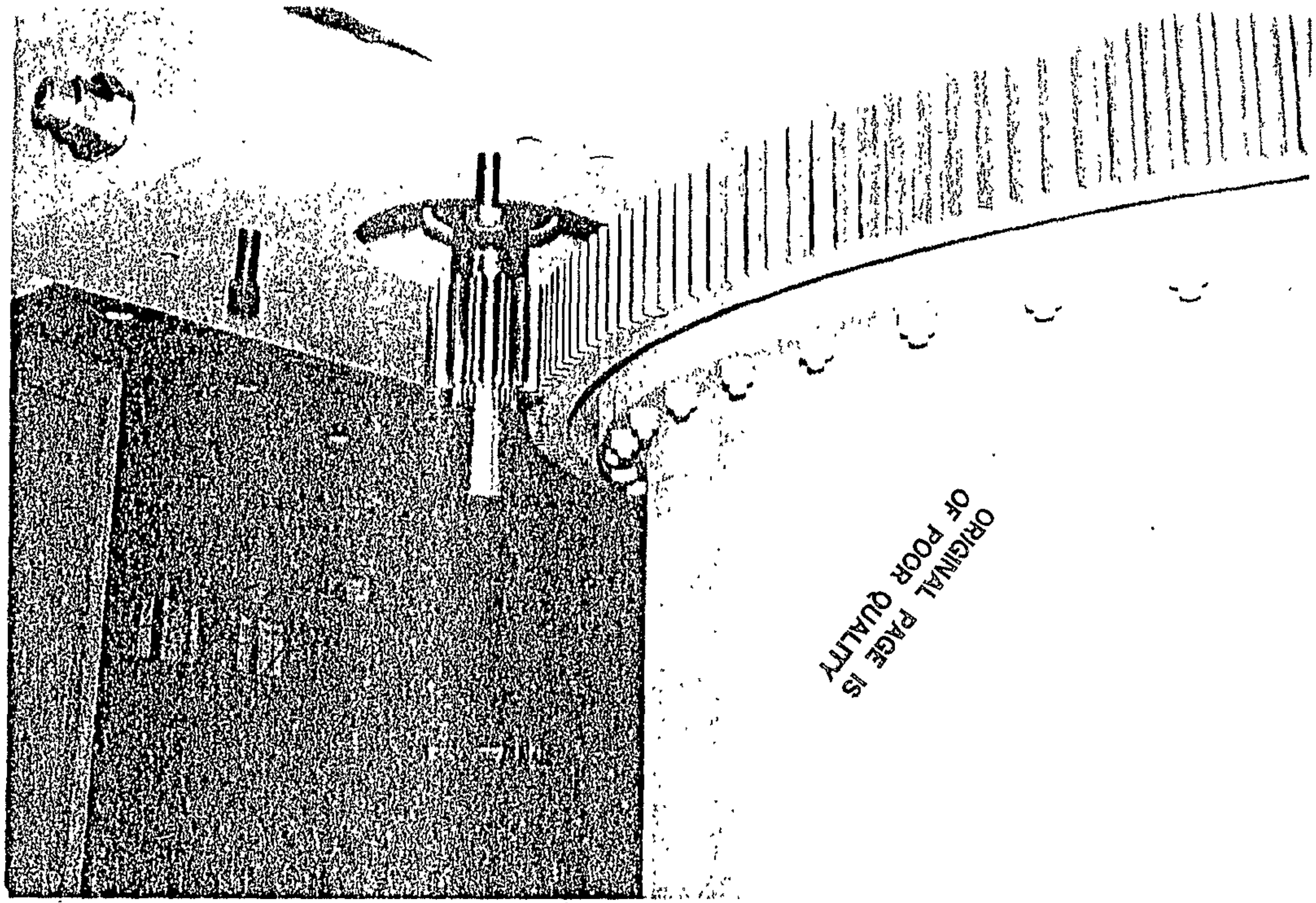



94-2-221

FIGURE 52. PHOTOGRAPH OF AN AZIMUTH DRIVE SYSTEM OF THE TYPE PROPOSED FOR SPS

pivots at the turret structure. The upper end of the screw is attached to a trunnion on the reflector, providing the full required elevation travel of 10 degrees to 90 degrees with an actuator stroke of approximately 15.5 feet. The machine screw rod is protected from the environment by an accordian-boot constructed of Vitron or similar long-lasting materials. Figure 53 illustrates a long stroke actuator used on the elevation drive of the 85 foot antenna at the JPL Mojave site.

Design studies have been made to determine maximum axis torques, maximum actuator loads and allowable loads. Safety factors have been applied to the worst case conditions. A summary of the major elevation drive system design parameters are listed in Table 26.

### 3.1.9 DRIVE CONTROL SYSTEM

The drive control system will employ AC induction motors, arranged in a sampled data loop which applies drive and dynamic braking commands in response to computer-generated axis step decisions. Each axis will have a drive motor which is controlled by solid-state switches driven by dedicated digital logic which converts the computer-generated drive commands into appropriate motor excitation commands.

3.1.9.1 Control Scheme. The concentrator motion is in discrete steps and upon receipt of a step command, the motor is excited and allowed to run at full speed in the appropriate direction until completion of the step is determined by pulse count from the axis incremental encoder. When this is reached, a dynamic braking sequence is initiated by the control electronics, and the motor is rapidly brought to a halt. Between steps, the concentrator is held in place by the inherent inability of the axis drive system to be backdriven.

Mechanization of the drive control is illustrated in Figure 54. The stations's microprocessor produces a drive enable signal and either a forward or reverse direction command. Upon receipt of these commands, the input logic in the motor controller produces direction commands to the direction steering logic, which in turn routes the commands to the particular pair of solid-state switches that apply line voltage to the motor, with phase rotation in the desired direction. As the motor runs the incremental encoder reports axis motion back to the microprocessor in the form of pulses corresponding to the direction of rotation. When the pulse count reaches the limit the microprocessor removes the direction command. This initiates the stop sequence by the dynamic braking subroutine. Inhibit signals are generated for both the input logic and direction steering logic to prevent application of external commands during dynamic braking. Once the subroutine is started, all commands are removed from the solid-state switches for a sufficient time to allow them to resume their non-conducting state, and then a series of stop pulses are produced and applied to the direction steering logic. These pulses are synchronized with the primary power lines by virtue of the reference A and B signals and are routed by the direction steering logic to the other pair of solid state switches.

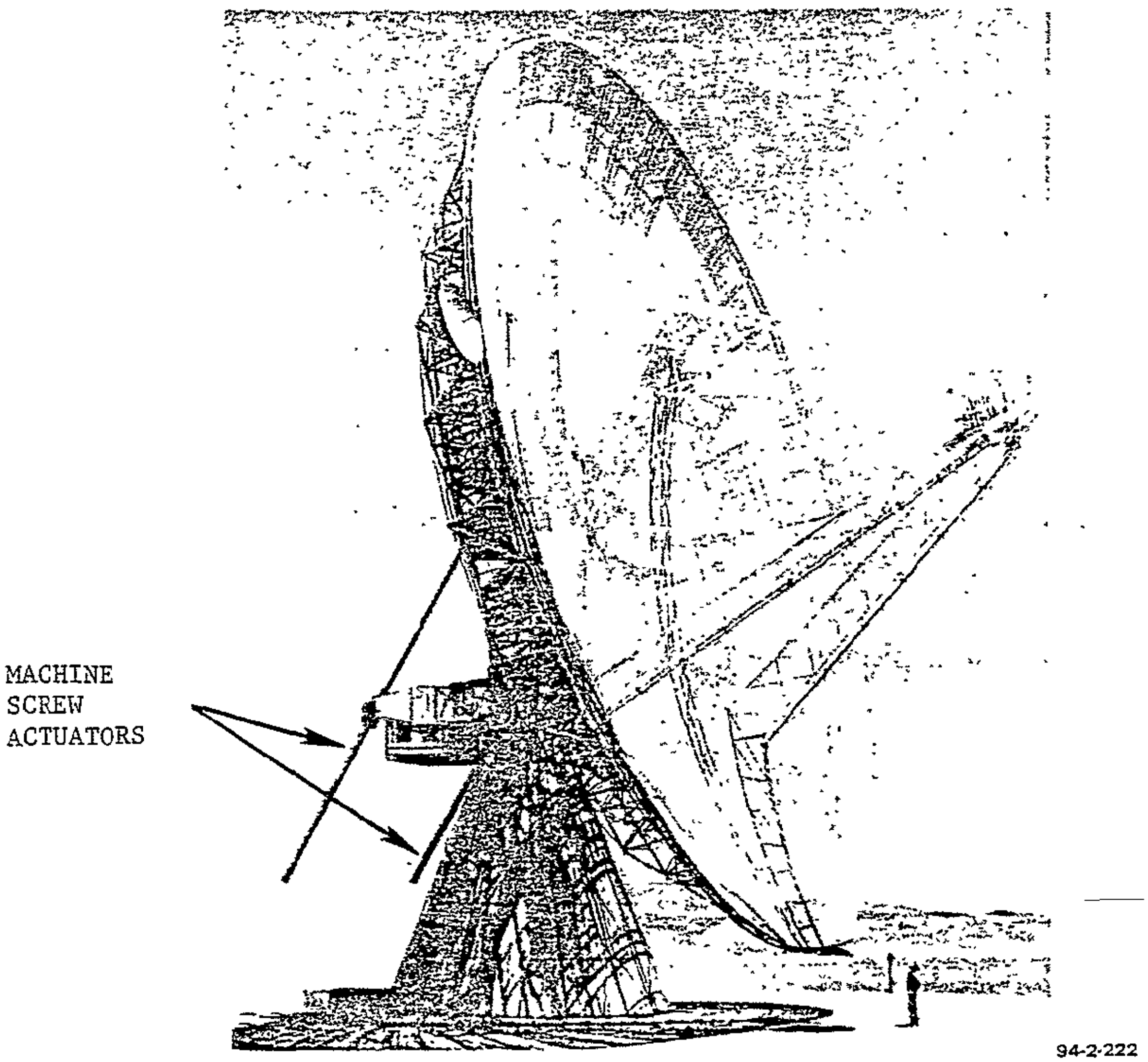


FIGURE 53. LONG-STROKE MACHINE SCREW ACTUATORS USED ON THE JPL 85 FOOT ANTENNA

TABLE 26. ELEVATION DRIVE SYSTEM DESIGN SUMMARY

| | |
|---|---|
| Axis Torque = | 198,500 Ft. Lb. (Refl. at 10° above Horizon) |
| Actuator Efficiency = | 19% |
| Speed Reducer Efficiency = | 88% |
| Motor RPM = | 1750 |
| Axis Speed = | 5.68 to 4.35°/min. |
| Average Speed = | 4.73°/min. |
| Gear Ratios for: | |
| • Actuator = | 11,100 to 14,500 |
| • Speed Reducer = | 10:1 |
| • Overall = | 111,000 to 145,000 |

### 3.1.10 TRACKING SYSTEM

Trade studies demonstrated that the optimum tracking system consists of a coarse programmed tracker with a fine (limited field of view) optical stepstrack. A block diagram of this configuration is shown in Figure 35 (paragraph 2.4.4.2).

3.1.10.1 Central Station Microprocessor. One input to the tracking system is the absolute azimuth and elevation angle commands. These signals are generated in the central station microprocessor and are transmitted serially to each concentrator. The central microprocessor will generate the ephemeris of the sun, convert the HA-DEC angles to Az-El angles, convert the El angles to corresponding jack position (corrected for concentrator dead load deflection and geometry of actuator drive) and transmit the axis position commands (in compatible format with the concentrator encoders) to the individual concentrators. The position commands will be updated approximately every 15 seconds to minimize loss of energy due to the sun's motion.

3.1.10.2 Motion Control and Encoding Logic. The following sequence of steps are required:

- Receive absolute position commands for each axis, decode the serial data and enter it into storage (15 to 30 second intervals).
- Add computed calibration correction to the input position command.

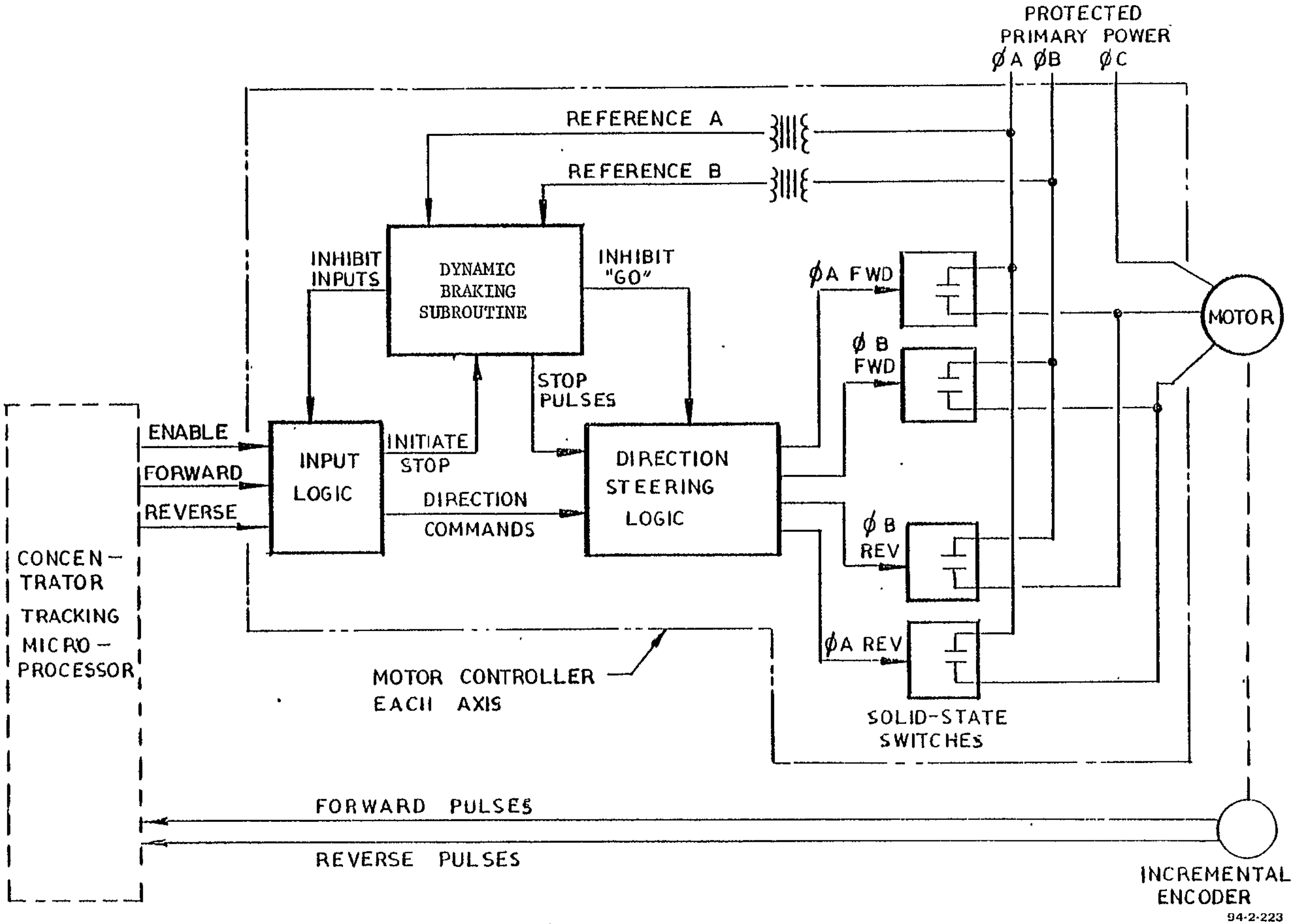


FIGURE 54. DRIVE SYSTEM BLOCK DIAGRAM

- Turn on axis drive motor in the direction to cause the concentrator to move towards the commanded position.
- Update encoded axis position data in response to position transducer data.
- Input digitized output of the optical sensor during stationary periods, average, and store this quantity.
- Stop axis drive motor when encoded position equals corrected position command.
- Determine calibration correction from digitized optical sensor data and store.
- Compute calibration correction for the next move from combination of stored data.

By alternating azimuth and elevation moves, the controller accomplishes one sequence (as described above) approximately every 15 seconds.

3.1.10.3 Incremental Position Transducer and Zero Reference. Each incremental position transducer will consist of two zero velocity type magnetic proximity probes operating at 90 degrees from each other on a cam driven by the axis motor shaft. Figure 55 shows the configuration and the typical output of each transducer. The resolution of the transducer will be approximately 0.003 degree.

3.1.10.4 Optical Self-Calibration Function. The optical self-calibration function will be accomplished by adding or subtracting a correction to the ephemeris tracking inputs. These corrections are developed from data supplied by a single photocell sensor with a narrow field of view, shown in Figure 56. The solar image is focused on the single photocell through an aperture equal in diameter to the solar image. Thus, pointing errors cause the image to move off the aperture and reduce the photocell output. Output data is stored in the microprocessor, and based on the stored data, the decision is made to increase or decrease the next step size from the ephemeris commanded position.

A typical elevation/azimuth tracking pattern is shown on Figure 57. Here the ephemeris slope (travel) is 2 units in elevation for 3 units in azimuth, therefore the step sizes chosen will be either 1 or 3 units in elevation and either 2 or 4 units in azimuth. The resulting error of this pattern is apparent from the difference between the steps and the ephemeris line. A decision process has been derived to determine which step size to take and how to apply the correction factor to the ephemeris command.

3.1.10.5 Control Arrangement and Cabling. A schematic of the concentrator cabling and control elements is shown in Figure 58. All control electronics for the concentrator is housed in a single NEMA-12 weatherproof enclosure, about 18" x 24" x 10" in size, mounted on one concentrator pedestal leg.

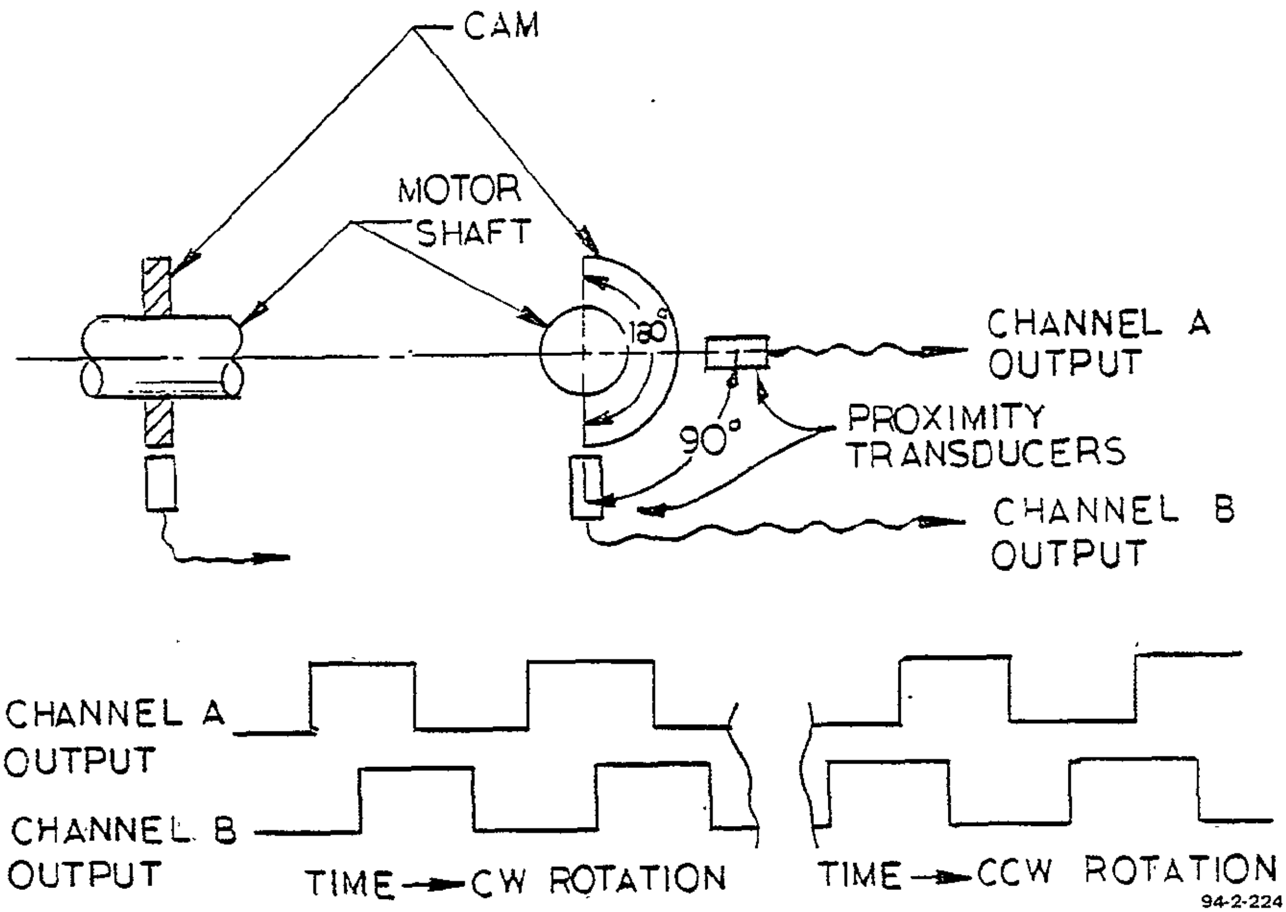


FIGURE 55. INCREMENTAL POSITION TRANSDUCER

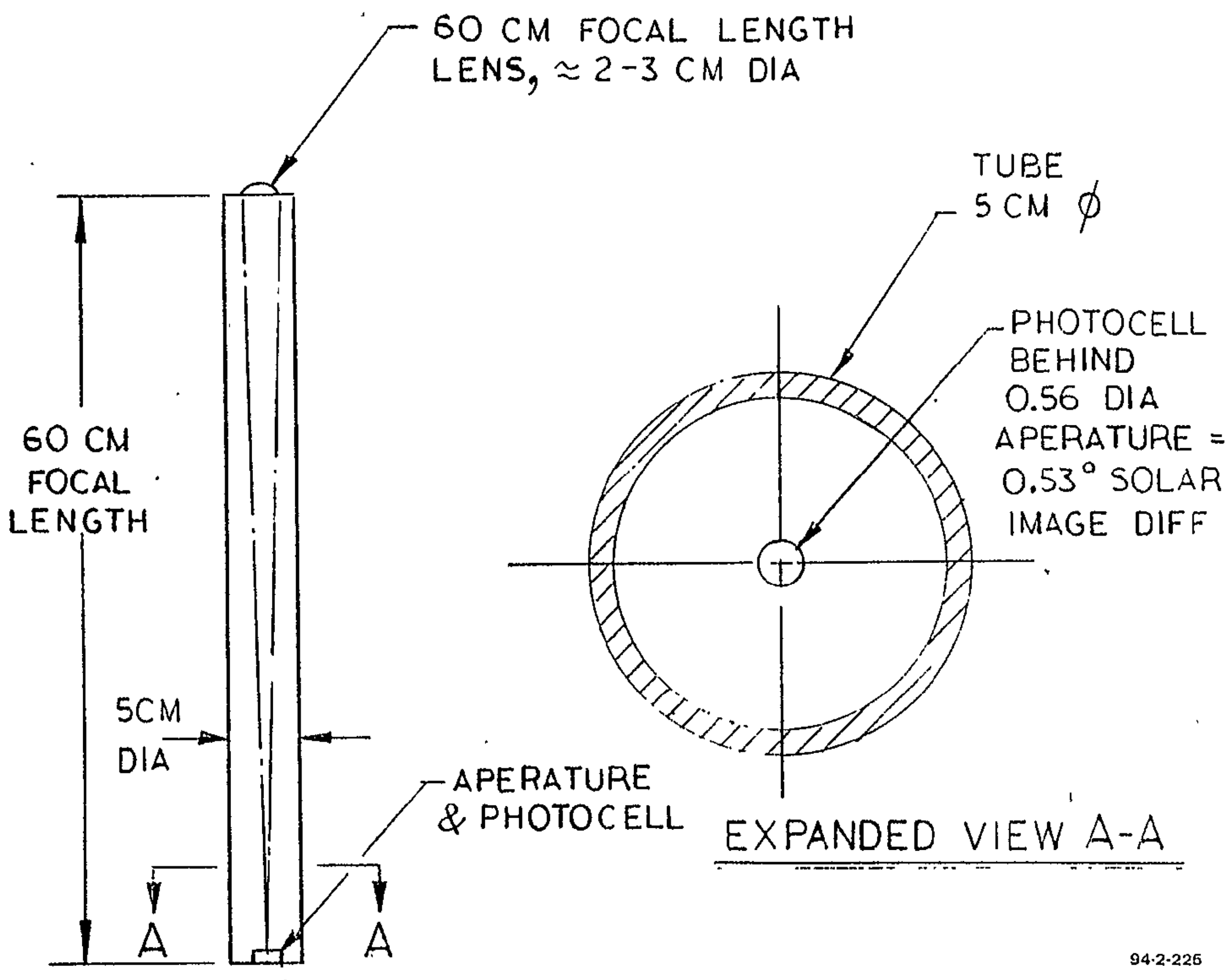


FIGURE 56. OPTICAL SENSOR USING A SINGLE PHOTOCELL

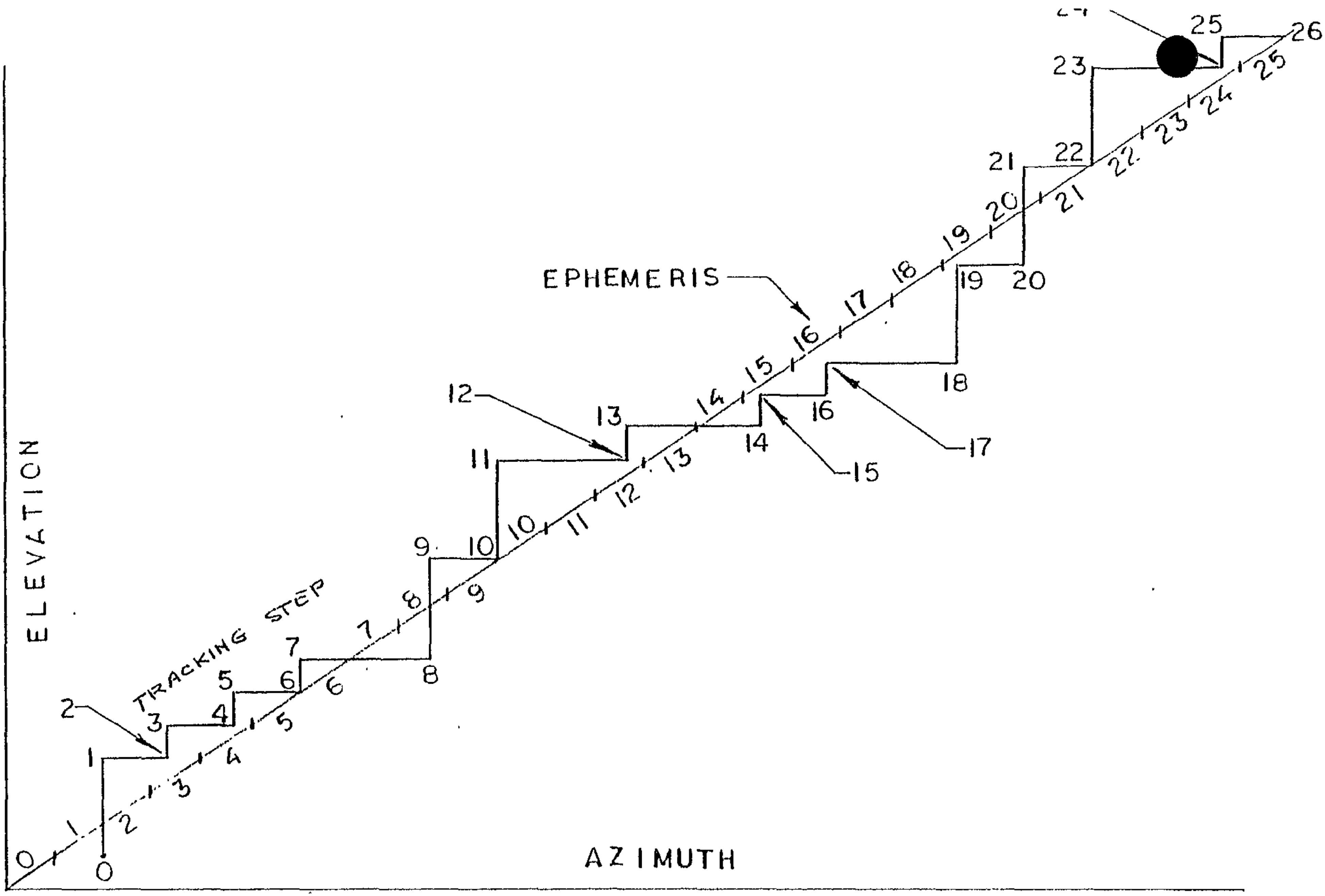


94-2-226

FIGURE 57. TYPICAL TRACKING PATTERN

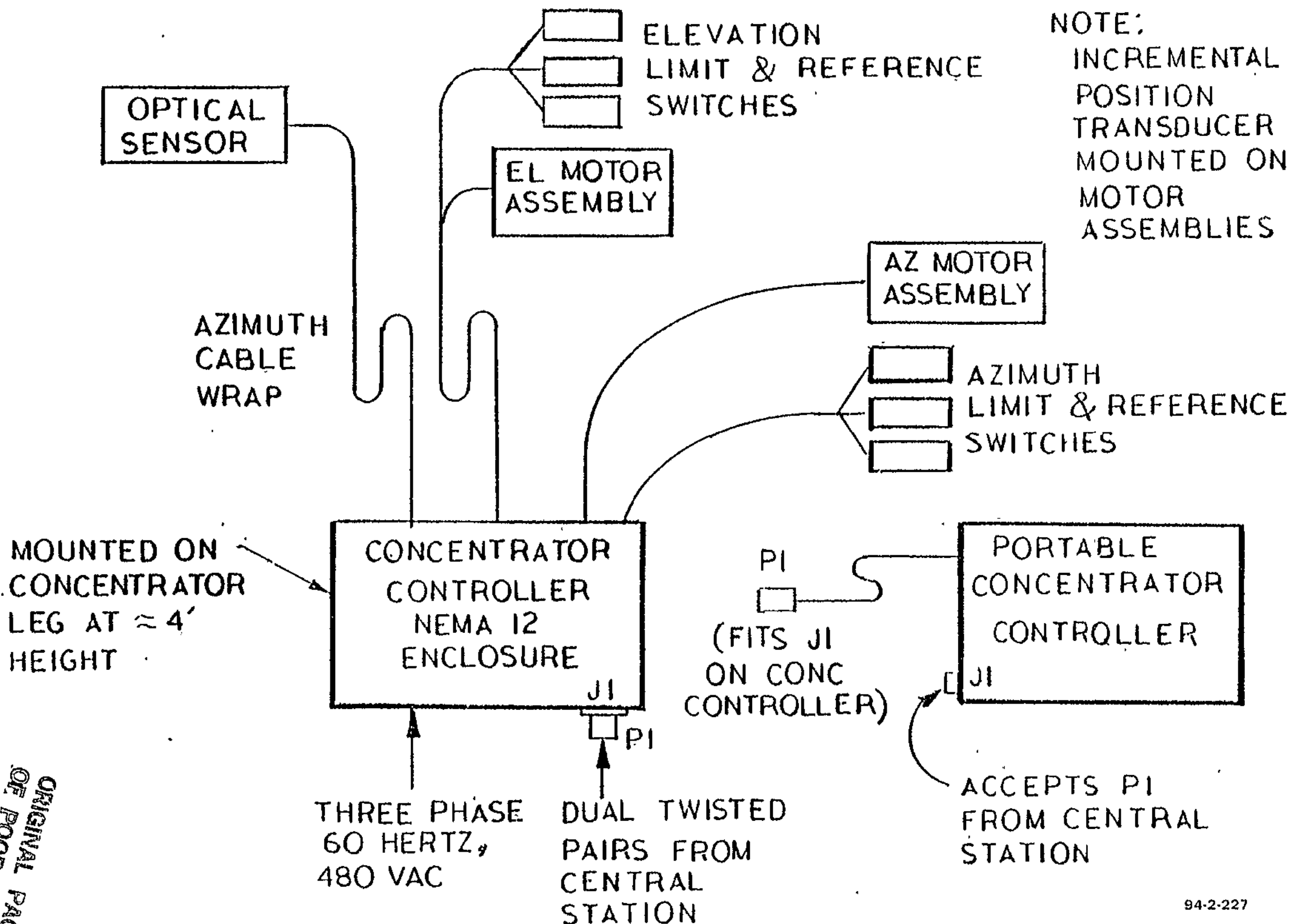


FIGURE 58. CONCENTRATOR CONTROL AND CABLING ARRANGEMENT

Flexible cable assemblies connect the drive motors, axis limit/reference switches and optical sensor to the concentrator controller. Local control for installation, checkout and maintenance is provided through the same connector PI normally used for central station control. The Portable Concentrator Controller provides economical local control and monitor while maintaining communication with the central station. Controls and indicators on the portable unit would provide the following capabilities:

- Allow normal operation of concentrator from central station while displaying command position and actual position.

- Provide on-off motor control for each axis with display of axis positions and digitized optical sensor output.

- Provide status data of limits, zero reference, etc.

3.1.10.6 Concentrator Operating Sequences. The following operations will be performed by the concentrator tracking system:

Night Sequence

- Determine time ($t_o$) and azimuth position ($AZ_o$) when following morning sun will reach minimum elevation angle (~5 to 10°).

- Determine if any concentrators are not in operating order

- Position each in-service concentrator to minimum EL and AZ = $AZ_o$.

Morning Start Sequence (for all in-service concentrators)

- At time = $t_o$ microprocessor will activate AZ and EL drives under program track control.

- When sun sensor indicates the solar insolation is above the minimum value: 1) start optical autotracking (AZ and EL), 2) station control will initiate engine start sequences including receiver cover opening, 3) station control will synchronize and connect engine/generator to station power bus.

Run Sequence

- Continue tracking.

Cloud Sequence During Run Sequence

- When insolation is interrupted to sun sensor: 1) continue program tracking; optical autotracking corrections will discontinue, and 2) receiver door will close.

- If cloud interruption continues engine/generator will shut down, and program tracking will continue.

- When adequate solar insolation returns: (1) open receiver door, (2) resume optical autotracking, and (3) receiver/engine/generator will proceed with start sequence.

Normal Afternoon Shutdown Sequence

- Stop concentrator drives (AZ and EL) when elevation angle reaches 10 degrees (or travel limit reached), or when insolation/power falls below a minimum level.

- Receiver/engine/generator shutdown sequences will proceed independently.

- At program command, proceed to night sequence.

Emergency Shutdown Sequence

- Defocus receiver when signal received from station control (El slew at 5 degrees/min for ~2 minutes).

- Reactivation depends on type of emergency: if high engine head/ receiver temperature, wait until temperature reduces, and return to tracking. Other emergencies: reactivation TBD.

High Wind Sequence (Above operating limits)

- When signal received from station control anemometer:

  - If running, stop suntrack (Az and El) and close receiver door.

  - Program control will instruct slew at $5^{o}$/min until 90 degree elevation position reached.

  - As wind velocities reduce, open door and return to normal program track.

  - If high winds continue, receiver/engine/generator will proceed with normal shutdown.

Cleaning/Maintenance Sequence

- Remain at afternoon shutdown position.

- After cleaning, resume in-service position.

Testing/Special Maintenance Sequence

- Manual local control

3.1.11 FOUNDATION

The foundation selected to support the solar collector is dependent on the soil conditions at the site. There are three common categories:

- Bedrock at a shallow depth. For this condition the use of a rock anchor would provide the most economical foundation.

- Soil with a high bearing value at a shallow depth. For this condition, the use of a spread footing would be most economical.

- Loose soil with low bearing value for a considerable depth. For this condition, a pile foundation would be the most economical.

The loose soil conditions are the most typical for the Southwest region of the United States, therefore a pile type foundation was selected as the baseline. A single timber friction pile under each concentrator leg provides the most economical foundation design for the soil conditions used in this study.

3.2 CONCENTRATOR PERFORMANCE

This section contains information concerning the optical characteristics of the collector (reflectance, blockage/shadowing, slope error), tracking accuracy, and axis drive energy consumption.

3.2.1 OPTICAL PERFORMANCE

Most of the information concerning the optical characteristics are discussed in previous sections and summarized below.

(1) Shadowing/Blockage. The loss of energy due to the front structure and tripod support is illustrated in Figure 59. Note that shadowing is defined as "primary blockage" and blockage of reflected energy from the mirror to the receiver is defined as "secondary blockage". A first-order analysis of the total shadowing/blockage indicates approximately 7.6 percent energy loss (based on the aperture area).

(2) Reflectivity and Specularity. The specular reflectance (reflectivity) of the second-surface draw fusion glass mirrors is 95 percent. An average dust correction factor of 95 percent is also used, resulting in an "average" reflectivity of 90.2 percent. Specularity of the reflected beam due to micro-roughness is 0.2 milliradians rms (maximum value of 0.5 mrad).

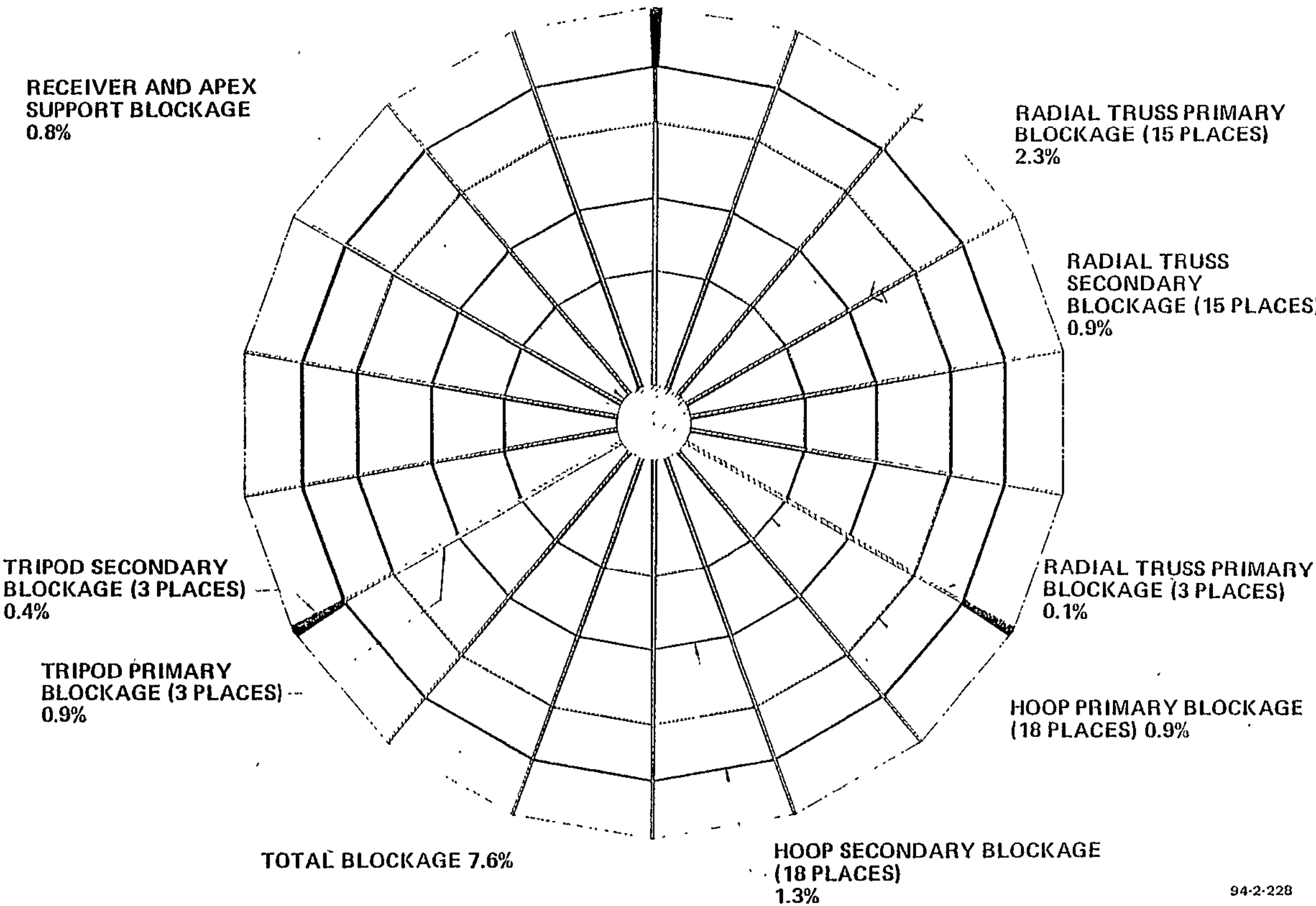


FIGURE 59. SHADOWING AND BLOCKAGE FOR THE BASELINE 18.6 METER CONCENTRATOR

(3) Surface Slope Errors. Surface slope errors were analyzed for the various sources listed in Table 27. The results gave an RMS error of 2.6 mrad for 98 percent of the time the plant is in operation.

### 3.2.2 TRACKING ACCURACY

In the baseline step-track system, the only significant tracking error contributors are:

- Steptrack process granularity
- Deflections caused by gravity between optical axis and tracking sensor
- Wind gust deflections
- Initial sensor misalignment

These are described below.

3.2.2.1 Tracking Process Granularity. The solar tracking system will use the steptrack technique in which the concentrator moves in finite increments in alternating axes. Using this tracking algorithm the rms error due to the offsets between steps is approximately 1.5 mrad for the baseline system.

3.2.2.2 Gravity Deflections. Analysis of the reflector and receiver support structures indicates that this error can be reduced to an acceptable value if the optical sensor is mounted on an appropriate front-structure member in the vertical symmetry plane. The relative deflection between the optical axis and the axis fo the tracking sensor will be less than 0.5 milliradians with this arrangement.

3.2.2.3 Wind Gust Errors. The steptracker will remove the effects of any constant structural deformation due to steady winds, since it will position the optical axis to the maximum gain point regardless of the deflected shape of the structure. However, fluctuations in beam pointing due to gusts between successive steps will result in random tracking errors. Digital computer simulation was performed to determine these effects. The models for time variation of the gust distrubances included random functions based on published spectrum models, and actual records of windspeeds recorded at 0.1 second intervals. The significant conclusions were:

(1) Neither the form of the wind gust spectral density nor the time interval between steps has any significant effect on the tracking error due to wind loading, within realistic step time intervals.

TABLE 27

SUMMARY OF SURFACE SLOPE ERRORS, 18.6 M CONCENTRATOR

| Source | Method of Analysis | RMS Error |
|---|---|---|
| (1) Panel Mfg. | Evalutation of Cost-Effective Manufacturing Techniques | 1.5 mrad |
| (2) Gravity Loads on Panels | Sag of panel calculated as a % of time spent at each elevation angle for 36°N. latitude | 0.3 |
| (3) Thermal Gradients | Analysis of front-to-back gradients due to heating, and bending due to mismatch in properties between front and back. | 1.2 |
| (4) Structural Panel Alignment | Assembly tolerances based on a precision jig used for field assembly and alignment. | 1.5 |
| (5) Gravity Loads on Support Structure | Detailed structural analysis of front-braced concept | 0.7 |
| (6) Wind Loads | Deflections calculated for various wind speeds; the % of time vs. wind speed then factored in:<br><br>Avg. Wind Speed / Percentage of Operating Time / Error<br>7 m/s / 98 / 0.2<br>15 / 1.8 / 1.1<br>20 / 0.2 / 2.0 | 0.2* |
| | RSS Total* | 2.6 mrad |

*Applies to 98 percent of the operating time; for the 1.8 percent of the time the wind averages 15 m/s the total error may increase to 2.8 mrad, and 0.2 percent of the time to 3.3 mrad.

(2) The magnitudes of errors attributable to gusty winds can be predicted by assuming that they have a zero mean Gaussian distribution with a standard deviation. Published data indicate that the rms gust-to-mean-speed ratio is normally about 20 percent, resulting in rms gust errors about half of the steady wind deflections.

The deflections for a steady wind of 13 m/s for several concentrator orientations are summarized in Figure 60 and a contour plot is shown in Figure 61. As in the case of surface slopes, an average wind speed of 7 m/s (representative of 98% of the time) is used in this analysis. Also, it is not realistic to assume the worst case concentrator orientation for long term rms error estimation. From the contour plot, it is seen that a typical average value is about 3.5 mrad at 13 m/s. Based on these considerations the rms error is estimated to be 0.49 mrad rms.

3.2.2.4 Tracking Sensor Misalignment. A budget of 0.5 mrad has been set based on the mount/reflector tolerance control of the site reflector erection fixture. Further analysis is required to verify this value.

3.2.2.5 Tracking Error Summary. The significant components of the tracking error budget are summarized in Table 28.

### 3.2.3 ENVIRONMENTAL PERFORMANCE

The major environmental factor that influences the concentrator design is survival wind loading. These winds directly effect the cost of the concentrator, which in turn has a major influence on the cost of the system. Consideration has also been given to the temperature, sand/dust, earthquake, etc., conditions defined in Table 5. Significant items are summarized below.

3.2.3.1 Temperature. The concentrator will be able to operate in the ambient temperature range from -30°C to +50°C (-22°F to +122°F). Components will be provided to meet these requirements without a significant cost penalty.

3.2.3.2 Sand/Dust. Sandstorm survival requires special design attention and will impose restrictions on most mechanical and electrical components. The glass panel surface is the best reflective material available to withstand sandstorms.

3.2.3.3 Earthquake. No features of the design are susceptible to zone 3 earthquake damage. The wide base of the concentrator is particularly resistant to earthquake loads.

3.2.3.4 Hailstorms. The principal component affected by the hailstorm survival specification is the mirror surface. Testing will be required to prove compliance.

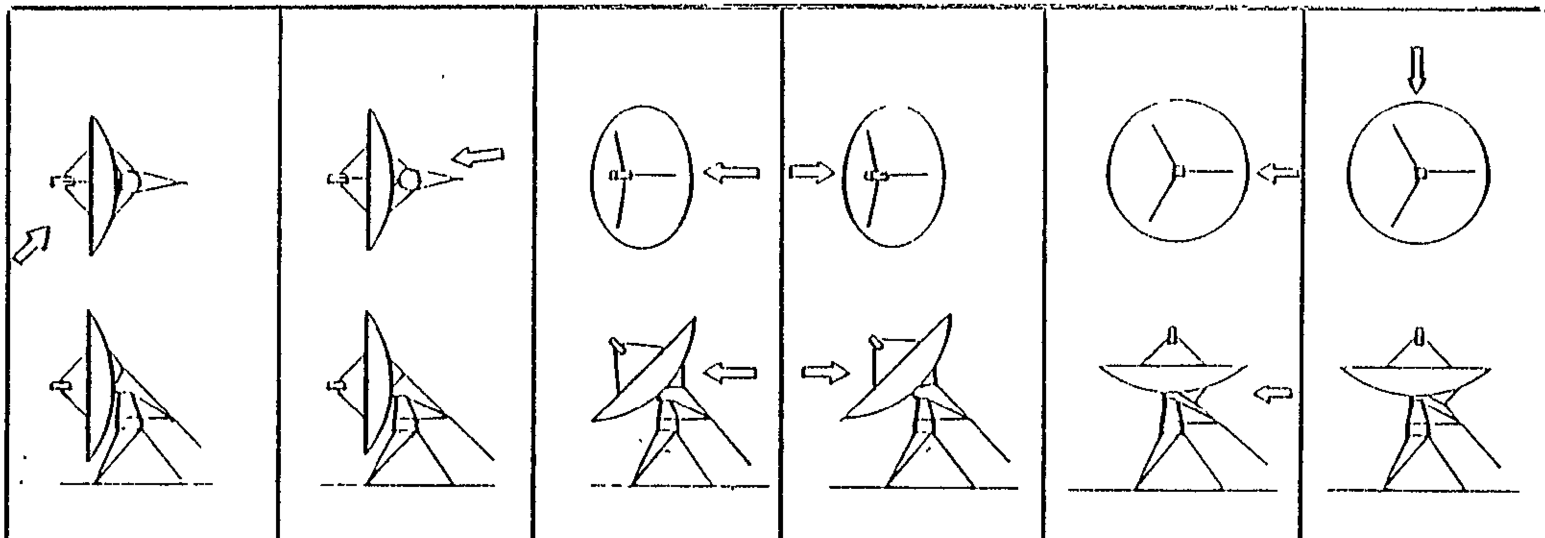

| COMPONENT | ERROR (MRAD) | | ERROR (MRAD) | | ERROR (MRAD) | | ERROR (MRAD) | | ERROR (MRAD) | | ERROR (MRAD) | |
|---|---|---|---|---|---|---|---|---|---|---|---|---|
| | EL | CROSS-EL | EL | CROSS-EL | EL | CROSS-EL | EL | CROSS-EL | EL | CROSS-EL | EL | CROSS-EL |
| OPTICAL SUPPORT STRUCT | 0 | 0.3 | 0 | 0.3 | 0.3 | 0 | 0.2 | 0 | 0.2 | 0 | 0 | 0.2 |
| GIMBAL ACTUATOR STRUCT | 1.5 | 0.3 | 0.9 | 0.3 | 0.6 | 0 | 0.5 | 0 | 0.8 | 0 | 0 | 0.6 |
| AZIMUTH TURRET/DRIVES | 0.2 | 0.3 | ≅0 | 0.5 | 0.2 | 0 | 0.1 | 0 | 0.1 | 0 | 0 | 0.1 |
| PEDESTAL STRUCTURE | 1.9 | 0.3 | 1.1 | 0.3 | 1.1 | 0 | 0.8 | 0 | 0.6 | 0 | 0 | 0.6 |
| FOUNDATION | 0.5 | 0.4 | 0.3 | 0.4 | 0.4 | 0 | 0.4 | 0 | 0.2 | 0 | 0 | 0.2 |
| AXIS TOTALS | 4.1 | 1.6 | 2.3 | 1.8 | 2.6 | 0 | 2.0 | 0 | 1.9 | 0 | 0 | 1.7 |
| VECTOR SUM | 4.4 (.25°) | | 2.9 (.17°) | | 2.6 (.15°) | | 2.0 (.11°) | | 1.9 (.11°) | | 1.7 (.10°) | |

94-2-230

FIGURE 60. POINTING ERRORS DUE TO 13 M/S WIND

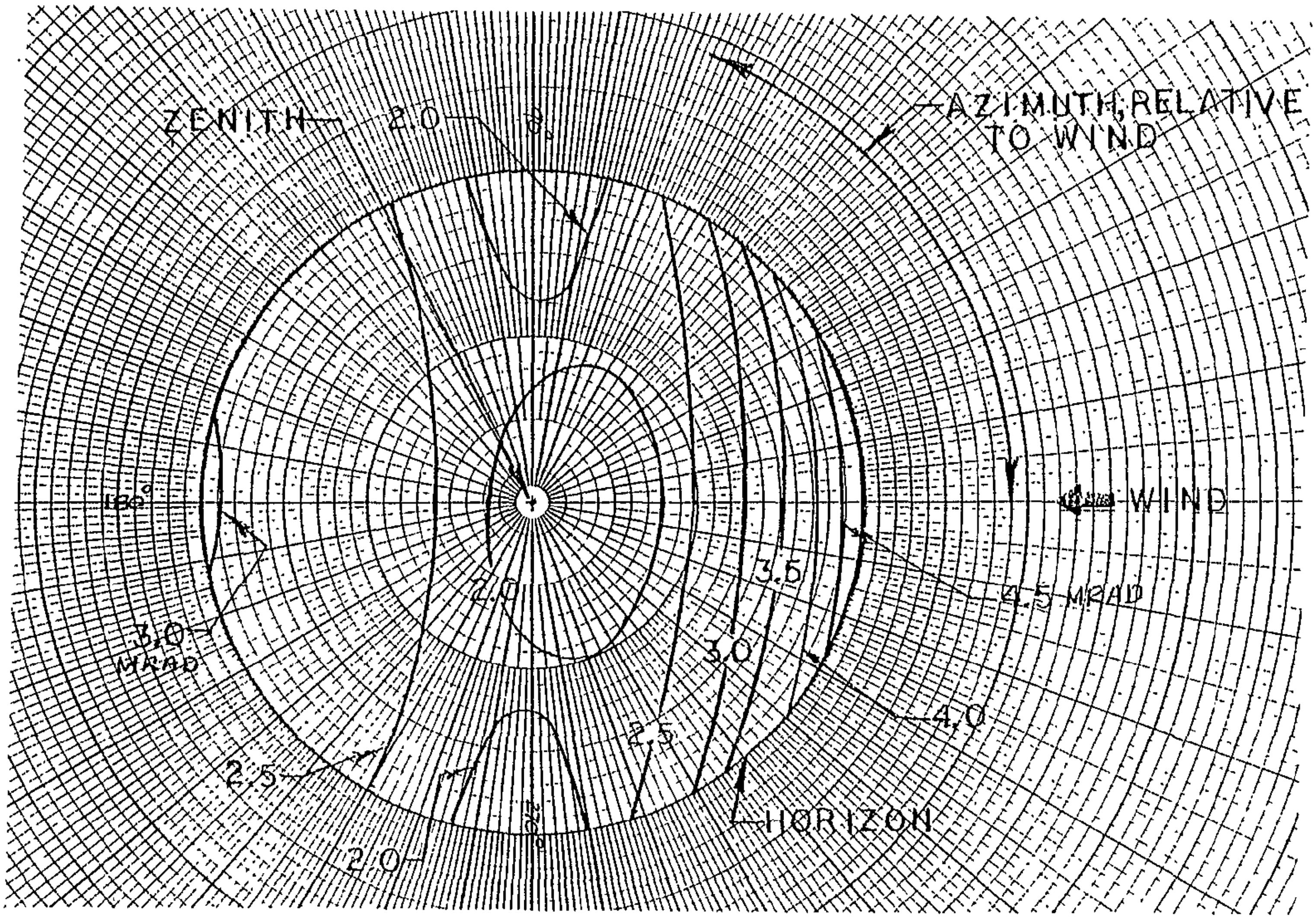


94-2-231

FIGURE 61. POINTING ERROR CONTOURS FOR 13 M/S WIND

TABLE 28

SOLAR TRACKING ERROR BUDGET

| Contributor | rms Error (mrad) |
|---|---|
| Process Granularity | 1.5 |
| Gravity Sag | 0.2 |
| Wind Gusts | 0.5 |
| Sensor Alignment | 0.5 |
| RSS Total | 1.7 mrad |

3.2.3.5 Wind Loads. A good background of wind loading data and analysis techniques has been developed for microwave dishes. However the survival wind loading stress for a solar concentrator must be evaluated more extensively because of the importance of both low cost and survival stresses (operating deflections usually govern microwave design, and cost is not such a significant factor). Conversely the operating wind loadings are less critical for solar installations than microwave. Microwave applications usually require that specified distortions can never be exceeded at any time during operation; however, solar applications can trade-off distortion versus cost during the operating time period.

a. Survival Wind. The concentrator will survive winds with a maximum speed, including gusts, from any direction, as follows:

(1) 40 m/s (90 mph) with the concentrator in the stowed position (zenith).

(2) 22 m/s (50 mph) with the concentrator in any possible orientation. These winds can occur suddenly with usually rapid wind rise rates, such as severe thunderstorm gust fronts.

Following wind storms of the above magnitude, the concentrator subsystem will suffer no degradation of operational performance nor have any requirement for parts replacement or realignment.

The drive-to-stow analysis is depicted in Figure 62, which also shows the frequency of wind storm in the Barstow/Daggett area. Based on 18 m/s (40 mph) as a start-to-stow condition, only two storms occurred during the year 1976 at this site. About half of the high winds occurred during non-operating night periods.

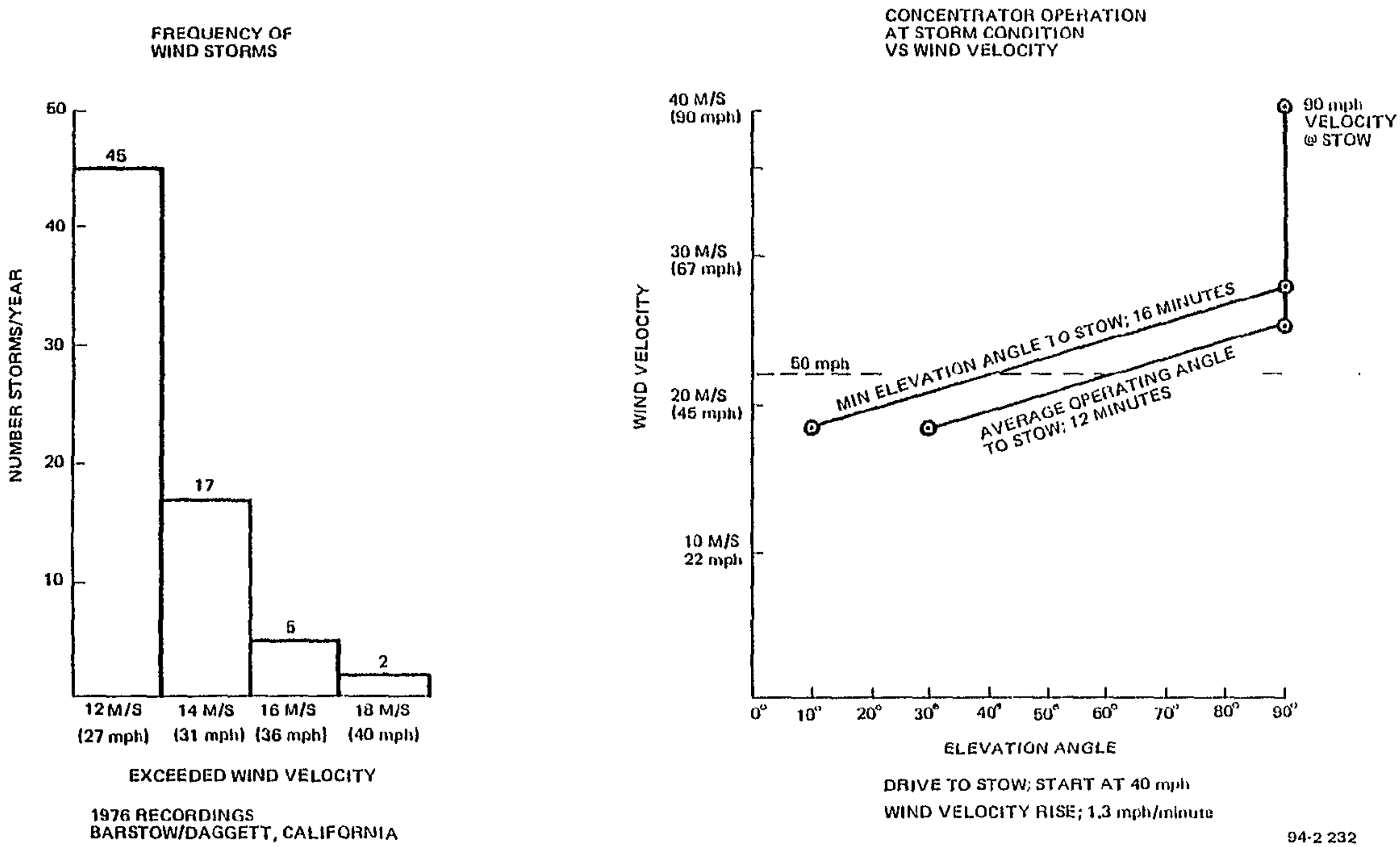


FIGURE 62. DRIVE TO STOW ANALYSIS

When the station anemometer measures winds which exceed 40 mph, the control subsystem and program track control will instruct the elevation drive to proceed to 90° elevation. The travel rate will average 5°/minute. When the wind velocity reduces to ~16 m/s (36 mph), the elevation drive will return to its normal location (either operational track or night horizon look).

b. Operational Wind. The operational wind speed is specified as follows:

| Wind Speed, m/s | Frequency, Percent |
|---|---|
| 0 - 2 | 29 |
| 2 - 4 | 21 |
| 4 - 6 | 19 |
| 6 - 8 | 14 |
| 8 - 10 | 8 |
| 10 - 12 | 5 |
| 12 - 14 | 3 |
| 14 - | less than 1 |

These values have been incorporated into the performance values summarized in Paragraphs 3.2.1 and 3.2.2.

### 3.2.4 ENERGY CONSUMPTION

The concentrator subsystem electrical requirements consist of power to drive the concentrator during tracking, stowing, etc., and power for the electronic units.

The drive system energy requirements calculations are summarized in Table 29. They include the system running loads (gravity imbalance, wind torques and axis bearing friction), the drive train and motor mechanical and electrical losses for both axes, and the work required to move the system each step. The total drive energy required for a typical day is:

| | Day | Night | Total |
|---|---|---|---|
| Azimuth Axis | 300 Whr | 130 Whr | 430 Whr |
| Elevation Axis | 590 | -- | 590 |
| Total | 890 | 130 | 1020 Whr |

TABLE 29

CONCENTRATOR DRIVE ENERGY CONSUMPTION

| DRIVE TORQUE: | | AZIMUTH AXIS | ELEVATION AXIS | COMMENTS |
|---|---|---|---|---|
| Tu | Unbalance Torque | N/A | 120 kNm | Average for 10-60° elevation |
| Tw | Wind Torque | 15 kNm | 20 kNm | 7.5 M/S Average Velocity |
| Tf. | Axis Friction Torque | 0.2 kNm | 0.1 kNm | - |
| T | Average Running Torque | 15 kNm | 140 kNm | T = Tu + Tw + Tf |
| $\eta_r$ | Mechanical Efficiency | 0.15 | 0.17 | Drive reducers |
| $\eta_m$ | Motor Efficiency | 0.65 | 0.65 | - |
| Te | Effective "Input" Torque | 150 kNm | 1300 kNm | $Te = T/\eta_r\eta_m$ |
| θ | Average Angular Travel | 2π rad | 1 rad | - |
| $Ed_1$ | Drive Energy (Torque) | 950 kJ(260 Whr) | 1300 kJ(360 Whr) | ED = Te θ (Whr = kj/3.6) |
| DISCONTINUOUS DRIVE CONTROL: | | | | |
| η | Number Daily Axis Moves | 1200 | 1200 | Step per ½ minute |
| J | System Inertia | 0.015 $kg.m^2$ | 0.021 $kg.m^2$ | Reflected to motor shaft |
| Ω | Rated Motor Speed | 183 rad/s | 183 rad/s | 1750 rpm |
| $Ed_2$ | Drive Energy (Control) | 600 kJ(170 Whr) | 840 kJ(230 Whr) | $Ec = \eta J\Omega^2$ |
| TOTAL | | | | |
| Ed | Average Drive Energy | 430 Whr | 590 Whr | $Ed = Ed_1 + Ed_2$ |
| | Distribution Day | 300 Whr | 590 Whr | - |
| | Distribution Night | 130 Whr | - | - |

The electrical power consumed by the tracking control system electronics is 22W continuous or 530 Whr per day. Thus, the total electrical energy consumed by each concentrator will be 1.55 kWhr per day.

## 3.3 CONCENTRATOR COMPONENT FABRICATION/PROCUREMENT

A key factor in the selection of the baseline concentrator concept was the utilization of proven, highly reliable materials and components, and also those that will contribute directly to the components required in large volume to achieve commercial success around 1990. The Ford Motor Company Production Planning Research Division has been consulted on techniques to minimize costs of volume production, and they will be utilized for any future work of this type. Their inputs are included in the following discussion.

All structural members will be fabricated to detailed piece-part shop drawings specifically adapted for the quantity to be provided and the type of shop equipment utilized. The design has maximized the use of automatic stampings; and minimized welding, the use of expensive shop assembly and the work required for site assembly. Even today the members could be economically assigned to high volume, production-line, fabrication shops with in-house galvanizing. Consideration of the geography of the most promising future solar sites will allow a logistics study of various mill costs, shipping costs, area labor rates, etc., for comparison of production costs. Similar piece-parts will be bundled together and trucked within weight limitations direct to the site for unloading in an organized area. Only the azimuth housing requires any shop assembly.

All mechanical components are basically standard industrial designs of proven, highly reliable components. Several well-qualified vendors are available for each component.

Several factors strongly suggest that the best solar panel economics can be achieved by vertically integrating the panel manufacturing with the glass source. The degree to which such integration would take place is strongly dependent on the volume. The low end of the production range (6 million sq ft/year) would require only one-tenth of the yearly capability of the existing fusion-glass plant. The mid-range would utilize the entire plant's capacity, thus good vertical integration of panel manufacturing and glass production could be achieved. At the high range (300 million sq ft/year), a new plant or plants with more than five times the existing capacity would be required.

## 3.4 CONCENTRATOR INSTALLATION AND CHECKOUT

Site implementation studies have been made for the baseline 1 $MW_e$ station, consisting of nineteen 18.6 meter concentrators per site. Between 100 and 5000 of these sites will be installed throughout the Continental United States annually. The discussion applies to a single 1 $MW_e$ station; multiple stations would simply require more of the same equipment and manpower. The installation checkout plan outlined below is based on the most economical approach and does not reflect the shortest installation time period that can be achieved. (The installation of the electrical and control cables are covered in the Electrical System Appendix.)

### 3.4.1 SITE LAYOUT

The centerline locations for each of the nineteen concentrators are to be surveyed and marked prior to the start of installation. The centers for the three foundation piles required for each concentrator will also be accurately located and marked as a part of the survey. Permanent bench marks will be established for future reference, as required.

A typical field layout would be in three columns, two of which would have seven concentrators and the third column five. This arrangement is shown in Figure 63. The spacings between concentrator centerlines is 26m in the N-S direction and 56m in the E-W direction. This corresponds to a 25% packing fraction within the immediate vicinity of the concentrators; the placement of the fence makes it appear the packing is less dense. Geological restrictions may dictate alternate field layout configurations but as long as there is access for equipment this does not affect the site implementation plan.

### 3.4.2 FOUNDATION CONSTRUCTION

Three friction piles are used for each concentrator. The exact diameter, length and type will be dictated by the local soil conditions and the availability of pile materials in the area. The foundation piles will be delivered to the site in one bulk lot (~60 piles including spares) and offloaded with the crane used during the pile driving operation. The first step would be to drive a test pile and load it to verify the soil bearing and friction characteristics.

Standard pile driving equipment will be used, consisting of the crane and hydraulic/pneumatic pile driving beam and hammer. The piles used will be approximately 20 feet long and will be driven vertically. Step (1A) on Figure 64 shows this simulated operation in process. An average pile length and diameter should be able to be driven in typical sandy/silt/clay type soil in approximately 20-30 minutes. Following driving, the tops of the piles will be prepared to accommodate the concentrator pedestal base leg attachment. Timber piles will be slotted to accept the pedestal leg blade.

### 3.4.3 CONCENTRATOR INSTALLATION

The basic concentrator components will be shipped to the site, offloaded and positioned close to the foundation in accordance with a predetermined staging plan. The necessary alignment fixtures, jigs, cribbing, supports, cranes, etc. will be mobilized to the site and set up in preparation for the start of erection.

Current plans call for three small crews (~4 men) of ironworker-type personnel to be used during the erection phase. The first crew would assemble radial trusses of the reflector structure on the ground. The second crew will work on the ground assembly of the reflector structure and surface panels. The third crew will ground-assemble the pedestal structure and tripod assembly. In addition, this crew will erect the pedestal, install the reflector assembly and mate the tripod to the reflector. As this is done the first and second

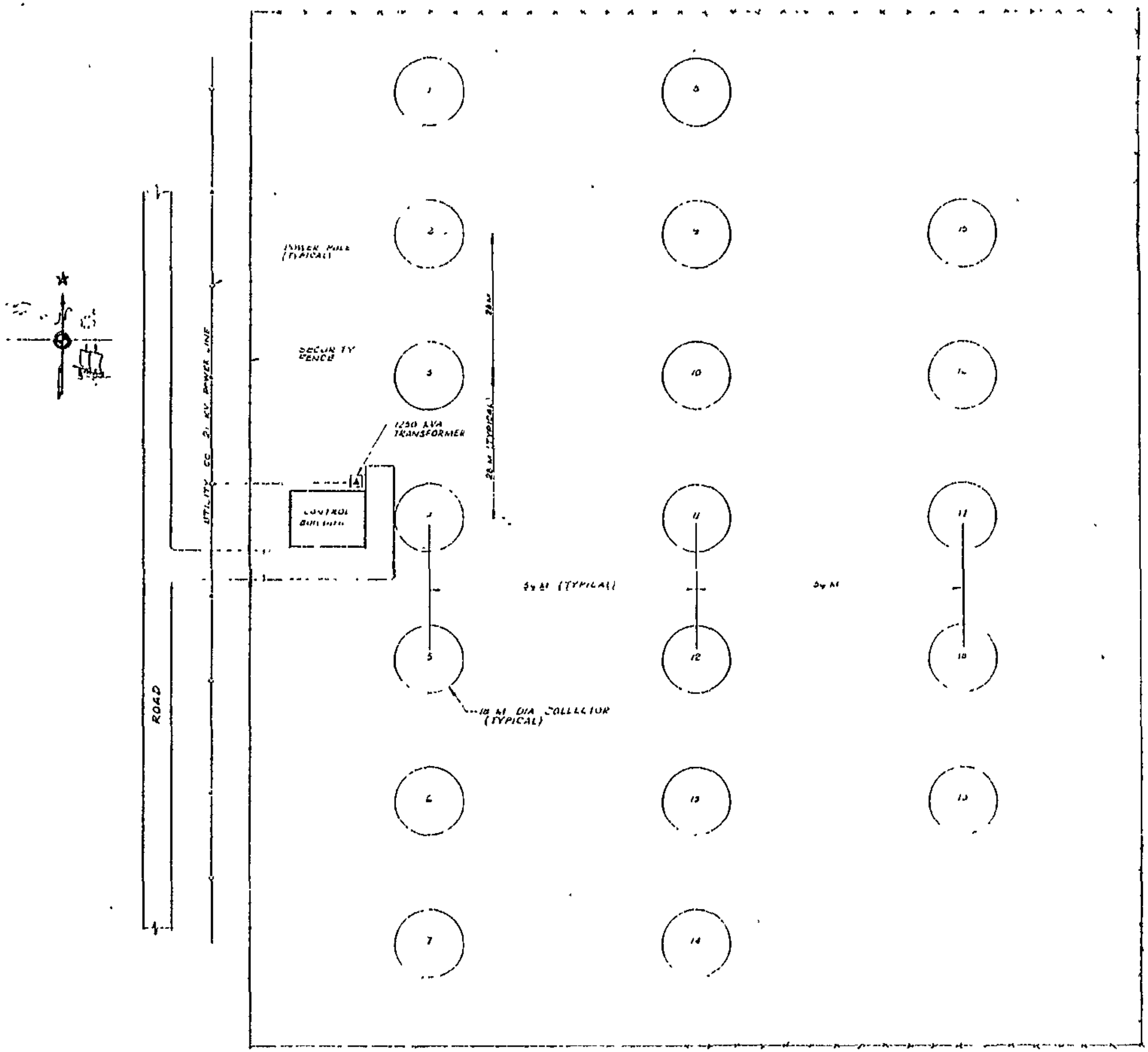


FIGURE 63. TYPICAL 1 MWe SITE LAYOUT

94-2-233

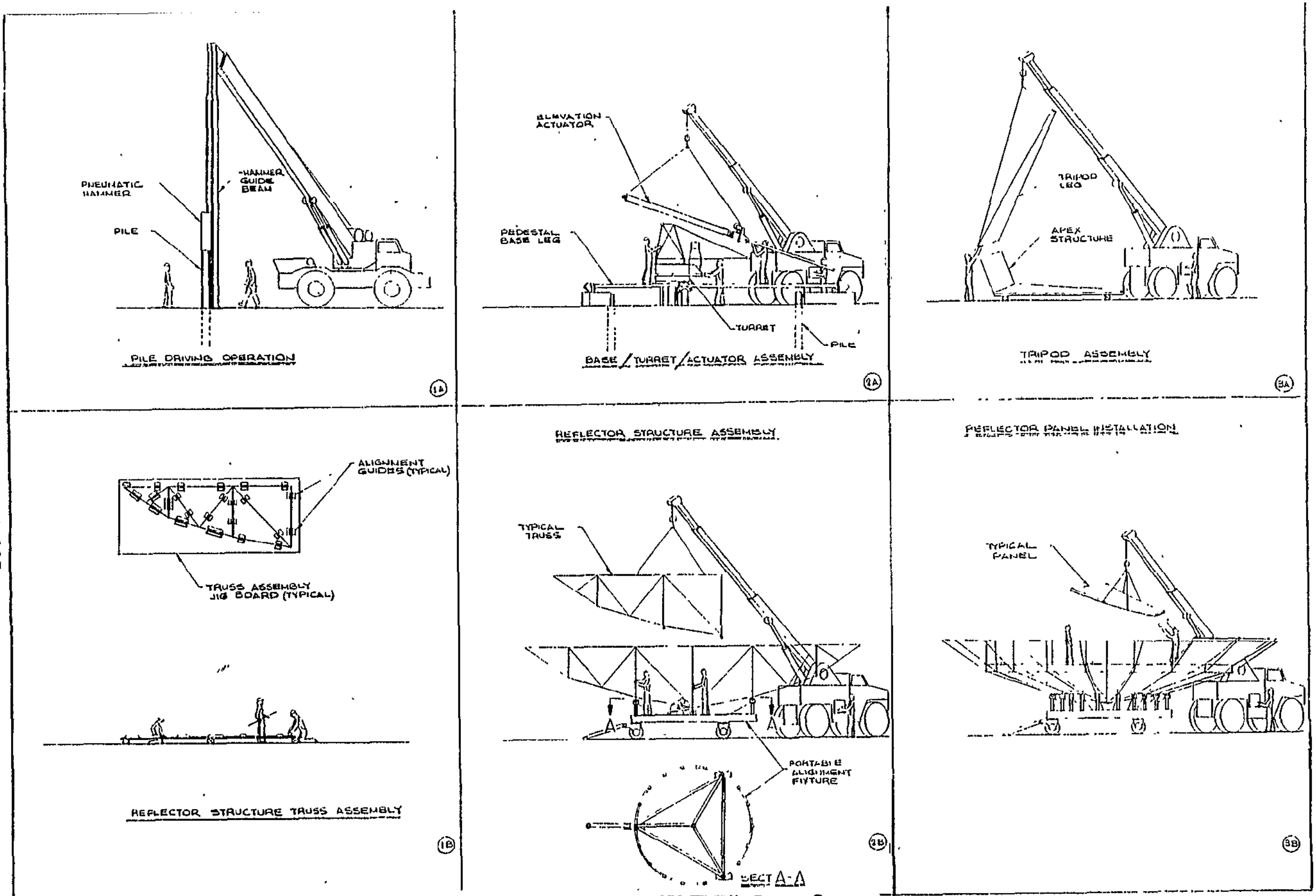


FIGURE 64. TYPICAL CONCENTRATOR INSTALLATION SEQUENCE (SHEET 1 of 2)

94-2 234a

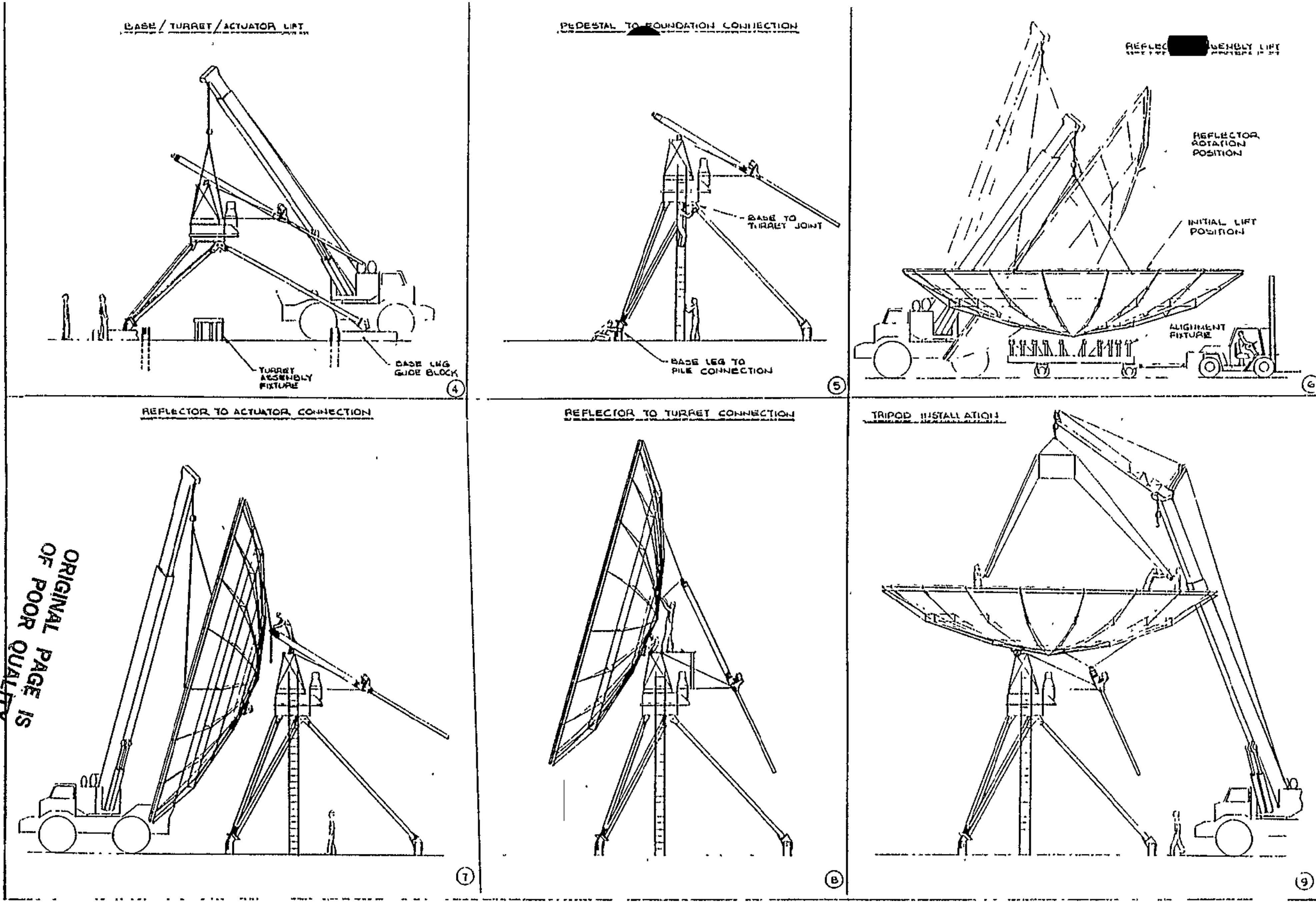




FIGURE 64. TYPICAL CONCENTRATOR INSTALLATION SEQUENCE (SHEET 2 of 2)

94-2-234b

crews continue assembling radial trusses and reflector assemblies, respectively. The most economical approach would be to serially install each concentrator, with the crews performing repetitive functions.

3.4.3.1 Reflector Radial Truss/Assembly. One crew would open the bundles of tubing packaged in accordance with a pre-planned site assembly sequence. All parts will be adequately marked to allow for easy identification. The tubular members will be assembled into two identical horizontal truss assembly jigs (a single typical jig is shown in Figure 64, Step (1B)). These jigs allow rapid assembly and precise alignment of radial truss members. All connections are huck riveted.

3.4.3.2 Reflector Structure and Panel Assembly. The second crew takes the assembled radial trusses and mounts them into a transportable reflector assembly jig (See Figure 64, Step (2B)). This fixture will be designed to perform the function of positioning each radial truss in its exact location without the requirement of alignment procedures. (Figure 65 shows the radial trusses of a typical microwave reflector installed on the ground.) As the radial trusses are installed, the tubular intermediate circumferential and diagonal members are added. All connections are huck rivet type, which affords a rapid and positive joint. (Figure 66 shows a typical microwave antenna reflector structure which had been assembled in a similar manner.)

Once all the reflector members have been installed and connections made, the reflector panels will be uncrated and installed. Each panel will be lowered in place using a crane and nylon slings to protect the glass panels from damage as shown in Figure 64, Step (3B). Since all trusses are automatically aligned via the jig, the reflector panels are simply bolted in place and become correctly positioned also without further adjustments or alignments. After the last panel is installed, the erection crew (third crew) lifts the entire reflector structure and panel assembly from the jig. The transportable fixture is then moved to the next concentrator location and the sequence is repeated.

3.4.3.3 Pedestal Assembly and Concentrator Erection. The third crew has the responsibility of assembling the pedestal structure and connecting all the concentrator subassemblies to each other. Their first task is to mount the azimuth bearing/gear housing portion of the turret assembly onto a support fixture located on the azimuth centerline of the concentrator, Step (2A). The six base-support-tubes are then connected to this housing and layed out horizontally. The ends are supported on guide blocks which position the pedestal leg pads at the correct height to allow them to freely slide as the assembly is raised. The tubular triangular framework above this housing is then assembled and riveted together. Since all members of this assembly have been precisely fabricated and toleranced in the shop, there is no requirement for field alignment. Finally, the elevation actuator is connected to the rear turret pivot and allowed to rest on the forward truss framework.

The third crew also assembles the tripod structure on the ground as shown in Step (3A). Two of the three legs are layed horizontal on the ground and connected to the power module support structure while the third leg is simply cantilevered in the air.

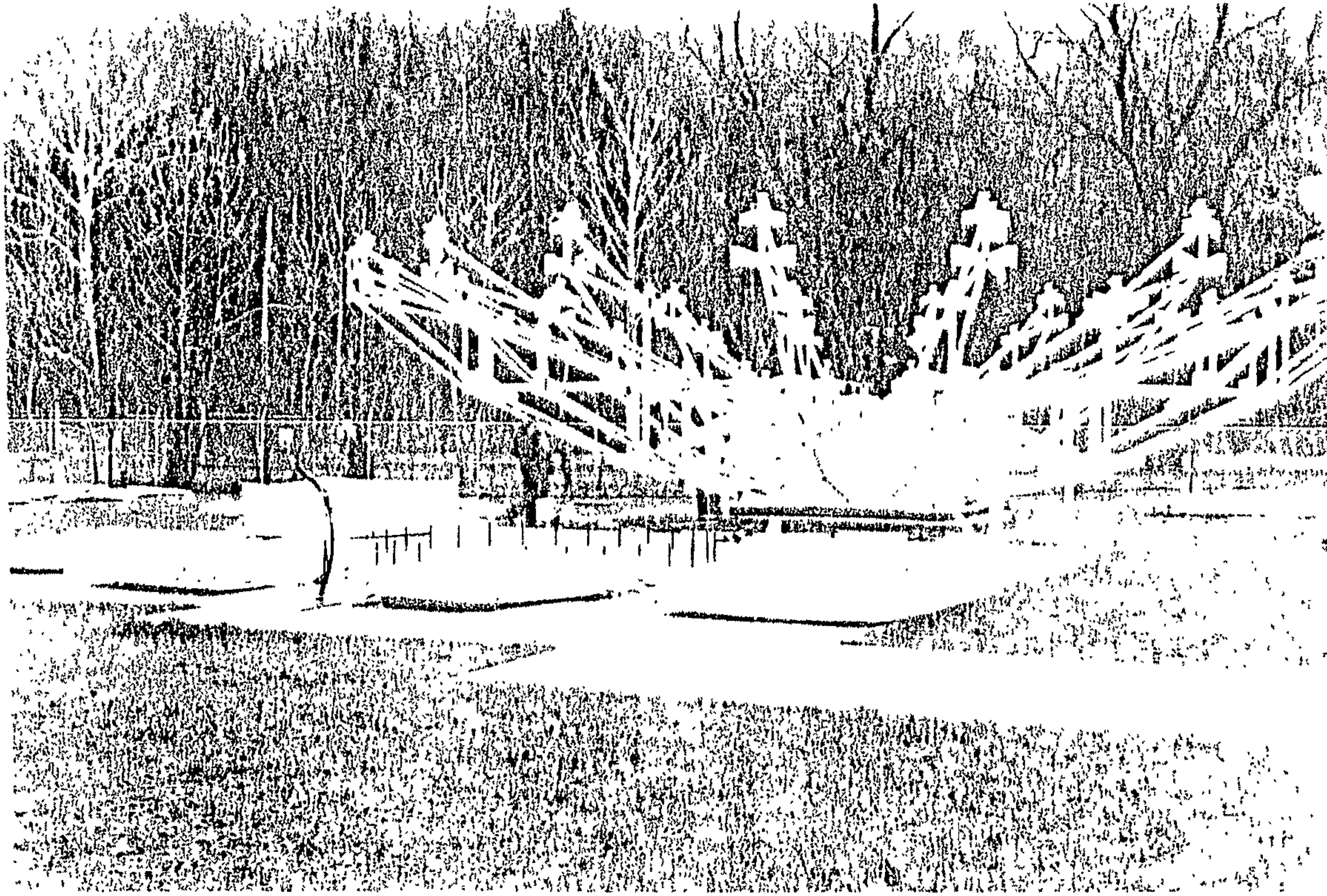

FIGURE 65. TYPICAL REFLECTOR RADIAL TRUSS INSTALLATION

94-2-235

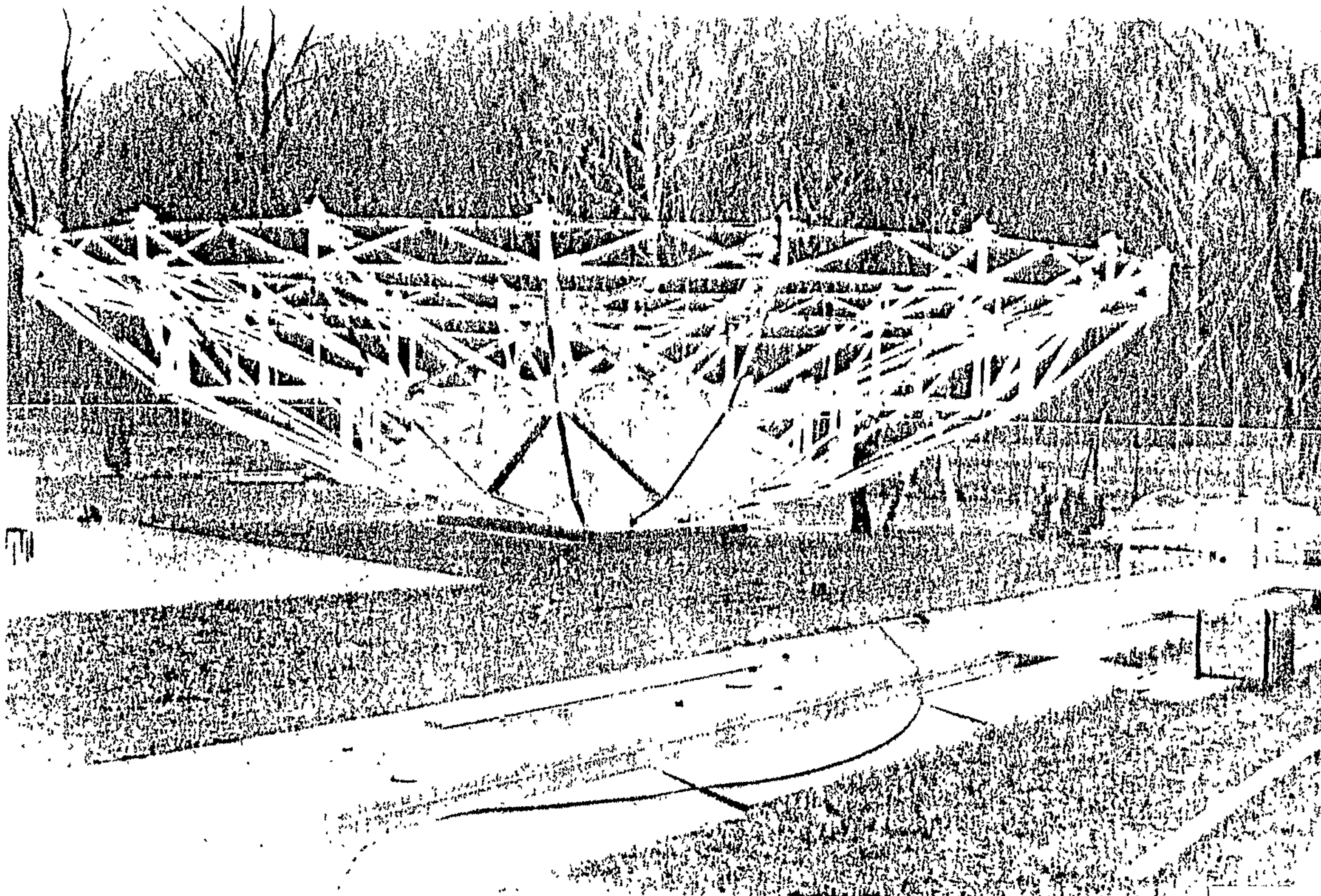

94-2-236

FIGURE 66. TYPICAL REFLECTOR STRUCTURE ASSEMBLY

The next major operation is to raise the base/turret/actuator assembly vertically in place, allowing the outboard ends of the base legs to slide along the support blocks while the inboard ends pivot about the pin joints (see Step (4)). As the outboard legs approach the foundation piles, they are guided into the correct position and bolted in place. The inboard pivots rotate to allow for the insertion of another bolt to form stiff connections to the azimuth bearing/gear housing (Step (5)).

As soon as the second crew completes their assembly of the reflector structure and panels, it is raised off the fixture (Figure 67 shows a typical microwave antenna being lifted), and the crane rotates this reflector assembly until it is facing approximately 20 degrees above horizon (see Step (6)). This will allow for the reflector to be raised to the correct height without requiring a long length of crane boom and consequently additional crane capability (and cost). The reflector is then brought up to the position shown in Step (7), where the connection is made between the elevation actuator clevis and the vertical link bar of the rear of the reflector structure. The reflector is then raised until the two elevation bearing connections can be made and also the other two reflector structure links to the actuator can be reached (Step (8)). The reflector assembly is released from the crane and the load taken by the pedestal structure.

The final step for this crew is to pivot the tripod structure from the ground and raise it in the zenith (elevation angle 90 degree) position. Due to its light weight, this piece can be lifted using the crane's jib extension. The reflector structure meanwhile was rotated to the zenith position via a hand-held drill motor attached to the elevation actuator drive shaft. The tripod structure is then swung around and slowly lowered to mate with the reflector as shown in Figure 64, Step (9). This sequence is then repeated for the next concentrator.

In summary, the installation is to be accomplished with experienced crews performing repetitive tasks, using special fixtures and jigs specifically designed to expedite assembly and eliminate the necessity for field alignment and utilizing standard handling and lifting equipment. When a typical 1 MWe station is completed, all personnel, fixtures and equipment will be mobilized to the next site where the erection pattern will be repeated again. (See Figure 68 of a typical installation of three 60 foot microwave antennas completed in a similar manner to that described above.)

### 3.4.4 CONCENTRATOR SERVO, TRACKING AND ELECTRICAL INSTALLATION

A specialized electrical crew consisting of only two men will install and checkout the electrical, servo and tracking subsystems. All the pigtails of the electrical power, signal and control cables from the central control facility which were previously buried are terminated into the appropriate electrical enclosures mounted to the pedestal base legs. From these enclosures, all pre-cut, pre-connectorized cables will be routed through the concentrator structure to the appropriate motors, encoders, sensor, limit switches, apex structure, etc. These cables will cross the axes in a service loop arrangement which will allow for full azimuth and elevation rotational capability without the need for elaborate cable wrap mechanisms.

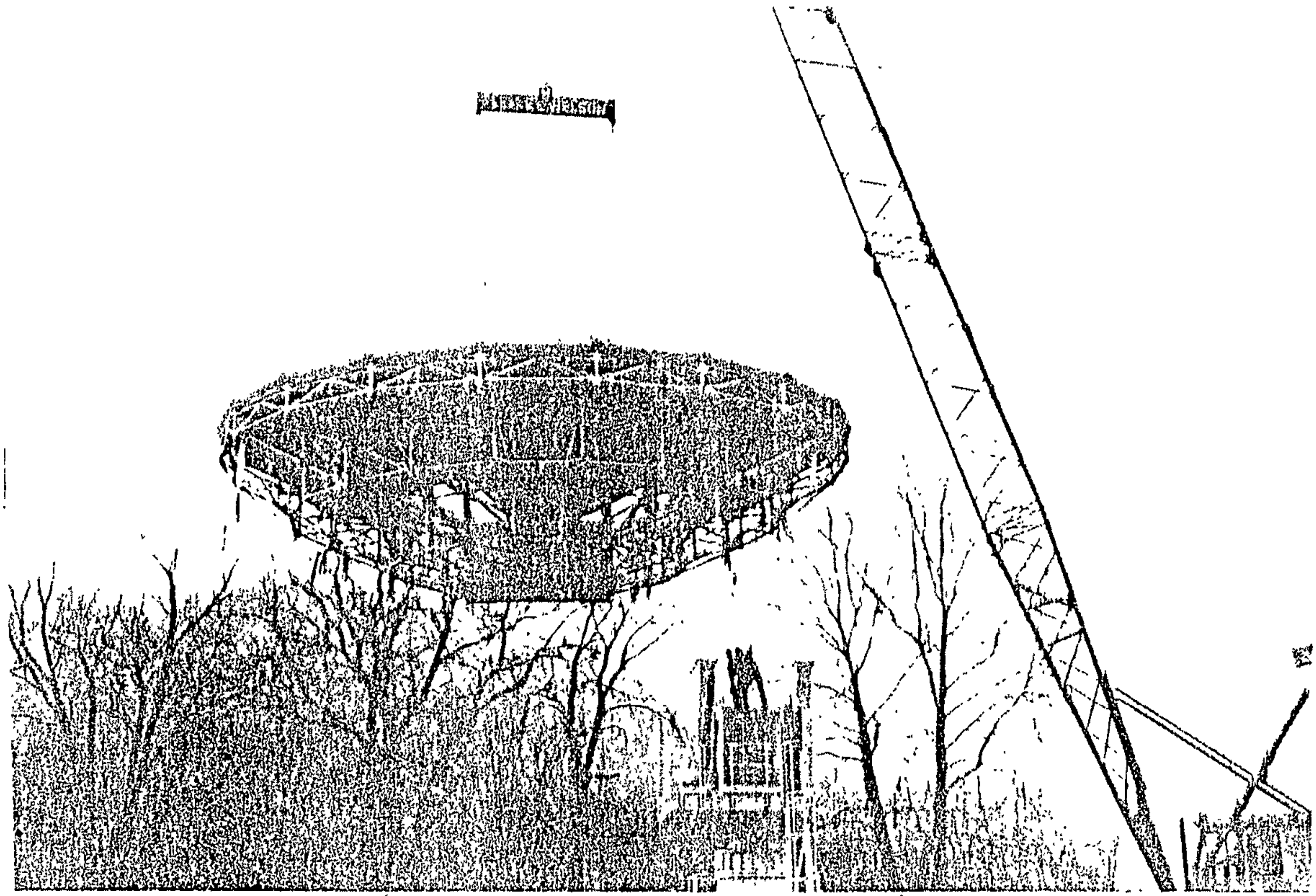

FIGURE 67. TYPICAL REFLECTOR STRUCTURE/PANEL ASSEMBLY BEING LIFTED

94-2-237

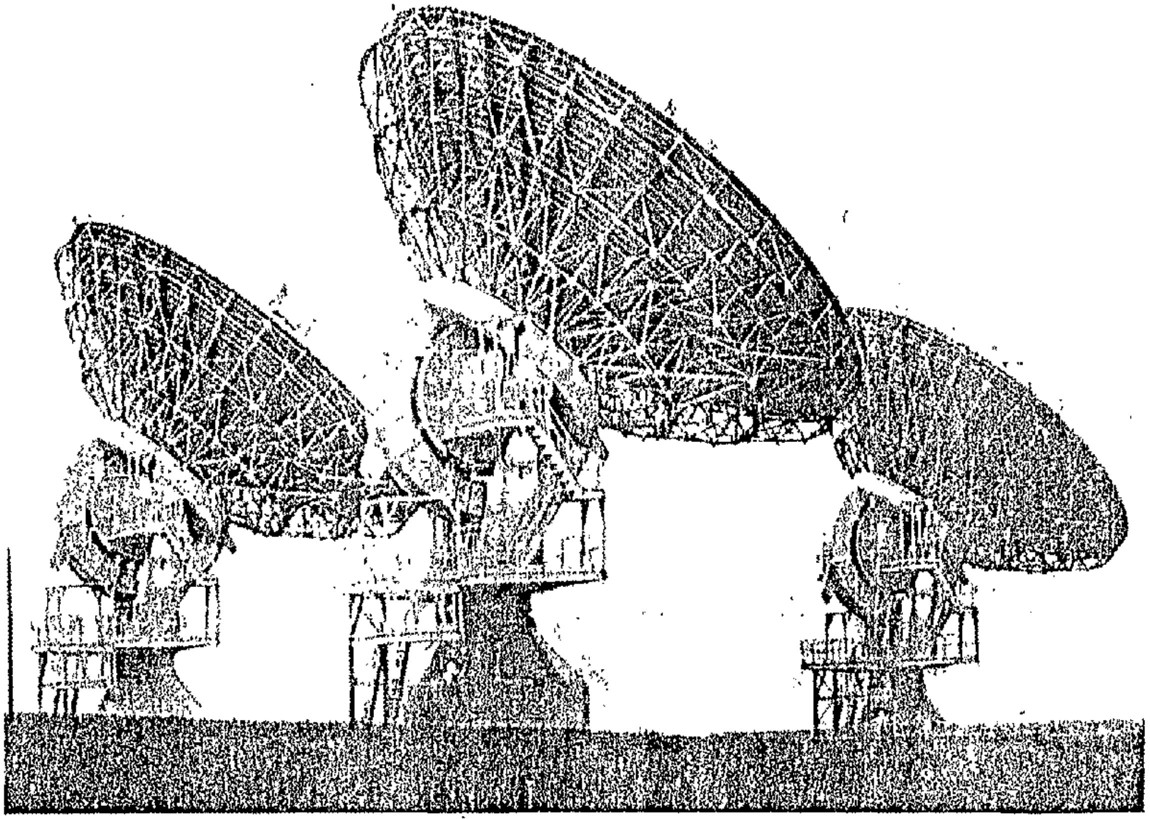

94-2-238

FIGURE 68. MULTIPLE 60 FOOT ANTENNA INSTALLATIONS

The sun sensor will be mounted and aligned to the primary reflector using a special alignment jig. Axis encoders will be electrically connected (encoders have been previously mounted in the shop). The elevation encoders will be aligned using predetermined reference markings on the encoder housing and mounting plate for a given actuator extension length. The azimuth encoders will be zeroed to true south by the use of a special polar magnetic sensing device. Drive motors will be hooked up and limit switches wired. Cables will be routed up one of the tripod support legs. The power module will be mounted in place using the specially equipped site maintenance and servicing vehicle. All electrical and cooling lines will be connected and the system will be ready for operation.

### 3.4.5 CONCENTRATOR ALIGNMENT, CHECK AND TEST

The computer in the central facility will be programmed to perform functional checks on the individual concentrator module. These checks will verify travel limits, axis drive velocities and accelerations, tracking accuracies, rated power output and monitor all the critical parameters of the system. After verification checks, the concentrator will be programmed into the normal operational mode for the start of a ~100 hour "burn-in" period - a period particularly appropriate for the electronic components.

## 3.5 OPERATION AND MAINTENANCE REQUIREMENTS

The 1 MWe station is designed for unattended operation except for maintenance functions. One visit per week by one utility company employe (or service company employe) will handle the scheduled maintenance and cleaning. Emergency and failure conditions will be sensed and an alarm transmitted to a manned utility station.

A great advantage of a modular concept in which electricity is generated at each collector is that the actual electrical performance of each individual collector is continually monitored at negligible cost. The need for cleaning, adjustment, or repair can be determined if any collector fails to deliver energy equal to the other units. Therefore, maintenance can be provided in an optimum manner.

During the weekly visit, the following maintenance will be performed:

- Weekly inspection of control equipment and investigation of any collector that is generating electricity below the nominal.
- Quarterly inspection check for two collectors (1/10 of system per week).
- Annual maintenance for one collector every third week.

### 3.5.1 REFLECTIVE SURFACE CLEANING

The frequency of reflective surface cleaning is highly site-, seasonal-, and weather-dependent. A 4-week cleaning interval has been chosen as representative of long-term average cleaning rates to maintain good mirror reflectivity. As illustrated in Figure 69, natural cleaners such as rain and frost will extend the cleaning period or improve reflectivity, while severe dust storms will require more frequent cleaning to maintain high reflectivity. Unusual local soil/dust/environmental conditions may also revise cleaning procedures. Since the performance level can be precisely determined with the modular concept, the cleaning cycle will be optimized on a cost/performance basis based on the results of current DOE-sponsored cleaning studies and procedures. (Statements by some operating managers at the Albuquerque STTF indicate that reflective surface cleaning can be omitted completely. However, FACC review indicates that the cleaning procedures described herein should maintain reflectance at minimum cost, and the possible danger of permanent surface deterioration due to lack of cleaning is elminated.)

The following cleaning procedure has been selected:

(1) Five concentrators will be selected for the weekly maintenance visit. These units will remain at the West horizon position overnight to be ready for early morning (or evening) cleaning.

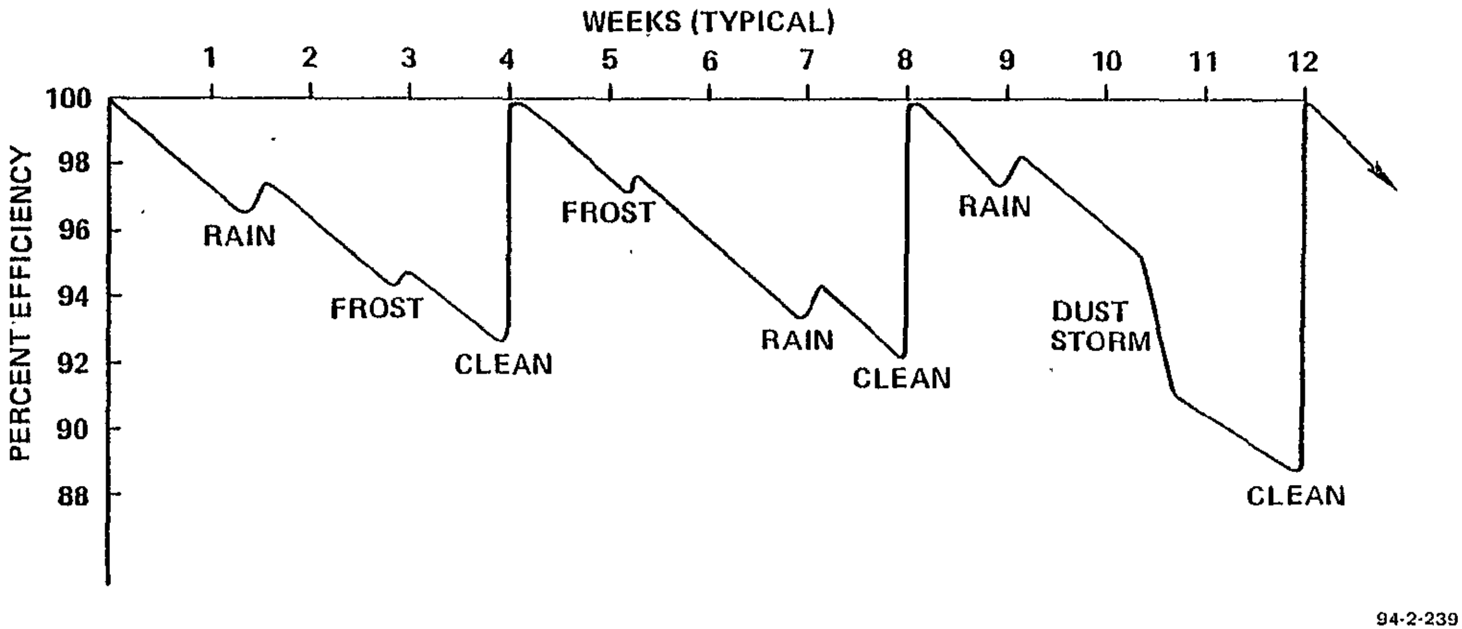


FIGURE 69. TYPICAL DIRT/DUST REFLECTIVITY LOSS

(2) The spray-soak-rinse cleaning method is proposed. Cleaning studies presently underway may determine that a one operation cleaning (without rinsing) is cost effective. A specially formulated cleaning solution is sprayed on the surface, allowed to soak for a predetermined length of time, and spray-rinsed with deionized water. The cleaning agent will be selected based on wetability (time and area), residue built-up and cost/performance. Total spray, soak, and rinse time per each 18.6m diameter concentrator is ~0.5 hours. The cleaning vehicle and concentrator position are shown in Figure 70. This vehicle is described in section 3.5.3 and is controlled by one man.

(3) Water use is 200 liters per concentrator, or a total of only 1000 liters per week. This could be important since water is scarce in desert regions.

(4) A mechanical scrub method was considered which uses deionized water (with or without a cleaning agent). After initial flushing, soft brushes scrub the surface, and it is then rinsed in deionized water. This method was not selected since it requires more sophisticated equipment, and introduces a danger of damaging the collector since the cleaning equipment must be closer to the reflector and particularly to the receiver support tripod. However, this is retained as an option since some scrubbing may be necessary to remove the surface film.

### 3.5.2 CONTROL AND MONITORING

During the weekly maintenance visit to the system control building, the utility employe will call-up and review the performance data of individual collectors on the CRT terminal. A specified collector can then be inspected and checked to identify and repair, replace, or correct a problem. The disc drive recorder will also be inspected for routine maintenance. The disc will be changed and previous data disc delivered to the utility network office for further analysis and recording of system performance.

Experience has shown that most electrical component failures occur during initial turn-on or during the first 100 hours. Consequently for a high reliability system, "burn-in" of all electornic components is considered essential.

Experience indicates that more maintenance is required during the first year of operation. Therefore, the following schedule has been developed:

<u>First Year</u>:

- Monthly inspection of each concentrator
- Semi-annual maintenance of each concentrator.

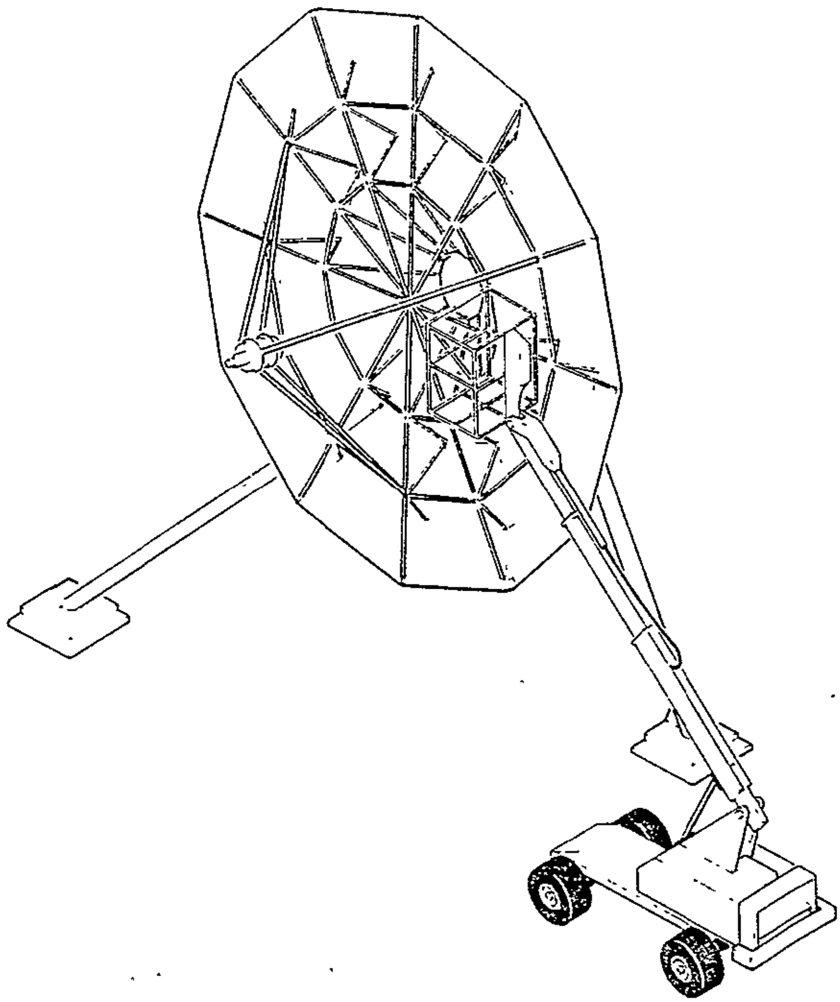


FIGURE 70. TYPICAL MAINTENANCE EQUIPMENT

Subsequent Years (2nd through 30th):

- Quarterly inspection of each concentrator
- Annual maintenance of each concentrator.

Inspection Items:

- Visual inspection of elevation actuator/gear reducer for possible oil leaks.
- Visual inspection of azimuth gear reducer for possible oil leaks.

- Reflective surface glass for possible cracks or silver deterioration.

- Visual inspection of structure for possible loose/bent members, corrosion, and loose fasteners.

- General visual checks for weathering, animal or bird intrusion or damage, and vegetation growth.

Maintenance Items:

- Visual inspection and lubrication of elevation actuator/ gear reducer.

- Observe condition of elevation actuator boot cover.

- Inspect azimuth bull gear for wear.

- Visual inspection of elevation bearings.

- Check generator bearing.

- Check electrical cables and junction boxes.

- Clean microprocessor circuit boards.

- Inspect azimuth bearing.

- Check operation of travel limit switches.

- Check defocus and stow sequences.

- Visually inspect for water collection pockets.

NOTE: Receiver and engine maintenance and inspection will also be performed as part of the overall control and monitoring process.

### 3.5.3 O & M EQUIPMENT REQUIREMENTS

Based on 100 to 5000 sites activated annually, an all-purpose maintenance and cleaning vehicle would be provided as a modification of existing commercially available equipment, (see Figure 70). Several sites can share the vehicle if they are close together, but this estimate assumes one $50,000 vehicle per site. Considering its limited use and routine maintenance, the vehicle should be serviceable for 30 years.

The principal feature of the vehicle would be an adjustable platform from which the maintenance man can clean the surface using two high pressure spray nozzles (wash and rinse) with piping to the two attached solution and water tanks. The platform will also provide access to the maintenance areas on the collector, particularly the power conversion module. A key feature of the vehicle is that all operations are controlled by one man from his platform position.

### 3.6 CONCENTRATOR RELIABILITY ANALYSIS

This section describes the approach to predicting the desired high reliability of the concentrator subsystem. The predicted failure rate and MTBF (Mean Time Between Failures) of each concentrator is 36 failures per million hours and 27,000 hours, respectively.

#### 3.6.1 BACKGROUND

FACC's broad experience with space communication antennas is directly applicable to the concentrator subsystems. The high reliability requirements associated with the tracking, telemetry, and command of military satellites has placed great emphasis on the proper selection of components, stress levels, and maintainability design. The unattended operation requirements of these terminals requires high reliability and low down-time just as the case for the solar applications.

#### 3.6.2 ANALYSIS AND CALCULATIONS

Definitions and ground rules are:

(1) Subsystem Failure. Any event attributable to a subsystem which prevents the SPS from performing its required function.

(2) Dimensions. All failure rates ($\lambda$) are quoted in the dimension of failures per million hours, and MTBF are quoted in hours.

(3) Functional and Total Failure Rate. Total failure rate is the summation of all the failure rates of each element in the subsystem. Functional failure rate takes into account redundancies and does not include non-critical equipment, and is one which will cause a subsystem failure. Only functional failure rates are given here.

(4) Duty Cycle. The concentrator subsystem is assumed to operate on a 100 percent duty cycle for the period of the day when solar energy is available, including reset time for the following day's operation. However, the electronics and tracking control is on 24 hours per day.

(5) Reliability Model. The reliability configuration block diagram for each concentrator is shown in Figure 71. The failure rate is obtained by a serial summation of equipment failure rates. The equipment items are considered in series, that is, the failure of any equipment is assumed to result in a functional failure.

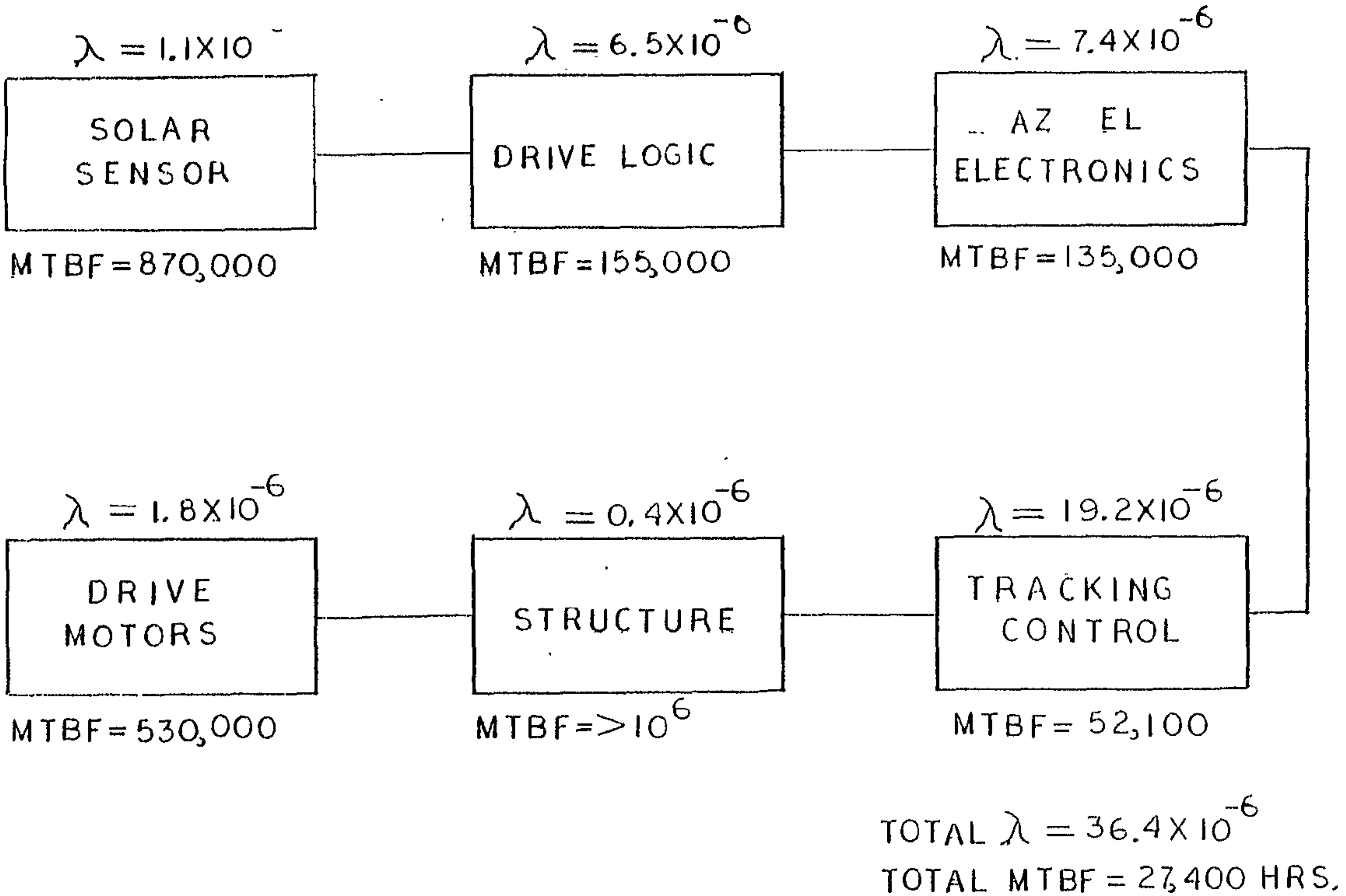


94-2-241

FIGURE 71. CONCENTRATOR SUBSYSTEM RELIABILITY MODEL

(6) Reliability Predictions. The predictions and estimates used were made in accordance with the procedures of MIL-STD-756A and MIL-HDBK-217B, Section 3. The parts count prediction using failure rates from Section3 and ground environment were used. A listing of the equipments and their failure rates are contained in Table 30 and the summary is shown in Table 31.

TABLE 30. SUMMARY OF CONCENTRATOR SUBSYSTEM RELIABILITY

| Concentrator Components | Quantity | Failure/$10^5$ hours | Group Failure/$10^5$ hours |
|---|---|---|---|
| Solar Sensor | | | |
| Solar Cell | 1 | 0.2 | 0.2 |
| IC, Driver | 1 | 0.95 | 0.95 |
| Subtotal, λ | | | 1.15 |
| Drive Logic | | | |
| Switches | 4 | 0.38 | 1.52 |
| Crystal | 1 | 0.20 | 0.20 |
| IC Digital | 9 | 0.30 | 2.70 |
| IC Linear | 2 | 0.95 | 1.90 |
| Resistors | 9 | 0.015 | 0.13 |
| Subtotal, λ | | | 6.45 |
| Azimuth Axis Electronics | | | |
| IC's | 8 | 0.3 | 2.4 |
| Relays, SS | 2 | 0.604 | 1.21 |
| Resistors | 10 | 0.01 | 0.10 |
| Subtotal, λ | | | 3.71 |
| Elevation Axis Electronics | | | |
| IC's | 8 | 0.3 | 2.4 |
| Relays, SS | 2 | 0.604 | 1.21 |
| Resistors | 10 | 0.01 | 0.10 |
| Subtotal, λ | | | 3.71 |
| Tracking/Servo Control, AZ & EL | | | |
| Capacitors | 12 | 0.026 | 0.31 |
| IC's Linear | 4 | 0.95 | 3.80 |
| Resistors | 31 | 0.015 | 0.46 |
| Switches | 2 | 0.38 | 0.76 |
| Potentiometer | 2 | 0.33 | 0.66 |
| IC's Digital | 12 | 0.30 | 3.60 |
| Encoders | 2 | 1.377 | 2.75 |
| Processor (4k) | 1 | 2.50 | 2.50 |
| Power Supply | 1 | 4.35 | 4.35 |
| Subtotal, λ | | | 19.19 |
| Structure | | | |
| El Bearing | 2 | 0.0005 | 0.001 |
| El Drive | 1 | 0.167 | 0.167 |
| Az Bearing | 1 | 0.002 | 0.002 |
| Az Drive | 1 | 0.204 | 0.204 |
| Subtotal, λ | | | 0.374 |

TABLE 31. FAILURE RATE SUMMARY (PER CONCENTRATOR)

| Concentrator Components | Failure/$10^6$ hours | MTBF (hours) |
|---|---|---|
| Solar Sensor | 1.15 | 870,000 |
| Drive Logic | 6.45 | 155,000 |
| Azimuth Electronics | 3.71 | 270,000 |
| Elevation Electronics | 3.71 | 270,000 |
| Tracking Control | 19.19 | 52,100 |
| Drive Motors (Az & El) | 1.86 | 530,000 |
| Structure | 0.37 | 2,700,000 |
| Total Concentrator | 36.4 | 27,400 |

SECTION 4

# CONCENTRATOR LIFE CYCLE COST ESTIMATES

Life cycle cost estimates for the concentrator subsystem for the Solar Power System program have been subdivided into (1) capital investment costs, (2) scheduled component replacement costs, and (3) maintenance costs. These costs are defined in the following paragraphs and are based on the selected concept, i.e., 1 $MW_e$ station, 0.4 capacity factor, 19 concentrators per site, 18.6 meter diameter.

## 4.1 CAPITAL INVESTMENT COSTS

Table 32 summarizes the concentrator subsystem capital costs for the production quantities of 100 to 5000 sites (1 $MW_e$ each) per year implemented in the late 1980's (1978 base year dollars).

## 4.2 SCHEDULED COMPONENT REPLACEMENT COSTS

Major spare parts and component replacement costs are insignificant (less than $\$0.5/m^2$). Reliability calculations indicate a failure rate less than 0.3 per site per 30 years for mechanical components.

TABLE 32. CONCENTRATOR CAPITAL INVESTMENT SUMMARY

| Concentrator Component Description | 100 Sites/Yr | 500 Sites/Yr | 1000 Sites/Yr | 5000 Sites/Yr |
|---|---|---|---|---|
| Reflective Panels | $\$38/M^2$ | $\$34/M^2$ | $\$32/M^2$ | $\$24/M^2$ |
| Structural | 59 | 56 | 54 | 48 |
| Mechanical | 24 | 20 | 19 | 16 |
| Drive Motors/Controllers | 2 | 2 | 1 | 1 |
| Tracking Control | 2 | 2 | 1 | 1 |
| Subtotal Hardware | 125 | 114 | 107 | 90 |
| Site Foundation | 11 | 10 | 10 | 9 |
| Site Installation/Checkout | 27 | 25 | 23 | 21 |
| Shipping to Site | 6 | 6 | 6 | 6 |
| Project Operation | 3 | 2 | 2 | 1 |
| Maintenance Equipment | 9 | 8 | 8 | 7 |
| Total ($\$/M^2$) | $\$181/M^2$ | $\$165/M^2$ | $\$156/M^2$ | $\$134/M^2$ |
| Total $\$(19 \times 272M^2)$ | \$935 K | \$853 K | \$806 K | \$693 K |

## 4.3 MAINTENANCE COSTS

Scheduled maintenance is defined in paragraph 3.5. For the first year of operation, the hours per week include 2-1/2 hours for reflector cleaning, 2-1/2 hours inspection and maintenance, and 1 hour commute travel time. (The 1/2 hour control building tasks are included in the electrical subsystem budget). For subsequent years of operation, the same tasks require 2-1/2, 1-1/4 and 1 hour per week, respectively. A summary of annual life cycle maintenance costs for the concentrator are listed in Table 33.

TABLE 33. LIFE CYCLE MAINTENANCE COSTS

| Annual Costs for 30 Years | 1st Year | 2nd through 29th Year |
|---|---|---|
| • Scheduled maintenance labor @ $17/Hr | $5.3 K | $4.2 K |
| • Commute mileage (50 miles/wk @ 14¢) | 0.4 | 0.4 |
| • Cleaning water and cleanser | 0.3 | 0.3 |
| • Lubricants and minor spares | 0.1 | 0.1 |
| • Servicing of maintenance vehicle | 0.1 | 0.1 |
| • Unscheduled maintenance @ $25/Hr | 0.4 | 0.1 |
| Total | $6.6 K | $5.2 K |

## SECTION 5

## SENSITIVITY ANALYSIS

The effect in reducing the plant rated power to 0.5 $MW_e$ or in raising it to 10.0 $MW_e$ is summarized along with the capacity factor variation from a no storage system up to a station having a 0.7 capacity factor rating.

### 5.1 CONCENTRATOR SUBSYSTEM SENSITIVITY TO PLANT SIZE (RATED POWER)

The concentrator design will be the same whatever the rated power, only the quantity of concentrators per site will vary (i.e., 10 modules for 0.5 $MW_e$, 190 for 10 $MW_e$). The production cost will remain constant since it is assumed that the annual quantities remain unchanged. Site implementation costs will vary with rated power since it is more efficient to install the same modules in larger quantities on fewer sites.

Figure 72 illustrates the far term total concentrator costs ($\$/m^2$) as a function of a plant size variation from 1/2 $MW_e$ to 10 $MW_e$ and for the specified annual quantities varying from 100 $MW_e$ to 5000 $MW_e$.

Operation and maintenance costs of the concentrator system will vary only slightly with plant size. The total area of reflective surfaces requiring cleaning and the total quantity of components requiring maintenance will remain constant. Concentrator costs would be slightly lower for one large 10 $MW_e$ plant than for ten 1 $MW_e$ or twenty 1/2 $MW_e$ plants if they were all located the same distance from the utility area maintenance depot and had similar commute time.

### 5.2 CONCENTRATOR SUBSYSTEM SENSITIVITY TO ANNUAL CAPACITY FACTOR

The concentrator modules will be identical whether the annual capacity factor is 0.7, 0.4 or zero storage, again only the quantity of concentrators will change. The total concentrator subsystem cost per site will, of course, vary with the quantity of modules required, which is a sizable variation. The cost/$m^2$ of aperture will be the same for zero storage or for 0.4 capacity factor since the difference is only 18 vs 19 concentrators respectively, but will reduce for the 0.7 capacity factor which requires approximately twice as many concentrators on each site.

Figure 73 illustrates the far term total concentrator costs ($\$/m^2$) with varying capacity factors and for the specified annual quantities varying from 100 sites to 5000 sites, each with 1 $MW_e$ rated power.

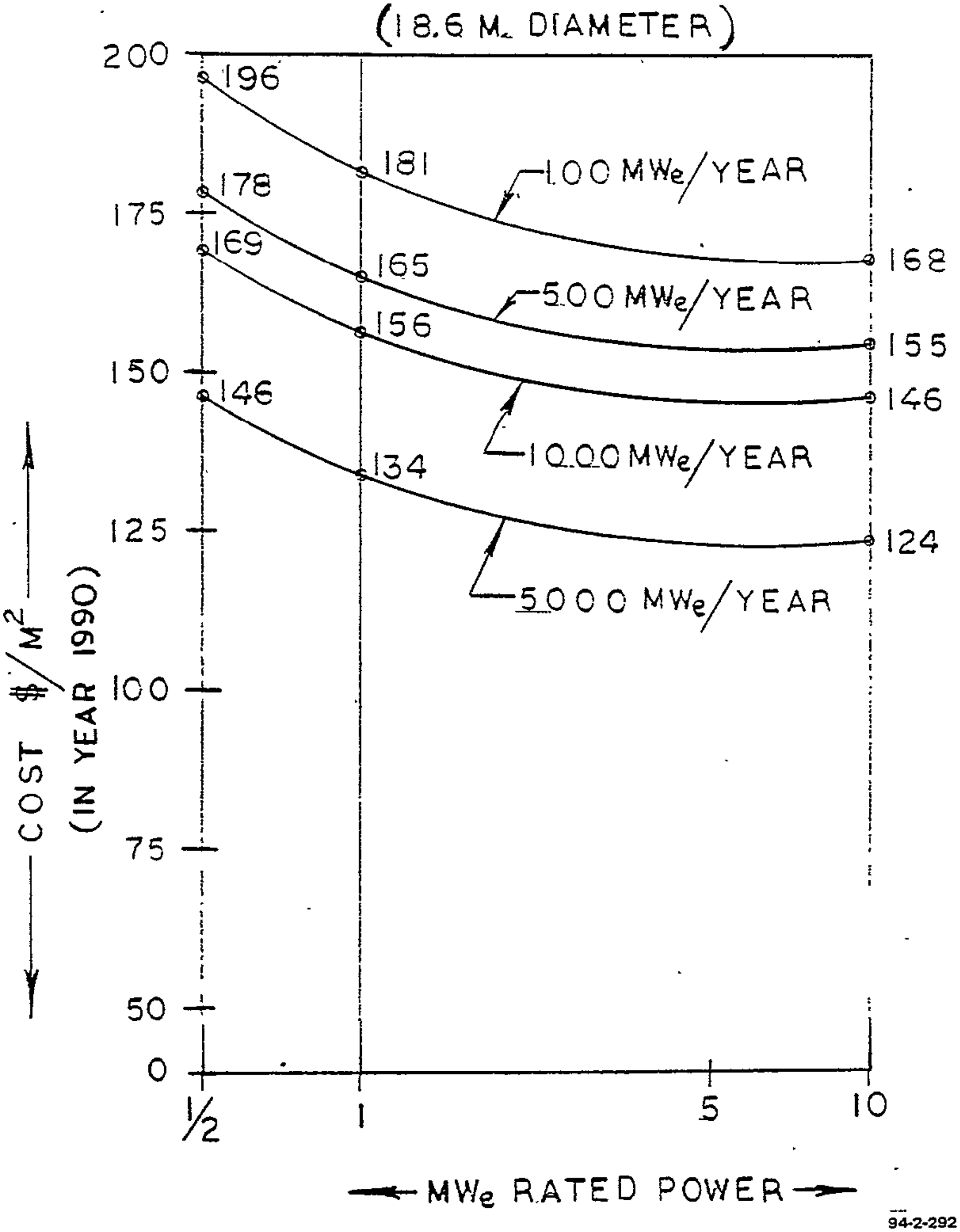


FIGURE 72. CONCENTRATOR COST SENSITIVITY TO PLANT SIZE AND QUANTITY (18.6 M. DIAMETER)

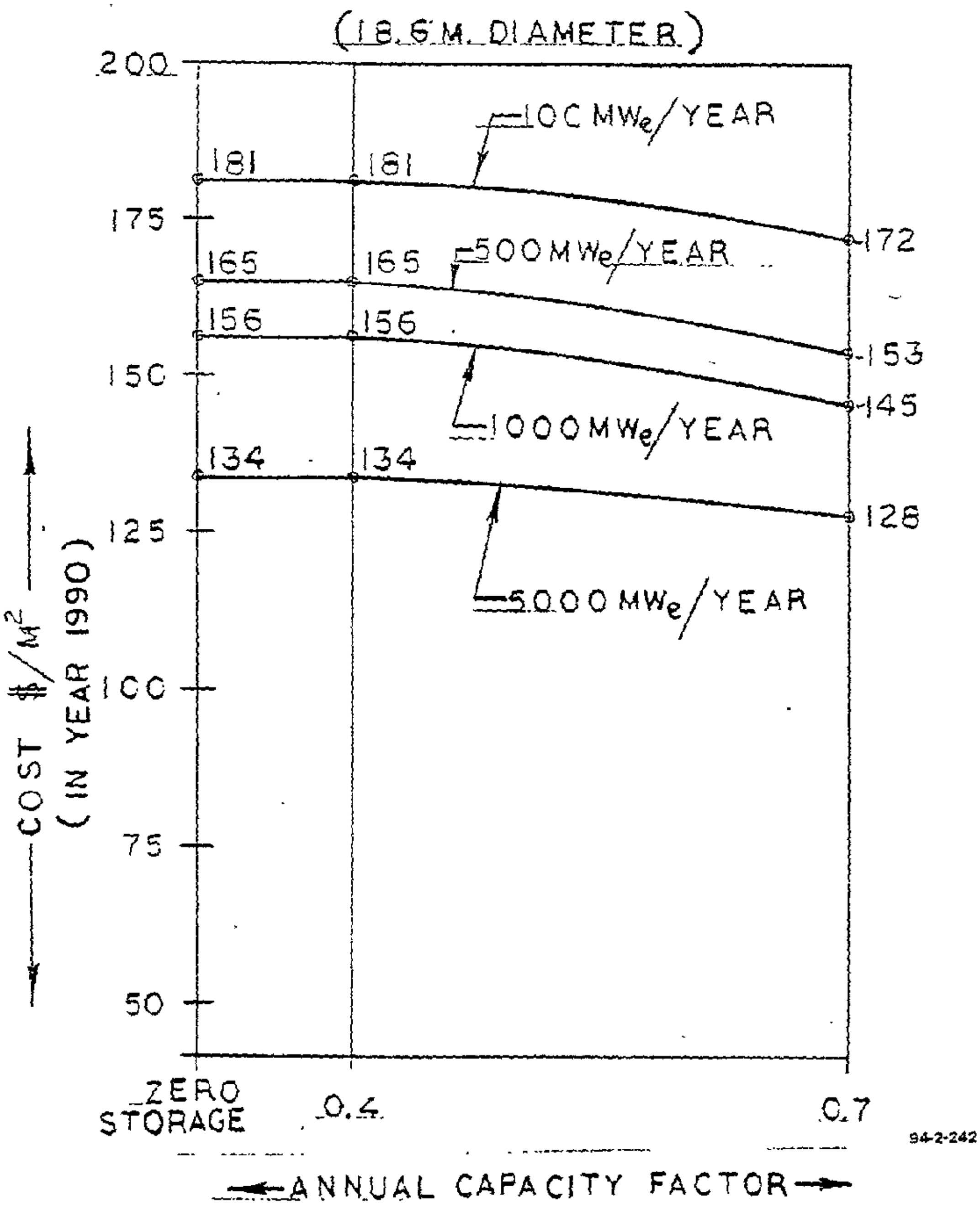


FIGURE 73. CONCENTRATOR COST SENSITIVITY TO ANNUAL CAPACITY FACTOR (18.6 M. DIAMETER)

REFERENCES


1. Pettit, R. B., "Characterization of the Reflected Beam Profile of Solar Mirror Materials", Solar Energy, Vol. 19, pp. 733-741, Pergamon Press, 1977.

2. Takitani, H., and Arden, W. M., "Mirrors for Solar Energy Application", MDC G7213 McDonnell Douglas Astronautics Company - West

3. Wen, L., (JPL), "Thermal Optical Surface Properties and High-Temperature Solar Energy Conversion".

4. Rausch, R. A., and Gupta, B. P., "Exposure Test Results for Reflective Materials".

5. Freese, J. M., "Effects of Outdoor Exposure on the Solar Reflectance Properties of Silvered Glass Mirrors", SAND 78-1649, Sandia Laboratories.

6. Shand, E. B., Glass Engineering Handbook, McGraw Hill.

7. Hutchins, J. R., III, and Harrington, R. R., "Glass" Reprinted from: Kirk-Othmer: Encyclopedia of Chemical Technology, 2nd Ed Vol. 10, pp. 533-604, John Wiley & Sons, Inc.

8. Argoud, M. J., "Investigation of Low Cost, Good Optical Quality, Reflective Elements for Paraboloidal Concentrator", JPL Document No. 900-735.

9. Easton, C. R. (MDAC), "Solar Central Receiver Prototype Heliostat", CDRL Item B.d Final Technical Report, Vol. 1, MDC G7399.

10. Fox, N.L. and Dayman, B., "Preliminary Report on Paraboloidal Reflector Antenna Wind Tunnel Tests", JPL CP-3 Internal Memorandum, February 1962.

11. Fox, N.L., "Load Distributions on the Surface of Paraboloidal Reflector Antennas", JPL CP-4 Internal Memorandum, July 1962.

12. Vermeulen, P.J., Bader, A. and Elfner, P., "Reduced Drag, Paraboloidal Type, Solar Energy Collectors", The University of Calgary, Alberta, Canada. T2N 1N4

# APPENDIX B

# ELECTRICAL SUBSYSTEM SELECTION AND DEFINITION

CONTENTS FOR APPENDIX B

CONTENTS FOR APPENDIX B (Continued)

## SECTION 1

## INTRODUCTION

This Appendix summarizes the results of the Phase I effort which was conducted to define a recommended conceptual design for the SPS electrical system. The electrical system is defined here as (1) the AC generator component of the power conversion subsystem, (2) the energy transport subsystem, (3) the energy storage subsystem, and (4) the electrical control subsystem. This Appendix presents the trades that were evaluated to arrive at a baseline electrical system and details of the recommended hardware. Also the baseline system is summarized in Paragraphs 3.1.4.2, 3.1.5, 3.1.6, and 3.1.7 of the Report.

### 1.1 OBJECTIVES

The basic objective of the work presented in this Appendix was to investigate various electrical subsystem and component configurations which would fulfill the requirements of the SPS program and to recommend the preferred concept in terms of reliability, performance and cost.

The primary criteria used for evaluation of the electrical subsystems are in descending order of importance:

(1) High operational reliability

(2) Minimum risk of program schedule failure

(3) High potential for commercialization

(4) Low Phase II and III program costs.

Other parameters which are considered and which posed potential risks were:

(1) Performance

(2) Efficiency

(3) Production costs

(4) Operational costs

(5) Unscheduled maintenance

(6) Human safety

(7) Community acceptance

### 1.2 STUDY APPROACH

The approach taken in this selection has been to synthesize candidate electrical systems in an optimum manner for the SPS application; to identify the relative advantages and disadvantages of each system concept; and to select the most promising.

A baseline system was established as one which can be designed and built within the 4.5 year startup time for a 1 MWe station with a 30-year life. Station capacity factor variations, i.e., no storage, 0.4, 0.7, or stand-alone, do not have any significant effect on electrical system concept selection, other than to change the required quantity and size of some electrical subsystem components.

# SECTION 2

# ELECTRICAL SYSTEM EVALUATION AND STUDIES

## 2.1 ELECTRICAL PERFORMANCE REQUIREMENTS, INTERFACES AND SPECIFICATIONS

The basic electrical system performance requirement is to convert the mechanical output of a number of collector-mounted heat engines to electrical energy and transport that energy to a single location for delivery to either a utility grid or to a local distribution network for "stand-alone" operation. Part of the energy is to be utilized to charge batteries for later input to the grid.

### 2.1.1 INTERFACE CRITERIA

Several interfaces exist between the electrical system and the heat engines at the one end and the electrical utility grid at the other.

### 2.1.2 ENGINE INTERFACE

It is planned to directly couple the generator to the engine. Control system interfaces also exist between power control microprocessor and; (1) the engine head temperature sensor for the case of the Stirling engine, (2) the engine electronic control unit, and (3) the concentrator drive and tracking system. These interfaces are discussed in later sections.

### 2.1.3 UTILITY GRID INTERFACE

Three important parameters must be accommodated for the the utility grid interface. They are: (1) the nominal line voltage at the point of interconnection, (2) the line frequency, and (3) the grid power factor.

Utility grid transmission voltages are typically in the range of 12,000 to 67,000 volts at the point of interconnection with a solar generating station. Pending final site selection, a nominal line voltage of 21,000 volts has been assumed. Although line voltages are usually carefully regulated by the utility operating companies, it is believed appropriate to design the SPS station to interface with a transmission line which might vary as much as ±10 percent from nominal.

Most major utility power systems in the United States are interconnected into power pools covering significant geographical regions and operate at a common frequency base of 60.0 Hz. Frequency bias is applied to area generation capacity to control the interchange of power between areas (or operating companies) of a region. Short term frequency excursions occur as a result of generating-capacity/load imbalances, sudden application or removal of large load blocks, failure of tie-lines, and/or failure of generating units of significant size. Small frequency offsets are periodically applied to all of the bias regulators of a region to maintain the integrated frequency within close tolerances so that synchronous clocks will be accurate. Although it is rare that short term frequency deviations resulting from these causes will exceed 0.2 Hz (usually they are much less), the SPS station will be designed to track deviations of ±3.0 Hz to prevent loss of synchronization and tripping of the station off-line.

The on-line power station must be capable of delivering power to the utility grid at the power factor which exists at the point of interconnection. This power factor is a function of both transmission and load power factors and will show both annual and diurnal variations. Utilities which have large electric motor loads such as irrigation pumps, heavy industrial machinery, or air conditioners tend toward lagging power factors, although power factor correction is used to keep the systems within reasonable bounds. Utilities which serve large metropolitan areas with large amounts of underground cable tend to have leading power factors (or less lagging power factors) during periods when the systems are lightly loaded. Discussions with utility personnel indicate that a solar power station designed for 0.8 lagging to 0.9 leading power factors should be suitable for all points of interconnection.

Since it is common design practice to design small generators and transformers for power factors from 0.8 lagging to 0.8 leading, no special requirements will be imposed on these items. Caution is, however, necessary in selection of any solid state (static) inverters which may be used in the storage subsystem, since many existing designs are not suitable for operation into loads with leading power factors.

### 2.1.4 ENVIRONMENTAL SPECIFICATIONS

Environmental conditions used as the basis for electrical subsystem design and component selection are listed in Table 5 of Appendix A. Some of the measures taken to ensure that the performance of the electrical system will not be degraded are as follows:

(1) The collector-mounted generators will be of drip-proof (DP) construction with windings and metal parts treated for operation in exterior environments. Custom weather shielding will be provided to preserve weather integrity at all required operational attitudes.

(2) All other electrical components located at the collectors will be housed in NEMA-12 enclosures.

(3) Lightning air terminals, down leads and ground rods will be provided at each collector in accordance with the requirements of the Lightning Protection Code (NFPA-78).

(4) Power and control cables between the individual collectors and the control building will be buried in accordance with the requirements of the National Electrical Code (NFPA-70).

(5) Opto-isolators will be provided on control cables.

(6) The main power switchboard, all of the storage subsystem components, and the power control subsystem components will be installed in a building. Air conditioning, ventilation and air filtration will be provided for the components which require it (computer, batteries, inverters/converters).

(7) Battery racks will include bracing and cell retaining features appropriate to the specified zone 3 seismic environment.

(8) A fully-enclosed, weatherproof, oil-immersed, self-cooled transformer with integral lightning arrestors will be used for the grid interface.

## 2.2 BASIC ELECTRICAL SYSTEM AND COMPONENT CANDIDATES

Six basic concepts have been identified and presented in the following paragraphs. The basic choices were found to be between DC and AC generation, radial versus bus collection, local versus centralized power inversion, and electromechanical versus static power conversion for energy storage and retrieval.

### 2.2.1 SYSTEM CONFIGURATIONS

The six basic concepts which warranted consideration for the SPS solar power station are shown in the block diagrams on Figures 1 through 6. Discussion of system selection and the efficiency values given on the figures is contained in Paragraph 2.3.

2.2.1.1 <u>System Configuration A</u>. This system utilizes DC power generation and DC bus collection. It offers three major advantages: (1) DC generators do not have to be synchronized which simplifies the required control equipment; (2) the output of the generators may be transported to the control building on a two-conductor bus, which has significant cost advantages for large collector fields; and (3) the output of the DC generators may be directly connected to the storage subsystem battery, which again is a significant cost advantage.

2.2.1.2 <u>System Configuration B</u>. This concept is identical to that presented as Concept A, except that an electro-mechanical (rotary) inverter is used in place of a static inverter. The desirable feature of this concept is that rotary inverters are much more tolerant of abnormal load conditions, such as transients, short-term overloads, and out-of-range power factor conditions. It also offers all of the advantages delineated for Concept A.

2.2.1.3 <u>System Configuration C</u>. This system is also a system using DC generation, but with static inversion at the individual collectors, rather than at the central control building. The unique advantage of this system is its complete modularity. It also offers control system simplicity inherent in a DC generation system.

2.2.1.4 <u>System Configuration D</u>. This system utilizes AC generation and cable (rather than bus) power collection. Power handling throughout the system is simple and direct which should result in high system efficiency, but at the cost of added control system complexity for generator synchronization.

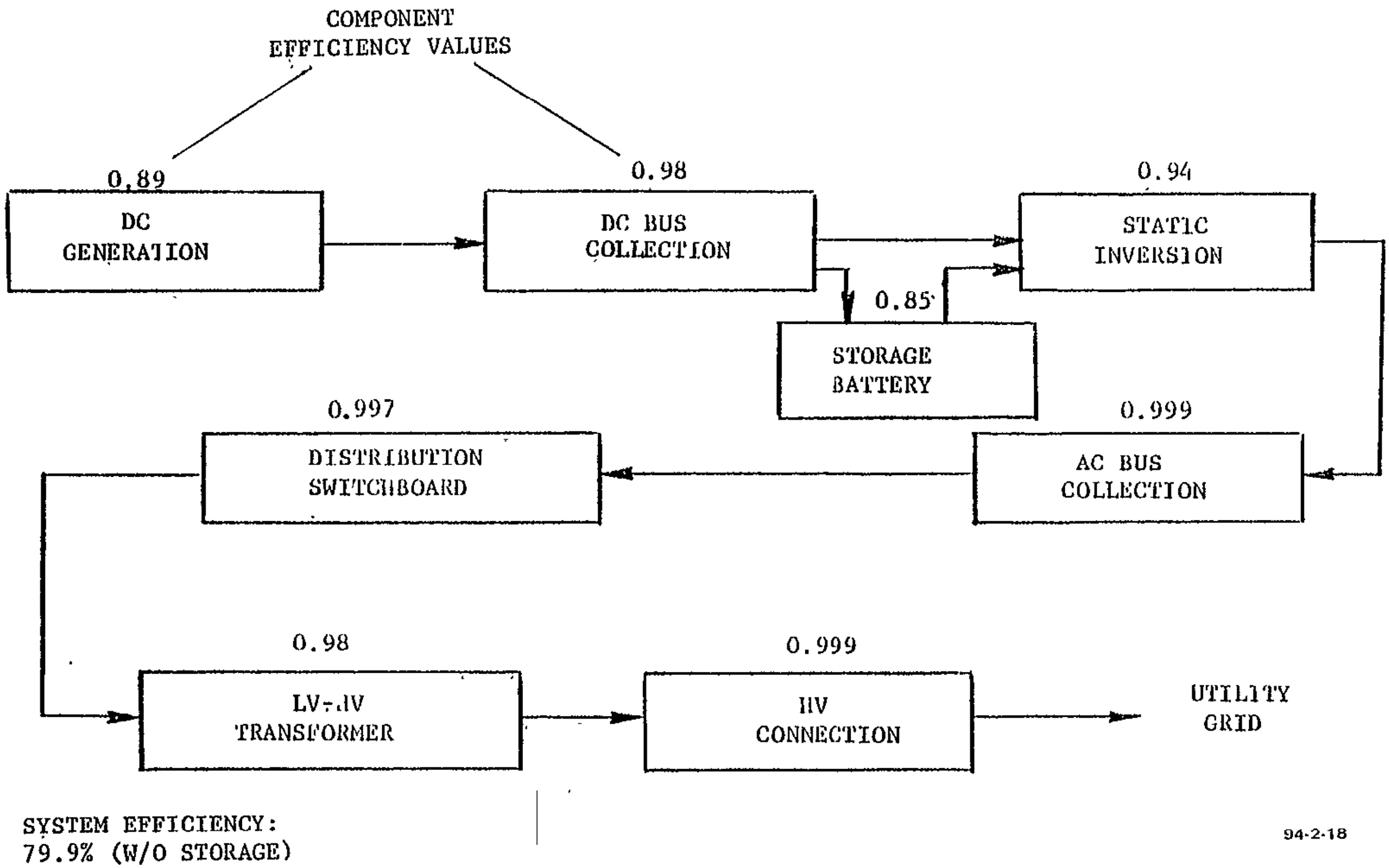


FIGURE 1. SYSTEM CONFIGURATION A

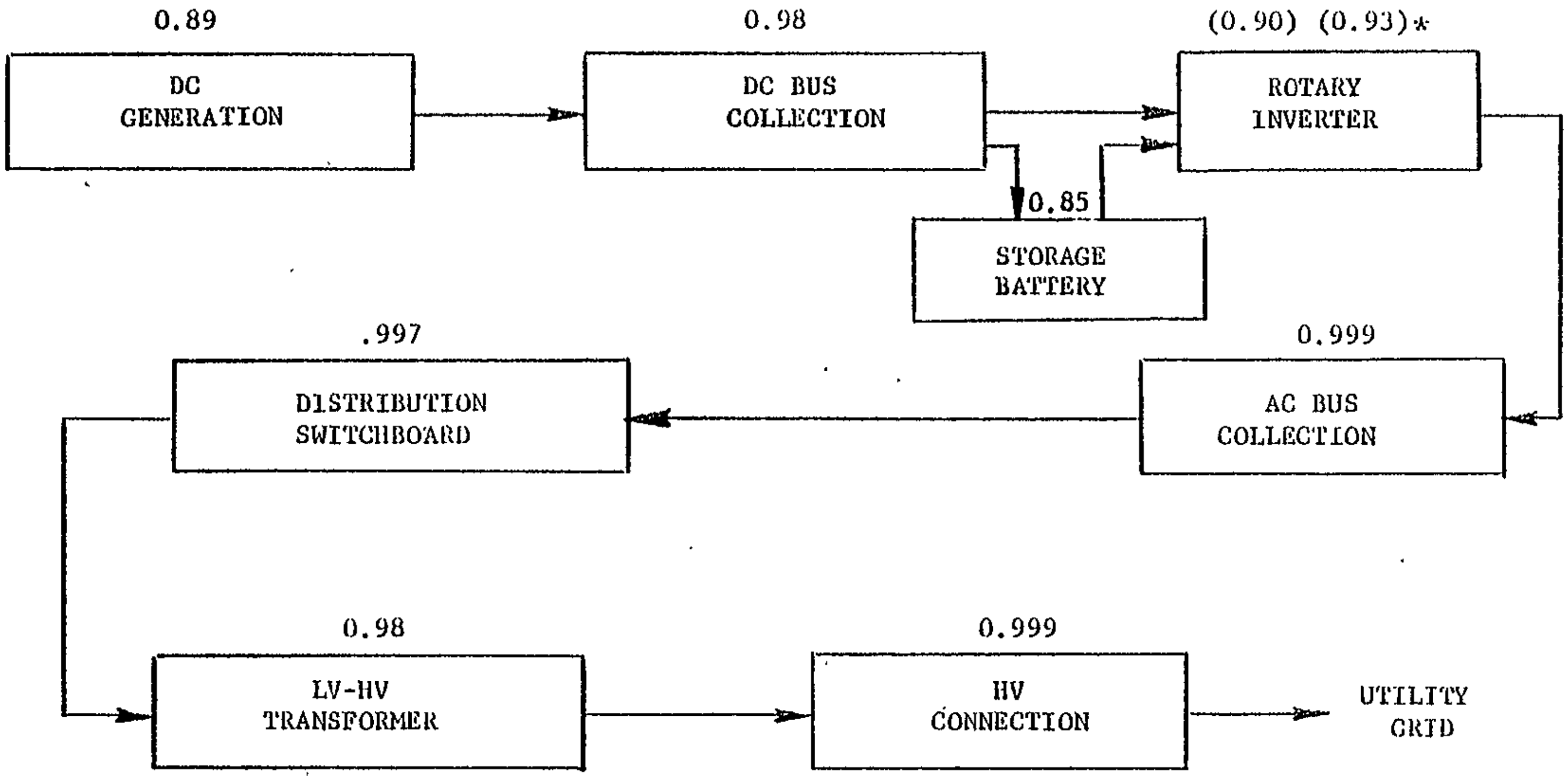


* Efficiencies of DC motor and AC alternator are expressed separately; composite efficiency is product of indicated values.

SYSTEM EFFICIENCY:
71.2% (W/O STORAGE)

94-2-19

FIGURE 2. SYSTEM CONFIGURATION B

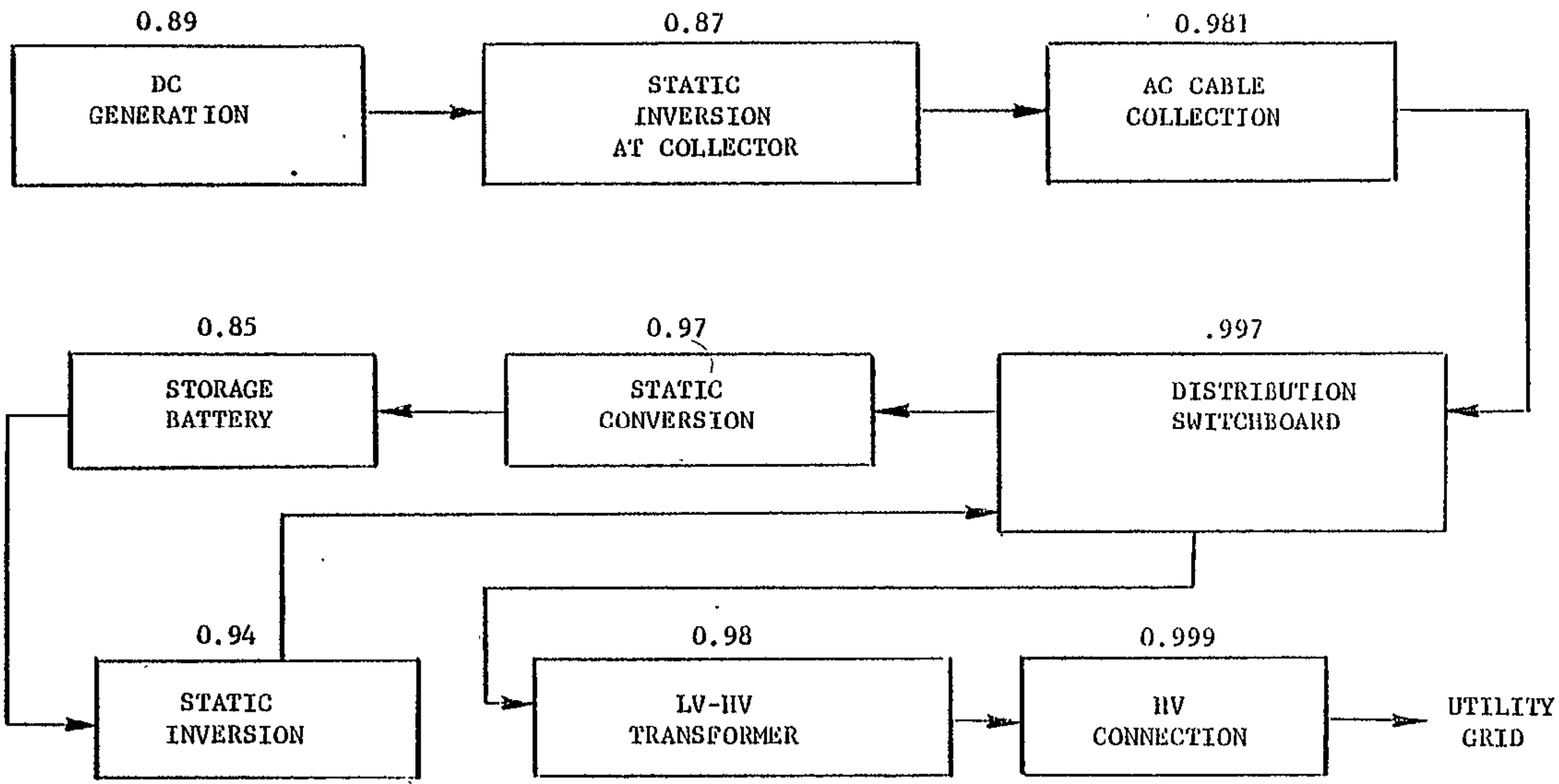


SYSTEM EFFICIENCY:
74.1% (W/O STORAGE)

94-2-20

FIGURE 3. SYSTEM CONFIGURATION C

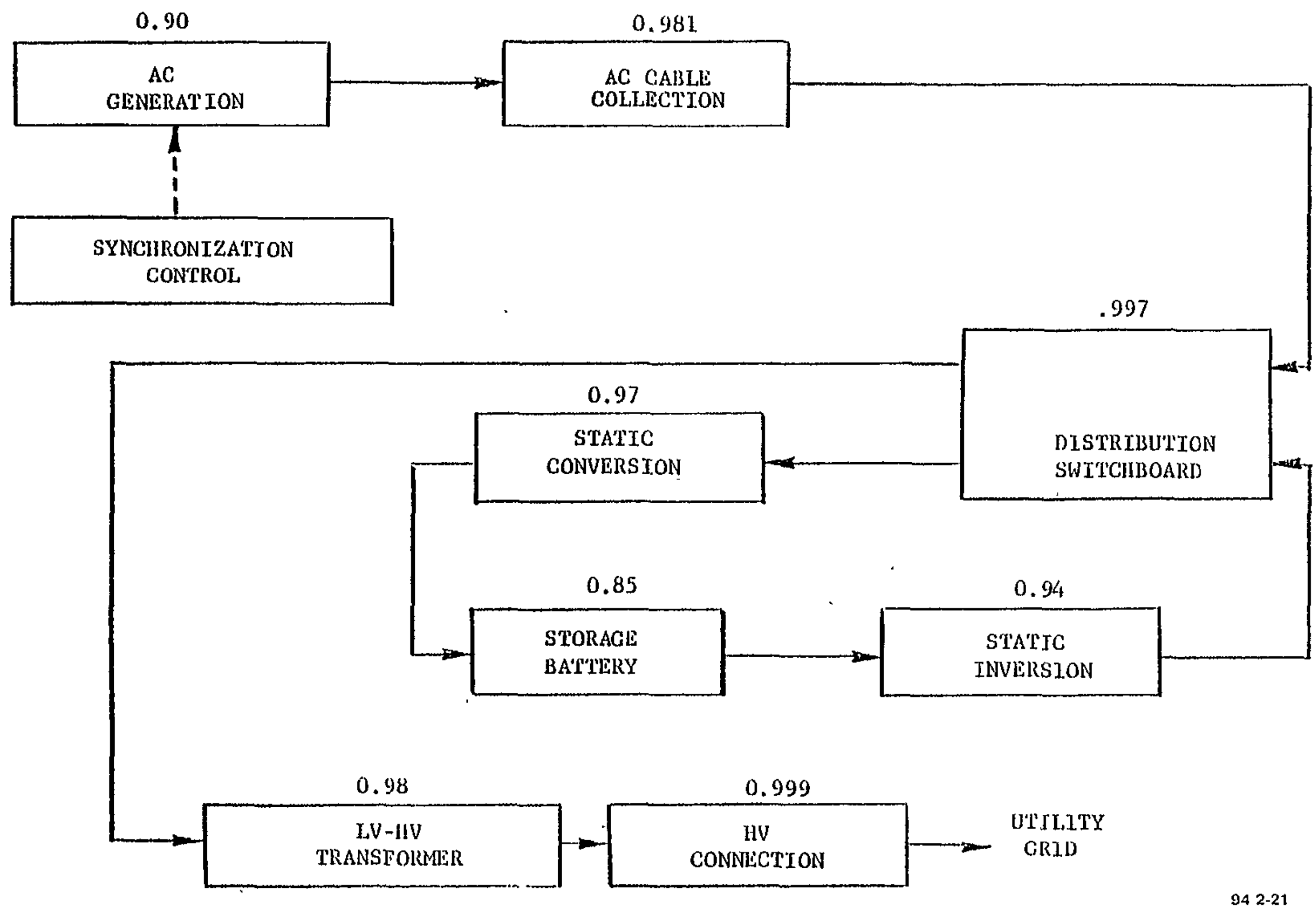


SYSTEM EFFICIENCY:
86.2% (W/O STORAGE)

FIGURE 4. SYSTEM CONFIGURATION D

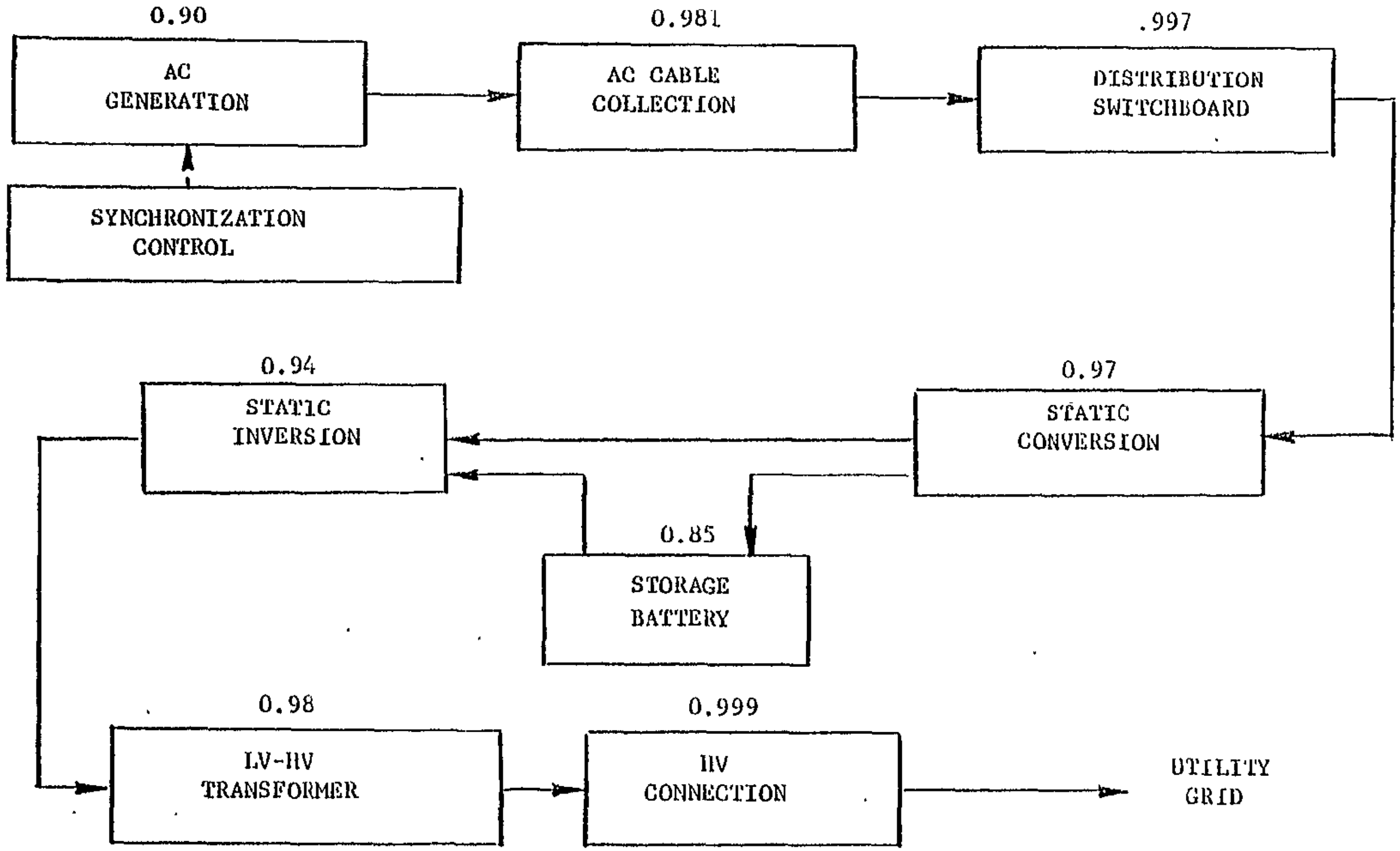


SYSTEM EFFICIENCY:
78.6% (W/O STORAGE)

94-2-22

FIGURE 5. SYSTEM CONFIGURATION E

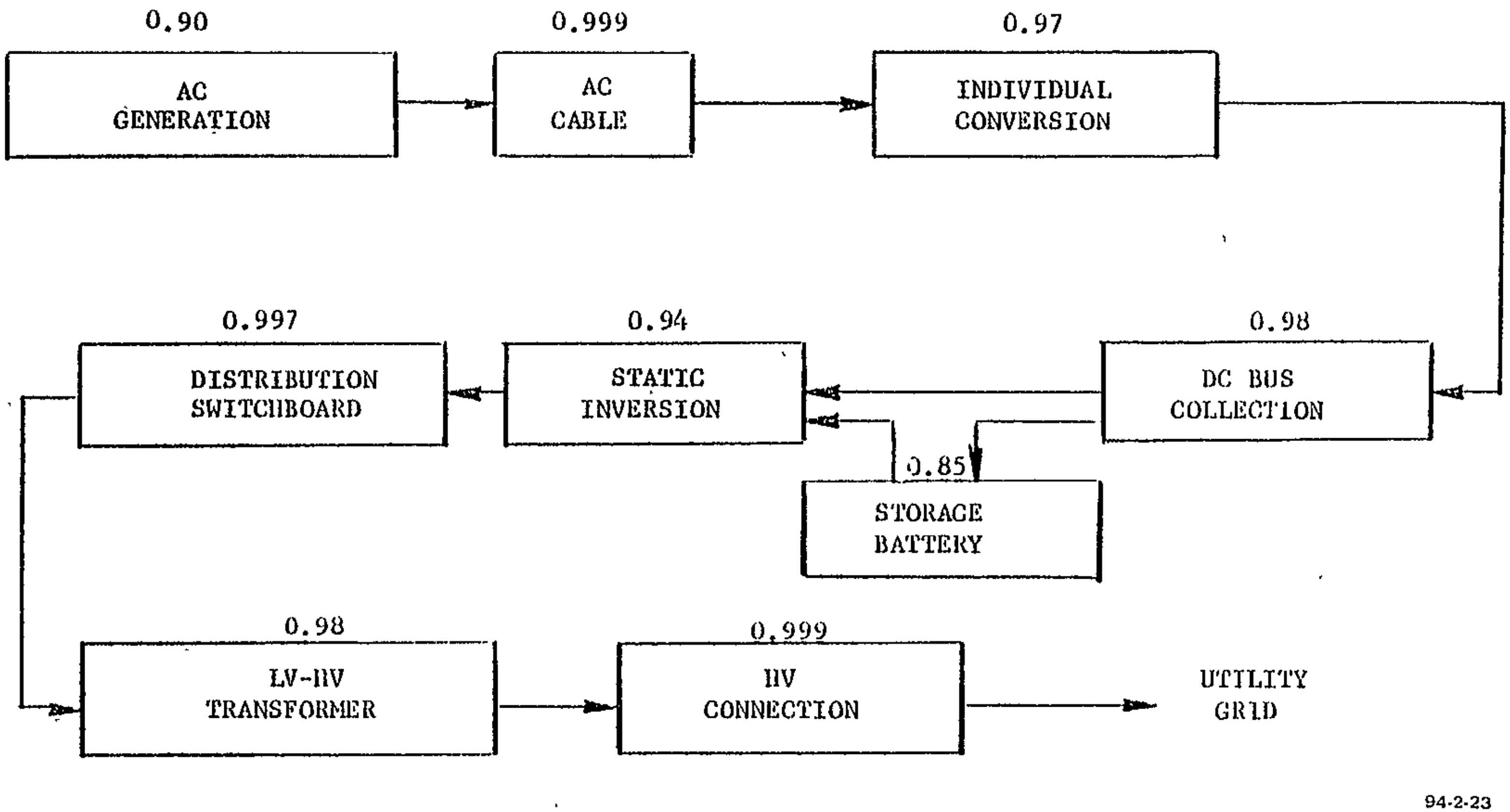


SYSTEM EFFICIENCY:
78.4% (W/O STORAGE)

FIGURE 6. SYSTEM CONFIGURATION F

2.2.1.5 System Configuration E. This concept also uses AC generation. All power, rather than just the power required for storage, passes through the conversion-inversion process. The desirable attribute of this system is simplified synchronization with the electric utility grid, although the control complexity associated with synchronizing the individual collector generators remains.

2.2.1.6 System Configuration F. This system is the inverse of Concept C. It avoids the control complexity inherent in the previously discussed AC generator systems and offers two-conductor bus collection.

2.2.2 GENERATORS

The output characteristics and the construction features of both AC and DC generators will be discussed in order to evaluate their selection for the SPS program.

2.2.2.1 AC Generator. The advantages of an AC generator (or alternator) are its alternating output which can go into a transformer directly, and the elimination of a commutator and brushes. The voltage output of commonly available AC machines of the size under consideration is 480 volts, 3 phase. Grid-connected alternators require precise speed and voltage matching when synchronized to a grid.

2.2.2.2 DC Generator. DC machines have several attractive features: (1) no need for a voltage regulator, (2) connecting the machines in parallel is simple since only their output polarity and voltages must be the same, (3) it is not necessary to make all the DC generators run at the same rotational speed, (4) the output can be used to charge batteries directly or can be used by inverters to generate AC power, and (5) the machines have stationary field pieces and rotating armatures. Output voltages of either 250 or 500V are available.

2.2.3 STORAGE SUBSYSTEM

The storage subsystem permits storing part of the generated electric power during sunshine hours for later distribution. Only battery storage is considered in this Appendix.

2.2.3.1 Storage Batteries. Two major kinds of batteries are currently available. These are lead-alloy plate batteries with an acid/water electrolyte, and the nickel/cadmium/iron plate batteries with an alkali/water electrolyte. Both kinds of batteries are rugged and both have a rated cycle life of nearly 2,000 cycles. The output voltage of alkali batteries does not vary significantly from fully charged to fully discharged. The acid batteries have variable voltage at their terminals and as the batteries discharge their output voltage drops until it becomes unusable. One other similarity is that the cost of the individual cells for a given current output is almost identical. The big difference is in the terminal voltage available from the cells.

The acid batteries can offer approximately 2 volts at their terminals; the alkali cells can only offer 1.2 volts. Therefore, for a given battery terminal voltage, the alkali cells will usually cost about twice as much as the acid cells, even though their current outputs are equal.

2.2.3.2 Battery Ancillary Equipment. Components must be selected to convert generated AC power to DC power to charge the batteries, and to reconvert the DC power to AC power. Batteries can be charged by any source of DC power, but the silicon controlled rectifier (SCR) has several advantages. The SCR solid state electronic converter is a controllable DC power machine which is efficient, safe, silent, has no moving parts and is relatively inexpensive. It is a modern design, and requires minimal maintenance. Being controllable, it can be set to act like a constant voltage charger when operating below full current, and it can be set to act as a constant current device when connected to discharged batteries.

Two kinds of inverters are available, rotary motor-alternator sets and solid state electronic inverters. Solid state inverters are the preferred choice because they are quiet, safe, essentially maintenance free, and efficient.

### 2.2.4 TRANSPORT/DISTRIBUTION SUBSYSTEM

The transport and distribution subsystem is the means of collecting power from the power conversion modules, transporting it to a single location, removing a portion of it for internal operation of the station, and distributing the rest to a grid or for stand-alone operation.

2.2.4.1 Power Collection. Power collection systems generally fall into geometric shapes (based on layouts of the system components location and connection) which can be described as radial-shaped, ring-shaped, or a combination of the two. In a radial system, there is a central point and branches radiate from the point out to each disk (module). In a ring system, all of the modules connect onto a ring, and there is no central point. In a hybrid system, there may be several radial systems connected onto a ring or there may be a central point connecting a group of ring-shaped subunits radially. As a general rule, the radial system is the simplest and least expensive to construct. Ring systems generally cost more to build but are more reliable because power can flow around the ring from two directions instead of just one.

2.2.4.2 Power Distribution Switchboard. The station rated output is achieved by combining the output of several generators at a central location. The electrical output of all the generators is to be transported to a single set of busses in an electrical switchboard. An alternative would be to connect the generators onto one set of wire busses. The switchboard busses have the advantage of being short whereas the wire busses are as long as the distance between the generators.

2.2.4.3 Utility Grid Interface Transformer. The output power will be delivered to a public utility grid for distribution to energy users. Obviously a utility grid interface transformer is required to match the voltage of the station generators to the voltage of the public utility lines. Note that for the special case of "stand-alone" operation, a transformer may not be required.

### 2.2.5 ELECTRICAL CONTROL SUBSYSTEM

The electrical control subsystem will control all facets of unattended station operation. Major functions required of the subsystem are: (1) daily collector selection, start-up, and synchronization with the utility grid proportional to the incident solar energy; (3) control of energy delivery to and from the energy storage subsystem (if provided); (4) status monitoring of all operating equipment, including an alarm system and emergency defocus sequence; (5) station diagnostics for maintenance purposes; and (6) data logging of selected station operating data for future analysis and a record of station performance. The control system will consits of a master power controller (MPC) and central control interface assembly (both located in the central control building), instrumentation cabling to the individual collectors, and remote control interfaces assemblies (RCIAs) and transducers at the collectors.

2.2.5.1 Master Power Controller. Four classes of equipment were considered for the master power controller (MPC): (1) a ladder diagram processor, (2) a solid state controller, (3) a micro-processor, and (4) a mini-computer.

The commonly-used ladder diagram (electro-mechanical relay) type processor offers a limited control technique which has been widely used in various forms for a number of years. The solid state logic controller is essentially a modernized version of a ladder diagram processor. It is capable of more complex control functions, higher speed switching, and has the ability to operate in adverse environments.

Of the classes of controllers considered, the micro-processor is the most advanced and therefore has the least operational history. The micro-processor operates under stored program control and thus can provide much more flexible and accurate control than currently available analog devices. Effective control algorithms can be written with little or no hardware impact.

The mini-computer offers all of the advantages mentioned above, plus substantially higher operating speeds and a greater overall device-handling capability. They can also be programmed in some extremely effective high level languages (such as APL), which have not generally been implemented for micro-processors.

2.2.5.2 Central Control Interface Assembly. The central control interface assembly (CCIA) consists of those devices necessary to make signal level and/or format conversions required to interface the master power controller (MPC) with sensors and controlled devices. For digital systems, it will include analogue to digital (A/D) and digital to analogue (D/A) converters.

2.2.5.3 Remote Control Interface Assembly. A remote control interface assembly (RCIA) will be required at each collector to convert logic power levels to the levels required by the controlled devices and to accomplish the physical fan-out of control signals to (and from) the concentrator tracking servo, the heat engine, and the electrical generator.

2.2.5.4 Instrumentation and Control Cabling. Instrumentation cabling is required from the MPC/CCIA equipment complex in the station control building to the RCIA at each collector. The basic choices to be made are the degree of signal isolation required by the individual signal paths and the cable jacket construction required for the planned method of installation.

2.2.5.5 Sensors. Sensors will be required to determine solar insolation level, heat engine speed and head temperature, generator voltage and current output, storage subsystem charge and energy delivery rates, real and reactive power delivered to the utility grid and various other "housekeeping" information.

## 2.3 CONFIGURATION VERSUS PERFORMANCE AND COST

The six previously defined system configurations and their various component alternatives are evaluated in the following paragraphs. Overall system efficiency has been given considerable weight because of its strong effect on station capital costs and the ultimate commercialization potential of the SPSE concept. Certain component alternatives, e.g., the use of AC or DC generators and static or rotary power conversion equipment; have such a direct bearing on system efficiency that the basic choices had to be made at the system level and the selected components thereafter optimized for less important parameters, regardless of how desirable some of the other performance features might have been.

### 2.3.1 ELECTRICAL SYSTEM CONFIGURATIONS

The six system configurations described in Figures 1 through 6 have been examined in terms of various system level considerations such as efficiency, reliability, cost, etc. In the following paragraphs each system is ranked according to these system level parameters and, finally, a preferred system concept is selected.

2.3.1.1 System Efficiencies. Figures 1 through 6 show the six system configurations with system blocks annotated with expected efficiencies based on current technology. Manufacturer's published data were used wherever possible and this represent off-the-shelf, no-risk hardware. Continued electrical component development is expected to improve system efficiencies constructed in the 1990 time frame by 3 to 5 percent over the values specified. Further increases in efficiency would be obtainable by increasing collector sizes so that larger, and hence more efficient, electrical generators may be employed. System "D" offers significantly higher efficiency than any other concept. This increase of 6.3 percent over the next highest system is of particular importance when considering the cost of the generated energy.

Overall system efficiency with storage cannot be determined by simply multiplying all the component efficiencies because only a portion of the generated power goes through the storage loop. The actual efficiency for this case is discussed in Paragraph 3.1.1.2 of the report.

Station auxiliary loads have not been included in the efficiency calculations shown here because they are essentially independent of the system used. The auxiliary loads are included in the system analysis calculations.

2.3.1.2 Other Selection Considerations. Other considerations of significant importance are listed below and discussed in the following paragraphs.

- Reliability
- Maintainability
- Cost
- Generator Weight
- Stability
- Complexity

a. <u>System Reliability</u>. Four system characteristics are important in evaluating the expected system reliability:

(1) Are AC or DC generators used for primary generation at the collectors? DC machines, because of the presence of brushes and a commutator, are less reliable than AC machines and are penalized 10 percent in this analysis.

(2) Is a common AC-DC converter used in the primary power delivery chain? If so, a single point failure of a device of some complexity would terminate all power delivery. Systems having this characteristic are penalized 10 percent.

(3) Is a common DC-AC inverter used in the primary power delivery chain? If so, a single point failure of a device of somewhat greater complexity would terminate all power delivery. Systems having this characteristic are penalized 15 percent.

(4) Is a rotary inverter used in lieu of a static inverter? Although rotary inverters have bearing systems which require maintenance, they have a significantly smaller component count, are more tolerant to abnormal load conditions, and have a much longer operational history. Therefore, systems which utilize rotary inverters are given a bonus of 15 percent.

Based on the foregoing factors, relative reliability of the various systems is summarized in Table 1. System D has an advantage in reliability.

TABLE 1. QUALITATIVE SYSTEM RELIABILITY

| System Configuration | DC Generation | Primary Chain Converter | Primary Chain Inverter | Rotary Inverter | Qualitative Reliability |
|---|---|---|---|---|---|
| A | -0.10 | 0 | -0.15 | 0 | 0.75 |
| B | -0.10 | 0 | -0.15 | +0.15 | 0.90 |
| C | -0.10 | 0 | 0 | 0 | 0.90 |
| D | 0 | 0 | 0 | 0 | 1.00 |
| E | 0 | -0.10 | -0.15 | 0 | 0.75 |
| F | 0 | 0 | -0.15 | 0 | 0.85 |

b. System Cost. Three major components vary significantly in cost for the various systems. They are the generators, the converters, and the inverters. Generator costs for various sizes and types of machines considered in this report are shown on Figure 7. For the baseline configuration, it will be noted that 75 kW direct-current (DC) machines of drip-proof (DP) construction cost 3.5 times as much as the equivalent alternating current (AC) machines. Converter costs and inverter costs vary with the size of the devices required by the various system configurations.

Table 2 presents a detailed breakdown of the component costs for each of the six candidate systems. This information was obtained from vendor information for off-the-shelf hardware, and demonstrates the variation for the three cost-variable components. Configuration D has a 6 percent cost advantage over the next best configuration, and considerably more compared to the remaining four candidates.

c. System Stability. System electrical stability is enhanced by the use of a small number of large generators. This option is not practical for SPS because of the modularity of the system, i.e., the need to generate power at several collectors of reasonable size. The system configurations utilizing DC generation (options A, B and C) do not require synchronization of the individual generators and are hence the easiest to control, particularly under dynamic conditions. Schemes A and C utilize static inverters which introduce second order control problems, since available static inverters of the power class under consideration are not particularly tolerant of output overloads, harmonic current feedback, transients, or leading power factors. Some development would therefore be required to ensure suitability of these devices for the primary power delivery chain. Concept B uses a single large rotary inverter for conversion of the output of the multiple DC generators which is well-developed technology. One inverter has the advantage of substantial mechanical inertia in its rotating mass and thermal inertia in its stator and rotor windings, and would be the easiest concept to control.

Configuration D utilizes multiple AC generators, which are directly connected to the utility grid (and to each other). Therefore all generators must be operated in phase synchronism and with the field excitation of each generator controlled in such a manner that reactive load currents will be shared in proportion to the power delivered from each unit. Since two parameters must be accurately controlled at each generator and each generator is connected to a utility grid which will impose dynamic load conditions directly on the generators, it is inherently the least stable system under consideration and therefore will require the most sophisticated control system.

System configuration E simplifies the control problem by first converting the output of all generators to DC and then inverting it back to AC with a phase-locked static inverter. This scheme achieves isolation of the generators from the grid, but not from each other. System configuration F goes a step further by providing individual conversion of the output of each generator. This system achieves isolation of each generator from all others, as well as from the utility grid. It is therefore a system with high inherent stability and relatively simple control requirements.

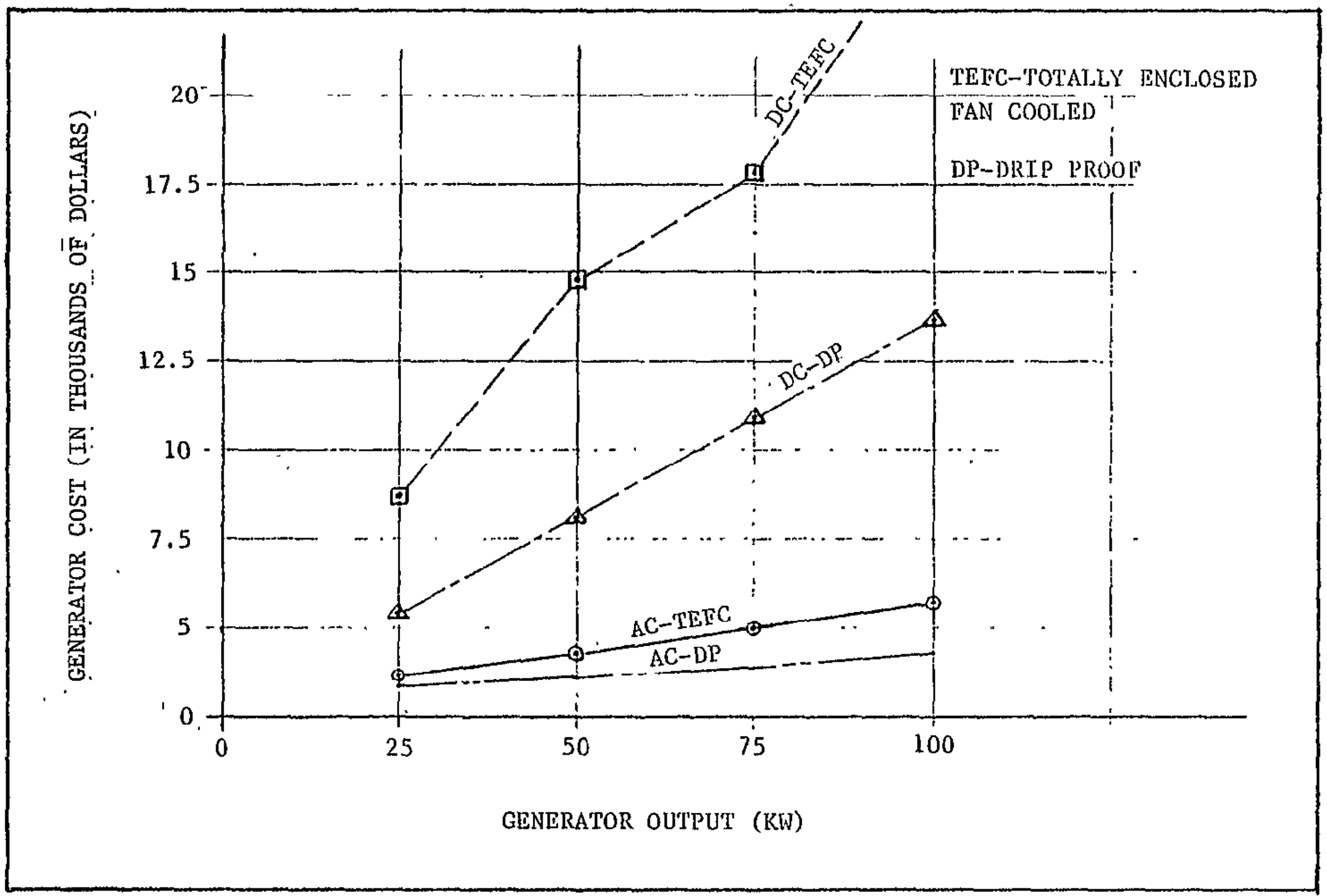


94-2-11

FIGURE 7. GENERATOR COST VS POWER OUTPUT RATING

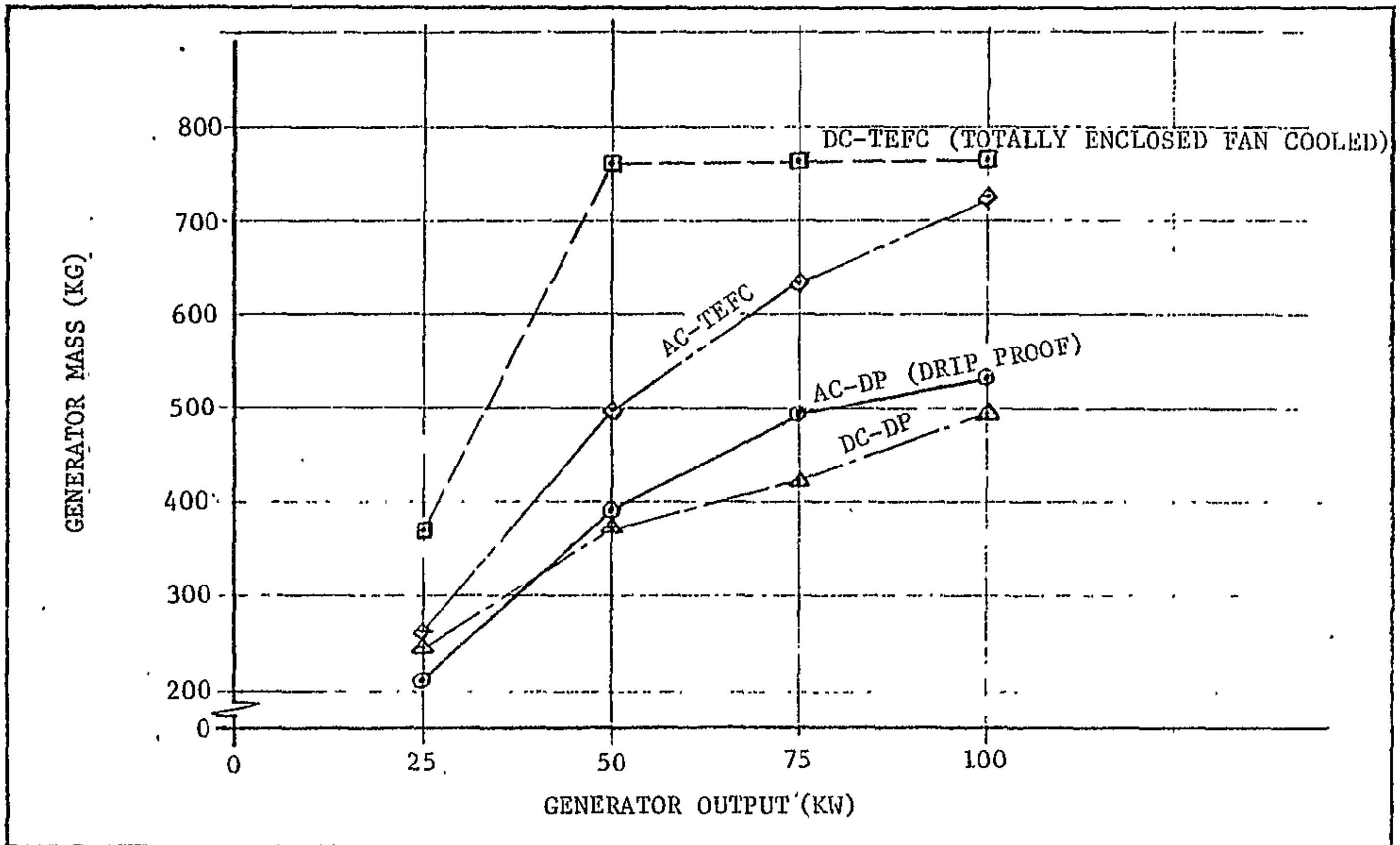


94 2-12

FIGURE 8. GENERATOR MASS VS POWER OUTPUT RATING

Table 2

COST* VS SYSTEM CONFIGURATION

(Single Station Procurement - 1978 Dollars)

| Equipment Item | System Configuration | | | | | |
|---|---|---|---|---|---|---|
| | A | B | C | D | E | F |
| **Power Conversion S/S:** | | | | | | |
| Generators | $209K | $209K | $209K | $60 | $60K | $60K |
| Ancilliaries | 68 | 68 | 68 | 68 | 68 | 68 |
| Sub-Total | 277 | 277 | 277 | 128 | 128 | 128 |
| **Transport/Distribution S/S** | | | | | | |
| Wire | 12 | 12 | 12 | 12 | 12 | 12 |
| Power Switchboard | 24 | 24 | 24 | 24 | 24 | 24 |
| HV Transformer | 32 | 32 | 32 | 32 | 32 | 32 |
| HV Switch | 1 | 1 | 1 | 1 | 1 | 1 |
| Ancilliaries | 8 | 8 | 8 | 8 | 8 | 8 |
| Sub-Total | 77 | 77 | 77 | 77 | 77 | 77 |
| **Control S/S:** | | | | | | |
| Computer & CRT Terminal | 13 | 13 | 13 | 13 | 13 | 13 |
| Central Control Interface Assy. | 19 | 19 | 19 | 19 | 19 | 19 |
| Cable | 17 | 17 | 17 | 17 | 17 | 17 |
| Remote Control Interface Assy. | 30 | 30 | 30 | 30 | 30 | 30 |
| Subtotal | 79 | 79 | 79 | 79 | 79 | 79 |
| **Storage S/S:** | | | | | | |
| Converters | - | - | 52 | 52 | 74 | 281 |
| Batteries | 498 | 498 | 498 | 498 | 498 | 498 |
| Inverters | 145 | 119 | 524 | 102 | 145 | 145 |
| Ancilliaries | 21 | 21 | 21 | 21 | 21 | 21 |
| Subtotal | 664 | 638 | 1095 | 673 | 738 | 945 |
| Grand Total | $1097K | $1071K | $1528K | $957K | $1022K | $1229K |
| Normalized Value | 1.15 | 1.12 | 1.60 | 1.00 | 1.07 | 1.28 |
| Reciprocal Value | 0.87 | 0.89 | 0.63 | 1.00 | 0.94 | 0.78 |

*Note current costs are shown for off-the-shelf hardware for baseline configuration, i.e., 1 MWe, 0.4 capacity factor.

A summary of the relative merit assigned to each concept is summarized in Table 3. As noted, system D introduces the greatest stability problems, i.e., requires the greatest amount of control hardware.

TABLE 3. SYSTEM STABILITY

| System Configuration | Index of Inherent Stability |
|---|---|
| A | 0.90 |
| B | 1.00 |
| C | 0.85 |
| D | 0.70 |
| E | 0.80 |
| F | 0.90 |

d. System Complexity. The basic elements of most of the concepts are very similar in nature so a measure of system complexity can be derived from the number of elements required. A summary of the elements are shown in Table 4.

TABLE 4. SYSTEM COMPLEXITY

| System Configuration | Direct Generation Elements | Total Elements | Normalized Value |
|---|---|---|---|
| A | 7 | 8 | 1.0 |
| B | 7 | 8 | 1.0 |
| C | 6 | 9 | 1.1 |
| D | 5 | 8 | 1.0 |
| E | 7 | 8 | 1.0 |
| F | 8 | 9 | 1.1 |

System configuration D has the least number of elements in the primary power delivery chain and thus appears best from this standpoint. However, it suffers from the control complexity problem described above.

e. System Maintainability. Most of the components in the various systems are very similar (or identical) in nature and thus would have no impact on relative maintainability. Two component alternatives are, however, believed to be of significance. They are:

(1) DC Generators vs AC Generators — DC generators will require more maintenance then AC generators due to their brushes and commutators. This is evaluated as a 20 percent penalty.

(2) Rotary Inverters vs Static Inverters — Repair of rotary inverters will be more difficult and time consuming than for static inverters. Since no power can be delivered during the repair period, the system using a single rotary converter is penalized a net 20 percent.

Relative system maintainability is shown below in Table 5, with systems D, E, and F having the advantage.

TABLE 5. SYSTEM MAINTAINABILITY

| System Configuration | DC Generator | Rotary Inverter | Index of Relative Maintainability |
|---|---|---|---|
| A | -0.20 | 0 | 0.80 |
| B | -0.20 | -0.20 | 0.60 |
| C | -0.20 | 0 | 0.80 |
| D | 0 | 0 | 1.00 |
| E | 0 | 0 | 1.00 |
| F | 0 | 0 | 1.00 |

f. Generator Weight and Size. Generator weight and size has no direct impact on the electrical system, but a heavier/larger unit located near the focal point of collector will require a stronger structural support and more elevation drive horsepower, both of which lead to increased collector cost. The larger size also results in additional aperture blockage. Current manufacturer's literature indicates that totally enclosed AC machines in the 75 kW power class weigh about 84 percent of comparable DC machines, as shown in Figure 8. Drip proof machines show a reverse trend. Size comparisons are shown in Figures 9 and 10 with DC machines generally showing a size advantage, although the differences are not large.

2.3.1.3 System Configuration Selection. The selection factors are weighted according to importance and are summarized in Table 6. The factors were arranged so that higher values always indicate greater merit.

The results show configuration D is clearly superior. The only potential problem is the inherent instability resulting from having several AC machines

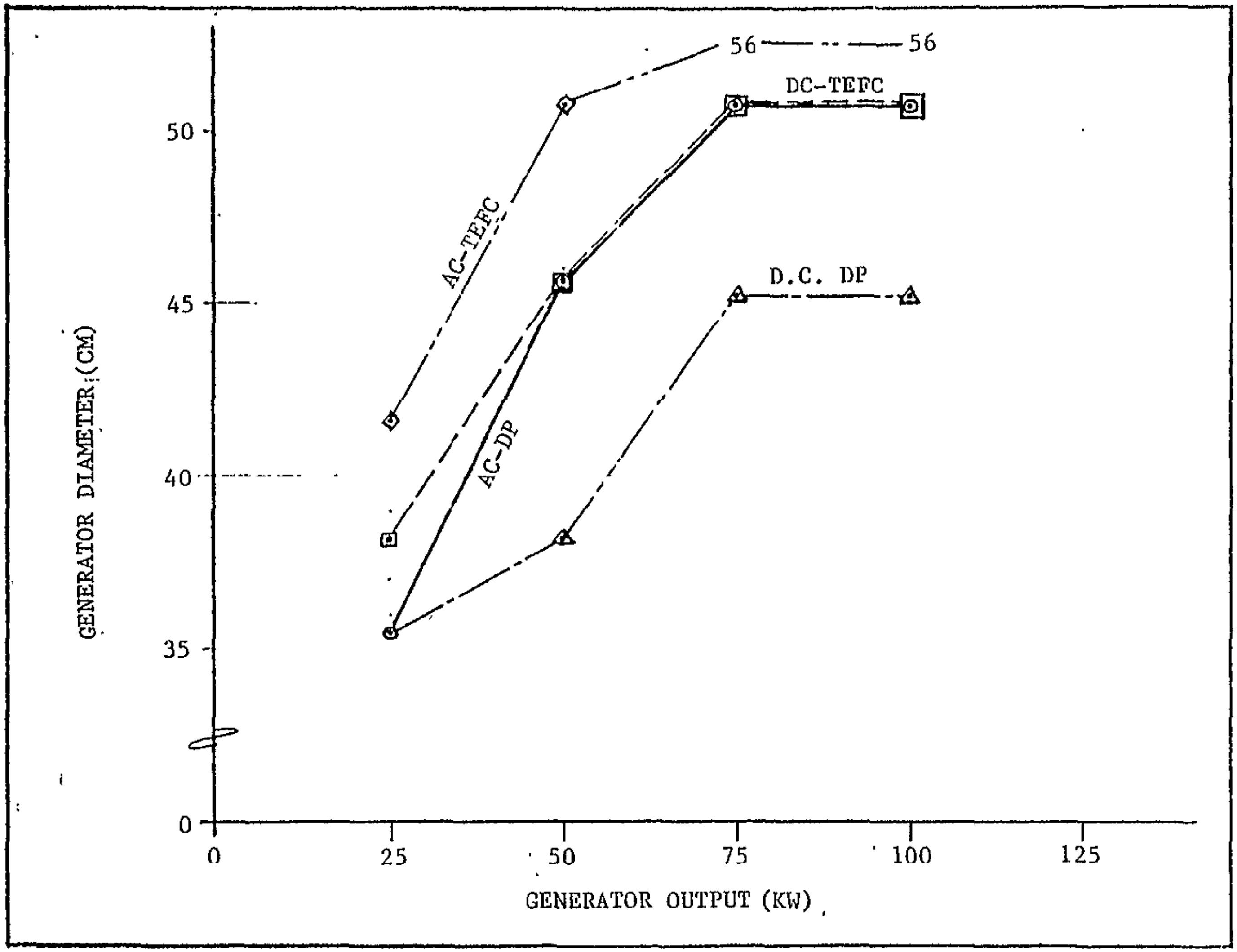


94-2-13

FIGURE 9. GENERATOR DIAMETER VS POWER OUTPUT RATING

C-3

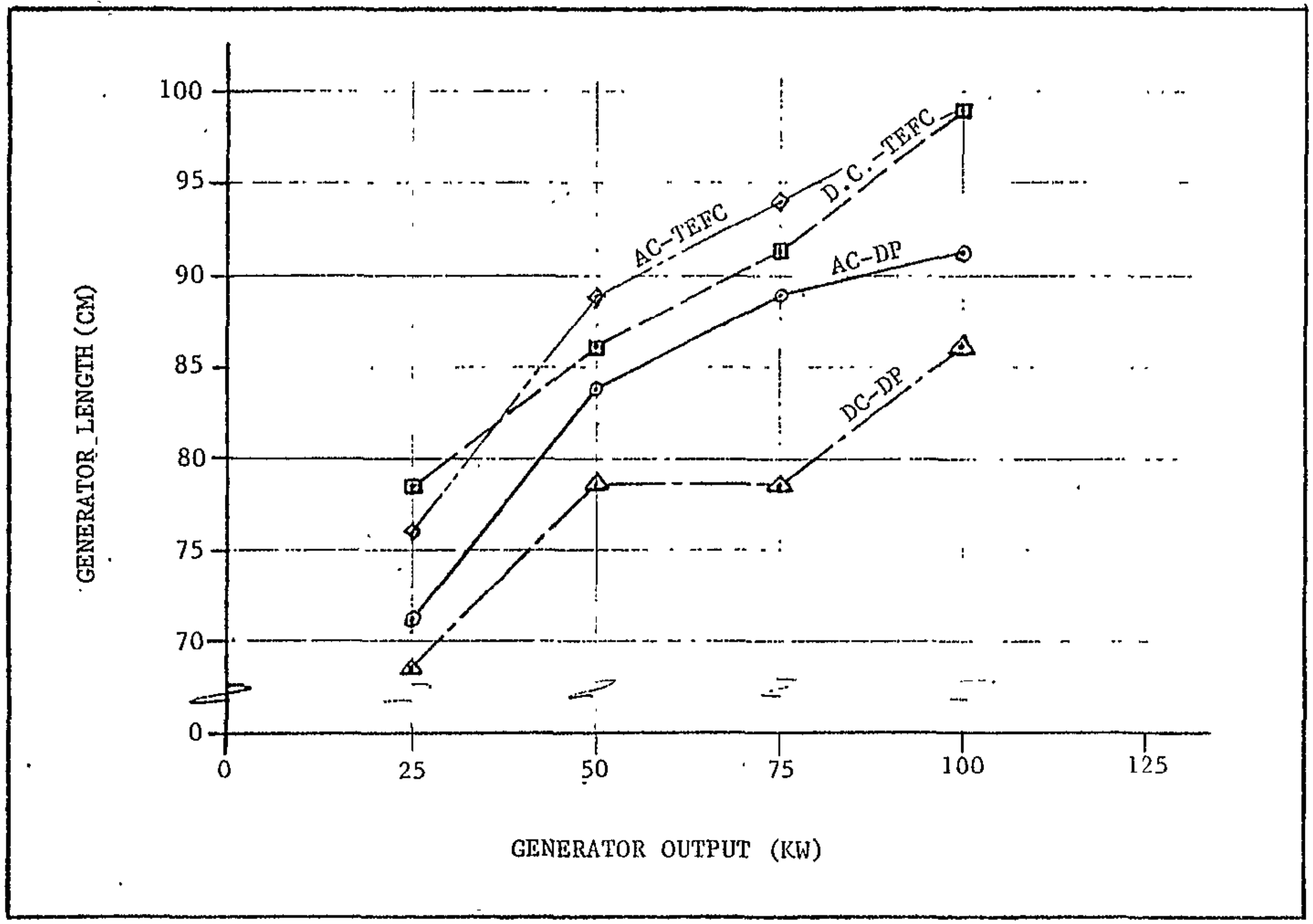


94-2-14

FIGURE 10. GENERATOR LENGTH VS POWER OUTPUT RATING

ORIGINAL PAGE IS OF POOR QUALITY

TABLE 6. SUMMARY OF SELECTION FACTORS

| Selection Factors | Weighting Factor | System Configuration | | | | | |
|---|---|---|---|---|---|---|---|
| | | A | B | C | D* | E | F |
| Efficiency | 1.0 | 0.94 | 0.84 | 0.86 | 1.00 | 0.92 | 0.92 |
| Reliability | 1.0 | 0.75 | 0.90 | 0.90 | 1.00 | 0.75 | 0.85 |
| Cost | 1.0 | 0.87 | 0.89 | 0.63 | 1.00 | 0.94 | 0.78 |
| Inherent Stability | 0.9 | 0.81 | 0.90 | 0.77 | 0.63 | 0.72 | 0.81 |
| Complexity | 0.7 | 0.70 | 0.70 | 0.63 | 0.70 | 0.70 | 0.63 |
| Maintainability | 0.5 | 0.40 | 0.30 | 0.40 | 0.50 | 0.50 | 0.50 |
| Generator Weight | 0.2 | 0.20 | 0.20 | 0.20 | 0.17 | 0.17 | 0.17 |
| Relative Merit | | 4.67 | 4.73 | 4.39 | 5.00 | 4.70 | 4.66 |

*System selected

directly coupled to a grid under dynamic energy source and load conditions. Since modern control technology can solve this problem in a cost effective manner, this subsystem configuration has been selected for further development.

### 2.3.2 ALTERNATOR SUBSYSTEM

Considerations related to the selection of the alternator are operating voltage, rotational speed, and characteristics concerning attitude and weather protection. Standard industrial practice dictates the use of a 480 volt output. Obviously 3-phase, 60 Hz output is also required for compatibility with existing grid systems. A 60 Hz frequency could be obtained with various alternator rotational speeds, depending on the number of poles. Selection of 1800 rpm allows the generator to be direct-coupled to the Stirling engine without the need of an expensive gearbox. Accurate alignment between the frame of the alternator and the engine will be provided so a single-bearing generator can be used. This design is smaller, lighter, has fewer parts, less tendency to vibrate, and lower in cost than a two-bearing design.

The generator will be required to operate in virtually all attitudes as the concentrator tracks the sun across the sky. Ball bearings can accept loading from nearly any radial or axial direction and are relatively low in cost, consequently, they will be specified for use. Sealed, permanently greased bearings have been selected as the best system.

Alternators for outdoor use are classified as drip-proof (DP) or totally enclosed, fan-cooled (TEFC). A fan-cooled drip-proof design has been chosen because of a much smaller diameter, less weight, and less cost. It was determined that a totally enclosed design is not necessary; a simple sheet metal enclosure with air filter will enable a drip-proof machine to operate in all environments. This enclosure will save weight, size and cost compared to a machine built with "totally enclosed" protection. A brushless design will be used since this greatly simplifies the maintenance.

In summary, the selected power conversion subsystem generator will be a 75 kW, 480 volt, 3-phase, 1800 rpm, 60 Hertz alternator with single, permanently greased ball bearing; flexible disc coupling, SAE size 3 adaptor; drip-proof frame; and built-in cooling fan.

2.3.3 STORAGE SUBSYSTEM

2.3.3.1 Storage Batteries. A comparison of acid and alkali batteries was summarized in Paragraph 2.2.3.1 of this Appendix. Lead-acid batteries have been chosen because the cost of alkali cells makes them uncompetitive at this time. Consideration was given to the type of lead acid battery plate, i.e., lead-antimony alloy, lead-calcium alloy, and pure lead plates. Pure lead is not desirable because of limited life. Calcium alloy plates are very resistant to erosion but deep charge and discharge cycles tend to cause plate growth which can damage the cells. Antimony alloy has more erosion than calcium but is more resistant to deep cycles. Since deep cycles will be used for the SPS application - and the costs are nearly equal - lead-antimony alloy plates were selected.

2.3.3.2 Ancillary Equipment. Trade studies between various options to charge the batteries (motor-generator sets, vacuum tube rectifiers, oxide reactifiers, and solid state rectifiers) demonstrated that a solid state silicon controlled rectifier (SCR) is by far the best choice. Also solid state inverters were chosen to convert battery DC to AC for use in the grid or stand-alone operation.

2.3.4 TRANSPORT/DISTRIBUTION SUBSYSTEM

Power is generated at each of the collectors which must be transported from the generator to the ground and then to a central location for distribution. The 480 volt, 75 kW/94 kVA, alternators can produce 113 amperes at full output, therefore the wires from the generators must be large enough to carry the current safely and with minimum voltage drop and power loss. The wires must also be flexible to accommodate tilt and rotation of the concentrator, yet durable enough to withstand daily flexing. Three conductor copper type "W" cable has been selected for the portion of the cable that is subject to flexing.

2.3.4.1 Grid Layout. The power from each alternator can be transported by bare wires overhead on poles, by insulated wires directly buried in the ground, by insulated wires in underground protective ducts or by wires placed in cable trays at the ground level. The type of layout selected is discussed below.

a. Radial Grid Distribution System. The radial system is like the spokes in a wheel, each concentrator module is connected to a central point. The first advantage of a radial system is low cost, which derives from the fact that the wires for a radial connection are the minimum size and length. The second advantage is its simplicity; there is only one point where all the radial lines connect. The instrumentation of this scheme is simple because every circuit is accessible at one point. The same is true of power circuit control; all of the system circuit breakers or switches can be built into one structure. The third advantage is circuit reliability. A fault on one radial line does not affect any other line. If a fault occurs, the radial line can be isolated by one device and the rest of the system can continue to operate. The major disadvantage of the radial system is that if trouble should disable the central point, the entire system goes out of service.

b. Ring Distribution System. In this system each module is connected to a ring. The central point of collection is bi-directionally connected and therefore can adjust to problems anywhere in its circuit without becoming disabled. Another advantage is that it generally has only the main ring bus circuit connecting all of its power points. In many applications, this results in minimum length circuit wires, hence reduced installation costs. Still another advantage is that a fault anywhere on the ring can be isolated while the rest of the ring continues to transport power. The major disadvantage is the ring bus wire size; it must be large enough to handle all of the power of the sources connected to it. Another disadvantage is the physical distance between element disconnect devices located along the ring itself. This same consideration applies to instrumentation; more sets are required and they will all be separated.

c. Hybrid Distribution System. There is a variety of hybrid connections which can be constructed which will fulfill the requirements of the SPS electrical transport/distribution subsystem. There may be radially connected groups of loads which are ring-connected. Conversely, there may be radially connected load units tied onto a large ring bus. Illustrations of these two examples are shown in Figure 11.

d. Collection Field Layout Selection. In Table 7, the comparative lengths of conductors, their sizes, and their unit costs have been combined to give a relative cost for each wiring method. Note that the radial system figure is only 73 while the ring main figure is 761. The ring main conductors cost 14 times more than the radial because they must handle 10 times the current. Both the hybrid numbers are similar and that their figures-of-merit lie roughly half way between the radial and the ring system figures.

The radial system has been selected as the connection scheme of the SPS station. The number of power sources and a requirement for high reliability for the generating units is ideal in the radial system. The advantages of small wire-size economy, short physical installation distances, central plant control, and minimum instrumentation make the radial system the best choice.

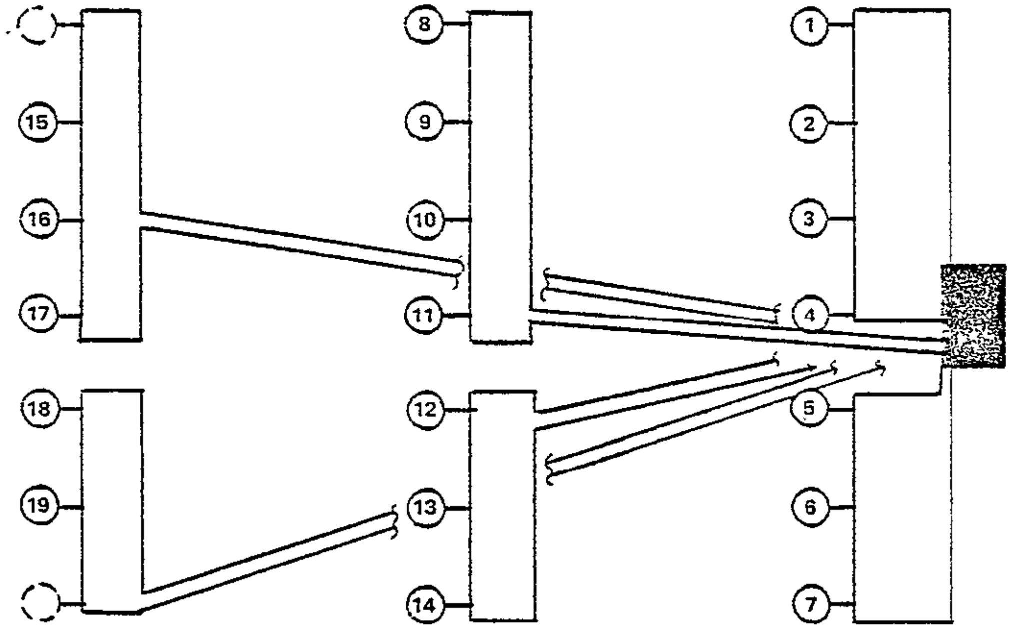


HYBRID: RADIALLY CONNECTED RINGS

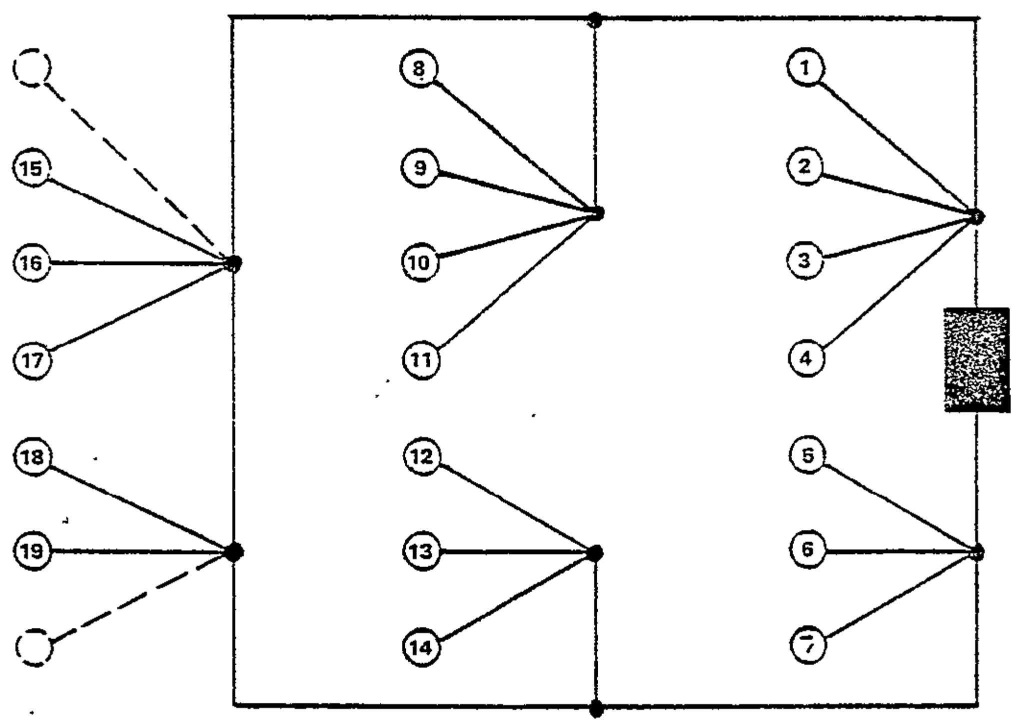


HYBRID: RING CONNECTED RADIAL GROUPS

94-2-15

FIGURE 11. EXAMPLES OF HYBRID DISTRIBUTION SYSTEMS

2.3.4.2 Cable Routing Studies

a. Overhead Power Lines. The concentrator/generator outputs could be connected to bare (or insulated) lines, and suspended on poles. One advantage is that only inexpensive hardware is needed to construct a pole line. Another is that the wires enjoy the benefit of substantial air cooling. They can handle far greater currents than the other options. They are easily accessible for maintenance and are readily visible. The disadvantage of pole lines for SPS is interference with dish operation for high packing fractions. This includes both physical interference and some solar blockage. A safety hazard is present because maintenance/cleaning equipment might contact the wires. A number of wood poles, crossarms and wires is not aesthetically pleasing. Another disadvantage is the susceptibility to weather damage, including lightning.

b. Underground Ducting. Burial of wires in underground ducts has unique advantages. No interference and increased safety are important considerations. The appearance is much better than exposed wires and the environmental problems are less severe, including protection from heat. The ground is relatively cool during the night and remains so during the day and so conductor insulations are not subjected to extreme temperature cycles. Finally, a circuit failure is confined to that one circuit; adjoining circuits are seldom affected. A major disadvantage of the underground ducts is that circuit failure, should it occur, is hard to pin point and once located, is difficult to repair. Often the best repair is to abandon the circuit and install a new one in a nearby duct.

TABLE 7. COMPARISON OF AC COLLECTION SYSTEMS

| Type of Distribution System | Estimated Length Units | Wire Size | Wire Unit Cost | Relative Cost |
|---|---|---|---|---|
| Radial (125 amp capacity) | 197 | #4/0 (AL) | $0.37/unit | 73 |
| Ring (2200 amp capacity) | 145 | 7#500 MCM (AL) | 5.25/unit | 761 |
| Hybrid-I Radial Connected (Rings 500 amp capacity) | 224 | 2#350 MCM (AL) | 1.25/unit | 280 |
| Hybrid-II, Ring Connected (2200 amp capacity) | 66 | 7#500 MCM (AL) | 5.25 | 346 |
| Radial Groups (250 amp) | 90 | #4/0 (AL) | 0.37 | 33 |
| | | | | 379 |

c. Direct Burial. It is possible to bury circuits in earth-filled trenches, without the use of ducts, thus saving the expense of installing ducts. Ground water immersion can be a problem, but direct burial allows improved access to line fault damage points compared to ducts. Fault incidents are minimized by conductor spacing.

d. Surface Power Runs. Another alternative is lines laid on or just above the ground. Cable trays (or racks) can be constructed, and the generator cables placed in the trays. The advantages are that the cables can be air-cooled, they are accessible, they are almost out of sight and are easy to install. The disadvantages are the very high cost of constructing the trays and installing them, their exposure to maintenance vehicles and the environment, and their susceptibility to fault damage.

e. Cable Routing Selection. The comparative costs for overhead, surface, and underground lines are shown in Table 8. These have been developed from estimates of 300 meter runs of each kind of construction.

The direct burial method of wiring has been selected for its many advantages: trenching to install the wire runs is relatively easy; conductor separation in the trenches minimizes fault incidence; the wires are cooled directly by heat conduction to earth; relatively low cost; the circuits are out of sight and protected; conductor installation is fast and easy; and the circuit faults are not difficult to repair when found.

TABLE 8. RELATIVE COST OF VARIOUS CABLE INSTALLATION METHODS

| Cable Routing Method | Cost/Meter ($) |
|---|---|
| Overhead Pole-Line<br>#4 B.C. wire | $20.00 |
| Underground Duct-line<br>1/C-#1 (AL)<br>(No concrete; heavy wall duct) | $26.00 |
| Direct Burial<br>Underground Line<br>#4 (AL) (USE) | $13.60 |
| Ground Level Surface<br>Cable Trays | $39.00 |

2.3.4.3 Electrical Conductor Material. The power cables can be made of aluminum or copper. The advantages and disadvantages of each are well known, e.g., copper is a standard material which has good conductivity but higher cost; aluminum has lower conductivity, the oxide layer can be a problem, flexing can cause work-hardening and breakage, but it has a substantial price advantage (approximately 50 percent). It has become standard electrical construction industry practice to install aluminum wiring for circuits requiring large size and long length due to the cost savings over copper wire. Therefore, the aluminum conductors have also been selected for this application, except for the portion on the concentrator which is subject to flexing.

2.3.4.4 Switchboard Selection. The best approach to supplying power to the SPS station loads is to install a single switchboard that will contain all the station's load circuit protective disconnects. The switchboard could be installed indoors or outdoors; an indoor application is the most cost-effective because a building is required for other equipment. Figure 12 is a sketch of a typical switchboard design.

The Switchboard busses must be large enough to handle the 2,200 amperes of station output and the bus mounting hardware will be designed for the alternator's output voltage of 480 volts AC. A standard 3,000 ampere rating has been selected for the switchboard bus. The choice of aluminum as busbar material was made for reasons discussed above. The standard practice of tin plating the aluminum busses will be used to eliminate the problem of surface oxide formation.

The switchboard power contactors can be either manually or electrically operated. Remote control of the circuit "breakers" is an important advantage since unattended, computer-controlled operation is planned. Therefore, electrically operated devices were chosen. The electrically operated, air insulated, drawout type breakers also have the advantages of high current handling ability, ease of maintenance and replacement, and fine control over trip characteristics. Their disadvantages are cost, size, need for mechanical maintenance, and complexity. The circuit protector of the main power line needs to be remotely controlled for safety, therefore a remotely controlled air breaker has also been selected for this application.

2.3.4.5 Transformer and Connecting Switch. The transformer requirements are a low voltage winding compatible with the generator output of 480 volts, 3 phase, 60 Hz, and a high voltage winding capable of delivering 1000 kW of power at the utility grid voltage (typically 21,000 volts). Off-the-shelf transformers to meet these requirements may have either one or two windings; it may be liquid, gas, or air cooled; it may be three single-phase units or a single 3-phase unit. Also consideration was given to its location.

a. Transformer Winding Selection. A two-winding transformer is customarily used throughout American utility industry. The windings are separated so they can be connected in delta, which prevents third harmonic currents in the output lines. The high and low voltages do not cross over between windings so the high voltage windings can be a small gage wire, and the low voltage windings can be insulated for 480 volts rather than 21,000 volts. For these reasons, the two-winding transformer device has been selected.

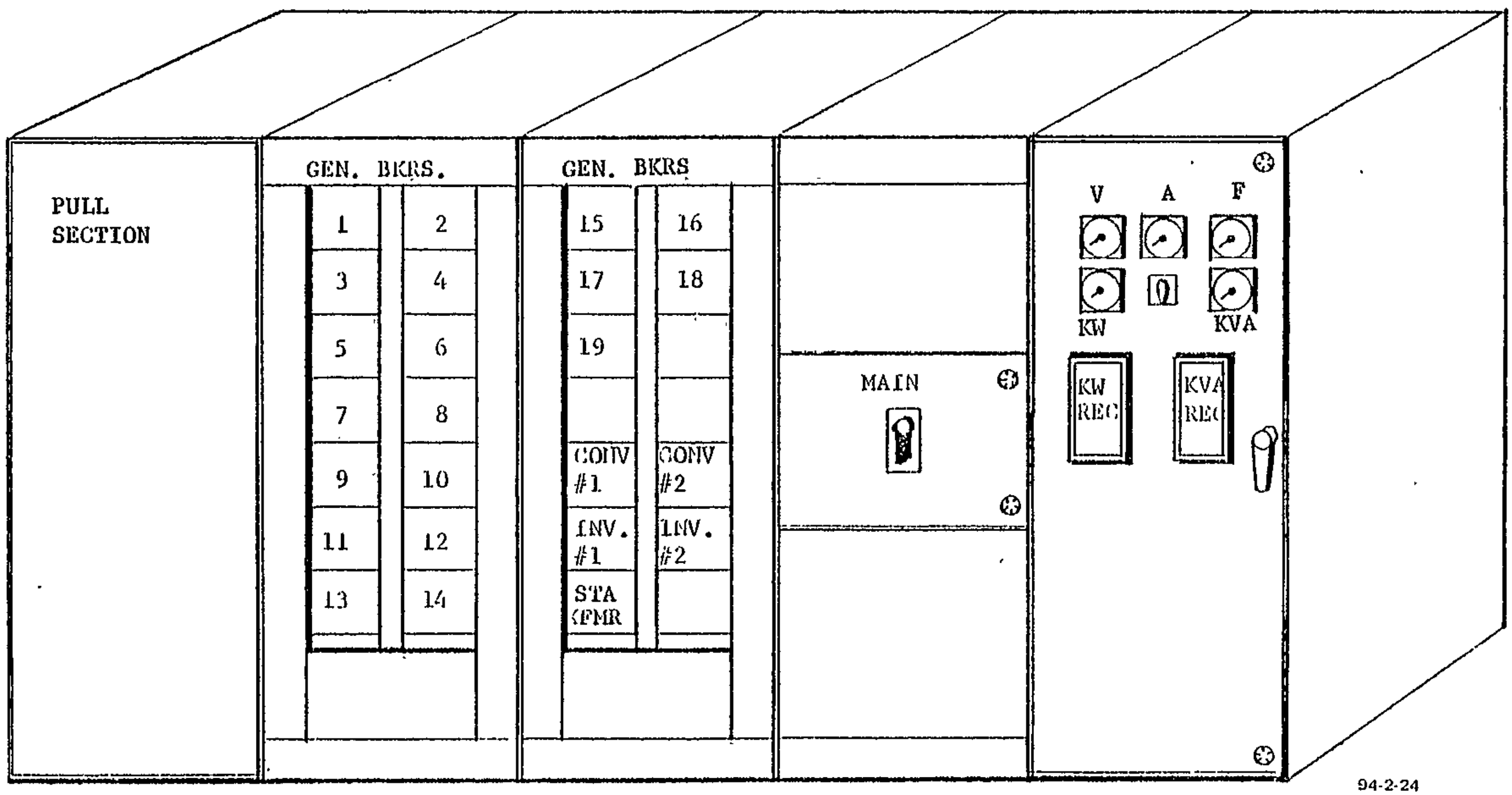


FIGURE 12. MAIN POWER SWITCHBOARD

b. Transformer Cooling. Liquid cooled transformers were chosen because they have the advantages of reliability, efficient heat transfer, small size, and high insulation value. Also they are dust-tight and are the best type to handle the high voltage and any thermal overloads.

c. Transformer Mounting. A weather-proof, pad-mounted outdoor unit was selected since it will meet all requirements and is considerably less expensive than a vault-mounted unit.

d. High Voltage Switch. A high voltage switch connects the transformer output to the utility line. Standard equipment exists for the 21,000 volts, 34 amperes, and 1250 kVA.

2.3.5 ELECTRICAL CONTROL SUBSYSTEM (GRID CONNECTED CASE)

Four types of master power controllers (MPC) have been considered. They are:

- Ladder diagram processors
- Solid state logic controllers
- Micro-computers (microprocessors)
- Mini-computers

The basic requirement of the MPC is to control power delivery from several AC generators into a utility grid with an unlimited capacity compared to an SPS system (i.e., infinite sink). It is both impractical and undesirable to vary the sun's input to the engine; impractical because of difficulty of either shuttering the solar input or bypassing part of the working fluid from the receiver, undesirable because of the wasteful loss of energy. Therefore, the control scheme must be designed to accept all the solar energy directed to the receiver. This is accomplished by "slaving" the existing Stirling engine power control loop to the engine head or receiver temperature. This permits output power from each engine to follow the solar input power curve while maintaining constant system temperature. Note that the engine/alternator remains at a fixed speed of 1800 rpm for all operating conditions. It is also necessary that all alternators operate in phase synchronism and that a means be provided for sharing reactive currents between generators in proportion to the power generated by each of them. The following real time analogue inputs are required from each collector's power conversion system (engine-generator).

- Engine head temperature
- Generator output voltage
- Generator output current

After each generator has been synchronized and placed on-line, it will be necessary to provide an analogue signal of generator excitation offset to each collector's power conversion system to control reactive current delivery.

Two digital signals must be sent (in common) to each collector's servo system at regular intervals for collector positioning. They are:

- Azimuth position
- Elevation position

Also, each collector will require the following discrete control and status signals:

- Engine start/stop
- Receiver door open/close
- Sodium blocking valve open/close
- Concentrator focus/defocus (Emergency defocus)
- Concentrator operate/stow
- Generator output contactor open/close
- Engine summary status
- Engine ready flag
- Concentrator summary status
- Generator contactor status
- Miscellaneous status signals such as receiver temperature(s), etc.

Monitoring and control of 19 collectors in the baseline (1.0 $MW_e$, CF = 0.4, P75 Stirling engine) station from the central MPC would require approximately:

- 57 analogue input signals
- 19 analogue output signals
- 2 digital output signals
- 76 discrete input signals
- 114 discrete output signals plus miscellaneous status

Adding in the other monitoring and control signals associated with the storage subsystem and other centralized station control functions would increase the number by approximately 20 percent. System stability considerations dictate that the analogue input signals be processed and returned as control values at least every 0.5 seconds. A change of status of a discrete input signal must be processed immediately on an interrupt basis and returned as an appropriate control signal. Digital position data for the collectors must be updated and transmitted every 15 seconds to ensure proper sun tracking.

In addition to the basic station control functions, the MPC would provide station performance data logging and station diagnostics.

2.3.5.1 MPC Device Selection. The MPC device was selected based on the selection factors summarized on Table 9. The ladder diagram processor and the solid state logic controller were quickly eliminated because of the factors listed on the table. Mini-computers were eliminated because of cost, leaving only a choice of 8-bit or 16-bit micro-computers (micro-processor).

a. Micro-Computer Capability. Existing micro-computers operate under stored program control, have semi-conductor memories and usually some form of mass storage. Clock rates for the 8-bit machines are usually in the range of 1 to 5 MHz. Current 16-bit processors operate at clock rates from 2 to 11 MHz. Although all internal processing is done digitally by manipulation of single data bits (8-bit bytes or 16-bit words) well-developed interface devices are commercially available.

Digital data processing in the control loops permits positive control of loop transfer functions and prevents cascading instabilities which may occur when attempts are made to operate multiple alternators in phase synchronism under dynamic loads, variable solar conditions and possible emergencies. Digital signal processing also avoids the problem of accumulative error.

A micro-computer system can utilize available perpherals for flexible, real-time display of station performance parameters, system diagnostic capability and station performance data logging in a form that is suitable for both local display and detailed off-site processing and analysis. Large-scale production has resulted in declining prices for a product of given capability. Currently, a top-of-the-line 8-bit micro-computer operating at 4 MHz with 65,536 bytes of addressable random access memory, 512,000 bytes of mass storage and a CRT terminal is available at a price of $8,600 which is very good compared to alternative MPCs. The ability to operate under stored program control is, however, the capability of greatest importance in developing a control system for this application.

b. 8-Bit Versus 16-Bit Micro-Computers. Two basic factors are of paramount importance in making the decision between 8-bit and 16-bit micro-computers. They are: (1) capability and (2) availability.

TABLE 9. EVALUATION OF MASTER POWER CONTROLLER

| Selection Factors | Ladder Diagram Processor | Solid State Logic Controller | Micro-Computer 8-bit | Micro-Computer 16-bit | Mini-Computer |
|---|---|---|---|---|---|
| Data throughput (relative) | 1 | 2 | 5 | 9 | 10 |
| Analogue or digital control loop | Analogue | Analogue | Digital | Digital | Digital |
| Proportional function capability | yes | yes | yes | yes | yes |
| Integral function capability | no | no | yes | yes | yes |
| Derivative function capability | no | no | yes | yes | yes |
| Generator synchronization capability | no | no | yes | yes | yes |
| Cross current compensation capability | no | no | yes | yes | yes |
| Software programmable | no | no | yes | yes | yes |
| Program development (relative difficulty) | 10 | 8 | 2 | 1.2 | 1 |
| Program modification (relative difficulty) | 10 | 8 | 2 | 1.2 | 1 |
| Flexible data display capability | no | no | yes | yes | yes |
| Diagnostic capability | no | no | yes | yes | yes |
| Data logging capability | no | no | yes | yes | yes |
| Estimated Cost (1978 $) | $58K | $51K | $9K | $15K | $33K |

The power control micro-computer should be able to provide up-dated data to all controlled devices at intervals not exceeding 0.5 second (desirably less). However when the number of control functions required is considered, this approaches the current processing capability of the best of the 8-bit machines. The control programs must therefore be optimized for execution time which will make assembly language programming mandatory. Sixteen bit micro-computers are typically about twice as fast as 8-bit machines for simple tasks and perhaps 10 times as fast for more complex tasks. These speeds, which rival mini-computer performance, would make it possible to provide increased stability margins or alternatively to allow software development to be done in a high level language (HLL) such as Pascal. Programming in Pascal (which shows promise of becoming an industry standard for 16-bit machines) would reduce software development time and cost to about 1/2 of that required for assembly language programming. It would also greatly facilitate upgrading software to accommodate future hardware developments. The penalty for this is approximately a two-fold increase in processing time. The 16-bit processors will therefore provide substantially improved performance for a modest increase in cost, or approximately equal performance at reduced total costs (software and hardware).

Sixteen bit processors would clearly be performance and cost effective for the experimental station and probably for the "far term" operational stations. They cannot, however, be recommended for an experimental station to be implemented on a 3½ or 4½ year schedule. Although the processor chips themselves have been delivered in commercial quantities for approximately one year, complete hardware systems are perhaps 1 to 2 years away and mature software will lag hardware availability by an additional 1 to 2 years.

Eight bit micro-processors are therefore believed to be the only realistic choice for an experimental station to be implemented in a 3½ or 4½ year time frame. The continuing development of 16-bit processors should be closely followed for possible use on a 6½ year program. Continuing hardware development and large scale production of 16-bit micro-processors will undoubtedly result in cost reductions which will reduce (or possibly eliminate) the indicated cost differential with present day 8-bit processors and make them the best choice for "far term" operational solar power stations to be implemented in the late 1980's.

## 2.4 ELECTRICAL SUBSYSTEM COST ANALYSIS

Three types of electrical subsystem costs were required for input to system optimization analysis:

(1) Costs for a 1 MWe station without storage at todays' prices, and for various numbers of stations for the far term (∿1990),

(2) Costs for battery storage (lead-acid battery subsystem for a single station now, and multiple stations in the year 1990), and

(3) Costs for a range of station power levels and capacity factors (sensitivity analysis).

These results are described in the following three paragraphs.

### 2.4.1 COSTS FOR 1 MWe STATION (NO STORAGE)

An electrical subsystem cost breakdown was derived for the 1.0 MWe plant for three typical sizes of Stirling engines:

| Engine | Number of Electrical Subsystems | Dia. of Concentrators |
|---|---|---|
| P-150 | 9 | 25.5 m |
| P-75 | 19 | 18.0 |
| P-40 | 40 | 13.2 |

These values were selected to give a representative range in the number of concentrators (number of electrical subsystems) required for a 1 MWe plant and are not necessarily optimum (especially for the P-40 engine).

Table 10 presents the results for the single electrical subsystem if purchased today. Tables 11 through 14 give the costs for 100, 500, 1000, and 5000 stations (1 MWe each) for circa 1990. Note that detailed cost breakdowns are given for the major components within the electrical subsystem as well as shipping and field assembly costs. In all cases there is a dramatic increase in electrical subsystem cost when quantity is increased, even though the power output of the station remains the same.

Figure 13 presents a plot of the no-storage electrical costs as a function of the number of (variable-size) concentrators. However, caution must be used when applying these values to systems with higher annual capacity factors (ACF). The reason is as follows: The results presented in Figure 13 are for a nominal 1 MWe plant for different numbers of collectors. These collectors provide the nominal system power directly to the grid when the solar insolation is at the rated value, i.e., 800 $W/m^2$. When the solar insolation is greater than 800 $W/m^2$, the excess power generated by these "basic modules" can be directed to a storage system for later delivery, or simply dissipated. If a larger ACF is desired than is achievable with the

TABLE 10. SINGLE 1 MWe ELECTRICAL SUBSYSTEM (LESS STORAGE) COSTS IN 1978 DOLLARS

| | No. of Concentrators | | |
|---|---|---|---|
| | 9 | 19 | 40 |
| Power Conversion S/S: | | | |
| Alternator/Regulator/Shroud | $59.4 K | $67.4 K | $118.2 K |
| Contactors | 22.8 | 31.6 | 35.7 |
| Ancillaries | 11.3 | 18.4 | 35.6 |
| Lightning Protection | 0.7 | 1.5 | 3.1 |
| Cables | 7.2 | 9.0 | 5.9 |
| Subtotal | 101.4 K | 127.9 K | 198.5 K |
| Transport/Distribution S/S: | | | |
| Cables | 17.0 | 16.4 | 17.9 |
| Power Switchboard | 20.0 | 24.0 | 26.0 |
| HV Transformer | 32.0 | 32.0 | 32.0 |
| Ancillaries/Switch | 6.0 | 4.4 | 4.6 |
| Subtotal | 75.0 | 76.8 | 80.5 |
| Control S/S: | | | |
| Computer/CRT Terminal | 10.2 | 12.7 | 22.8 |
| Central Interface Assembly | 9.9 | 19.4 | 38.6 |
| Remote Interface Assembly/Sensors | 14.2 | 30.0 | 63.2 |
| Cables | 8.7 | 17.0 | 33.0 |
| Subtotal | 43.0 | 79.1 | 157.6 |
| Shipping to Site: | 2.9 | 3.9 | 6.0 |
| Field Assembly: | | | |
| Cable Installation | 2.2 | 4.0 | 8.3 |
| Installation (Other) | 22.5 | 36.2 | 63.1 |
| Test/Check-out | 6.8 | 8.8 | 13.0 |
| Subtotal | 31.5 | 49.0 | 84.4 |
| Total | $253.8 K | $336.7 K | $527.0 K |

NOTE: Non-recurring engineering not included in above costs.

TABLE 11. 100 - 1 MWe ELECTRICAL SUBSYSTEM (LESS STORAGE BASELINE COSTS IN FAR TERM (LATE 1980's)

| | No. of Concentrators | | |
|---|---|---|---|
| | 9 | 19 | 40 |
| **Power Conversion S/S:** | | | |
| Alternator/Regulator/Shroud | $51 K | $58 K | $100 K |
| Contactors | 18 | 25 | 29 |
| Ancillaries | 9 | 15 | 28 |
| Lightning Protection | 1 | 1 | 3 |
| Cables | 6 | 8 | 5 |
| Subtotal | 85 | 107 | 165 |
| **Transport/Distribution S/S:** | | | |
| Cables | 15 | 15 | 16 |
| Power Switchboard | 16 | 19 | 21 |
| HV Transformer | 26 | 26 | 25 |
| Ancillaries/Switch | 5 | 3 | 4 |
| Subtotal | 62 | 63 | 66 |
| **Control S/S:** | | | |
| Computer/CRT Terminal | 6 | 8 | 8 |
| Central Interface Assembly | 6 | 12 | 14 |
| Remote Interface Assembly/Sensors | 8 | 18 | 38 |
| Cables | 8 | 15 | 30 |
| Subtotal | 28 | 53 | 90 |
| **Shipping to Site:** | 3 | 4 | 5 |
| **Field Assembly:** | | | |
| Install Cables | 2 | 4 | 7 |
| Installation (Other) | 23 | 32 | 57 |
| Test/Check-out | 6 | 8 | 12 |
| Subtotal | 31 | 44 | 76 |
| **Recurring Engineering:** | 5 | 5 | 5 |
| Total | $214 K | $276 K | $407 K |

TABLE 12. 500 - 1 MWe ELECTRICAL SUBSYSTEM (LESS STORAGE) COSTS FOR FAR TERM (LATE 1980's)

| | No. of Concentrators | | |
|---|---|---|---|
| | 9 | 19 | 40 |
| Power Conversion S/S: | | | |
| Alternator/Regulator/Shroud | $44 K | $50 K | $88 K |
| Contactors | 16 | 22 | 25 |
| Ancillaries | 8 | 13 | 25 |
| Lightning Protection | 1 | 1 | 2 |
| Cables | 6 | 8 | 5 |
| Subtotal | 75 | 94 | 145 |
| Transport/Distribution S/S: | | | |
| Cables | 14 | 13 | 15 |
| Power Switchboard | 14 | 17 | 18 |
| HV Transformer | 23 | 23 | 23 |
| Ancillaries/Switch | 4 | 3 | 3 |
| Subtotal | 55 | 56 | 59 |
| Control S/S: | | | |
| Computer/CRT Terminal | 5 | 6 | 6 |
| Central Interface Assembly | 5 | 9 | 11 |
| Remote Interface Assembly/Sensors | 6 | 14 | 29 |
| Cables | 7 | 14 | 27 |
| Subtotal | 23 | 43 | 73 |
| Shipping to Site: | 3 | 4 | 5 |
| Field Assembly: | | | |
| Install Cables | 2 | 3 | 7 |
| Installation (Other) | 19 | 30 | 52 |
| Test/Check-out | 5 | 7 | 11 |
| Subtotal | 26 | 40 | 70 |
| Recurring Engineering: | 4 | 4 | 4 |
| Total | $186 K | $241 K | $356 K |

TABLE 13. 1000 - 1 MWe ELECTRICAL SUBSYSTEM (LESS STORAGE) COSTS FOR FAR TERM (LATE 1980's)

| | No. of Concentrators | | |
|---|---|---|---|
| | 9 | 19 | 40 |
| Power Conversion S/S: | | | |
| Alternator/Regulator/Shroud | $42 K | $47 K | $83 K |
| Contactors | 15 | 21 | 24 |
| Ancillaries | 7 | 12 | 23 |
| Lightning Protection | 1 | 1 | 2 |
| Cables | 5 | 7 | 5 |
| Subtotal | 70 | 88 | 137 |
| Transport/Distribution S/S: | | | |
| Cables | 14 | 13 | 14 |
| Power Switchboard | 13 | 16 | 17 |
| HV Transformer | 21 | 21 | 21 |
| Ancillaries/Switch | 4 | 3 | 3 |
| Subtotal | 52 | 53 | 55 |
| Control S/S: | | | |
| Computer/CRT Terminal | 4 | 5 | 6 |
| Central Interface Assembly | 4 | 8 | 9 |
| Remote Interface Assembly/Sensors | 6 | 12 | 13 |
| Cables | 7 | 13 | 26 |
| Subtotal | 21 | 38 | 54 |
| Shipping to Site: | 3 | 4 | 5 |
| Field Assembly: | | | |
| Install Cables | 2 | 3 | 6 |
| Installation (Other) | 17 | 28 | 49 |
| Test/Check-out | 5 | 7 | 10 |
| Subtotal | 24 | 38 | 65 |
| Recurring Engineering | 3 | 3 | 3 |
| Total | $173 K | $224 K | $319 K |

TABLE 14. 5000 - 1 MWe ELECTRICAL SUBSYSTEM (LESS STORAGE) COSTS FOR FAR TERM (LATE 1980's)

| | No. of Concentrators | | |
|---|---|---|---|
| | 9 | 19 | 40 |
| Power Conversion S/S: | | | |
| Alternator/Regulator/Shroud | $34 K | $39 K | $68 K |
| Contactors | 12 | 16 | 18 |
| Ancillaries | 6 | 9 | 18 |
| Lightning Protection | 1 | 1 | 2 |
| Cables | 5 | 7 | 4 |
| Subtotal | 58 | 72 | 110 |
| Transport/Distribution S/S: | | | |
| Cables | 13 | 13 | 14 |
| Power Switchboard | 13 | 15 | 17 |
| HV Transformer | 20 | 20 | 20 |
| Ancillaries/Switch | 4 | 3 | 3 |
| Subtotal | 50 | 51 | 54 |
| Control S/S: | | | |
| Computer/CRT Terminal | 3 | 3 | 3 |
| Central Interface Assembly | 3 | 5 | 6 |
| Remote Interface Assembly/Sensors | 4 | 8 | 16 |
| Cables | 6 | 12 | 23 |
| Subtotal | 16 | 28 | 48 |
| Shipping to Site: | 3 | 4 | 5 |
| Field Assembly: | | | |
| Install Cables | 2 | 3 | 5 |
| Installation (Other) | 14 | 23 | 41 |
| Test/Check-out | 4 | 6 | 8 |
| Subtotal | 20 | 32 | 54 |
| Recurring Engineering: | 2 | 2 | 2 |
| Total | $149 K | $189 K | $273 K |

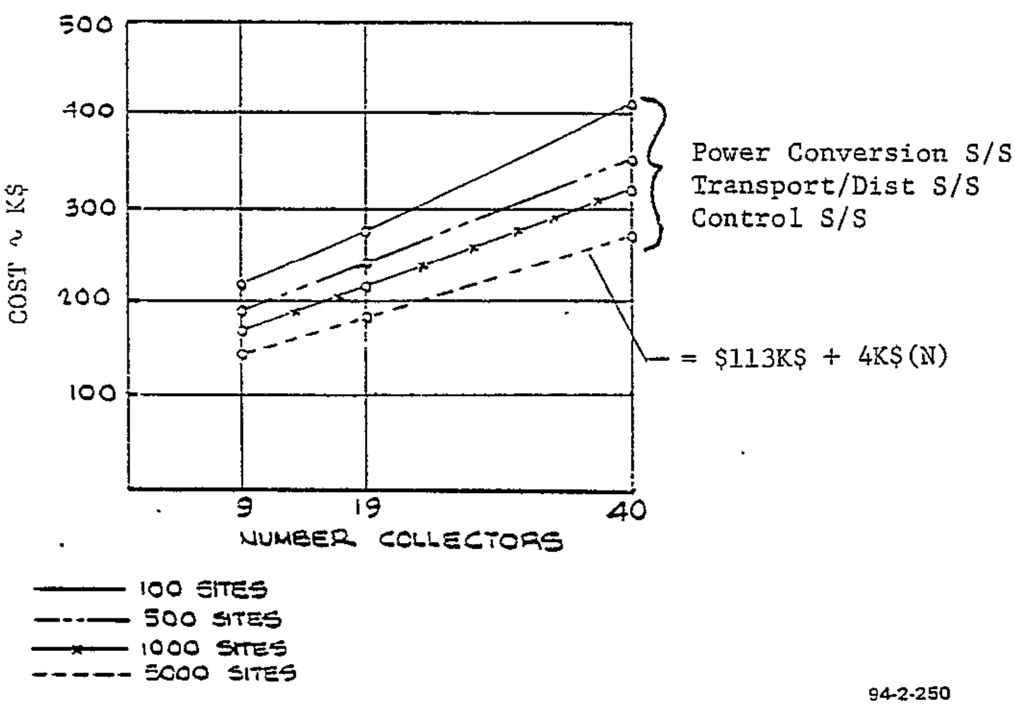


FIGURE 13. NO-STORAGE ELECTRICAL COSTS VS NUMBER OF COLLECTORS (1 MWe) (FAR TERM - LATE 1980's)

basic modules, additional collectors must be provided but the results shown in Figure 13 cannot be used since the total generated power will exceed 1 MWe (although the excess power is delivered entirely to the storage system and not directly to the grid). To obtain the correct electrical subsystem costs for larger ACFs, the additional cost of the components over the cost for the basic modules given in Figure 13 is obtained by scaling. This scaling involves costs which are directly proportional to the number of added collectors plus fixed costs.

## 2.4.2 BATTERY STORAGE SUBSYSTEM

Battery subsystem costs (including inverter/converter, racks, shipping, installation, etc.) were computed for a typical subsystem capable of delivering 1646 kWh to the grid. (Note this is a representative value, not the baseline.) Table 15 presents these values for a 1 MWe station at today's prices and the values for 100 to 5000 sites in the 1990 era. Table 16 presents the costs for 5000 sites in 1990 as a function of energy delivered to the grid from storage. Values of 648 to 7850 kWh were selected to cover the range of expected values.

TABLE 15. ELECTRICAL STORAGE SUBSYSTEM BASELINE COSTS (1646 KWH)

| | Single 1 MWe Site (1978 $'s) | 100 Sites (Late 1980's) | 500 Sites (Late 1980's) | 1000 Sites (Late 1980's) | 5000 Sites (Late 1980's) |
|---|---|---|---|---|---|
| Batteries | $475 K | $410 K | $393 K | $385 K | $377 K |
| Inverter | 102 | 83 | 73 | 69 | 64 |
| Converter | 52 | 42 | 37 | 35 | 33 |
| Auxiliaries | 21 | 17 | 15 | 14 | 13 |
| Battery Racks | 23 | 12 | 11 | 10 | 8 |
| Subtotal Hardware | 673 | 566 | 529 | 513 | 495 |
| Shipping | 14 | 13 | 13 | 13 | 13 |
| Site Installation | 90 | 73 | 69 | 65 | 59 |
| Site Testing | 8 | 6 | 6 | 6 | 5 |
| TOTAL | $785 K | $658 K | $617 K | $597 K | $572 K |

TABLE 16. ELECTRICAL STORAGE SUBSYSTEM COSTS FOR 5000 SITES IN 1990 (1978 PRICE BASE)

| | Energy Delivered to Grid from Storage | | | |
|---|---|---|---|---|
| | 648 kWh | 1646 kWh | 5000 kWh | 7850 kWh |
| Batteries | $216 K | $377 K | $ 758 K | $1129 K |
| Inverter | 64 | 64 | 64 | 64 |
| Converter | 18 | 33 | 84 | 134 |
| Wiring | 8 | 13 | 20 | 28 |
| Battery Rack | 4 | 8 | 12 | 24 |
| Hardware | $310 K | $495 K | $ 938 K | $1379 K |
| Site Installation | $ 37 | $ 59 K | $ 112 K | $ 165 K |
| Site Testing | 4 | 5 | 8 | 11 |
| Shipping | 9 | 13 | 26 | 39 |
| Total | $360 K | $572 K | $1084 K | $1594 K |

Note: Air conditioning/ventilation costs, building cost, and handling costs and profit not included. Discharge rate based on 700 kW.

### 2.4.3 SENSITIVITY ANALYSIS

An electrical subsystem cost sensitivity analysis was performed for plant sizes (rated power) from 0.5 to 10 MWe and for annual capacity factors (ACF) from the value for no storage to 0.7 ACF. All calculations were performed for 5000 sites per year in about the year 1990 for the P-75 system.

Table 17 presents the results for the no-storage electrical system for the three plant sizes. The 0.5 MWe case is represented by ten collectors (10 P-75 engines with 74 kW max. power), the 1 MWe case by 19 collectors, and the 10 MWe by 190 collectors. Table 18 summarizes the corresponding costs for the lead-acid battery storage subsystem.

Table 19 details the no-storage electrical subsystem costs for the 1 MWe plant for ACFs from zero storage to 0.7. Table 20 summarizes the corresponding values for the lead-acid battery storage subsystem. (Note that the 1646 kWh for the 0.4 ACF in Table 20 is not the baseline value; the baseline is 2100 kWh.) One striking change that is required for a lead-acid storage system for an ACF of 0.7 is the size of the room to house the batteries. This is illustrated in Figure 14 (plans for the control building for zero storage and 0.4 ACF are shown in Paragraph 3.1.7 of the report). The costs of this building and the added air conditioning units required have not been included in the preceding tables.

TABLE 17. NO-STORAGE ELECTRICAL SUBSYSTEM COSTS FOR 1/2 MWe, 1 MWe and 10 MWe

- CA 1990 Costs (1978 Dollars)
- 5000 Sites/Year

| Electrical Subsystem Breakdown | 10 @ 74 KW ½ MWe | 19 @ 74 KW 1 MWe | 190 @ 74 KW 10 MWe |
|---|---|---|---|
| Power Conversion S/S: | | | |
| Alternator/Regulator/Shroud | 21 | $39K | $390K |
| Contactors | 8 | 16 | 160 |
| Ancilliaries | 5 | 9 | 90 |
| Lightning Protection | 1 | 1 | 10 |
| Cables | 4 | 7 | 70 |
| Subtotal | 39 | 72 | 720 |
| Transport/Distribution S/S: | | | |
| Cables | 5 | 13 | 130 |
| Power Switchboard | 10 | 15 | 150 |
| HV Transformer | 13 | 20 | 200 |
| Ancilliaries/Switch | 2 | 3 | 30 |
| Subtotal | 30 | 51 | 510 |
| Control S/S: | | | |
| Computer/CRT Terminal | 2 | 3 | 30 |
| Central Interface Assembly | 3 | 5 | 50 |
| Remote Interface Assembly/Sensors | 4 | 8 | 80 |
| Cables | 6 | 12 | 120 |
| Subtotal | 15 | 28 | 280 |
| Shipping to Site: | 2 | 4 | 40 |
| Field Assembly: | | | |
| Install Cables | 2 | 3 | 30 |
| Installation (Other) | 15 | 23 | 200 |
| Test/Check-out | 4 | 6 | 50 |
| Subtotal | 21 | 32 | 280 |
| Recurring Engineering: | 2 | 2 | 20 |
| Total | $109K | $189K | $1850K |

TABLE 18. STORAGE SUBSYSTEM COSTS FOR 1/2 MWe, AND 1 MWe and 10 MWe

- CA 1990 Costs (1978 Dollars)
- 5000 Sites/Year

| Storage S/S Components | 1/2 MWe | 1 MWe | 10 MWe |
|---|---|---|---|
| Batteries (Lead-Acid) | $188 K | $377 K | $3770 K |
| Inverter | 32 | 64 | 640 |
| Converter | 17 | 33 | 330 |
| Auxiliaries | 7 | 13 | 130 |
| Battery Racks | 4 | 8 | 80 |
| Subtotal Hardware | 248 | 495 | 4950 |
| Shipping | 7 | 13 | 130 |
| Site Installation | 30 | 59 | 550 |
| Site Testing | 3 | 5 | 50 |
| TOTAL | $288 K | $572 K | $5680 K |

TABLE 19. NO-STORAGE ELECTRICAL SUBSYSTEM COSTS FOR VARIOUS CAPACITY FACTORS (1 MWe)

- CA 1990 Costs (1978 Dollars)
- 5000 Sites/Year

| Electrical Subsystem Breakdown | Zero Storage<br>19 @ 74 KW | 0.4 CF<br>10 @ 74 KW | 0.70CF<br>41 @ 74 KW |
|---|---|---|---|
| Power Conversion S/S: | | | |
| Alternator/Regulator/Shroud | $37K | $39K | $84K |
| Contactors | 15 | 16 | 35 |
| Ancilliaries | 8 | 9 | 19 |
| Lightning Protection | 1 | 1 | 2 |
| Cables | 7 | 7 | 15 |
| Subtotal | 68 | 72 | 155 |
| Transport/Distribution S/S: | | | |
| Cables | 12 | 13 | 36 |
| Power Switchboard | 15 | 15 | 29 |
| HV Transformer | 20 | 20 | 20 |
| Ancilliaries/Switch | 3 | 3 | 3 |
| Subtotal | 50 | 51 | 88 |
| Control S/S: | | | |
| Computer/CRT Terminal | 3 | 3 | 6 |
| Central Interface Assembly | 5 | 5 | 10 |
| Remote Interface Assembly/Sensors | 8 | 8 | 17 |
| Cables | 11 | 12 | 29 |
| Subtotal | 27 | 28 | 61 |
| Shipping to Site: | 4 | 4 | 6 |
| Field Assembly: | | | |
| Install Cables | 3 | 3 | 8 |
| Installation (other) | 22 | 23 | 51 |
| Test/Check-out | 6 | 6 | 14 |
| Subtotal | 31 | 32 | 73 |
| Recurring Engineering: | 2 | 2 | 2 |
| Total | $182K | $189K | $385K |

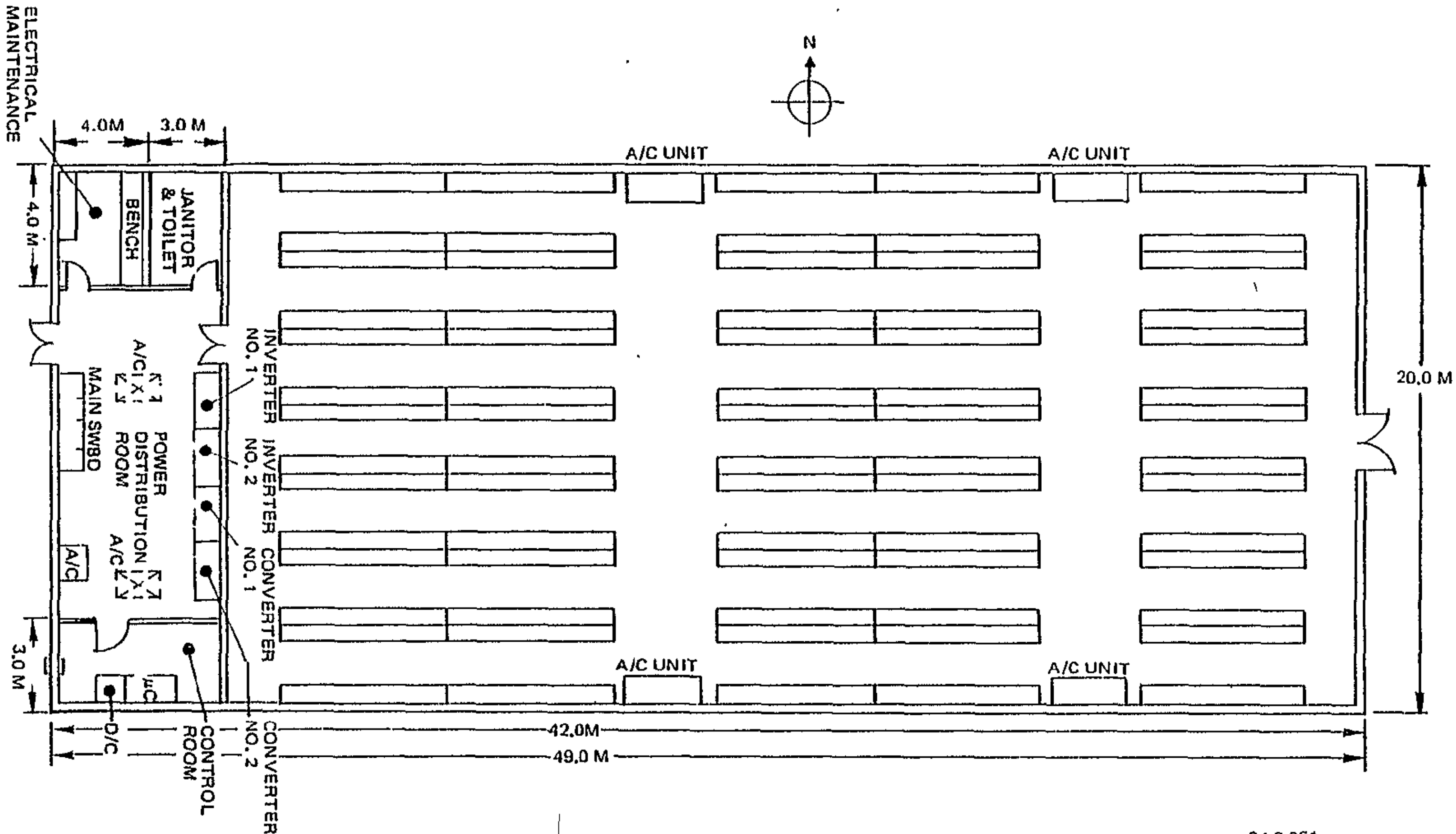


FIGURE 14. CONTROL BUILDING FLOOR PLAN FOR 0.7 CAPACITY FACTOR

TABLE 20. STORAGE SUBSYSTEM COSTS FOR VARIOUS CAPACITY FACTORS (1 MWe)

- CA 1990 Costs (1978 Dollars)
- 5000 Sites/Year

| Storage S/S Components | Zero Storage | 0.4 CF (1646 kWh) | 0.7 CF (14,671 kWh) |
|---|---|---|---|
| Batteries (Lead-Acid) | -------- | $377 K | $2462 K |
| Inverter | -------- | 64 | 64 |
| Converter | -------- | 33 | 128 |
| Auxiliaries | -------- | 13 | 30 |
| Battery Racks | -------- | 8 | 21 |
| Subtotal Hardware | -------- | 495 | 2705 |
| Shipping | -------- | 13 | 85 |
| Site Installation | -------- | 59 | 320 |
| Site Testing | -------- | 5 | 20 |
| TOTAL | "0" | $572 K | $3130 K |

## SECTION 3

## SELECTED ELECTRICAL SYSTEM AND COMPONENT DEFINITION

Electrical system configuration "D" (AC generation of the module) has been selected for the SPS because it offers several significant advantages over the other system. These advantages are listed below:

- Highest operating efficiency
- Lowest cost
- Most reliable components
- Least system complexity
- Adaptable to various operating modes

This system configuration, together with its components and control system is discussed in the following paragraphs.

### 3.1 ELECTRICAL SYSTEM CONFIGURATION

The system using the P-75 Stirling engine collects power from nineteen 75 kW AC generators (18 "basic modules" plus one for storage), each located near the prime focus of a collector and transports that power to a central power distribution switchboard located in the control building. Then it goes through a step-up transformer and fused switch to nearby high voltage utility transmission lines. General characteristics of this system have been described in preceding paragraphs.

Generating capacity in excess of that required to meet the rated station power output requires the charging of two lead acid battery banks through two converters during most of the operating day. Energy stored in the battery banks may then be withdrawn from the battery banks, inverted back to AC and delivered to the utility grid in accordance with a pre-programmed or adaptive operating schedule.

A one-line diagram showing mechanization of the selected concept and identifying the size of the major circuit elements is shown in Figure 15. The system will operate under the control of a microprocessor-based master power controller (MPC) and is designed for unattended operation. The microprocessor controls the complete operation of the station from start-up each morning, synchronization of the individual modules, to shut-down at dusk. The functions performed by the computer are summarized in Paragraphs 3.1.1.5 and 3.1.7 of the report, and Paragraph 2.3.5 of this Appendix.

The output of each power conversion module is collected by means of a simple radial cable system and conveyed to the switchboard. From the switchboard,

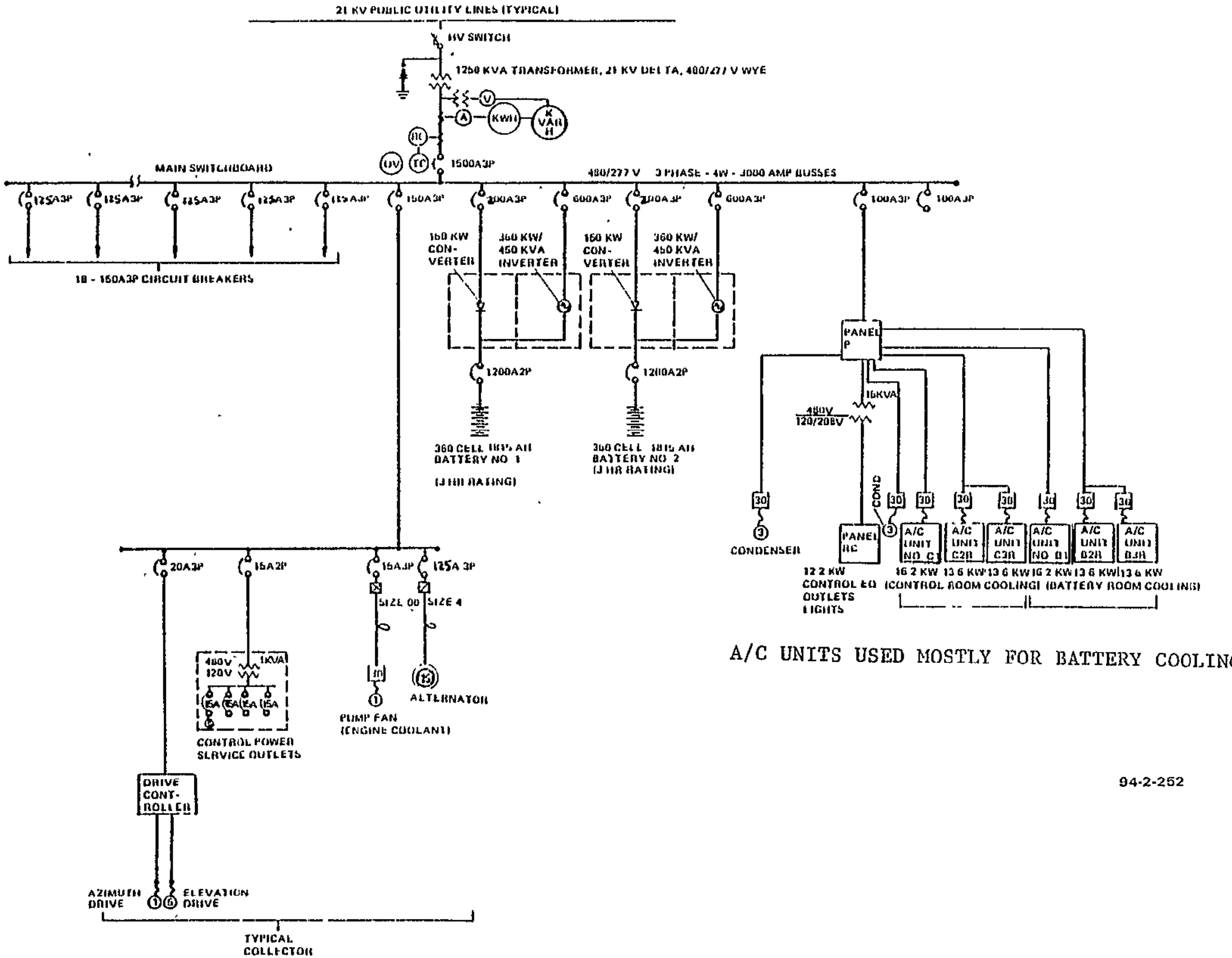


FIGURE 15. ONE-LINE DIAGRAM FOR SPS ELECTRICAL SYSTEM INCLUDING BATTERY STORAGE

it is stepped-up by the 1,250 kVA transformer for delivery to the utility grid or part may be conveyed to the power converters for storage. Power flow through the converters to the storage batteries and from the storage batteries through the inverters to the main switchboard would again be under control of the MPC in accordance with a pre-programmed or adaptive schedule. Power is also returned from the switchboard to any off-line collector (over the same radial feeder used to convey its on-line output to the switchboard) to operate the collector auxiliaries, such as the azimuth and elevation drives. Power required to operate the control building air conditioners is derived from Panelboard "P", a 480V 3Ø distribution panel fed from a branch circuit of the main power distribution switchboard. Power required to operate the MPC, CCIA and control building lighting system is derived from Panelboard "RC", which is fed from Panelboard "P" through a 480-120/208 volt step-down transformer.

The main power switchboard includes an electrically operated main circuit breaker, which can be controlled from the MPC to connect or disconnect the main switchboard to the utility grid. Protective features of the breaker operate independently of the MPC and thus will provide a second level of station protection against failures. The switchboard also includes standard switchboard instruments (described below) for display of bus voltage, frequency, line current, kilowatts, and kilovars.

Details of the electrical hardware and its predicted performance are discussed in the following paragraphs. (Note that all the equipment for the electrical system is off-the-shelf, and typical make/model numbers of applicable hardware is given in the body of the report.)

### 3.1.1 GENERATOR (ALTERNATOR)

The generator will be 75 kW/93.5 kVA, 480 volt, 3-phase, 60 hertz, 1800 rpm, single ball bearing, drip-proof, brushless, AC power unit connected directly to the Stirling engine shaft. It will have Class F insulation, suitable for a 50 degree C rise above ambient and be fan cooled. The generated voltage will have a maximum imbalance between phases of 1 percent, a maximum waveform deviation from pure sinewave of 5 percent, and a maximum harmonic content of 5 percent.

The alternator voltage will be regulated by an SCR-type electronic voltage regulator which can hold machine output voltage to the 480 volts ±0.5 percent at any load between 0 percent and 100 percent. The regulator will be able to absorb any transient caused by a 50 percent load change and restore normal line voltage within 0.1 second (6 Hz). The voltage regulator will be in an all-weather enclosure mounted on the alternator.

### 3.1.2 TRANSPORT/DISTRIBUTION SUBSYSTEM CABLING AND EQUIPMENT

Weather-proof, flexible, insulated power cables will be used from the generator across the rotational axes of the concentrator and to the ground. The cable will have three conductors consisting of No. 2/0 extra flexible, stranded copper wires, insulated to withstand usage at 600 volts AC, and jacketed with sunlight resistant, waterproof, neoprene.

A weather-proof control box containing all of the electrical apparatus for the collector will be located near ground level. This NEMA-12 enclosure will house all of the electrical apparatus which consists of:

(1) Alternator Power Contactor. This power contactor will be a 3-pole, NEMA size 4, 480 volt, magnetic contactor with a 120 volt AC magnet coil, a red pilot light, and a three position (HAND-OFF-AUTO) control selector switch.

(2) Alternator Circuit Breaker. This circuit breaker will be a molded plastic case, 3-pole, 125 ampere, thermal-magnetic trip, 480 volt and manually operated.

(3) Pump/Fan Motor Starter (for engine coolant). The pump/fan motor starter will be a standard NEMA size 0 starter rated at 480 volts, 15 amperes, having a 120 volt AC magnet coil, three thermal overload relays, a red pilot light, and a three position (HAND-OFF-AUTO) control selector switch.

(4) Pump/Fan Motor Circuit Breaker Disconnect. The pump/fan circuit breaker disconnect will be a molded plastic case, 3-pole 480 volt, 15 ampere, thermal-magnetic trip, and manually operated.

(5) Circuit Breaker for Transformer. The circuit breaker serving the transformer will be a 2-pole, 480 volt, 15 ampere, thermal-magnetic trip, and manually operated.

(6) 1 kVA Transformer (for power supply to operate concentrator). This transformer will be a 1 kVA, single phase, 480 to 120 volt, 60 hertz, transformer with class F or H insulation.

(7) Circuit Breaker Panelboard. The output of the concentrator transformer will be the power input to a small circuit breaker panelboard supplying control power to the electronics, the starter and contactor, and the general purpose maintenance outlet. The Panelboard will be a conventional 120 volt, 70 amp bus panelboard fed with two 15 ampere and 2 20 ampere plug-in circuit breakers. The panelboard will have a ground bar and a neutral bar and a cover door for the branch breakers.

(8) Circuit Breaker for Concentrator Drives. This circuit breaker will be a 3-pole, 480 volt, 20 ampere thermal-magnetic trip, and manually operated.

(9) Utility Outlets. The receptacle for the maintenance workmen will be a standard duplex convenience outlet, rated at 20 amperes, 120 volts.

Power wires and signal wires are routed from the NEMA-12 box to the central control building. These wires will be buried underground without ducts. The power wires will be single-conductor stranded aluminum, No. 4/0 and No. 250 MCM sized, with 480 volt RHW-USE 600 volt insulation suitable for direct burial in the earth.

In the control building, all of the power cables will terminate at circuit breakers in the main switchboard. The main switchboard will be a metal enclosed, free standing Underwriter Laboratories (UL) approved, 480 volt, 3-phase (40 wire), 3000 ampere bussed, indoor type. Figure 12 shows a recommended configuration for this switchboard. It will have tin-plated aluminum busses, a neutral bus, a ground bus, main circuit breaker, branch breakers and instruments. The generator branch circuit breakers will be 125 ampere, 3-pole, 480 volt, manually operated, having an interrupting capacity of 20,000 amperes symmetrical. The main 480 V circuit breaker will be a 1500 ampere, 2-pole, and air insulated. It will be electrically operated (120 volt AC) spring powered drawout type, with adjustable long-term current, short-term current and time delay trip circuits, a manual operating handle and trip indicators. Interrupting capacity will be 25,000 amperes at 480 volts, symmetrical. The board will also have nineteen 125 amps, 3-pole; two 200 amp, 3-pole; two 600 amp, 3-pole; and two 100 amp, 3-pole circuit breakers.

The instruments mounted on the switchboard will be standard 4-1/2 inch square switchboard-type meters, showing the bus operating voltage, the output current, the output frequency, the kilowatts and the kilovars. There will also be two recording meters, one for kilowatt-hours and the other for kilovar-hours. The recording meter charts will travel at one inch per hour.

From the switchboard, the station's 480 volt power will go to a utility line voltage-matching transformer. The 1500 amperes capacity of the switchboard will require six paralleled No. 500 MCM stranded aluminum wires, with 600 volt polyethylene USE type insulation along with USE neoprene jacket for burial protection. The transformer will be a metal enclosed, weather-proof, pad-mounted unit. The transformer will be a 1250 kVA/100 kW, 60 hertz, 3-phase, silicone liquid filled, air-cooled assembly. Primary voltage will be 480 volts, secondary voltage will be 21,000 volts, maximum impedance 5 percent and overall efficiency 98 percent. The unit will have a liquid level indicator, a temperature indicator, a drain valve, a filling neck and cap, an expansion reservoir and an electric overtemperature alarm device. The high voltage side of the transformer will contain a 40 amp fused, 35,000 volt, air-insulated mechanically operated switch and three lightning arrestors.

From the transformer, power will be routed in a 3-conductor, No. 4 stranded copper, shielded, 35 kV class butyl-rubber insulated cable with jacketing suitable for direct burial. The cable will terminate in a 3-conductor, 35 kV class, cast metal "pothead", suitable for pole mounting. The pothead will be constructed to receive 3/c-No. 4 copper wires, shielded, and jacketed with an O-ring sealed cable connector. The pothead will be filled with a void-free plastic insulating compound. A 200 ampere, non-fused, 35 kV, manually-operated, pole-top switch will be mounted between the cable pothead and the utility lines.

### 3.1.3 STORAGE EQUIPMENT

Power that is diverted to battery storage is first converted to DC using silicon controlled rectifiers (SCRs). The rectifiers will be computer controlled to accept power from the switchboard only during daylight, generating hours. The converter will have current limiting on charging to prevent overload on initial charging of run-down batteries, then current limiting at the float voltage level of 405 volts DC.

Power from the converters is stored in conventional lead acid batteries. The batteries will have lead-antimony plates, immersed in sulfuric acid and water electrolyte contained in polycarbonate cases. The battery cells will have a nominal 2 volts DC output at their terminals. Their amp-hour rating will be approximately 1800 ampere hours (3-hour rating). The cells will be connected in series to give a nominal terminal voltage of 360 volts DC (405 volts at float voltage, and 333 volts at end of discharge). Strings of battery cells with a 360 volt terminal voltage will be connected in parallel so as to provide approximately 2100 kWh delivered to the grid (for 0.4 ACF). Therefore, the storage capacity of the batteries must be 10 to 20 percent greater to account for the losses in the system.

The batteries will be mounted in two-high, earthquake-resistant racks, built of acid-resisting coated metal members. Figure 16 provides a major manufacturer's data on cells of the type applicable to SPS. A typical battery installation is shown in Paragraph 3.1.6 of the report.

By the time a battery cell has been charged and discharged 2000 times, the plate erosion is such that only 80 percent of the original plate materials remain and the plates are reduced to 80 percent of their capacity. At this capacity, the cells are considered to be unserviceable and should be replaced.

Present day inverters can accept a maximum of 405 volts DC. Therefore an inverter battery needs 180 cells (at 2.25 volts) connected in series to supply this voltage. The battery configuration for one inverter is two battery units (180 cells each) connected in parallel to furnish power to one inverter. DC power from the batteries goes to the inverters on three parallel-sets of No. 500 MCM wire (a total of six conductors). The wires are stranded copper with 600 volt class black THW polyvinyl-chloride insulation. The power enters the inverters through a 2-pole, 1200 ampere, manually operated circuit breaker.

The SCR inverters take 405 volt DC power from the batteries and convert it to 480 volt, 3-phase, 60 hertz power. (Figure 17 shows a typical converter and inverter assembled into an uninterruptible power supply configuration.) The voltage will be regulated to within 0.5 percent of 480 volts, and the sinewave output will contain no more than five percent harmonics. The imbalance between output lines and the phase-to-phase voltage will not vary more than one percent. In case of transient loads, the circuitry will restore the voltage to within one percent in less than 1 second. Output frequency will be determined by an internal clock oscillator which is phase-locked to the utility grid. If the AC line voltage disappears, the inverter will switch to its internal 60 hertz oscillator. The inverter will be fully protected from faults.

The computer will turn the inverter on after the alternators have been shut down either at the end of the day or temporarily during cloud cover. The computer will send AC power to the collectors to position them for morning start-up independent of an outside utility line.

**C&D**

# STATIONARY BATTERIES

**FOR COMMUNICATIONS**

# 2525 to 3500 Amp. Hrs.
# MT - Lead Antimony
# MCT - Lead Calcium

NEMA

## TYPICAL SPECIFICATIONS

| | | | |
|---|---|---|---|
| CAPACITY | 2525 to 3500 Amp. Hrs. at 8 Hr. Rate to 1.75 F.V. | | |
| PLATES | Height | Width | Thickness |
| Positive . . . . . . . . . . . . | 18" (457 mm) | 13" (330 mm) | .270" (6.9 mm) |
| Negative . . . . . . . . . . . . | 18" (457 mm) | 13" (330 mm) | .210" (5.3 mm) |
| SPECIFIC GRAVITY . . . . . . | 1.210 @ 77°F (25°C) | | |
| CONTAINERS . . . . . . . . . . . | Hi Impact Plastic | | |
| CELL COVERS . . . . . . . . | Hi-Impact Rubber | | |
| SEPARATORS . . . . . . . . . . . | Microporous | | |
| RETAINERS . . . . . . . . . . . | Fibrous glass mats | | |
| ELECTROLYTE WITHDRAWAL TUBES . . | Two per cell | | |
| SEDIMENT SPACE . . . . . . . . . | 0.75" (19 mm) | | |
| ELECTROLYTE . . . . . . . . | Height above plate 3" (76 mm) | | |

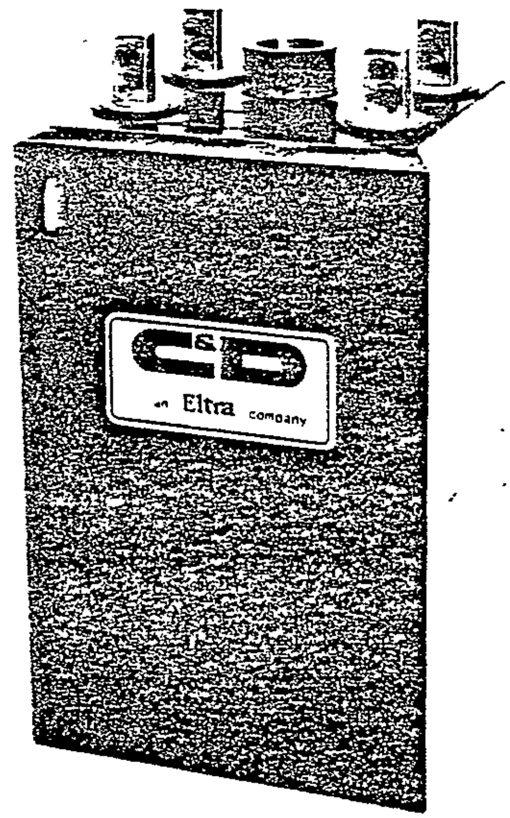


- **High-Impact Structural Foam Container with Cross-linked Polyethylene Liner** - Impact resistant double container system virtually eliminates breakage.
- **Built-In Level Indicator** - Makes it easy and convenient to check water level without removing vent.
- **Flame Arrestor** - Prevents accidental spark or flame from entering cell. Water can be added without removing vent.
- **Electrolyte Withdrawal Tubes** - Allows electrolyte to be removed from a level about one-third down from the top of the plates. Gives an accurate reading of specific gravity.
- **Hard Rubber Cover** - Virtually eliminates cover leakage.



| Type of Cell: Calcium | Type of Cell: Antimony | Plates per Cell | Nominal Capacities 1.75 VPC @ 77°F (25°C) (Includes Connector Voltage Drop) Ampere Hours: 8 Hr. | 5 Hr. | 3 Hr. | 1 Hr. | Overall Dimensions: L | W | H | Approx. Wt. (lbs.) (kgs.) Net Filled | Dom. Packed | Elect. per Cell (lbs.) (kgs.) |
|---|---|---|---|---|---|---|---|---|---|---|---|---|
| MCT-2525 | MT-2525 | 27 | 2525 | 2170 | 1815 | 1010 | 17.25 in. | 17.00 in. | 28.03 in. | 538<br>244 | 560<br>254 | 189<br>86 |
| MCT-2720 | MT-2720 | 29 | 2720 | 2345 | 1955 | 1085 | | | | 553<br>251 | 585<br>265 | 184<br>83 |
| MCT-2910 | MT-2910 | 31 | 2910 | 2500 | 2095 | 1165 | | | | 578<br>262 | 610<br>277 | 180<br>82 |
| MCT-3105 | MT-3105 | 33 | 3105 | 2680 | 2235 | 1240 | 438 mm | 432 mm | 712 mm | 604<br>274 | 635<br>288 | 175<br>79 |
| MCT-3300 | MT-3300 | 35 | 3300 | 2835 | 2375 | 1320 | | | | 629<br>285 | 660<br>299 | 170<br>77 |
| MCT-3500 | MT-3500 | 37 | 3500 | 3025 | 2520 | 1400 | | | | 654<br>297 | 685<br>311 | 166<br>75 |

FIGURE 16. TYPICAL BATTERY CELL SPECIFICATION

NOTE: Electrolyte weighs approximately 10 lbs. per gallon (1.20 kgs. per liter.)

94-2-253

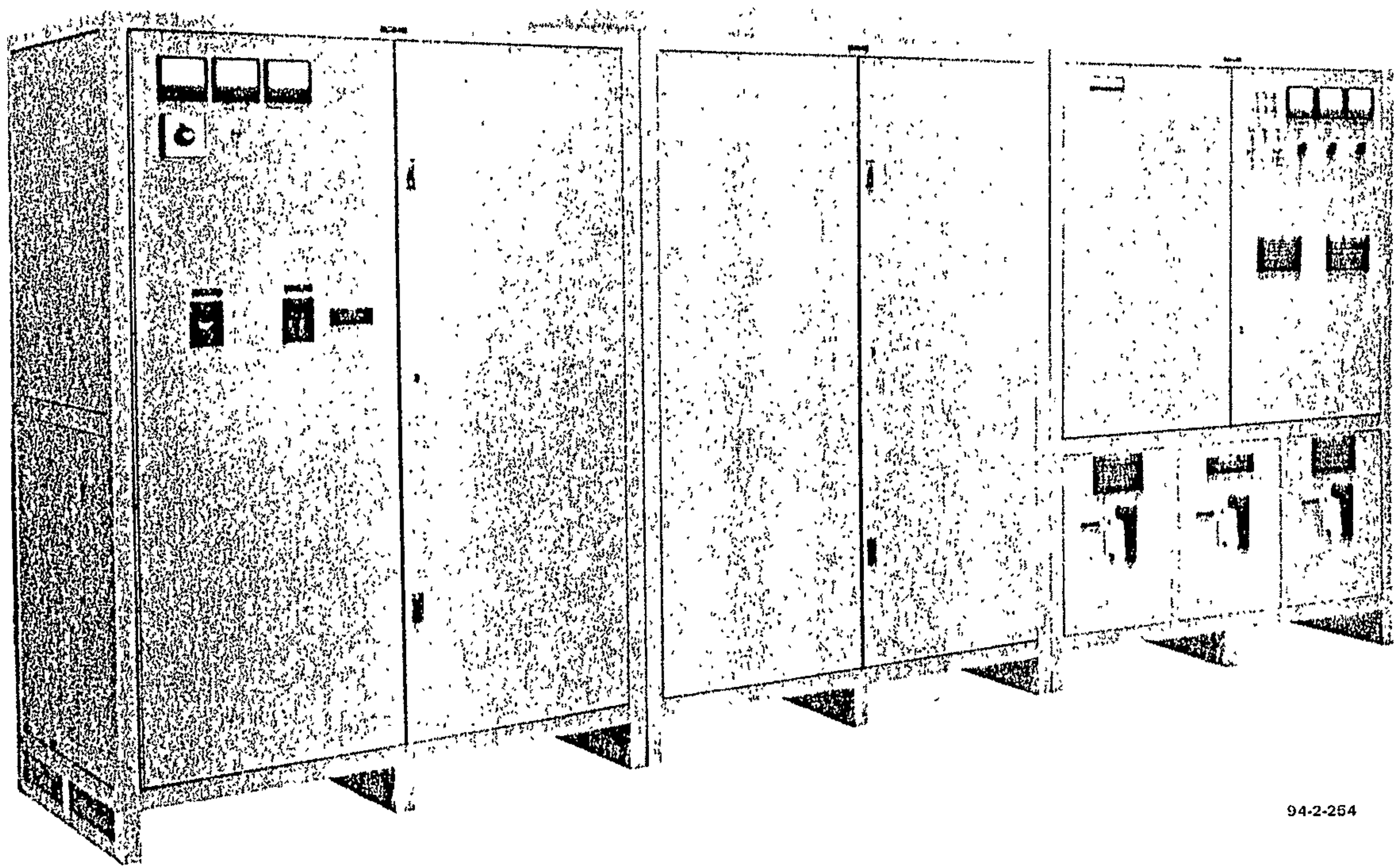


FIGURE 17. INTERNATIONAL POWER MACHINES 330 KW CONVERTER AND INVERTER ASSEMBLED IN UPS CONFIGURATION

3.1.4 CONTROL SUBSYSTEM

Figure 18 is a block diagram of the basic elements of the control subsystem and the interfaces. Operations performed by the control system are documented in Paragraphs 3.1.1.5 and 3.1.7 of the Report and Paragraph 2.3.5 of this appendix. Additional details of the hardware are described below.

3.1.4.1 Master Power Controller. The master power controller (MPC) consists of a Cromeco CS-3 microcomputer (microprocessor), a SOROC Technology IQ-120 CRT terminal and a Texas Instruments Model 810 line printer.

The CS-3 is a professional grade, 8-bit, Z-80A based machine operating in a S-100 bus configuration at a 4 megahertz clock rate. It uses a main frame power supply and 18 circuit boards. The CS-3 will be equipped with two 8 inch floppy disk drives and a PROM programmer (1st experimental station only). The architecture and interfaces with the CS-3 is described in Paragraph 3.1.4.5 below.

The SOROC IQ-120 CRT terminal incorporates a 12 inch CRT, formatted to display twenty-four 80 character lines of data, a standard alpha-numeric keyboard and a separate numeric key pad. It will be interfaced to the microprocessor over a standard EIA RS-232 serial data link operating in a full duplex mode. The CRT terminal provides the means for a maintenance technician to "call up" real-time or historical station performance data for observation and/or analysis. It also provides the means for performing selected diagnostics on the electrical control subsystem, should that be necessary.

The Texas Instruments Model 810 line printer provides the means for obtaining a "hard copy" of station performance or maintenance data. It is a bi-directional 9 x 7 wire matrix character impact printer and operates at 150 cps (characters per second). It will also be interfaced with the microprocessor over the standard EIA RS-232 serial data link.

3.1.4.2 Central Control Interface Assembly. The central control interface assembly (CCIA) will provide the means for interfacing the microprocessor with the main switchboard, converters and inverters, and the instrumentation cables to the remote control interface assemblies (RCIA's) located at the concentrators. It will perform the following functions:

- Signal level conversions on local (control building equipment) signals
- Transient suppression and optical isolation on incoming remote (concentrator) signals
- Analogue multiplexing of measured parameters
- Analogue to digital conversion of multiplexed signals
- Digital to analogue conversion of outgoing control signals

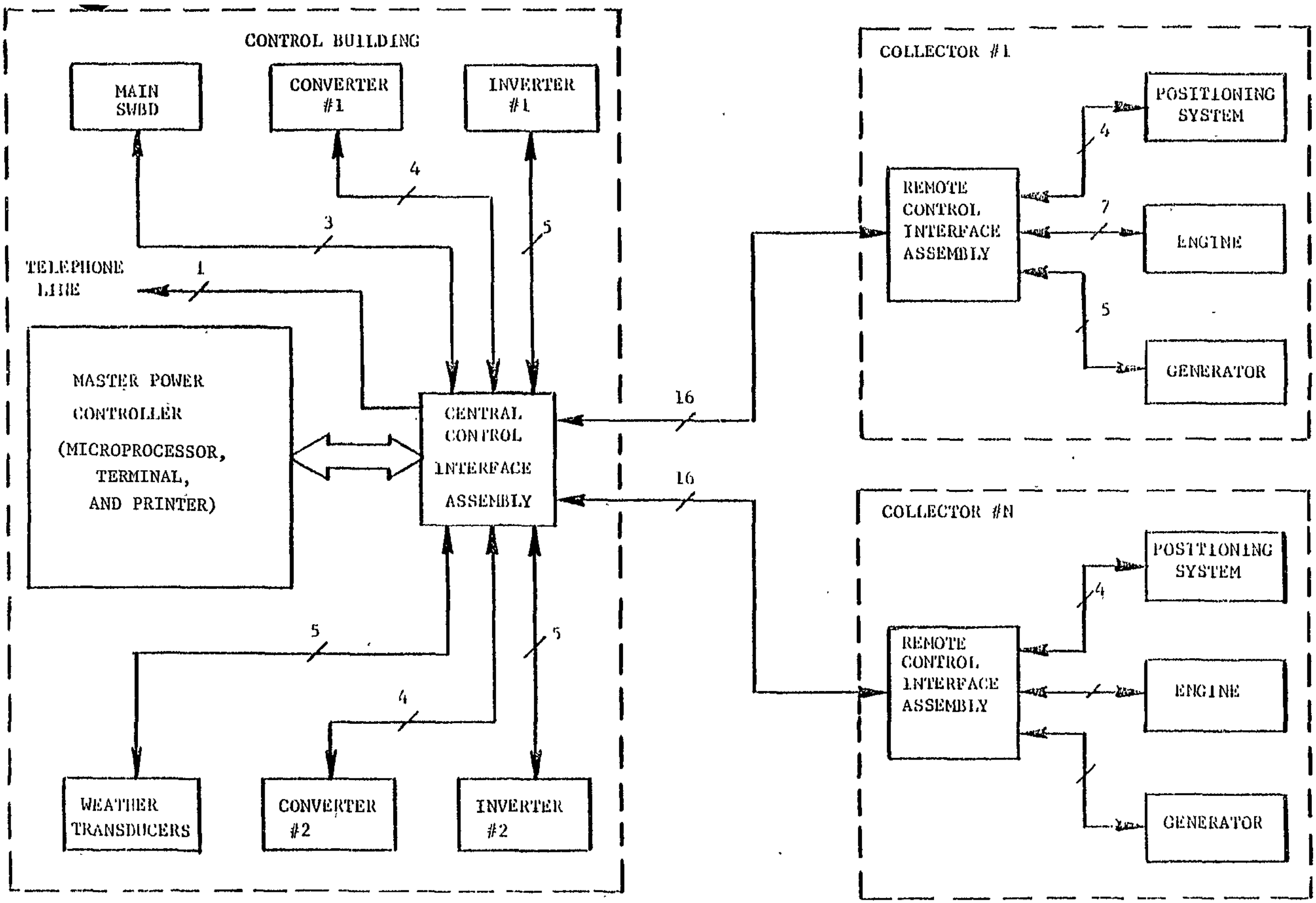


94-2-255

FIGURE 18. CONTROL SUBSYSTEM HARDWARE BLOCK DIAGRAM

- Line drivers for analogue signal outputs
- TTL to 20 ma current loop conversion of bi-state control signals
- Transient suppression and optical isolation of output signals
- Automatic telephone dialing for alarm conditions.

The CCIA will be housed in two cabinets, each will contain the necessary circuitry to interface the CS-3 with one converter, one inverter and up to ten collectors.

3.1.4.3 Remote Control Interface Assembly. A remote control interface assembly (RCIA) will be packaged in the NEMA-12 enclosure at the base of each concentrator. Its purpose is:

(1) To fan out the signals on the 18 pair cable coming from the control building into smaller cables to the engine, generator, and concentrator drive system.

(2) To provide signal level conversions as required to connect to the interfaced devices.

(3) To provide line driving capability for analogue transducer signals.

3.1.4.4 Control and Status Cables. All control and status cabling will be manufactured in pre-fabricated lengths with suitable connectors on each end. The long cables from the control building to the RCIA's will consist of 18 individually shielded pairs of No. 20 AWG stranded conductors (similar to Belden No. 9886) with a high density polyethylene jacket suitable for direct burial installation. The short cables from the RCIA to the engine, generator and concentrator drive system will also be prefabricated with weatherproof connectors on both ends. These cables will be of 6-pair construction (Belden 9886 or equal).

3.1.4.5 Microprocessor Architecture and Interfaces. The Cromenco CS-3 microprocessor is a structured bus-oriented system with 13 control lines, a 16-bit address bus and an 8-bit data bus as shown schematically on Figure 19. The 16-bit address bus makes it possible to directly address $2^{16}$ or 65,536 memory locations, 256 of which may be input-output (I/O) ports. The baseline SPS system will use 104 parallel and three serial ports. Memory in the experimental station configuration will be divided into 4K (4,096 8-bit bytes) of read only memory (ROM) and 60K of random access memory (RAM). The ROM will contain the bootstrap loader for the disk operating system (DOS) and monitor programs. The DOS, SPSE control program and the SPSE diagnostic routines will be on Floppy Disk No. 1. Floppy Disk No. 2 will be used to store station performance data for later inspection and analysis. When the system is started the bootstrap loader will down load the DOS from disk into RAM. The DOS will then execute an auto load of the control program into RAM. The real-time clock is initialized to calendar date and time and the control system will then be operational.

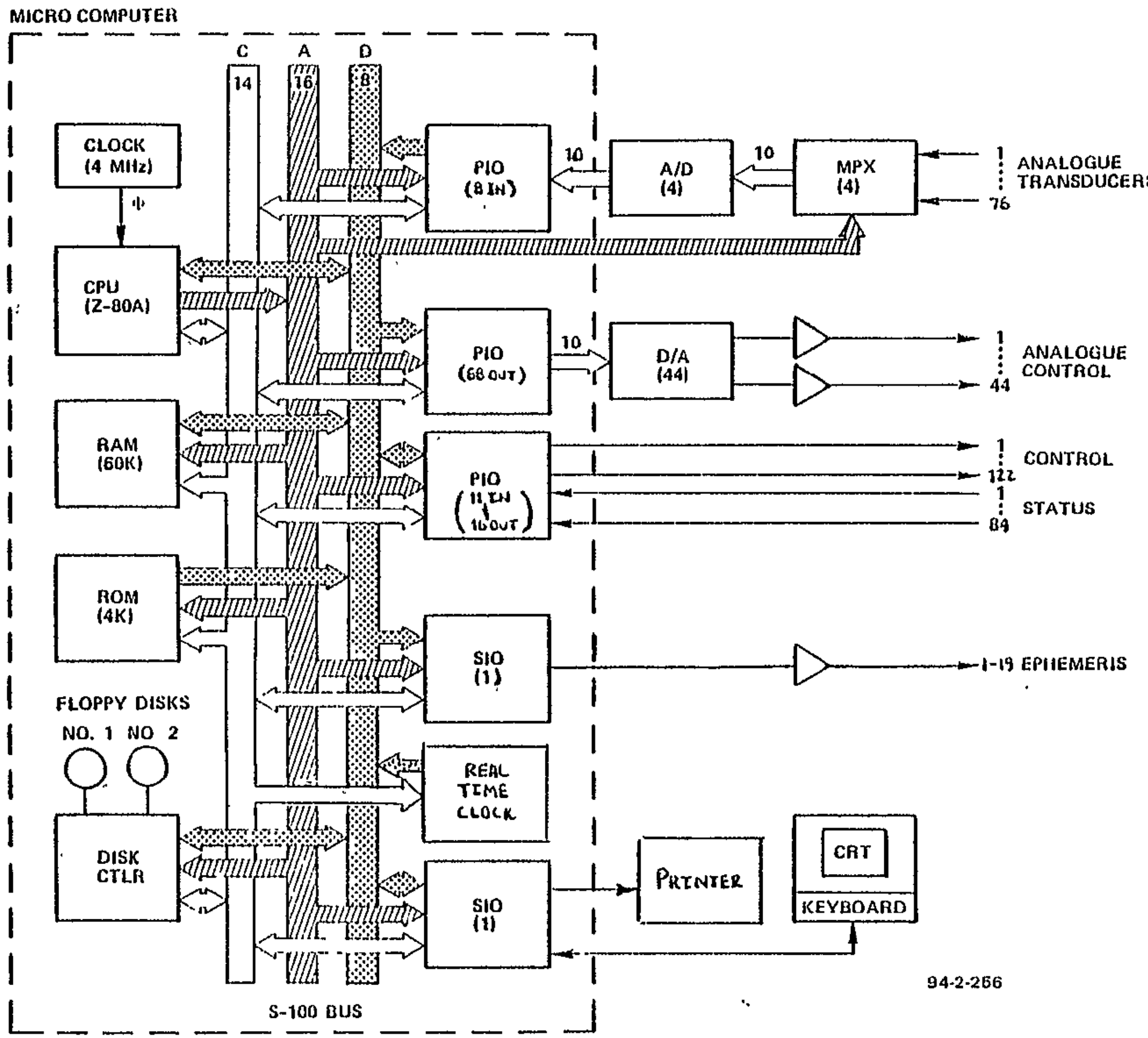


FIGURE 19. MICRO-COMPUTER (MICROPROCESSOR) ARCHITECTURE AND INTERFACES

Analog data received from the various transducers, voltage and current transformers will first be multiplexed, converted to 10-bit digital form and introduced into two 8-bit parallel input ports (PIO's). The ports will then be read sequentially into the accumulator ("A" register of CPU) and thence into memory to await processing in accordance with the various control algorithms. Computed 10-bit values for analogue control signals will then be sent sequentially to two adjacent output ports and latched until such time as updated information is received. The latched data will be converted from digital to analogue form and transmitted to the controlled devices.

Bi-state status signals received by the computer will set or reset single bits of the 8-bit parallel input ports; eight signals may thus be accommodated by a single port. Similarly, bi-state control signals generated by the computer will set or reset (and latch) single bits of the 8-bit output ports.

Ephemeris data will be sent to the collectors in asynchronous serial bit groups through a serial input-output (SIO) port. The CRT terminal and line printer will be interfaced with the computer in a similar manner.

Selected performance parameters may be routed to a section of RAM allocated as a buffer for data logging at required intervals. When the buffer is full, the data will be automatically off-loaded onto Floppy Disk No. 2 for permanent storage. The data may then be called up for display on the CRT terminal or printed out on the line printer, as requested by an operator on the CRT terminal keyboard. The floppy disk may be stored on site for future reference or transported to a remote location for more detailed analysis.

After software development has been completed and fully validated the DOS, control programs and diagnostic routines will be down loaded from disk into eraseable programmable ROM chips (EPROM's) or "burned" into ROM's for use at the future operational stations. This will change the allocation of memory space to 32K of EPROM (or ROM) and 32K of RAM and will allow the operational stations to run with only a single disk if desired.

3.1.4.6 Engine/Alternator Synchronization. The synchronization of all the power modules with the utility grid is one of the more complex tasks that the control system performs. The basis of the selected control technique is described in Paragraph 3.1.1.5 of the report; tasks performed by the computer are described here. When each engine reaches the predetermined conditions (head temperature ~600°C, 1800 rpm), it will return an engine ready "flag" to the microprocessor, and the flags will be stored in a queue. Synchronization of each engine/alternator with the station power bus (which was previously connected to the utility grid) will then be initiated in the order that they reported their readiness. The microprocessor will first compare the alternator output voltage to the bus voltage and (if necessary) send an offset signal to the voltage regulator to achieve a match. Next, the half periods of the bus and alternator voltage waveforms will be compared and a speed control signal will be sent to the engine's electronic control unit to achieve a match, which indicates that the alternator output frequency is equal to the bus frequency. Finally, time displacement between the positive-to-negative zero crossings of the bus and alternator voltage waveforms is measured and a small speed adjustment signal is sent to the engine's electronic control unit to minimize this displacement. With an effective A/D conversion throughput rate of 53 kHz, digitized samples of the two waveforms will be available approximately every 38 microseconds which should allow time displacement measurements between the two waveforms of less than one electrical degree. When time displacement has been reduced to an acceptable pre-set valve a control signal will be sent to the alternator's output contactor, directing it to close and connect the alternator to the station main power bus. The remaining engine/alternators will be synchronized and connected to the main power bus in rapid order. Two new control loops will now become active for each engine/alternator when nominal operating conditions are reached ($\sim 800^{\circ}C$ engine head temperature). They are: (1) the power control loop which senses Stirling engine head temperature and adjusts the power control valve (i.e., engine torque) to maintain constant engine head temperature, and (2) the reactive current control loop which adjusts alternator field excitation to maintain the power factor of each alternator equal to the power factor of the utility grid. The most important control consideration is that the "time constant" of each engine/alternator's control loop not exceed 1/2 the "time constant" of the utility grid or any of the controlled devices. This implies that each of the 38 engine/alternator control loops plus six storage subsystem control loops must be serviced at least every 11,364 micro-seconds. This requires that optimized assembly language coding of the control program be used to provide reasonable system stability.

### 3.1.5 LIGHTNING PROTECTION

Lightning protection has been designed to satisfy the safety requirements of the Lightning Protection Code (NFPA No. 78) and the SPS environmental performance requirements.

3.1.5.1 Concentrator Lightning Protection. Concentrators will be equipped with standard 18-inch air terminals at the top of the reflector and at the forward end of the power module so that protection will be provided regardless of collector operating attitude. Flexible copper flat cable (e.g. Thompson Lightning Proteciton Company No. 32F), will be used to bridge the two elevation bearings. Two flexible copper round cables (Thompson No. 32S or equal) will pass through the center of the azimuth turntable to connect the upper turret to two of the three lower support legs. The bottom end of the two lower support legs will be jumped with round copper cable to two 5/8" x 10' long copperweld ground rods. The ground rods will be connected to each other by a buried No. 2/0 AWG ring counterpoise, which circles the collector foundation piles. These methods have been used on a large number of microwave communications antennas and have proven to provide effective protection.

3.1.5.2 Power Transport/Distribution Subsystem Lightning Protection. Power cables from the collectors to the main switchboard in the control building will be buried and hence not subject to direct lightning strikes. All power system components in the control building will be connected to the station ground system, which will consist of ground rods and/or a counterpoise ring as appropriate to the soil conditions (resistivity) at the selected site locations. The pad-mounted transformer will be protected by standard surge arrestors.

3.1.5.3 Control Subsystem. Control cables from the collectors will be buried and thus not subject to direct lightning strikes. The cables will consist of 100 percent foil shielded-pairs which will maximize protection against induced lightning strike currents. All control cable conductors entering the control building will be protected with fast acting ($<1 \times 10^{-12}$ second) transient voltage suppressors and optical isolators to provide a final measure of protection to the master power controller and its associated signal conversion equipment.

## 3.2 ELECTRICAL SYSTEM INSTALLATION

The installation of the major components of the electrical system is discussed in this section.

### 3.2.1 ELECTRICAL CABLE INSTALLATION

The major installation task for the electrical subsystem is laying the cables between the concentrators and the control building. The centerline of the concentrators are typically spaced 28 meters apart in the N-S direction and 56 meters apart in the E-W direction. A computer program was developed to select cable sizes and field layouts to minimize cable and installation costs. Based on this, north-south columns of 7, 7, and 5 concentrators have been selected as optimum. Direct burial cable runs are recommended to minimize installation costs and to protect the cables.

A procedure recommended to be used in direct burial of the cables has been shown in Figure 20. Step ① of this Figure shows the trenching plan for the 7 X 7 X 5 field layout. Since the pedestal base support pads can be placed in any orientation without imposing any effect on the structural design, the trench is planned to be excavated directly in line with the concentrator centerlines allowing the exposed pigtails to be protected by the concentrator structure and to be within a few meters of any of the three legs. The layout of the foundation piles will be positioned to avoid the trench. As shown, the trench grid is basically three parallel N-S columns with a single connecting trench.

The trenching operation shown in Step ② is planned to be performed using a conventional "wheel scoop" type machine. An extension on the soil dumper permits the excavated material to be deposited far enough off to the side of the trench to allow for equipment to straddle the trench.

After the trench has been opened and before any cables are put in place, a sand truck with a special feeder for this application passes over the trench and deposits a layer of sand (~3 to 6" deep) throughout the length of the trenches (see Step ③ of Figure 20).

A vehicle with a rack for holding approximately 9 to 12 spools of cables with a special guide-and-feeder arrangement will be used for laying the cables. There is a variation in cable size depending upon the distance from the building. The cable vehicle will travel between the control building and each concentrator, laying the appropriate cable size (Step ④). Trench bridges will be

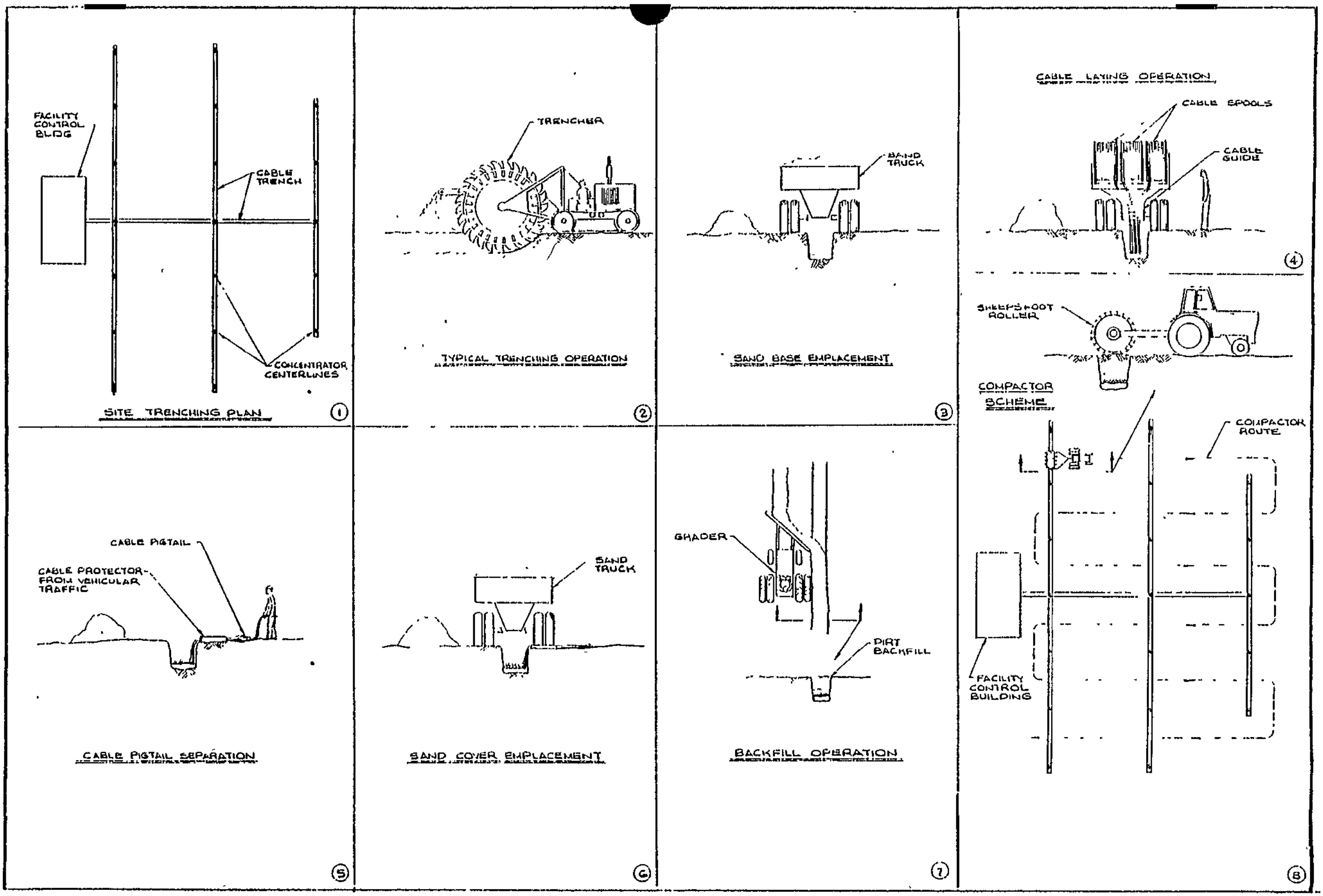


94-2-257

FIGURE 20. TYPICAL ELECTRICAL CABLE BURIAL SEQUENCE

used to allow the vehicles to cross the trenches, and cable guide fixtures will be used to make the 90 degree trench transitions.

After the cables have been cut to length for each concentrator, they will be pulled up from the trench at the concentrator centerline location and coiled to the side (Step ⑤). Vehicle bridges will be placed over the pigtails to protect them from damage. After all the cables have been laid, the sand truck will make another pass (Step ⑥), depositing another 3 to 6" layer of sand. This sand barrier will provide protection to the cables from vehicle traffic or from differential settlement. A grader will then be used to push the excavated material back into the trench as shown in Step ⑦.

Finally, it will be necessary to compact the excavated areas between concentrators which will have vehicle traffic (otherwise the natural settlement of the soil would produce ruts). This is accomplished using a tractor and sheeps-foot roller in the travel areas (Step ⑧).

### 3.2.2 INSTALLATION OF BATTERIES AND RACKS

The battery racks are framed members which require bolting together on site. The seismic 3 specification requires the racks be securely braced to the wall and/or to one another. Each battery weighs approximately 500 to 600 lbs so they must be handled individually with a small hydraulic lift.

### 3.2.3 INSTALLATION OF OTHER EQUIPMENT

Installation of the remaining equipment (invertors, converters, switchboard, etc.) is standard within the electrical industry and no special requirements are needed.

### 3.2.4 ELECTRICAL SUBSYSTEM CHECKOUT

All electrical installation work will be in accordance with the National Electrical Code. The ends of all cables will be provided with proper cable markers identifying the standard to-and-from designation, phase identification, and power, control or signal notation for quick reference during checkout. All cabling will be "cold" checked for continuity and all power cables will be checked for proper insulation characteristics using a "megger".

Once all the individual electrical system components have all been checked, the system will be ready to be brought on-line. A sequential step-by-step procedure will be used to gradually and safely bring each of the various subsystems on-line to verify performance. First the power into and out of the transformer will be checked followed by the power available at the main switchgear. After correct voltage, current, and phasing has been verified, breakers will be turned on one-by-one to provide power to the individual subsystem equipment. The system checkout and test procedure will be conducted using the master computer. Verification of all power, logic, control and statusing functions will be followed by a 100 hour burn-in period. This is a critical test since most premature failures of equipment occurs during this period.

## 3.3 ELECTRICAL RELIABILITY ANALYSIS

The predicted failure rate and MTBF (Mean Time Between Failures) of the electrical equipment per concentrator is 26 failures per million hours and 39,000 hours, respectively. The predicted failure rate and MTBF of the system microprocessor is 148 failures per million hours and 6760 hours, respectively.

The predictions and estimates were made in accordance with the procedures of MIL-STD-756A and MIL-HDBK-217B, Section 3. The parts count prediction using failure rates from Section 3 and ground environment were used. A listing of the equipments and their failure rates are shown in Table 21 and 22.

TABLE 21. MICROPROCESSOR RELIABILITY SUMMARY (EQUIPMENT PER 1 MWe STATION)

| Electrical Component | Failure/$10^6$ HRS ($\lambda$) | MTBF (hours) |
|---|---|---|
| Microprocessor PIO | 15.0 | 67,000 |
| Microprocessor CPU | 51.0 | 19,500 |
| Microprocessor 64K RAM | 52.0 | 19,200 |
| Microprocessor Power Supply | 30.0 | 33,330 |
| Total | 148.0 | 6756 |

TABLE 22. ELECTRICAL SUBSYSTEM RELIABILITY SUMMARY (EQUIPMENT PER CONCENTRATOR)

| Electrical Component | Failure/$10^6$ HRS ($\lambda$) | MTBF (hours) |
|---|---|---|
| Converter: | | |
| • A/D | 3.75 | 266,700 |
| • D/A | 3.75 | 266,700 |
| Alternator | 11.925 | 83,860 |
| Contactor | 2.0 | 500,000 |
| Voltage Regulator | 4.425 | 226,000 |
| Total | 25.85 | 38,700 |

## SECTION 4

## STAND-ALONE SYSTEM

In the SPS concept presented in this report, each collector delivers electrical power as a short term function of the solar insolation level available to it. Although some integration occurs as a consequence of the thermal mass of the receiver and heat transport systems, it is not possible to accommodate the wide variations in power load requirements implied by the stand-alone application without a significant amount of buffering, which cannot realistically be provided as part of the collectors themselves. Thus, external buffering or hybrid generation is clearly required.

Electrical system configuration "E", which was discussed previously, is a possible solution to the problem. This configuration is very similar to the recommended system configuration "D" except that it places the storage subsystem equipment in the direct power delivery chain and thereby isolates the collector power conversion subsystems from the short term load circuit demands. This system will be stable in operation and can have reasonable operating efficiency in the direct generation mode if collectors are brought on and off line as the integrated load schedule demands. However, it is not an effective alternative because of the cost of battery storage required. The most optimistic analysis of a daily load demand schedule for a small community would indicate that battery storage requirements (and cost) would be about 8 times that proposed for the basic SPS requirement even if no allowance is made for days with inclement weather.

It appears then that hybrid generation must be considered. Such a system can be mechanized by adding ten ground-mounted United Stirling P-150 engine-generator units to the power system configuration recommended for the basic application. These can be connected to the main station bus in the same manner that the solar collectors are connected and can be fueled with any available hydrocarbon material. In operation, the solar collectors would always provide the base generation capability and the P-150's would be used for daytime peaking, nighttime and inclement weather requirements. The storage subsystem, incorporated in the baseline station to meet the specified capacity factor requirements, would have no purpose in the hybrid station and thus could be eliminated at a very substantial cost saving. Preliminary estimates indicate that this savings would more than offset the cost of adding the hybrid generation capability. This approach therefore appears to be the optimum way to provide stand-alone power generation capability for the small community application.

# APPENDIX C

# DEVELOPMENT HISTORY OF USS STIRLING ENGINE

## PART I

## UNITED STIRLING ENGINE DEVELOPMENT - HISTORY SUMMARY

United Stirling of Sweden (USS) has 10 years of experience in advanced Stirling engine technology and development. During this period USS has developed an outstanding background of basic Stirling technology, component and engine development, and integration of Stirling engines into complete power systems.

### ENGINE DEVELOPMENT

Basic Stirling technology was obtained from N.V. Philips (Eindhoven, Netherlands) in 1968. Since then a number of engine configurations have been developed and evaluated at United Stirling.

Initial development at the company started with design of a 150 kW, four cylinder in-line concept, 4-615 (this designation refers to 4 cylinders, 615 cc displacement). Figure 1 shows an upscaled version of the Philips 4-235 single-acting rhombic drive engine. Four 4-615 engines were built and tested in the laboratory during 1971-1973. Total accumulated operational time was about 1,000 hours. Some disadvantages with this engine were high complexity, e.g., one preheater, heater and combustor per cylinder, low power-to-weight ratio, large size and high production costs.

The double-acting concept (Figures 2 and 3) with one piston in each cylinder seemed to offer considerable advantages in these respects. Arrangement of components allowed four cylinders to be energized from one combustor and the number of pistons to be reduced to half (Figure 4). Two drive mechanisms were considered - the swashplate and the V4-drive. Since the latter design utilized more conventional components and technique, it was chosen over the swashplate.

The first V4-engine (Figure 5) was successfully run in December 1971. During the next two years another two generations of this 35 kW engine were designed, built, and tested. In total seven engines of this power range were built and tested in the laboratory and in various installations. The accumulated number of operating hours was approximately 5,000 of which one engine represented 2,600 hours.

In 1972 the formal decision was made to base the 75 kW and 150 kW engine development programs on this configuration. The first 75 kW engine, representing the fourth generation V4 was successfully run in a test rig in 1974 (Figures 6A and 6B). Another three engines of this type were built and over 1,000 operating hours have so far been accumulated.

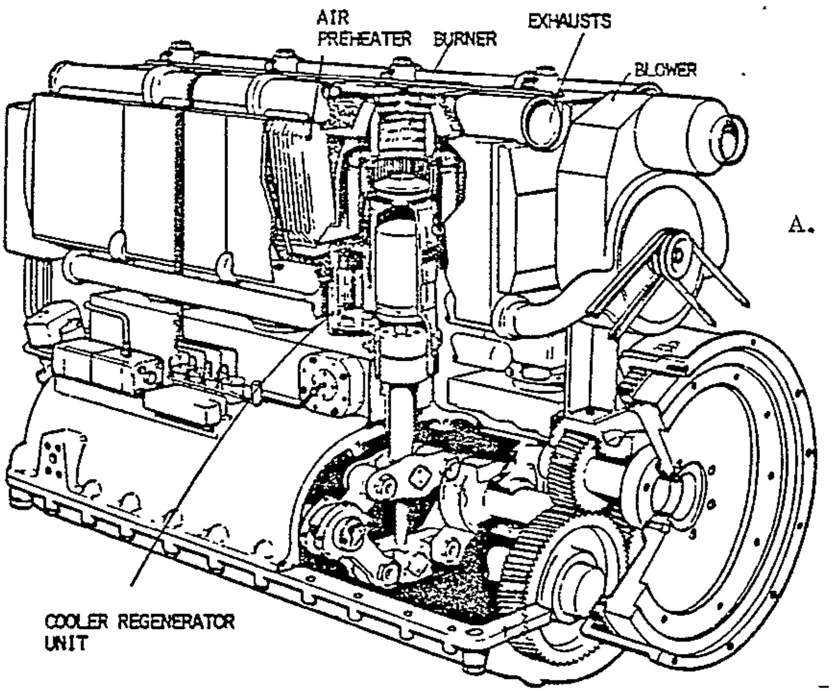


A. SKETCH ILLUSTRATING
MAJOR ENGINE COMPONENTS

94-2-259

B. 4-615 ENGINE
INSTALLATION
IN TEST CELL

94-2-260

FIGURE 1. UNITED STIRLING 4-615 DISPLACER TYPE ENGINE

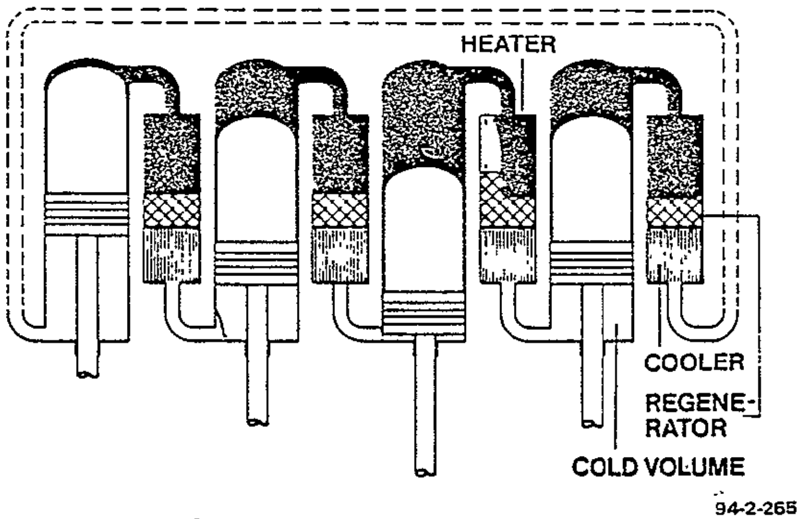


FIGURE 2. DOUBLE ACTING PISTON CONCEPT

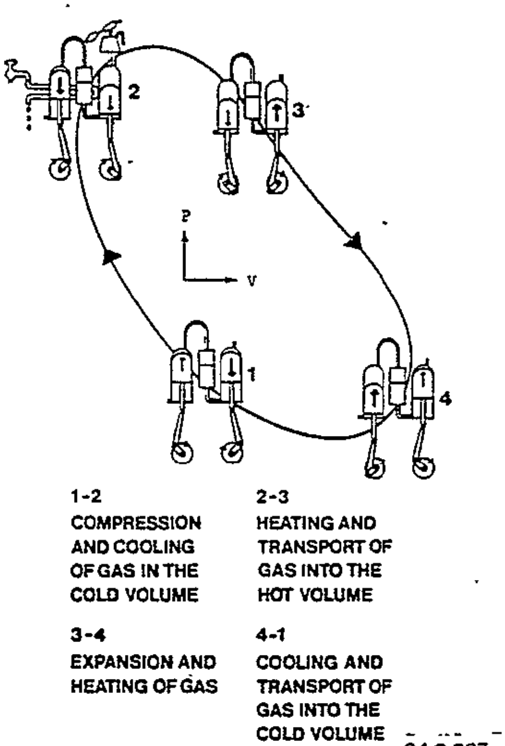


FIGURE 3. SCHEMATIC OF DOUBLE ACTING PISTON CONCEPT

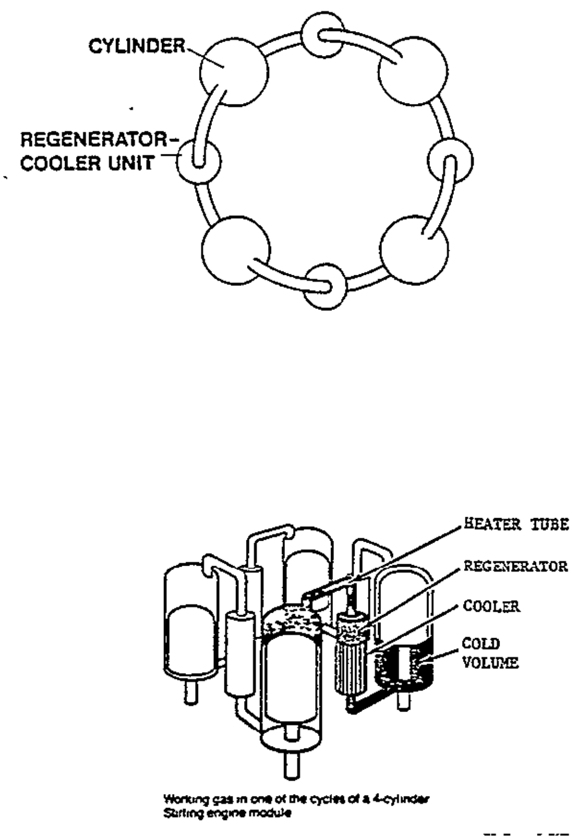


FIGURE 4. PISTON ARRANGEMENT OF DOUBLE ACTING CONCEPT

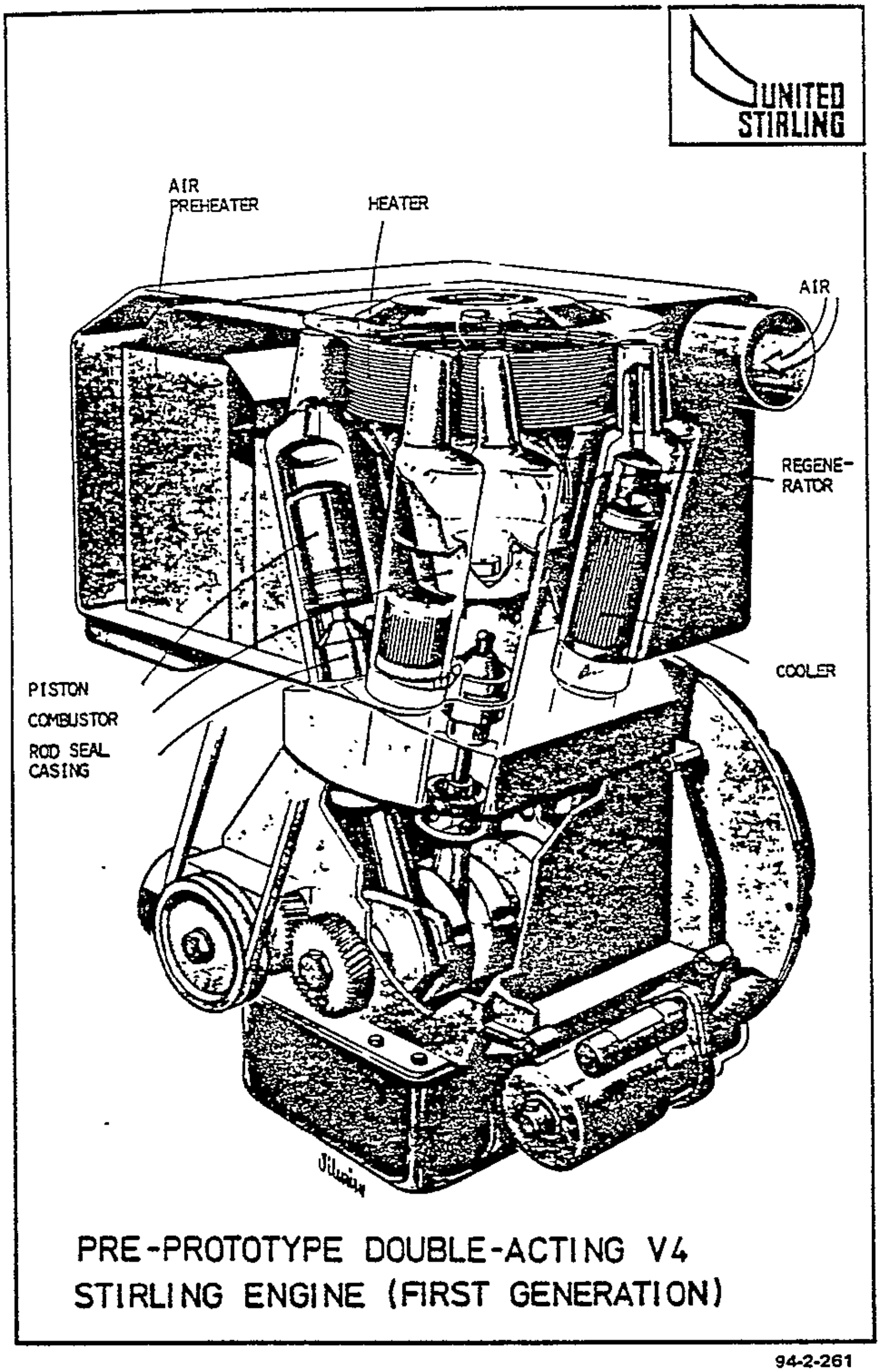


FIGURE 5. PRE-PROTOTYPE DOUBLE-ACTING V4 STIRLING ENGINE (FIRST GENERATION)

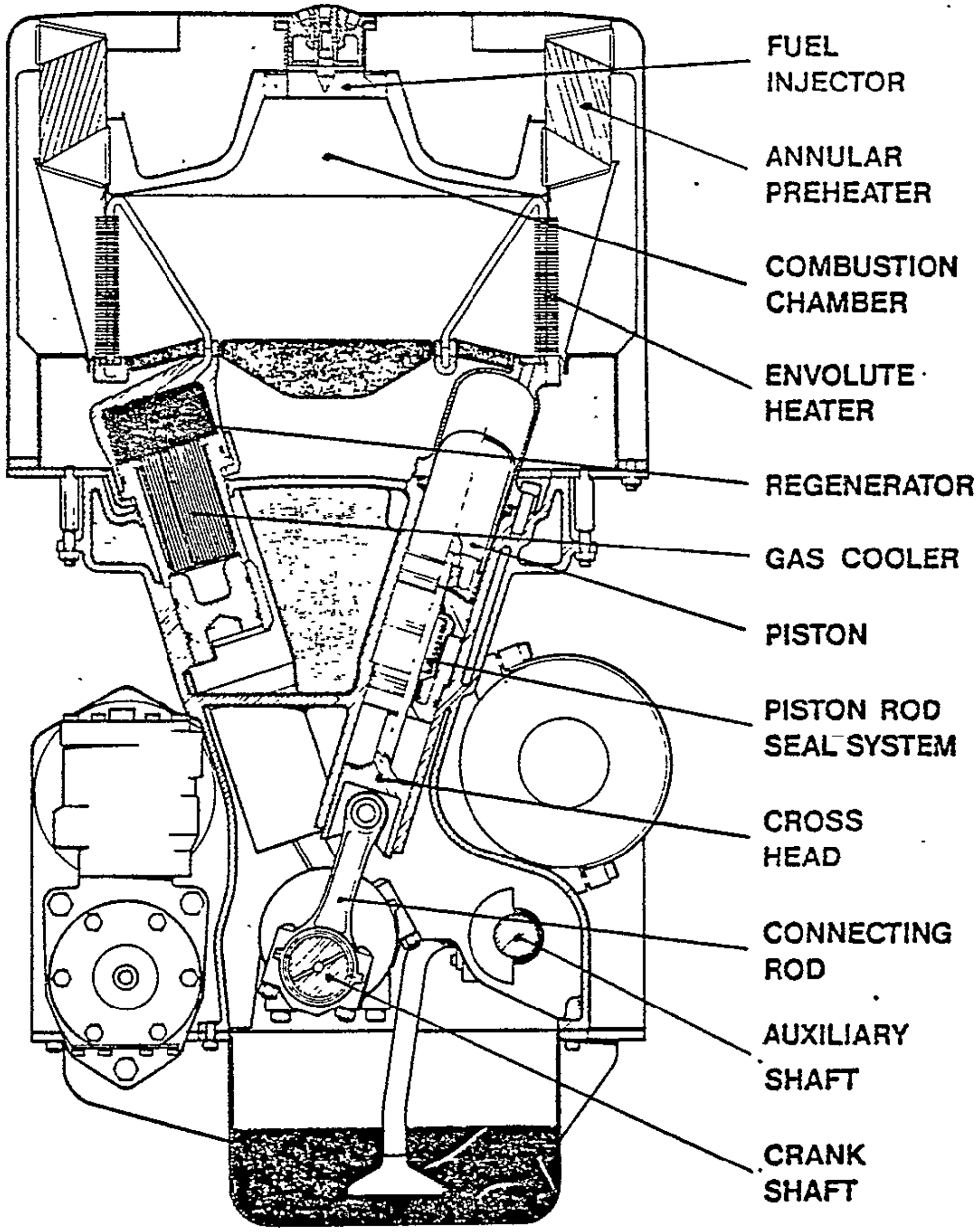


FIGURE 6B. SCHEMATIC OF P-75 DEMONSTRATING MAJOR COMPONENTS

United Stirling has recently designed and manufactured a new double-acting four-cylinder cluster configuration with dual crankshaft (U4) (Figure 7). This design is less complex than previous engines, which permits easier servicing during maintenance. The design has also been engineered for volume production. The first engine of this type, the P40 - a 40 kW experimental engine - was run successfully in test for the first time at the beginning of 1977 (Figures 8 and 9). Eleven P40 engines have been built and tested so far with ~3,000 hours of operation accumulated. Another six engines are under construction at this time.

This U4-configuration has served as a base for USS development of 75 - 150 kW engines for mass production during the eighties. Two V4-configured P-75 engines were built and tested during 1977-1978; a de-rated version of this engine has been installed in a truck with very good test results. Seventeen P-75 engines of U4 configuration are now under construction with one engine presently undergoing dynamometer testing; four engines will be available for such testing in 1979. The 150 kW engine, based on two 75 kW engines in line, will be built for testing in 1980; two P-150 engines are scheduled for this effort.

A summary description of the U4 concept is given in Part II of this appendix.

COMPONENT DEVELOPMENT

The design philosophy of United Stirling is to develop components in separate test rigs to a certain confidence level and to follow this by integration of the component into the engine for testing and evaluation.

During the development of the Stirling engine, a number of problems have been identified and characterized as classic Stirling problems:

- high temperature heat exchangers (preheater, heater head, regenerator)
- low temperature heat exchanger (water/gas cooler)
- control systems (power control, air/fuel control)

Some important progress has been made during recent years, some of which could even be characterized as break-throughs. A survey of present component development, with problems identified and solved, is given below. As evidence of USS confidence in the component state-of-the-art, present component development is mainly focused on improvement of reliability and life, rather than design or evaluation of technical solutions.

AIR PREHEATER*

In any Stirling engine application where low specific fuel consumption is of importance, the heating system must include a regenerative heat exchanger for

*Note that the air preheater and combuster are not used in the solar application, and the heater head is a simplified design. Also helium will be used as the working fluid rather than hydrogen.

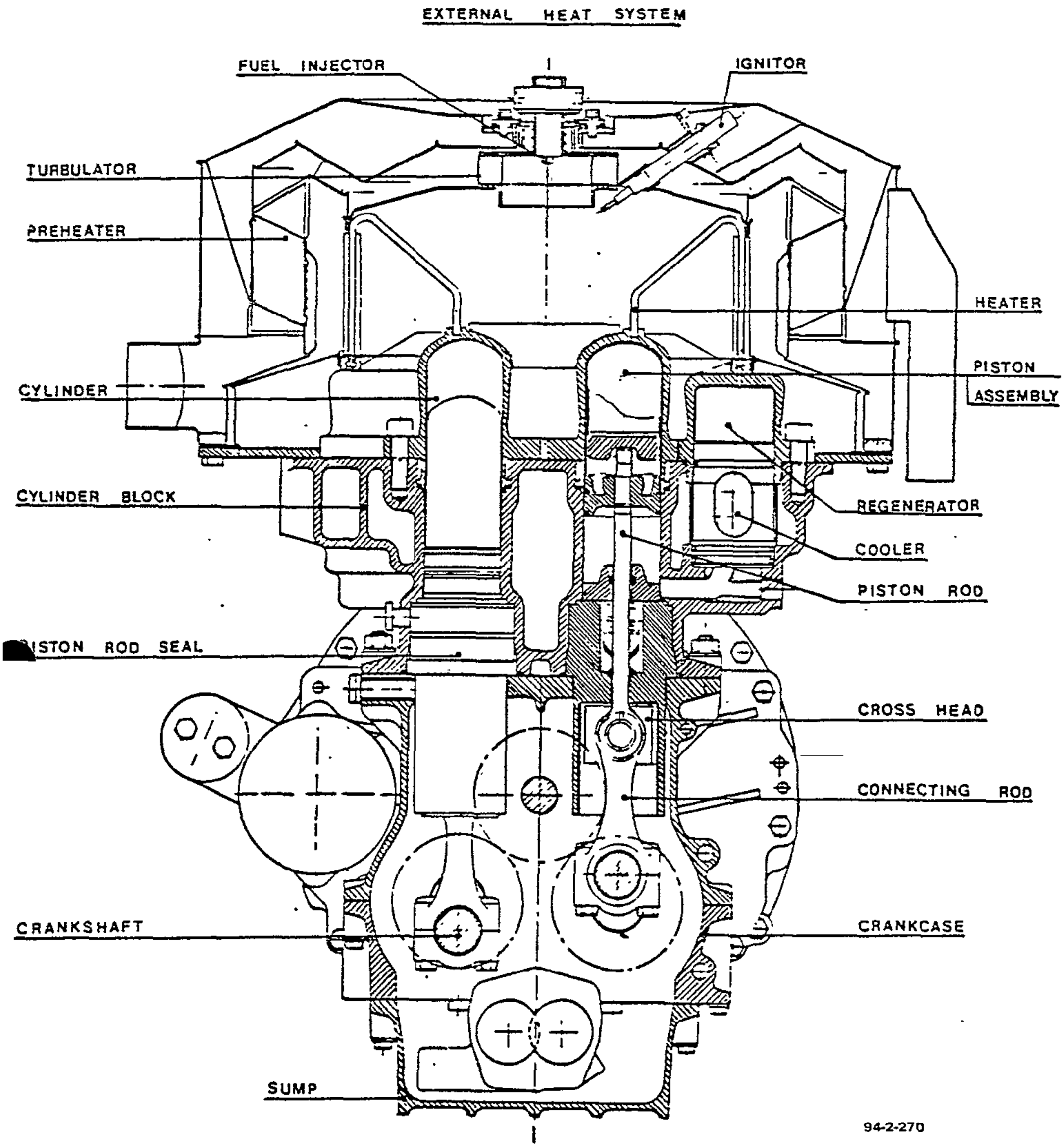


FIGURE 7. SCHEMATIC OF USS P-40 STIRLING ENGINE; U-CRANK CONFIGURATION

preheating the incoming air by extracting energy from the high temperature exhaust products leaving the heater. This heat exchange process is accomplished essentially at an atmospheric pressure which implies the need for large surface areas for heat transfer. The further requirement for high specific output imposes limits on the size and weight of the heat exchanger. Work is therefore in progress regarding tests of specially designed air preheaters involving recuperative as well as regenerative types.

An annular type of preheater (Figure 10) has been developed, using extremely thin foil technology. Characteristic features are uniform gas flow and low pressure drops, combined with compact design. Current engines employ this preheater which is now being tested for performance and endurance. Considerable increase in efficiency has been obtained, as well as reduced production costs. The number of operating hours accumulated in component and engine test rigs is about 7,500.

Tests are also being performed on the regenerative preheaters manufactured by Corning Glass Works, Corning, New York. A special seal system design is being tested for leakage, wear and mechanical integrity. The tests are run in special test rigs in which engine conditions are simulated under control conditions, as well as on engines in dynamometer test cells.

COMBUSTOR*

The combustion of distillate fuels in a Stirling engine is similar to that of regenerative gas turbines. Since the combustion air is preheated, precombustion temperatures are of the order of 500-700 degrees C. Although this high preheat temperature enables rapid fuel evaporation and combustion, it also greatly accelerates the rate of formation of oxides of nitrogen. Therefore other measures must be taken to limit $NO_x$ formation.

There are certain advantages to integrating the combustor inside the heater cage volume. This compact design approach, followed by United Stirling in most of their engine design, is illustrated by the current P40 engine combustor design shown in Figure 7. Combustion air, after passing through the preheater, is directed through an annular conduit surrounding the upper combustion chamber wall and enters the combustion chamber through a turbulator plate encircling the fuel nozzle. Fuel and air mix and burn in the central cumbustion chamber and the hot combustion gases then pass radially outward through the heater tube cage and then back through the preheater core to exhaust.

United Stirling selected a "one-stage lean-burn" concept for the combustors. This implies no intermediate zone between a rich primary and a leaner secondary zone. In order to get good stability the combustion air is introduced through the turbulator in a strong vortex pattern with internal recirculation. This flow pattern also yields nearly homogeneous combustion conditions by introducing fuel into the highly turbulent layer between the axial and recirculating flows in the upstream parts of the combustor. An air-assisted atomizer is used to assure good fuel atomization over the full operating

*Not used in solar applications.




PRECEDING PAGE BLANK NOT FILMED

range. This type of combustion system has been developed to provide relatively uniform combustion gas temperature and velocities over the heater tubes while maintaining good control response, stability, and low exhaust emissions. Exhaust gas recirculation has been employed to reduce $NO_x$ emissions. The number of hours accumulated in component and engine test rigs is about 7,500. Exhaust emissions from current engines utilizing this lean-burn concept are well below even the most stringent United States requirements for the eighties.

HIGH TEMPERATURE HEAT EXCHANGER ASSEMBLY (HEATER HEAD)*

The Stirling engine cycle inherently calls for high temperatures and high pressures of the working medium in order to yield high efficiency and high specific output. Accordingly, the heater head is one of the most critical Stirling engine components. Presently, the 4-cylinder double-acting Stirling engine designs incorporate a circular high temperature heat exchanger having two concentric rows of closely spaced tubes. Internal flow of working gas is sequential from one row to the next rather than in parallel. Generally the inner row, which is adjacent to the central combustion chamber are ordinary tubes, whereas those in the outer row are finned. This is done in order to equalize the temperature in both rows of heater tubes thereby maximizing performance.

The circular array is further divided into quarter-sections, with the end of each tube in one section being connected by a short header to one cylinder head (hot space), while the opposite end of each tube is connected by short headers to two regenerator housings. A cooler tube housing is attached to the base of each regenerator, as seen in Figure 7. At the base of each of the two cooler housings a duct leads to an adjacent cylinder, entering the cold space under the piston. Thus, the four cylinders and eight regenerator-cooler units are interconnected for the double-acting functions.

Major problems encountered by Philips and United Stirling in developing heater heads include minimizing head volume and pressure losses in the heaters, leakage of combustion gases between the quarter sections and around the combustion chamber where it contacts the heater tube array, non-uniform temperature distribution between quarter-sections, as well as general fabrication and brazing difficulties. United Stirling's heater designs have progressed from the "tower", to the "temple" and the most recent "envolute" design. The latter (shown more clearly by the photograph in Figure 11), has substantially reduced the leakage and thermal expansion problems; simplified and reduced the dead volume in the headers; and made fabrication much easier. Characteristic features of the envolute heater head include simple design, homogeneous temperature distribution, high efficiency, potential for long life, and cost effectiveness. Each tube in the heater is alike, and headers are cast integral with the cylinders and regenerator housings. The heater tubes are subject to the greatest creep of any component in the engine, and careful attention must be given to this problem. The material selected for the heater tube must have good high temperature creep and ductility properties,

*Solar application requires a new heater head of greatly simplified design.

good oxidation resistance, and must not be susceptible to hydrogen embrittlement. In the present configuration, Multimet is employed which is an iron-base super-alloy.

Results from component and engine testing are most promising, indicating increased efficiency, power, and life. Overall thermal efficiency was increased from about 32 percent with the tower heater design to over 36 percent with the envolute design, while the power has increased 25 percent for equal mean pressures. Over 7,500 hours of operation in component and engine rigs test have been accumulated and no envolute heater head breakdown has occurred.

REGENERATOR AND COOLER ASSEMBLY

The present cycle regenerators (Figure 12) are fabricated from sintered stacks of stainless steel screens sealed within a number of individual cups (regenerator housings) located around the cylinders. Tests have been performed with regard to heat transfer, wire dimensions, filling factors, pressure drop, etc., in order to arrive at the current configuration. Although the stacked screen configuration is expensive and alternate cheaper matrix configurations are being sought for automotive use, the screen regenerator provides excellent performance.

The cycle coolers (Figure 12) are formed from bundles of small tubes surrounded by an annular shell through which cooling water is circulated. These tubes are currently made of stainless steel or a copper-chromium alloy. In a more advanced configuration, it is projected that they could be made from aluminum alloy if the proper joints can be fabricated.

MECHANICAL ELEMENTS

Mechanical elements are the crank and piston mechanisms, which consist of crankshafts, connecting rods, crossheads, piston rods, sliding seals and piston with domes.

Crankshafts, connecting rods, and crossheads (Figure 13) have the same engine technology as common gasoline and diesel engines. Crankshafts and connecting rods have plain journal bearings which are hydrodynamically lubricated, as are the crossheads which take up the side loads from the connecting rods.

The piston rods are ground and hardened to provide the best wear and leakage properties compatible with the RULON* sliding seals. The lower working gas seal ring is "minimum lubricated" in order to obtain long life and low leakage. An efficient separation in the seal system prevents the oil from migrating to the upper seal and into the Stirling cycle. The oil that enters the gas seal ring is separated in an oil/gas separator and drained to the crankcase (Figure 14). Hydrogen leakage is low, and only requires a refill of hydrogen at intervals of 500 hours of operation or at 3 months, whichever comes first. Endurance testing with sliding seals is currently going on in

*Trade-name for a proprietary mix of Teflon, Fiberglas, and other materials.

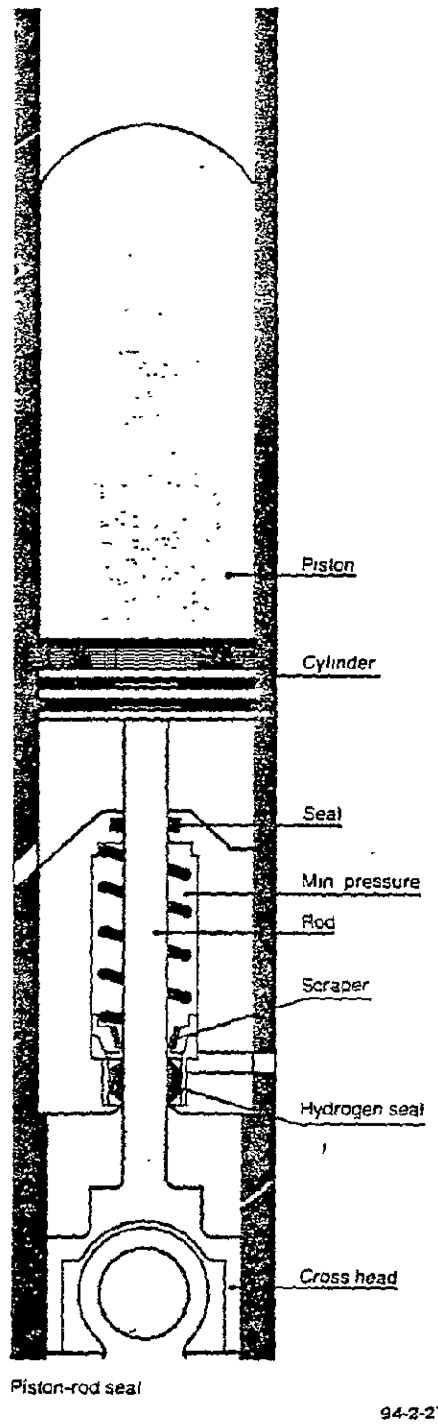


FIGURE 14. SKETCH SHOWING PISTON-ROD SEALS

component and engine test rigs. So far the test results are indicating more than 6,000 hours of life, and is continuously being improved.

The pistons have a rider ring to prevent metal-to-metal contact. The material for the piston rings and the rider ring is RULON with special filling compound. The pistons and the upper seal ring run oil-free as oil would influence the thermodynamic performance of the heat exchangers. On top of the pistons are piston domes which limit heat transfer from the hot to the cold side of pistons to acceptable rates. Life of piston seals and piston rod seals is about the same (6000 hrs).

START SEQUENCE

The heater tubes in a Stirling engine must be heated up before the starter motor is engaged. The burner blower, normally driven by the engine, is driven by a separate electric motor during the heat-up period. When the heater tube temperature has reached 200-300 degrees C, the starter is engaged.

Figure 15 shows a cold starting sequence test on a typical engine. After a 12 second heat-up period, the starter is engaged for about 2 seconds. The engine runs at idle speed and a vehicle would be able to move away slowly. After an additional 30 seconds, the heater temperature has reached its normal level and the engine can deliver full power. This start is representative for 20 degrees C ambient temperature. Tests at -32 degrees C have been made with a slight increase in cranking time due to higher hydrodynamic losses in the drive mechanism.

ENGINE INSTALLATIONS

Initial tests with the original 2-435 Philips engine were made in a number of installations, including one in a city bus and one in a pleasure-boat. These verify the environmental qualities of the engine and its ability to fulfill the commercial requirements.

A number of V4 engines have been tested in similar applications. The first installation of a 40 kW V4-engine (third generation) was made in 1974 in a Ford Pinto passenger car to get an early experience of driveability and control and cooling systems. This installation was made in collaboration with the Ford Motor Company.

In 1976, a 40 kW V4-engine was installed in a Ford Taunus Station Wagon (Figure 16). A somewhat improved version of the V4-engine was combined with a 4-speed manual transmission. Driveability is excellent and engine torque characteristics reduce the number of gear shifts to a minimum. Noise level is about 6 dB(A) lower than the original gasoline engine installation. Reliability is good and the passenger car is still in operation, accumulating over 500 hours of operation.

In 1977 a 65 kW V4-engine was installed in an 8-ton delivery truck (Figure 17). Driveability is excellent with few gear shifts in city traffic. Low noise and vibrations in the driver's cabin makes the driving very comfortable. The

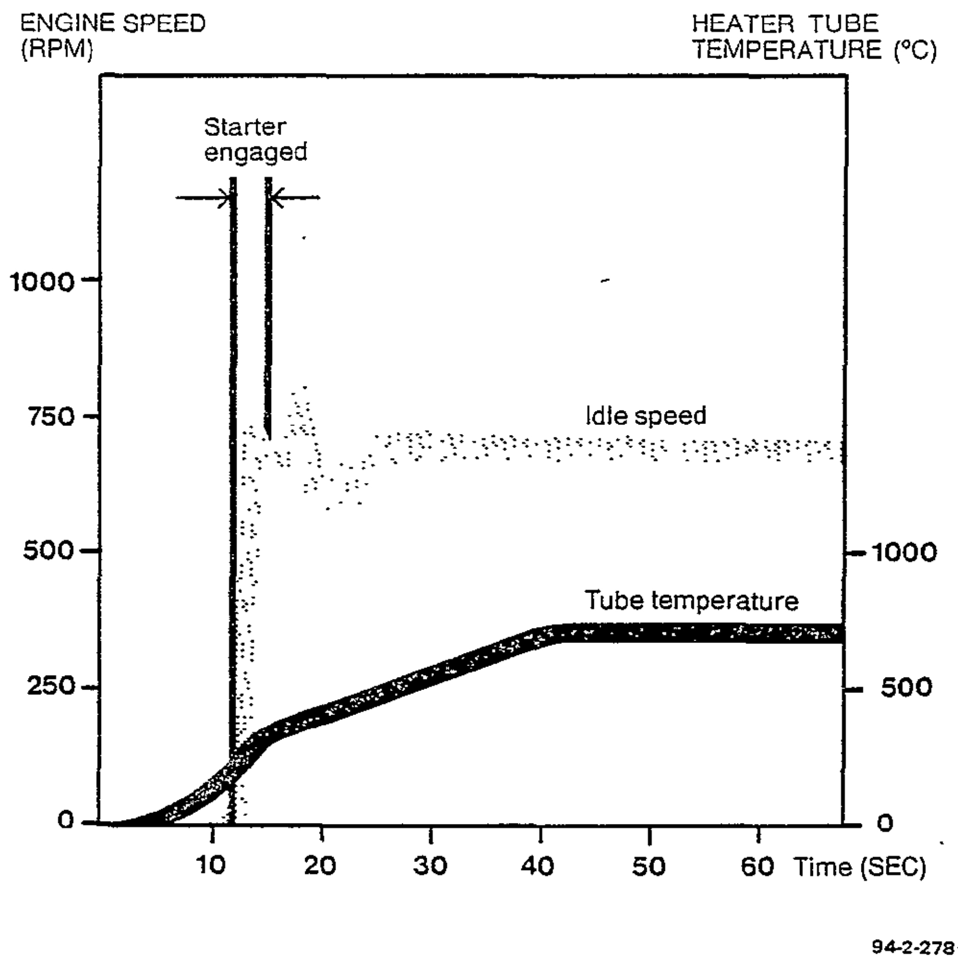


FIGURE 15. TYPICAL STARTING SEQUENCE

vehicle is extremely quiet - external noise level is about 15 dB(A) lower than the original diesel installation. The reliability is satisfactory and tests are still in progress. Over 250 hours of operation have been accumulated.

In 1978 a V4 Stirling engine powered heat pump for residential heating (maximum capacity 30 kW at -4 degrees C) was tested (Figure 18). Its potential for energy conservation and low environmental impact is of great interest.

In 1978 a NASA contract was awarded to USS for development of a Stirling engine-powered car. United Stirling installed a P40 (U4) engine (Figure 19) in an Opel passenger car (Figure 20). An existing P40 engine, not optimized for passenger car application, was used to allow the earliest possible installation. Evaluation tests have been going on for some time. Driveability is equivalent to current passenger cars; fuel economy is equal to the original diesel installation. Noise level in drive-by tests is 11 dB(A) below the diesel installation. Exhaust emissions are fulfilling original 1976 standards. The car was recently demonstrated at a Contractors' Meeting in Detroit, where over 150 persons were given an opportunity to take a ride in this car.

## PART II

## SUMMARY DESCRIPTION OF THE (P-40, P-75) U4 CONFIGURATION

Presented herein are the design features of the U4 configuration. As described earlier, the U4 configuration is easier and cheaper to manufacture than the V4 configuration - particularly on the general purpose tooling appropriate to the relatively low (~10,000/yr) production rate planned by USS.

### DESIGN FEATURES

The design of a double-acting square four (U4) unit has the following characteristics:

- Symmetrical arrangement of cycle components, providing good thermodynamic balance between different cylinders.
- One combustor and air preheater unit per four cylinders.
- Conventional drive mechanism (dual crankshaft, connecting rods and crossheads).

### COMBUSTION SYSTEM COMPONENTS

The arrangement of the external combustion system components, i.e., preheater, turbulator, combustor and heater were shown previously. The latest envolute heater head design is comprised of four identical quadrants, with curved inner row tubes and vertical outer row tubes with brazed fins.

Cylinder block - The cylinder block (Figure 21), made of nodular cast iron, contains four cylinders arranged in a square pattern, two coolers/regenerators per cylinder and ducts for the working medium and cooling water.

Crankshaft and connecting rod assembly - The crankcase assembly contains two crankshafts, each running in three plain main bearings. Each crankshaft is geared to a common drive shaft on which the flywheel is attached. The four connecting rods have forked small ends which accommodate the wrist pin, crosshead and eye of the power piston rod. The crossheads run in individual liners which are located concentrically with the cylinder block.

Oil pump - The oil pump is located in the sump and chain drive from the front end of the right hand crankshaft. Oil is fed from the pump through a pressure relief valve to the full flow oil filter mounted on the side of the crankcase. Provision has been made in the design to include an oil cooler if required. From the filter, the oil passes to the main bearings and drive shaft bearings. Drillings in the crankshafts feed the oil to the end bearings. Oil jets in the top of the crankcase lubricate and cool the piston rods. A spring controlled ball valve limits the flow of oil from the jets until oil pressure reaches a safe minimum level.

Auxiliary equipment - Outside the crankcase, a starter motor is attached on the right-hand side and engages with the flywheel ring gear. The burner blower motor is located on the left-side of the engine and drives the blower independently from the engine until the engine speeds up to take up the drive. The reciprocating pump for the hydrogen or helium working gas is driven from an overhung pin on the front end of the left-hand crankshaft. The central drive shaft can also be used to drive other accessory equipment at engine speed, as required.

The auxiliary gear drive at the flywheel end of the engine has been designed to accommodate a gear preload device to avoid excess gear noise, and the tooth loading on the idler gear to the burner blower motor is sufficiently low to allow the use of a glass-fiber filled nylon gear. Pressure controlled oil jets have been designed-in to lubricate the crankshaft gears if required.

## PART III

## STIRLING ENGINE HEAT PIPE SYSTEMS*

This section describe the results of experimental work carried out by USS to evaluate a concept for remote heating of the engine - for possible multi-fuel applications as well as for solar applications.

### STIRLING ENGINE CHARACTERISTICS

The efficiency of the Stirling engine is strongly dependent on:

- The temperature level at which energy is transferred to the working medium
- Speed of rotation
- Choice of working medium

Inherently, the Stirling engine process requires high temperatures and high pressures of the working medium to yield a high efficiency. The efficiency of a given engine tends to drop at high operational speed. High specific power requires that the working medium be helium or hydrogen.

The speed of the Stirling engine is mainly limited by the design of its heaterhead. Due to the relatively low heat transfer from the combustion gas to the heater tube walls, a fairly large surface area is needed. Optimization of the heat transfer on the outside tends to increase the heater tube diameters. However, such an increase in diameter is detrimental to the heat transfer to the working fluid on the inside surface of the tube. Therefore the heater assembly must be a compromise, and one which becomes more severe as the specific power of the engine is increased.

The problems with limitations of external heat transfer rates to the external surface of the heater tubes can be eliminated by using a heat pipe. Heat pipes allow large amounts of energy to be transported to small surfaces with very low temperature differences. Using this principle, the Stirling cycle may be optimized without regard to the previously limiting factors. Thus, short heater tubes of smaller diameters may be used, making possible a design with considerably lower pressure loss in the working gas and thereby allowing an increase of the rotational speed. This will improve the power-to-weight ratio of the engine.

---

*Note that vapor pipes are identical to heat pipes in terms of performance. The only difference is that gravity is used to return the liquid in a vapor pipe whereas a wick is used for heat pipes. Thus, heat pipes can be used where the heat source (evaporator) is above the heat sink (condenser).

DESIGN

Calculation, design, manufacturing, and testing of a Stirling engine heat pipe system have been carried out at United Stirling. This was performed as an experiment with the objective to demonstrate the feasibility of using a sodium heat pipe in conjunction with a Stirling engine.

The total heat convection loop in this experiment consisted of:

- A Stirling engine functioning as a condenser in the heat pipe
- The sodium heat pipe (a total of 9 used in the experiment)
- Electrical resistance heaters functioning as the heat source

A brief summary of this experiment is given below. Additional details are contained in IECEC Transactions, 1973 (Paper No. 739073) pp. 165-173.

ENGINE DESIGN

The engine used in this experiment was a single cylinder displacement-type engine. The difference in the engine for the heat pipe application was in the simplified design of the heater head. Sodium heat transfer allows the number of tubes in the heater head to be reduced, the tube diameter to be reduced, and larger tube radii to be used (see Figure 22); all of which allow increased engine speed and efficiency. The dimensions of the heater head were optimized for maximum power using an existing program. The cooler-regenerator units were not modified.

HEAT PIPE DESIGN

The evaporator section of the heat pipes was designed and manufactured from a stainless steel tube of outer diameter $d_o$ = 121 mm and wall thickness t = 3.5 mm. The total length of the tubes was 450 mm. The heat pipes were connected to the Stirling engine via a conical-shaped adiabatic section to a dome (Figure 23). This dome was welded to a plate that was brazed to the cylinder and regenerator cups to make a completely sealed vessel.

The condensed sodium on the heater tubes flowed onto a cover plate to which stainless steel gauze layers were attached. From this layer the liquid sodium was transported back to the evaporator section by means of the capillary structure.

The heat supply to the evaporator section was provided by electrical resistance wires brazed in grooves at the outside of the tube to assure perfect contact between the element and the evaporator wall.

EXPERIMENTAL APPARATUS AND RESULTS

The test unit was installed in a test cell and connected to a Schenk U 16 water-brake. The shaft power output of the engine was controlled by varying the mean working pressure in the cycle. The brake was fitted with a DC Motor for remote control of the torque. All control functions were mounted on a panel in the control room. Safety precautions were taken to prevent water and sodium contact in case of accidental leakage from the heat pipe.

Temperatures were measured on the outside of the heatpipe vessel, in the liquid as well as the vapor phase in several different locations, and were recorded continuously. Approximately 180 hours of engine operation were clocked. The general results showed that a Stirling engine equipped with a high temperature sodium heat pipe resulted in an appreciable improvement in performance when compared to a conventional combustor-type engine. This result is shown in Figure 24. There is a reduction in performance if helium is used in place of hydrogen for a conventional burner-head engine (curve 3 compared to curve 2). However, curve 1 shows there is a dramatic gain in performance when helium is used with a heatpipe - even greater than the original hydrogen burner-head version. This is called the 'bonus' effect by using a heat pipe source. The 'bonus' occurs because the power-consuming blower and air/fuel controls are eliminated; the greatly increased heat transfer due to condensing sodium; and simplified heater head design with fewer tubes and reduced dead volume.

SUMMARY

With its proved experience in Stirling engine heat pipe systems, United Stirling is well qualified to modify and adapt its P40 or P75 engines to be used in a solar application where sodium vapor, rather than combustion gases, is utilized as the source of heat.

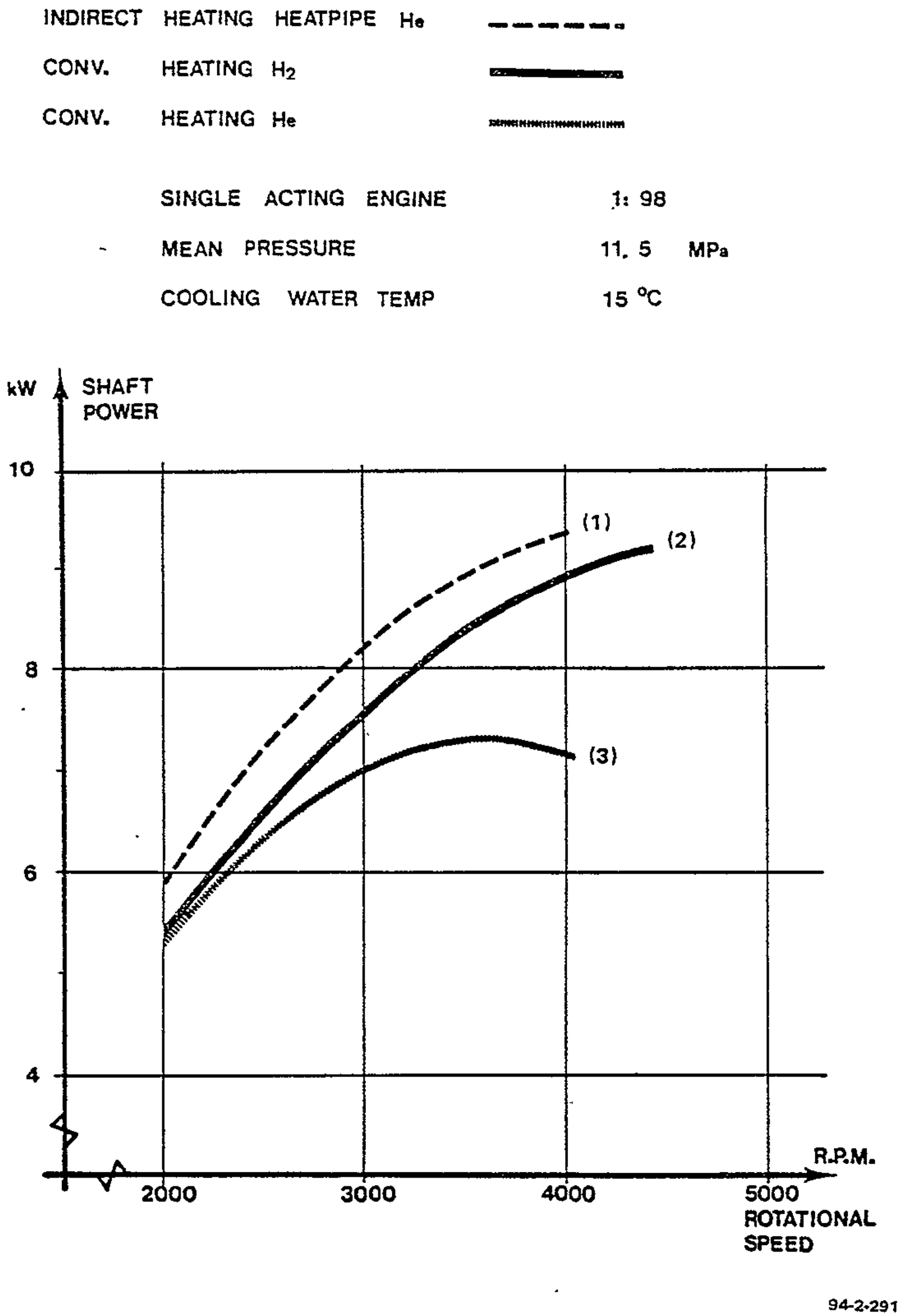


FIGURE 24. COMPARISON OF INDIRECT HEATING (HEATPIPE) WITH CONVENTIONAL HEATING

# APPENDIX D

# ORGANIC RANKINE CYCLE ENGINE FOR SPS APPLICATION

Source: Sundstrand Energy Systems

# APPENDIX D. ORGANIC RANKINE CYCLE

The engine proposed by Sundstrand Energy Systems of Rockford, Illinois is a 75 $kW_e$ organic Rankine cycle (ORC) operating with an 800°F turbine inlet temperature. The choice of an organic Rankine cycle versus steam Rankine cycle was based on engine availability as well as design simplicity and state-of-the-art technology.

A brief trade off between the two systems is shown below:

| | Organic | Steam |
|---|---|---|
| Turbine Inlet Temperature (°F) | 800 | 1350 |
| Approx. System Eff. | 27% | 27% |
| Availability (Month) | 15 | 32 |
| Technology | State-of-the-art | Advanced Concept |

Sundstrand's background in organic Rankine cycles began with the ASTEC program in 1962 (Figure 1). Figure 2 indicates that Sundstrand has worked on organic Rankine cycle projects for nearly 20 years.

## 1. ENGINE CONTROL CONFIGURATION

Organic Rankine cycle engines are usually started by employing a blow-down start, utilizing fluid trapped in the vaporizer to spin up the rotating assembly to self-sustaining speeds by opening a start valve. Unfortunately, this method will not work with a hot restart because the small boost pump delivers insufficient pressure to fill a hot vaporizer. Consequently, a start pump has been added to the solar system design to allow working fluid to be pumped through the hot vaporizer to start the turbine; when self sustaining speeds are reached, the electrically driven start pump can be switched off.

It has been assumed for this study that the system will operate into a large grid, in parallel with other units. It is this conditioning efficiency (93 percent) which has been used for the system performance analysis. For a single unit operating into a grid, however, a line-commutated inverter would be slightly more efficient (94 percent).

During steady state operation the turbine inlet temperature is kept constant at the design point by varying flow through the boiler. This is achieved by sensing turbine inlet temperature and controlling an electromechanical flow control valve at the feed pump outlet. As heat input varies the available turbine power varies, and turbine speed control is necessary. This is achieved by varying the excitation to the alternator and delivering variable amounts of power into the grid. An emergency shut down valve is included upstream of the turbine to protect the wound rotor alternator from damage in the event of an overspeed malfunction. In general, organic Rankine systems operate at speeds low enough to preclude turbine burst due to runaway speeds.

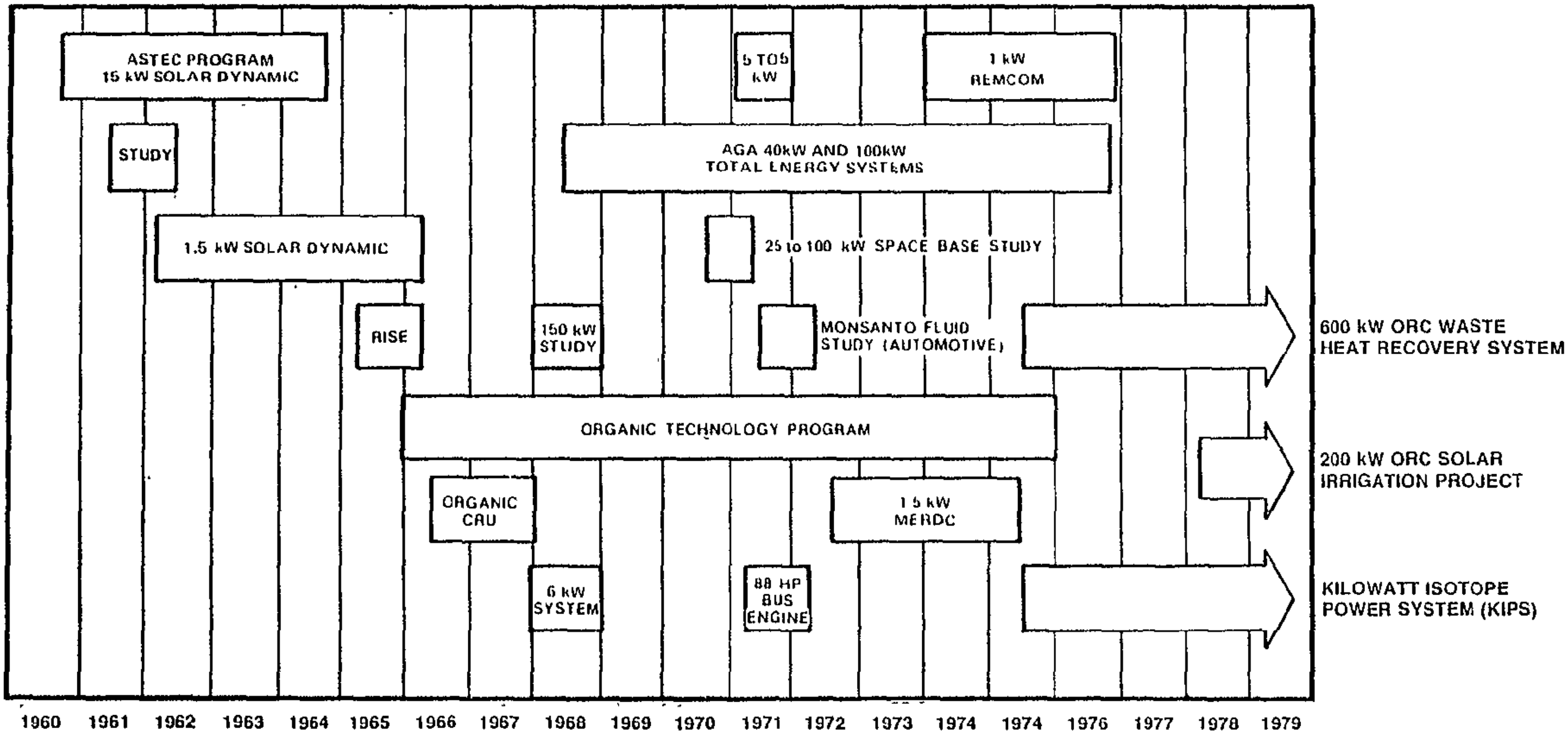


94-2-166

FIGURE 2. ORGANIC RANKINE CYCLE PROGRAMS AT SUNDSTRAND

The effect of reducing turbine and fan speeds at part power was investigated and significant performance improvements were noted. The logic for controlling at these speeds would be incorporated in a microprocessor control unit. Electrical load would be applied to the generator as the desired function of speed by sensing output frequency and output power and adjusting excitation appropriately.

2. SYSTEM PERFORMANCE

System design analyses were performed for three ambient air temperatures: 70°F, 95°F and 112°F. Each design was then investigated in the off-design mode as a function of air temperature and heat input. The 95°F air temperature was selected for the design point since it gives best performance over the investigated range of temperatures and heat input. The design point was selected at 85.7 percent of peak power and investigated at 100 percent, 75 percent, 50 percent, and 25 percent thermal input power.

Figure 3 shows the effects of ambient air temperature and heat input on the final design operating at constant turbine and fan speeds. As part of the control study, an investigation was made of the effect of reducing fan and turbine speeds at part power conditions. Considerable improvement in performance is feasible at the low power levels. These effects are shown in Figure 3. At the high ambient air operating condition (112°F) and low thermal input (80 $kW_{th}$) the system performance increases from 14.5 percent to 22 percent, i.e., net output increases from 11.8 $kW_e$ to 17.9 $kW_e$.

The system has been configured to utilize an alternator and system feed pump directly driven from the turbine, supported on liquid-lubricated tilting pad bearings. This allows a system to be designed which is completely hermetic, having no requirement for gearbox seals and greatly improving reliability. A wound rotor aircraft-type alternator keeps the electromagnetic weight to a minimum.

A large fan draws air through the annular condenser and is directly driven by an electric motor.

A summary of design point component efficiencies and system characteristics is given in Table 1.

3. WEIGHT AND DIMENSIONAL STUDY

The condenser size selected is dictated by the condenser fan. To handle the required flow rate and keep fan power to reasonable values a large propellor fan (54-inch diameter) is required. The condenser length is determined by the required heat exchanger area. The system and component dimensions and weights are given in Table 2.

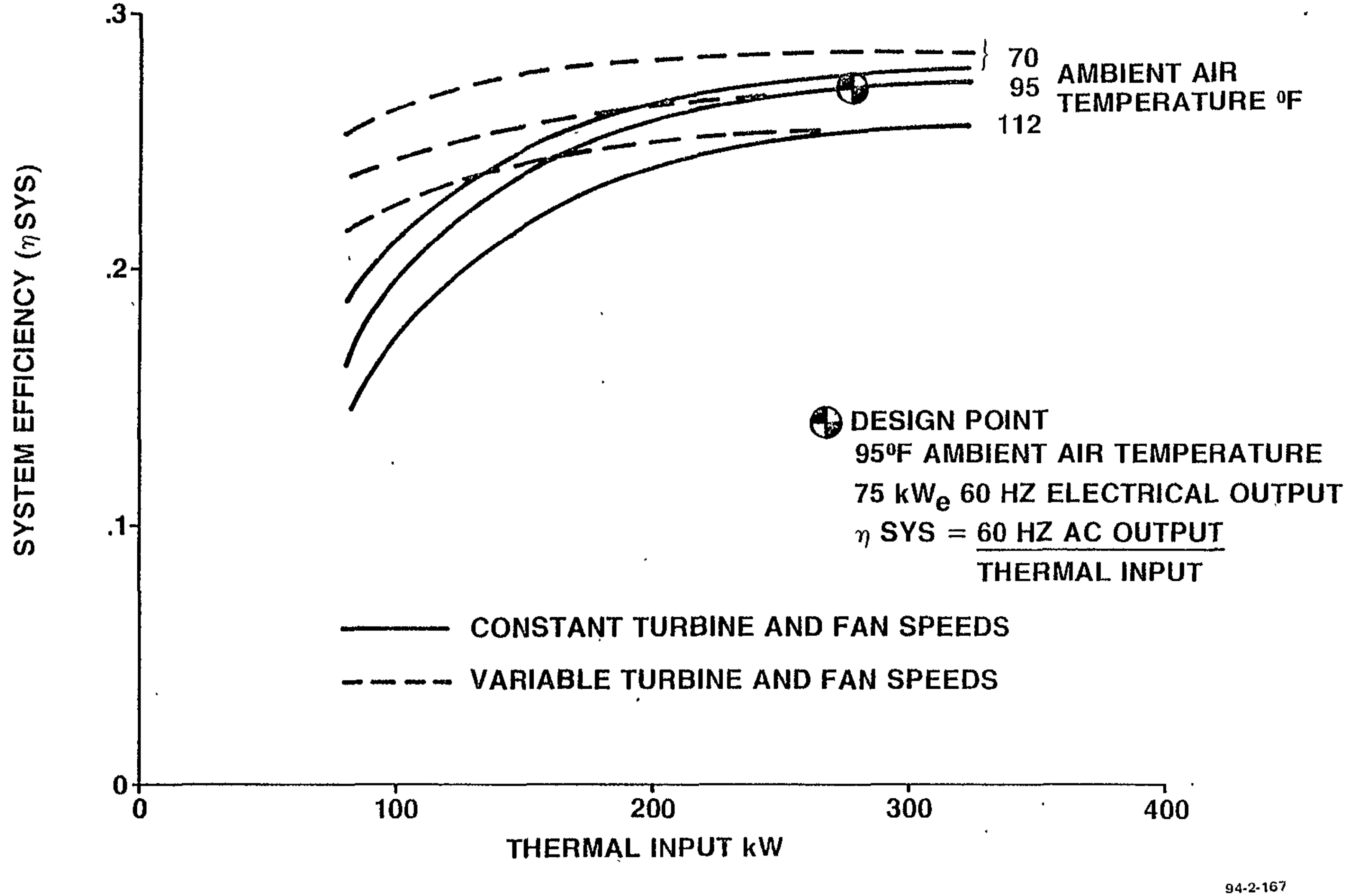


FIGURE 3. SOLAR POWERED ORGANIC RANKINE SYSTEM PERFORMANCE

TABLE 1. SYSTEM DESIGN POINT CHARACTERISTICS

| | |
|---|---|
| 60 Hz ac Power Out (kW) | 75 |
| Thermal Power In (kW) | 280.1 |
| System Efficiency (%) | 26.8 |
| Fan Power (kW) | 6.5 |
| Parasitic Power* (kW) | 0.2 |
| Conditioning Efficiency (%) | 93 |
| Alternator Efficiency (%) | 92 |
| Pump Efficiency (%) | 58 |
| Turbine Efficiency (%) | 75 |
| Regenerator Effectiveness (%) | 95 |
| Bearing Losses (kW) | 0.15 |
| System Flow (lb/hr) | 3480 |

*Includes controls and boost pump

TABLE 2. SYSTEM AND COMPONENT WEIGHTS - DIMENSIONS

| | Weight (lb) | Diameter (in.) | Length (in.) |
|---|---|---|---|
| • System (Total) | 1185 | 54 | 96 |
| Component: | | | |
| Condenser | 630 | 54 | 60 |
| Fan/Motor | 125 | 11 | 20 |
| Combined Rotating Unit | 70 | 8 | 14 |
| Regenerator | 130 | 18 | 27 |
| Start Pump | 75 | 0.75 | 1.5 |
| Electronic Controller | 30 | - | - |
| Fluid (Inventory) | 80 | - | - |
| Miscellaneous | 75 | - | - |

A typical configuration is shown in Figures 4, 5 and 6, starting with the combined rotating unit, CRU (Figure 4), then showing the CRU and regenerator, then the entire organic system (Figure 6).

Figure 7 is a functional block diagram of the ORC system, and Table 3 lists the design pressures and temperatures for the corresponding vapor/liquid state points on the block diagram.

4. SCHEDULE AND PRODUCTION CAPABILITY

Sundstrand projects the availability of a 75 $kW_e$ ORC engine which will support the requirements of the 4.5 year Phase II program. A complete system (power conversion module, condenser assembly and controls) will be available 15 months ARO.

Meeting the requirements of SPS, Sundstrand will, in addition to the Research and Development Facility, will be able to call on the following production capability:

| Location | Product | Units/Year |
|---|---|---|
| Ames, Iowa | hydrostatic transmissions | 600,000 |
| Denver, Colorado | fluid handling systems | 300,000 |
| Bristol, Virginia | air conditioning compressors | 2 million |
| Rockford, Illinois | fuel oil burners | 2 million |

TABLE 3. DESIGN CONDITIONS

| State Point At: (See Block Diagram) | Pressure (psia) | Temperature (°F) |
|---|---|---|
| 1. Turbine Inlet | 629 | 800 |
| 2. Regenerator Vapor Inlet | 2.07 | 572 |
| 3. Condenser Vapor Inlet | 1.92 | 167 |
| 4. Feed Pump Inlet | 10 | 124 |
| 5. Alternator Cooling Inlet | 717 | 135 |
| 6. Regenerator Liquid Inlet | 707 | 146 |
| 7. Vaporizer Liquid Inlet | 702 | 465 |
| 8. Vaporizer Outlet | 639 | 800 |

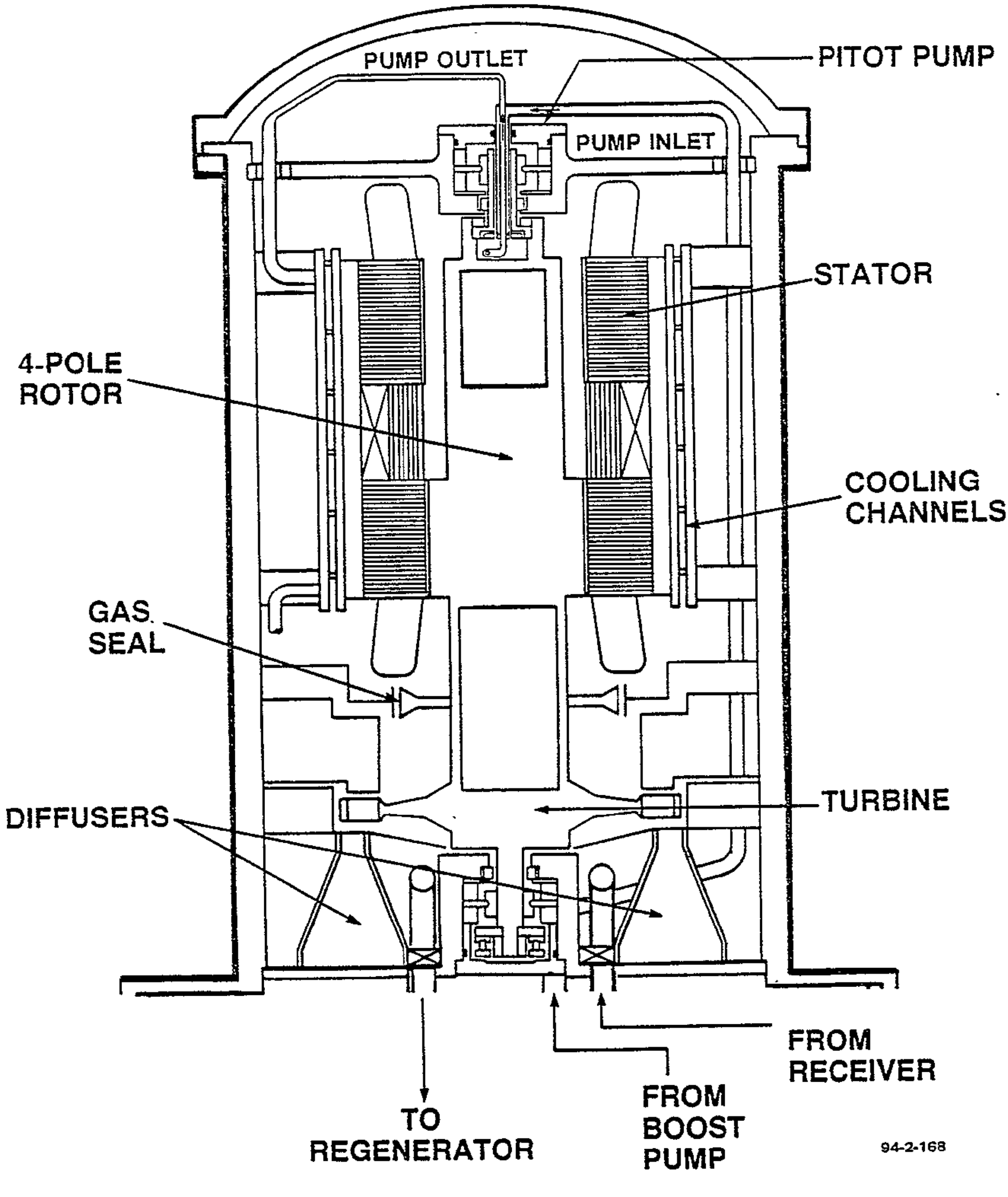


FIGURE 4. ORGANIC COMBINED ROTATING UNIT (CRU)





ORIGINAL PAGE IS
OF POOR QUALITY

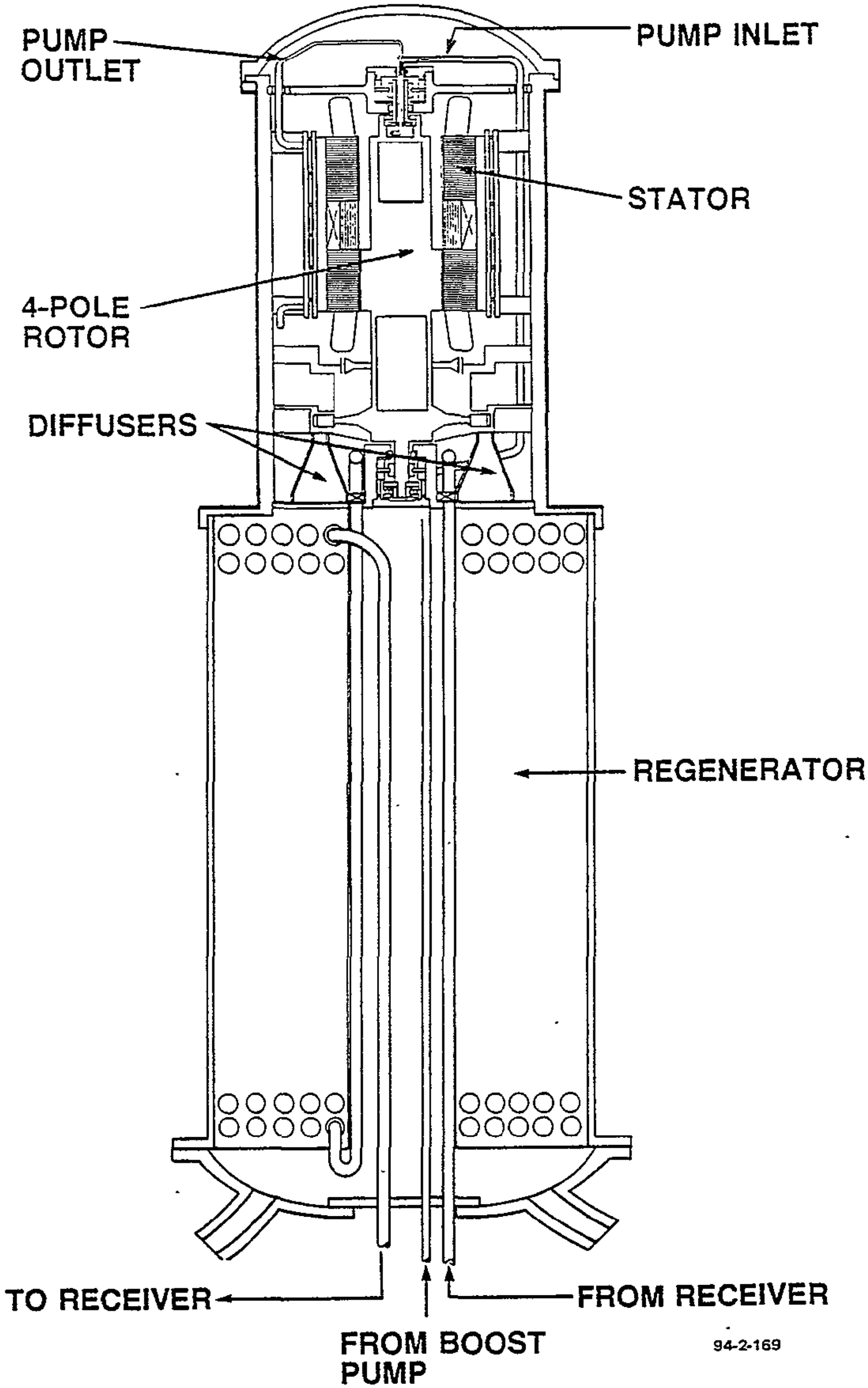


FIGURE 5. ORGANIC CRU AND REGENERATOR

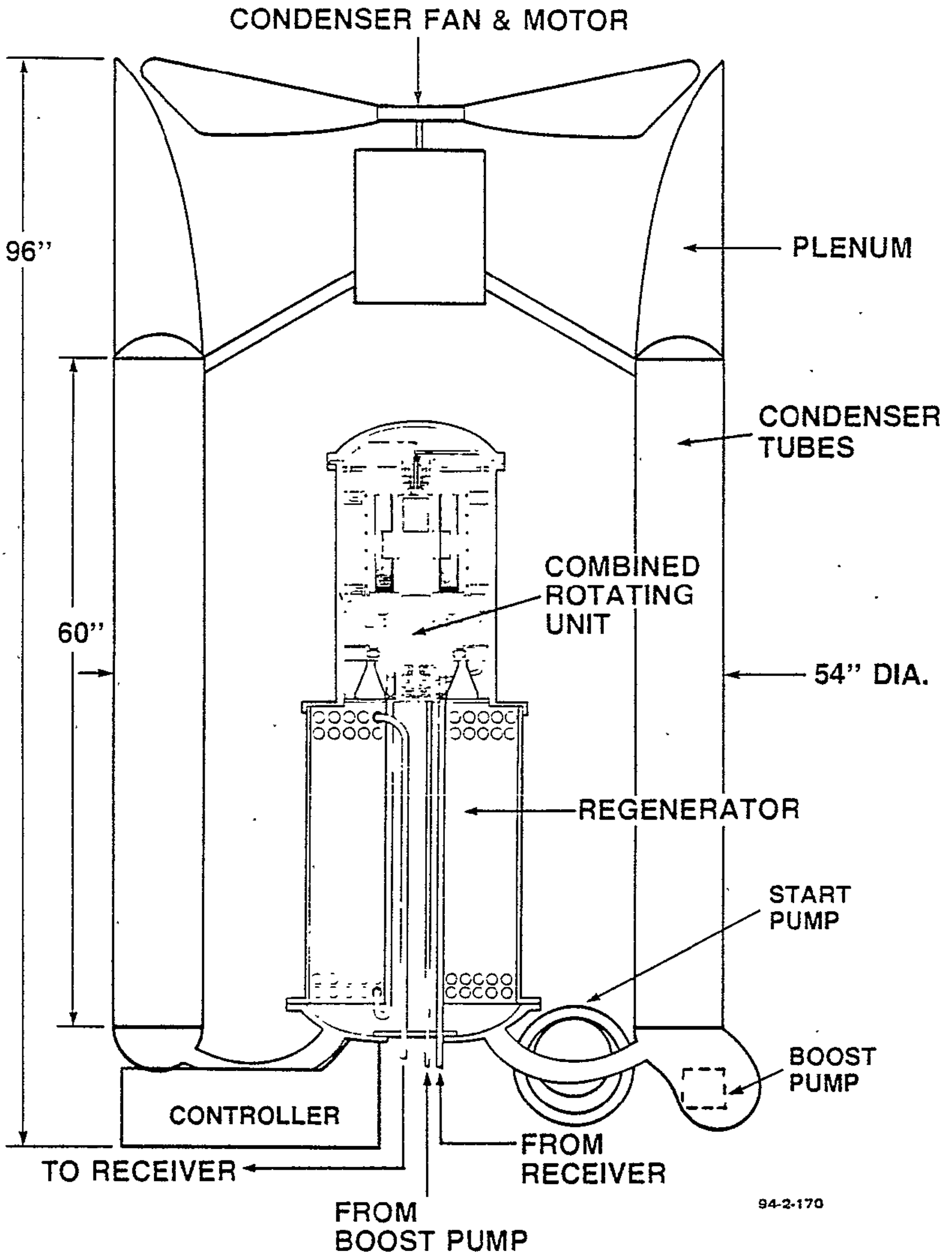


FIGURE 6. ORGANIC SYSTEM

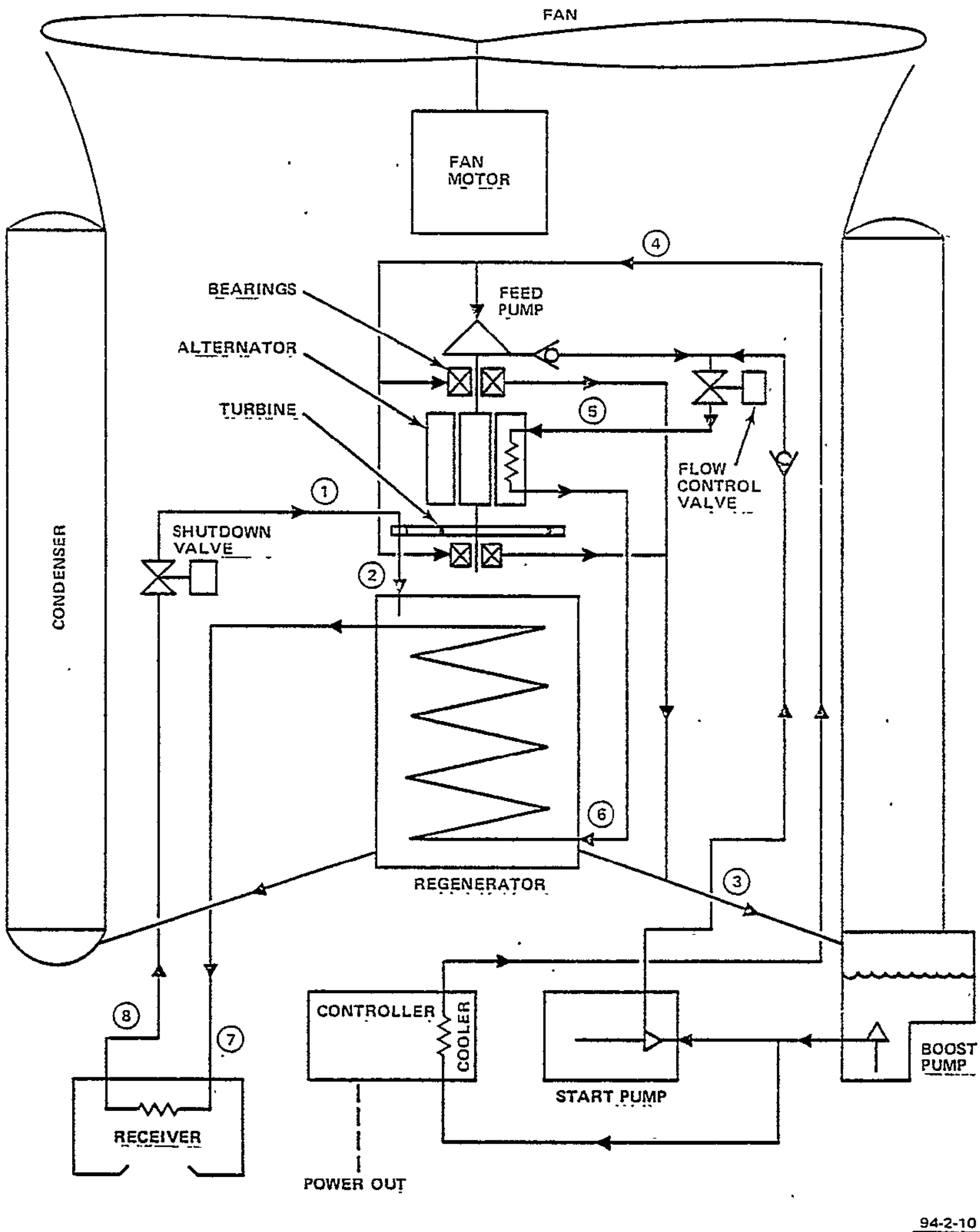


FIGURE 7. FUNCTIONAL BLOCK DIAGRAM: ORGANIC SYSTEM

5. COST DATA

Cost figures for organic Rankine cycle engines as developed by Sundstrand are given below:

(a) One deliverable engine plus operating spares
Approximately $2.0 million
(The bulk of this figure is nonrecurring costs)

(b) Production of an additional (25) deliverable engines plus operating spares
Approximately $1200/kW$_e$

(c) Production of 100 units/year to subcontractor's maximum current production capacity
Approximately $800/kW$_e$

NOTE: Maximum current production capacity will depend on the facility where the systems are produced, whether it be existing or new. When production levels reach approximately 300 units per year the system would no longer be produced in Rockford.

(d) Production of 10,000 units/year
Approximately $700/kW$_e$

(e) Production of 400,000 units/year
Approximately $400/kW$_e$